BEREITSCHAFT, BRADLEY JAMES FRANK, Ph.D. Urban Form and Air Quality in U.S. Metropolitan and Megapolitan Areas. (2011)
Directed by Dr. Keith Debbage. 390 pp.

The spatial form, or morphology, of urban areas may significantly affect the anthropogenic production of air pollutants. This dissertation explores the relationships between air quality and urban form at the metropolitan and megapolitan (multi-metropolitan) scale. Urban form was quantified for 86 metropolitan and 19 megapolitan areas using both pre-existing sprawl indices and multiple spatial metrics derived from remotely sensed landcover data. Air quality was assessed by measuring several key air pollutants, including the ambient concentration of ozone (O_3), the non-point source emissions of the two O_3 precursors nitrogen oxides (NO_x) and volatile organic compounds (VOCs), the ambient concentration and non-point source emissions of fine particulate matter ($PM_{2.5}$) and coarse particulate matter (PM_{10}), and the mobile emissions of carbon dioxide (CO_2). The ambient concentrations of air pollutants were averaged over the 5-year period 1998 to 2002. While controlling for industrial emissions, climate, population and geographic area, multiple linear regression was used to evaluate the degree of association between measures of urban form and air quality. The results suggest that urban form has a measurable impact on both the non-point source emission and ambient concentration of air pollution. Urban areas that exhibited more "sprawl-like" urban forms (i.e. lower residential density, less street network connectivity, less contiguous urban development) generally had higher non-point source emissions and/ or ambient concentrations of air pollution. Pre-existing sprawl indices were most significantly associated with ambient concentrations, while two spatial-metrics based

measures of urban structure, urban “continuity” and urban “shape complexity,” were most significantly associated with non-point source emissions. The relationships between measures of urban form calculated using spatial metrics and air pollution were most significant at the metropolitan scale. The extent of the urban area (i.e. high versus low urban threshold), however, did not significantly affect the associations between urban form, as assessed using spatial metrics, and air pollution. Understanding the relationships between urban form and air quality is an important step in identifying effective urban land use configurations and developing healthier cities.

URBAN FORM AND AIR QUALITY IN U.S. METROPOLITAN AND MEGAPOLITAN AREAS

by

Bradley James Frank Bereitschaft

A Dissertation Submitted to
the Faculty at The Graduate School at
The University of North Carolina at Greensboro
in Partial Fulfillment
of the Requirements for the Degree
Doctor of Philosophy

Greensboro
2011

Approved by

Dr. Keith Debbage
Committee Chair

To Kathryn Louise Rutledge Bereitschaft

tui vires est mihi vires

APPROVAL PAGE

This dissertation has been approved by the following committee of the Faculty of The Graduate School at the University of North Carolina at Greensboro.

Committee Chair Dr. Keith Debbage

Committee Members Dr. Zhi-Jun Liu

Dr. Jay Lennartson

Dr. Anna Marshall-Baker

March 2, 2011
Date of Acceptance by Committee

March 2, 2011
Date of Final Oral Examination

ACKNOWLEDGEMENTS

I would foremost like to thank my advisor, Dr. Keith Debbage, and committee members Dr. Jay Lennartson, Dr. Zhi-Jun Liu and Dr. Anna Marshall-Baker for their invaluable guidance, insight and support throughout this project. I would also like to thank my fellow graduate students, and the faculty of the Department of Geography, for providing the stimulating, collegial environment essential to my development as an academic.

This work would not have come to fruition without the additional support of friends and family. Dr. Eliza Nelson was instrumental in providing both intellectual and emotional support, particularly during the final stages when it was needed most. I am infinitely thankful for my parents, Frank and Kathy Bereitschaft, for their unconditional love and unwavering belief that I "will be anything and all [I] strive to be." To my mother, who lost her battle with cancer a year before completion, this is for you.

TABLE OF CONTENTS

Page

LIST OF TABLES

Page

LIST OF FIGURES

Page

CHAPTER I

INTRODUCTION

Cities account for less than three percent of the Earth's land surface, yet they produce 78 percent of anthropogenic carbon emissions and substantial quantities of airborne toxins and pollutants (O'Meara 1999; United Nations 2006). These emissions are believed to play a significant role in both global climate change and the deterioration of air quality at local and regional scales (Grimm 2008). Although many factors contribute to the air pollutant "footprint" of an urban area, including climate, topography, and economics, the way in which cities grow and evolve spatially is a crucial component (Lu and Turco 1995; Newton 1997; Stone 2008). The spatial distribution and arrangement of the urban landscape (i.e. urban form or morphology) dramatically affects how cities function, how efficiently they utilize resources, and how much pollution they produce (EPA 2001; Ewing 2003; Borrego et al. 2006). By quantifying components of urban form systematically across multiple urban areas, it may be possible to not only assess the degree to which urban form and air quality are related, but also identify the particular aspects of urban form most likely to affect the abundance of specific air pollutants. This information can help inform urban planning strategies designed to improve air quality and promote a healthful, sustainable urban environment.

The mass adoption of the automobile and the proliferation of supporting infrastructure over the last six decades have not only transformed the shape of the American city, but also the way in which it functions. Throughout the suburban and exurban portion of most large U.S. cities, the traditional pedestrian and transit-oriented neighborhood design has given way to auto-centric land use patterns. Although more extensive in some regions than others, most American cities today contain large tracts of low-density, single-use developments that spread across the landscape in a seemingly haphazard and non-contiguous (or "leap-frog") pattern. Commonly referred to as "urban sprawl," this pattern of land use has been associated with a variety of social, environmental, and economic ills (Ewing 1997; Bruekner 2000; Frumpkin 2002; Stone 2008).

The relationships between urban form and air quality are well documented (Newman and Kenworthy 1989; Larivi`ere and Lafrance 1999; Frank and Pivo 1994; Ewing, Pendall, and Chen 2003; Handy, Cao, and Mokhtarian 2005; Borrego et al. 2006). Most notable is the impact of urban form on travel behavior and associated tail-pipe emissions. The logic is straight-forward: as urban areas become less contiguous, more widely dispersed, and land uses become increasingly segregated and low-density, residents are forced to drive further and more often to reach their destinations. As people drive more and walk or use transit less, the emission of tail-pipe pollutants, including carbon dioxide (CO_2), nitrogen oxides (NO_X), particulate matter (PM), and carbon monoxide (CO), increases. Although this relationship has received considerable attention, it is important to consider that urban form can affect air quality through additional means,

including influencing building energy use and local meteorology (Taha and Bornstein 1999; Weng 2003; Ewing and Rong 2008).

The production and emission of air pollutants and carbon dioxide affects human health and well-being on a local, regional and global scale. While local air pollution causes a variety of health concerns, carbon dioxide contributes to rising global temperatures, which is expected to affect the well-being – and survival – of millions worldwide (Khasnis and Nettleman 2005; Cline 2007; Dasgupta et al. 2007). Although advances in technology may comprise part of the solution, they are not likely to mitigate these issues entirely. Mass adoption of the electric car, for example, would likely reduce the ambient concentration of air pollutants within urban environments. Total emissions of air pollutants and carbon dioxide, however, would not be reduced as long as most electricity in the U.S. is derived from fossil fuel-based power plants (EIA 2010). It is therefore important to consider not only how we derive energy, but also how our built environment affects energy use. Gaining a better understanding of how and to what degree particular aspects of urban form affects air quality is a critical component in the broader effort to create a more healthful urban environment.

In this dissertation, I quantitatively evaluate the strength of association between measures of urban morphology and the emissions of air pollutants and their ambient concentrations at the metropolitan and megapolitan scale. In doing so, I seek to answer the question: to what degree does urban sprawl and associated land use configurations affect air quality and the release of the greenhouse gas carbon dioxide? Although previous studies by Ewing et al. (2003) and Stone (2008) have examined the relationships

that exist between ozone levels and the multi-variable sprawl index developed by Ewing et al. (2003), this dissertation is the first to quantitatively evaluate the relationships that exist between levels of multiple air pollutants and multiple sprawl indices.

The sprawl indices included in this analysis capture a variety of spatial characteristics, such as residential density, street network connectivity, and heterogeneity of land uses, but they do not explicitly quantify the spatial configuration of urban patches. Therefore, in order to provide a more complete and revealing assessment of the specific linkages between urban form and air quality, spatial metrics (or landscape metrics) are applied to remotely sensed land cover data at both the metropolitan and megapolitan scale. Megapolitan areas represent a scale of urban form beyond the single metropolitan area, and may generally be described as multi-metropolitan urban agglomerations with overlapping commuter sheds (Lang and Knox 2009). Furthermore, spatial metrics are calculated for each scale at a high urban threshold (i.e. central city and surrounding suburbs) and low urban threshold (i.e. central city, surrounding suburbs, and outer exurban areas) to evaluate the influence of urban extent on the strength of associations. A comprehensive review of the literature suggests that spatial metrics have not previously been used to evaluate the relationships between urban form and air quality, nor have similar analyses incorporated separate urban thresholds or been carried out at the megapolitan scale.

Using a series of regression models that control for confounding factors including climate, population and industrial production, measures of urban form are regressed against the ambient concentration and number of annual exceedances (i.e. days in which

the concentration is above 75 ppb) of ozone (O_3), the ambient concentration and annual non-point emission of particulate matter ($PM_{2.5}$ and PM_{10}), the combined annual non-point emission of the O_3 precursors volatile organic compounds (VOCs) and nitrogen oxides (NO_x), and the mobile "on-road" emission of the greenhouse gas carbon dioxide (CO_2). Air quality data was collected for 86 of the most populous metropolitan areas in the U.S. and the 19 megapolitan areas identified by Lang and Knox (2006). In accordance with previous studies (Ewing et al. 2003 and Stone 2008), I expect to find that cities exhibiting higher levels of sprawl experience more air pollution than those with lower levels of sprawl. I further hypothesize that the more comprehensive, multi-variable Ewing et al. sprawl index will exhibit a more significant and consistent relationship with air pollutant levels than less complex, single-variable sprawl indices. Finally, I expect that both scale and urban extent will significantly affect the degree of association between measures of urban form derived from spatial metrics and both the ambient concentration and annual average non-point emission of air pollutants. Specifically, spatial metrics-based measures of urban form (i.e. urban form factors) calculated at the metropolitan scale and low urban threshold are expected to exhibit a greater degree of association with levels of air pollution than those calculated at the megapolitan scale and high urban threshold. In summary, this dissertation addresses five primary hypotheses:

1) Urban areas with morphological features associated with higher levels of sprawl, as assessed using urban sprawl indices and spatial metrics-based urban form factors, are associated with higher non-point source emissions of the O_3 precursors VOCs and NOx, $PM_{2.5}$, PM_{10}, and CO_2.

2) Urban areas with morphological features associated with higher levels of sprawl, as assessed using urban sprawl indices and spatial metric-based urban form factors, are associated with higher ambient concentrations of O_3, $PM_{2.5}$, and PM_{10}.

3) Composite urban sprawl indices that incorporate multiple measures of urban form (i.e. Ewing et al. (2003)) have a higher degree of association with levels of air pollutants than indices that incorporate a single measure (e.g. Sutton (2003)).

4) Measures of urban form calculated at the low urban threshold will exhibit a higher degree of association with levels of air pollution than those calculated at the high urban threshold.

5) Measures of urban form calculated at metropolitan scale will exhibit a higher degree of association with levels of air pollution than those calculated at the megapolitan scale.

CHAPTER II

LITERATURE REVIEW

In order to evaluate the empirical relationships that may exist between urban form and air quality, it is necessary to first consider the chemical, spatial, and temporal properties of air pollutants, the different components of urban form and the methodologies employed in their operationalization and quantification, and the theoretical causal pathways that unite them. In the literature review that follows, properties of the four air pollutants ozone (O_3), fine particulate matter ($PM_{2.5}$), coarse particulate matter (PM_{10}), and carbon dioxide (CO_2) are reviewed in detail, followed by a discussion of urban form, including an historical overview of urban form in the United States, a review of the theoretical models used to describe and conceptualize urban morphology as it evolved over the 20^{th} century, and a description of some of the contemporary strategies and methodologies used to quantify urban form. The causal links between urban form and air quality, which provide the theoretical basis for this investigation, are explored in the final section of this chapter.

Effects of Air Pollution

As centers of transportation and industrial activity, urban areas are the progenitors of a wide variety of common air pollutants, including ozone (O_3), volatile organic compounds (VOCs), nitrogen oxides (NOx), carbon monoxide (CO), sulfur dioxide (SO_2), heavy metals, and particulate matter (PM2.5 and PM10) (Mayer 1999; Grimm 2008). These and other air pollutants may impair respiratory and cardiovascular function in humans, decrease productivity and growth among certain species of plants and degrade or disrupt entire ecosystems (Likens, Driscoll, and Buso 1996; Jerrett et al. 2009; USDA 2009). The World Health Organization (2007) estimates that exposure to outdoor air pollution is responsible for 865,000 premature deaths annually, primarily due to cardiopulmonary effects. These effects are especially acute among the elderly, the very young, and individuals with asthma and other respiratory problems (McConnell et al. 1999). Air pollution, particularly ground-level ozone, is estimated to reduce the net primary production of crops and other vegetation in the U.S. by 3 to 7 percent annually, costing the agricultural industry $3 to $6 billion each year (Murphy et al. 1999; Felzer et al. 2004). Acid rain, formed when SO_2 and NOx react with water vapor, oxygen, and other chemicals in the atmosphere, can cause significant long-term damage to many ecosystems, particularly freshwater lakes, rivers, and streams (Schindler 1988; EPA 2007).

In addition to local and regional concerns, anthropogenic air pollution is a global environmental issue. Urban areas contain a significant concentration of point and non-point sources of carbon dioxide (CO_2) and other greenhouse gases that contribute to

global climate change (Pataki et al. 2006). It is estimated that the 20 largest cities in the U.S. produce nearly five times more CO_2 annually than the United States can naturally assimilate (Luck et al. 2001). The net production of carbon from urban activities represents about 80 percent of all anthropogenic carbon emissions (O'Meara 1999). These emissions are expected to contribute greatly to the rise in average global temperature, which has the potential to significantly affect human and biological systems over the next century (IPCC 2007). A rise in global temperature of only a few degrees will likely force millions of coastal inhabitants to relocate due to sea level rise (Nicholls and Mimura 1998), alter many of Earth's natural ecosystems and biomes (Scholze et al. 2006), lower agricultural productivity in some areas, and intensify tropical cyclones and other extreme weather events (IPCC 2007). While global warming is expected to continue throughout the 21st century, significant reductions in greenhouse gas emissions can help moderate its impact (IPCC 2007).

Air Pollutant Properties and Trends

This dissertation focuses on CO_2 and three of the EPA's seven criteria air pollutants: O_3, $PM_{2.5}$ and PM_{10}. Although not historically regulated by the U.S. Clean Air Act, CO_2 is considered here as an air pollutant, pursuant to the U.S. Supreme Court finding in *Massachusetts v. Environmental Protection Agency* (2007) that CO_2 and other greenhouse gases "fit well within the Clean Air Act's capacious definition of air pollutant." The properties of these four air pollutants, including the nature of their formation, emission, and dispersal, dictate how and to what degree they affect people and the environment.

Ozone (O_3)

Ground-level ozone is a secondary air pollutant; it is not emitted directly, but forms in the atmosphere when nitrogen oxides (NO_x) and volatile organic compounds (VOC) react in the presence of sunlight (EPA 2010). Nitrogen oxides are released from a number of sources, most notably fossil fuel combustion, which is responsible for 40 percent of all NO_x emissions. The majority of nitrogen oxides are released in the form of NO; about 10 percent are released as NO_2 (Jenkin and Clemitshaw 2000). While NO_2 is a common O_3 precursor, it is also regulated by the EPA as a criteria air pollutant due to its adverse effects on respiratory function (Latza, Gerders and Bauer 2009) . VOCs, which include non-methane hydrocarbons (NMHCs) and carbonyl compounds, are a diverse group of chemicals emitted from a wide range of anthropogenic sources including fossil fuel combustion, paints and lacquers, cleaning supplies, pesticides, organic solvents, and air conditioning units. The majority of worldwide VOCs emissions, however, are from natural sources including vegetation, soil microbes and sea water (Kansal 2009).

The chemical pathways by which NO_x and VOCs may produce O_3 are numerous and complex. A general mechanism, however, has been described by Warneck (1988):

$$R_1CH_2R_2 + 3NO + 3O_2 \rightarrow 3NO_2 + R_1COR_2 + R_1`CHO + H_20 \quad (1)$$

$$NO_2 + hv \rightarrow NO + O_3 \quad (2)$$

where R_1 and R_2 are alkyl groups, and $R_1`$ is an alkyl group containing one less carbon atom than R_1. In this reaction, an n-alkane molecule is converted into one ketone and one

aldehyde, oxidizing three molecules of NO to NO_2. The photodissociation of NO_2 then produces a molecule of O_3 (Aneja, Adams and Arya 2000). Ozone may subsequently be destroyed by reacting with NO to form oxygen (O_2) and NO_2, or by undergoing photolysis, forming an oxygen atom (O) and an oxygen molecule (O_2) (Jenkin and Clemitshaw 2000): Warneck (1988):

$$O_3 + NO \rightarrow NO_2 + O_2 \text{ or} \quad (3)$$

$$O_3 + hv \rightarrow O + O_2 \quad (4)$$

Spatial and temporal variations in ambient ozone levels are sensitive to the relative abundance and distribution of VOCs and NOx, topography, and local meteorological conditions (Gao and Niemeier 2008; Rimetz-Planchon et al. 2008). The coupled reactions that create and destroy ozone in the troposphere help sustain a discernable diurnal and annual cycle in many locations (Seinfeld and Pandis 1997). Ozone is produced during the daytime hours when sunlight and NO_2 are plentiful, typically reaching highest concentrations around mid-to-late afternoon (Hubbard and Cobourn 1999; Rimetz-Planchon et al. 2008). Ozone concentrations may decrease by 50 percent or more overnight, often reaching their lowest levels between 5:00 and 8:00 AM. In addition to dispersal by wind, O_3 levels within dense urban centers may decrease substantially due to interaction with abundant NO from vehicle exhaust. In large metropolitan areas, these reactions are suspected to be main cause of the "ozone weekend effect" (OWE), in which O_3 levels are consistently lower on weekends, despite a

reduction in precursor emissions relative to weekdays (Sadanaga et al. 2008). The interaction between NO and O_3 may also have the effect of reducing O_3 levels in dense urban centers below those in surrounding suburbs. In addition to diurnal and weekly fluctuations, O_3 concentrations are generally highest during the summer months when high temperatures and abundant solar insolation help drive O_3 formation (Rimetz-Planchon et al. 2008).

Although O_3 forms readily in urban areas where precursor emissions from vehicle exhaust and other anthropogenic sources are abundant, elevated concentrations of O_3 are often widespread, covering significant portions of a region's suburban, exurban, and rural area (Liu and Rossini 1996; Bereitschaft 2008). In addition to mesoscale intra-urban transport, synoptic-scale dispersal between metropolitan areas and larger multi-state regions is common (Galvez 2007). Ozone levels above the EPA standard of 0.075 ppm, for example, were found throughout the Carolina Piedmont megapolitan (multi-metropolitan) area of North and South Carolina between 1999 and 2007 (Bereitschaft 2008). The most populous metropolitan area within the region, Charlotte, produced a discernable plum of elevated ozone levels that extended well into the nearby metropolitan areas of the Piedmont Triad and Research Triangle (Bereitschaft 2008). Elevated levels of ozone throughout the rural portions of the Carolina Piedmont indicate long-range transport and influx of O_3 and O_3 precursor emissions from the Mid-Atlantic, Ohio Valley, and Tennessee Valley (Aneja et al. 1999).

Ambient levels of tropospheric O_3, like many other pollutants, have steadily declined over the last three decades, in large part due to the various regulations imposed

by the Clean Air Act of 1963 and subsequent amendments (Smith 2009). Ozone concentrations nationwide decreased by 29 percent between 1980 and 1990, 16 percent between 1990 and 1999, and an additional 5 percent (one percent when adjusting for weather) between 2001 and 2007 (EPA 2008; Smith 2009). In 2007, however, 57 percent of all monitoring sites still recorded ozone levels above the new, stricter 8-hour ozone standard of 0.075 ppm (reduced from 0.080 ppm) imposed in 2008. Sites with the highest ozone levels between 2001 and 2007 were located in the vicinity of southern California, Atlanta, GA, Charlotte, NC, Philadelphia, PA and western Massachusetts (EPA 2008). It is within these regions that residents are most frequently exposed to unhealthy levels of ozone.

While ambient ozone concentrations within urban areas have generally declined over the last three decades, it is estimated that background levels of O_3 have risen by 0.5 to 2 percent per year (Vingarzan 2004). Background ozone refers to that proportion of the total ozone concentration "that is not attributed to anthropogenic sources of local origin" (Vingarzan 2004). Background ozone levels ranged from 19 to 33 ppb at six remote monitoring stations positioned around the world, between 1992 and 2001 (Vingarzan 2004). This is a considerable increase over measurements taken between 1876 and1910, which indicated 5 to 16 ppb in France (Volz and Kley 1988; Vingarzan 2004). It is believed that the increase in background levels of O_3 is primarily due to long-range transport of ozone and ozone precursors from populated areas, and in North America, from China in particular. Transport models have indicated that air pollution originating in Asia has increased the background levels in the U.S. by 3 – 10 ppb during the spring

months (Vingarzan 2004). Worldwide background levels of O_3 are expected to rise over the next century, potentially increasing to 35 – 48 ppb by 2040 (Vingarzan 2004); levels already reached in northern California (Oltmans et al. 2008)

Particulate Matter ($PM_{2.5}$ and PM_{10})

The term particulate matter (PM) refers to any small (typically < 10 μm) solid or liquid particle, or mixture of particles, suspended in air (EPA 2010b). There are two classes of particulate matter based on size: larger, coarse particulates with diameters between 2.5 and 10 μm (PM_{10}), and fine particulates with diameters less than 2.5 μm ($PM_{2.5}$). Particulates may be emitted from natural and anthropogenic sources as primary air pollutants, or form as secondary air pollutants in the atmosphere (EPA 2010b). While a single source may produce particles of varying sizes, PM_{10} is generally associated with mechanical generation, as dust, soil, soot and other debris are either released or resuspended by agricultural activity, road traffic, mining, construction, or biological activity (Laden et al. 2000). The finer particulates, $PM_{2.5}$, are emitted primarily from fossil fuel combustion (e.g. coal-fired power plants, vehicle exhaust), but may also include finely ground soil, dust and minerals (Harrison et al. 1997; Laden et al. 2000).

As with ozone, seasonal fluctuations in the concentration of PM_{10} and $PM_{2.5}$ are often apparent. In Switzerland, for example, the concentrations of both PM_{10} and $PM_{2.5}$ were highest during the winter months, with a slight rise observed in mid-to-late summer (Gehrig and Buchmann 2003). Thermal inversions, which are typically stronger and more frequent in winter, reduce vertical mixing thereby trapping particulates near the surface. The ratio of $PM_{2.5}$ to PM_{10} also exhibited a discernable seasonal variation throughout

Switzerland. The ratio was greatest in winter and lowest in spring, presumably due to the release of pollen and other PM_{10}-sized biogenic particulates (Gehrig and Buchmann 2003). Rather than a single peak, there were three elevated periods of PM_{10} observed in Dunkerque, France: spring, mid-summer, and mid-winter (Rimetz-Planchon et al. 2008). A similar pattern was observed for $PM_{2.5}$ in Hamilton, Ontario, with peak concentrations occurring in early spring, summer, and fall under inversion conditions (Wallace and Kanagolou 2009).

Diurnal and weekly fluctuations in PM concentrations have also been observed. Wallace and Kanagolou (2009) found a strong diurnal cycle for $PM_{2.5}$ at all three air monitors in Hamilton, Ontario. The two maximums were reached around 8 am and 8 pm, closely coinciding with peak traffic hours. This illustrates the sensitivity of ambient $PM_{2.5}$ levels to traffic volume; much of the finer particulates in urban areas originate from tailpipe exhaust, and therefore higher concentrations may be expected near busy roadways. The spatial sensitivity exhibited by $PM_{2.5}$ has also been observed for other "tailpipe pollutants" including CO and NO_2 (Liu, Chan and Jeng 1994; Nguyen and Kim 2006). As anticipated, a slight weekend effect was also observed for $PM_{2.5}$, with concentrations reaching their minimum on Saturday and Sunday, and their maximum on Wednesday (Wallace and Kanagolou 2009). A similar diurnal and weekly pattern was observed for PM_{10} throughout Switzerland, however the authors note that neither fluctuation was significantly different from average levels (Rimetz-Planchon et al. 2008).

Air quality standards for particulate matter in the U.S. have been in place since 1971, and the EPA has monitored PM_{10} since 1987, and $PM_{2.5}$ since 1997. A reduction in

industrial activities and the installation of pollution control devices such as smokestack scrubbers have reduced levels of PM_{10} by 31 percent between 1990 and 2008 and $PM_{2.5}$ by 19 percent between 2000 and 2008 (EPA 2009; Smith 2009). In 2006, the EPA revised their PM standards, lowering the acceptable $PM_{2.5}$ 24-hour standard from 65 to 35 $\mu g/m^3$. The PM_{10} standard of 150 $\mu g/m^3$ was revoked however due to insufficient evidence that PM10 adversely affects human health (EPA 2009).

Carbon Dioxide (CO_2)

Although ambient levels of carbon dioxide are not continuously monitored throughout the U.S. as O_3 and PM are, measurements indicate that the global atmospheric concentration of CO_2 has been rising at an exponential rate since the beginning of the industrial revolution in the late 1700s (Hofmann, Butler and Tans 2009). Charles Keeling of the Scripps Institution of Oceanography began recording ambient CO_2 levels at the Mauna Loa observatory in Hawaii in 1958, which now paired with NOAA measurements constitutes the longest-running record of ambient CO_2 levels (Keeling 1976; Tans 2010). The records at Mauna Loa indicate that CO_2 levels have risen from 316 ppm in 1959 to 387 ppm in 2009 (Tans 2010). The annual rate of increase has also grown from 0.5 – 1 ppm in the 1960s to 1.5 – 2.5 ppm since 2000. Climate models indicate that CO_2 may reach a concentration of 550 ppm by 2050; nearly double that of pre-industrial levels (IPCC 2009).

The rise in global CO_2 levels correlate strongly with an increase in CO_2 emissions over the last two centuries, primarily from anthropogenic sources (Hofmann, Butler and Tans 2009). Humans facilitate the annual release of 8.4 billion of tons of carbon dioxide

into the atmosphere, most notably by burning fossil fuels for transportation, electricity generation and industrial production, and removing forests that act as carbon sinks (Raupach et al. 2007). While CO_2 emissions from forest removal have leveled off in recent years, emissions due to fossil fuel combustion have continued to grow. The rate of increase in global CO2 emissions is evident among datasets from both the Energy Information Administration (EIA) and U.S. D.O.E. Carbon Dioxide Information and Analysis Center (CDIAC), which both estimated a growth rate of approximately 1 percent in the 1990s and over 3 percent from 2000 to 2005 (Raupach et al. 2007). Much of this increase has been fueled by burgeoning fossil fuel use among developing nations. As of 2009, China and the surrounding nations of Vietnam, North Korea, and Mongolia (a region termed "Centrally Planned Asia" or CPA by the CDIAC) emitted 1.72 billion metric tons of carbon, making CPA the leading CO_2 emitting region in the world. Carbon dioxide emissions in North America, about 90 percent of which are from the U.S., have decreased only slightly from a record high of 1.72 billion metric tons in 2005 (Boden, Marland and Andres 2009). About 40 percent of the emissions in North America are attributable to the transportation and residential sectors, which are concentrated in urban areas (Pataki et al 2006).

An Overview of Urban Form

Within the context of this dissertation, urban form refers to the two-dimensional spatial configuration and composition of urbanized landscapes. This includes, for example, the spatial distribution of buildings, people and infrastructure; the geometric pattern and density of roadways and other transportation corridors; the proportional

abundance of land uses; and the spatial adjacencies of urban patches (i.e. areas with urban development) and land uses. Urban form also has a three-dimensional component that can influence air quality at the micro-scale (e.g. the "street canyon" effect created by tall buildings) (Taseiko et al. 2009). However, because this study is concerned with macro-scale interactions, the three-dimensional micro-scale effects are not addressed. While the cumulative effects of micro-scale influences may be significant, their influence here is expected to be of such complexity that they warrant a separate investigation and are beyond the scope of this dissertation. In the following sections, the concept of macro-scale urban form is explored in greater detail by examining the history of urban form in the United States, and the various models and measurements used to conceptualize urban patterns.

A Brief History of Urban Form in the United States

The pattern of urban development that characterizes the American city is one primarily of two transportation eras: the first centered around pedestrian locomotion and the second around the automobile. As Patrick Condon (2008) aptly observed, "Fly over any North American metropolitan region and look out the window. Two different cities lie below." The first city, having been built prior to the mid-20th century, is one of contiguity, of connectivity between streets. The roads, whether perfectly straight or winding, form a contiguous matrix in which nearly any location can be reached along multiple routes. Automotive arteries are apparent, but interconnectivity of the street network precludes any one street from dominating the flow of traffic in any particular direction. Land uses are relatively interspersed with commercial and residential areas

sharing some blocks and not others. Most residents are within walking distance of shops, commercial offices, and transit stops that afford intra-city access (Duany, Plater-Zyberk and Speck 2000; Codon 2008).

While the American city has evolved considerably over the last 400 years, the urban pattern of the city described above shares much in common with the first European settlements. A number of early settlements, including New Amsterdam (New York) and Boston, adopted a distinctly medieval character with irregular, winding streets that are still apparent today (i.e. the Wall Street district in New York and the North End in Boston) (Gallion and Eisner 1986). Most towns in the New World, however, were surveyed in advance of settlement and exhibited a grid-like pattern of perpendicular streets and avenues. Williamsburg, Virginia, for example was laid out by the surveyor Theodorick Bland in 1632. The city was characterized by a central avenue running from the capital building in the east to the College of William and Mary in the west, and a number of smaller streets extending parallel or perpendicular to the main avenue. The city was further subdivided into individual residential parcels, each one-half acre in size. Williamsburg, designed for an initial population of about 2,000, exhibited a formal pattern, but was built such that "a human scale characterized the environment" (Gallion and Eisner 1986); no part of the city or countryside was beyond a kilometer or two walking distance (Reps 1965; Gallion and Eisner 1986).

Many other cities of the colonial period, such as Philadelphia and Savannah, also exhibited a pattern of formality and regularity with rectilinear street networks and purposefully situated parks and squares. Savannah in particular has been lauded as having

an especially well-coordinated design based on a series of interconnected neighborhoods or "cellular units" composed of twelve blocks, each surrounding a central square or park. John Reps (1965) suggested that this layout was particularly advantageous because it "provided not only an unusually attractive, convenient and intimate environment but also served as a practical device for allowing urban expansion without formless sprawl" (quoted in: Bacon 1974). Even those settlements that took on a more disorganized pattern, particularly in New England, were small in scale, limited in population, and intimately connected with the surrounding agrarian countryside (Reps 1965; Gallion and Eisner 1986).

With the dawn of the industrial revolution in American at the beginning of the 19th century, cities grew both in number and in population at an unprecedented rate. People migrated to the cities from the countryside and from abroad to work in factories and mills powered by the newly invented steam engine (Gallion and Eisner 1986). The number of cities with 8,000 or more inhabitants rose from just 6 in 1800 (Philadelphia, New York, Baltimore, Boston, Charleston and Salem) to 448 in 1890. The population of New York City grew from 62,500 in 1800 to 660,000 in 1850, and 2.7 million in 1890. Only London, with a population of 5 million in 1890, could claim more residents (Platt 2004). Recognizing that outward expansion was inevitable, a New York commission developed a plan in 1811 to divide up the remaining undeveloped area of Manhattan Island into a regular grid of rectangular city blocks. Although little open space was appropriated in the original plan, Central Park was later established in 1853 at significantly greater cost to the city (Gallion and Eisner 1986; Platt 2004).

The unprecedented urban growth in the early 19th century left many cities unprepared and ill-equipped to meet the basic needs of residents. Overcrowding, poor sanitation, and severely degraded air and water quality led to outbreaks of infectious diseases and a decline in life expectancy (Haines 2002; Platt 2004). Although various regulations and acts of redevelopment helped to mitigate the often deplorable conditions of the newly industrialized cities, many people chose to relocate beyond the city centers (Mumford 1961). First introduced to the United States in 1829, the steam locomotive began shuttling affluent commuters to and from the city by the 1840s (Muller 1995). Forty years later, the first electric street cars were replacing horse-drawn "horse cars" in most major cities (Gallion and Eisner 1986). With increasing speeds and declining fares, commuter trains and streetcars made it possible for large numbers of people to live outside the main city center while retaining reliable access to work opportunities and other urban amenities (Warner 1978; Muller 1995). New peripheral development, however, was primarily confined to linear corridors along transit lines, giving rise to the term "street-car suburb" and creating a regional "hub and spoke" pattern. These suburbs typically exhibited rectilinear street networks that later became extensions of the older city gridiron (Sanders and Rabuck 1946; Southworth and Ben-Joseph 2003).

As the 19th century came to a close, planned suburban communities were quickly becoming a standard component of the American urban landscape. While many street car suburbs were primarily residential, other planned communities, as inspired by Ebenezer Howard's Garden City concept, contained commercial and civic amenities (Gallion and Eisner 1986; Morris 2005). Industrial operations that had largely been confined to

railway hubs and waterfronts within the central city also began to expand into the urban periphery. At least two decades before the mass introduction of the automobile, commuter railroads, subways, streetcars, and interurban electric railways were already facilitating the dispersal of people and industry into the metropolitan countryside (Muller 1995; Muller 2001). Industrial towns (or "industrial suburbs") sprang up along railroad lines, perhaps ten or twenty miles beyond the expanding urban core where land was still relatively inexpensive (Muller 2001; Platt 2004). In Pittsburgh, PA, the outward migration of steel, glass, railroad equipment and coke industries produced an expansive metropolitan skeleton reaching 30 to 50 miles beyond downtown (Muller 2001).

Although the various urban transportation systems development during the 19th century allowed cities to expand outward as they continued to grow in population, development was still relatively clustered and confined within the extent of the metropolitan region. Most residents living within suburban corridors or nodes formed by linear rail lines were within a five to ten minute walking distance of the local transit depot and other daily amenities. Decentralization during this period was therefore largely constrained by the necessity to live within close proximity of a transit corridor. With the introduction of the automobile in the early 20th century, the metropolitan skeleton composed of linear street-car suburbs and peripheral industrial towns began to transform into a more disorganized patchwork of interspersed development (Sanders and Rabuck 1946; Muller1995).

The formation of the second city alluded to at the beginning of this section began in earnest prior to World War II, during the roaring decade of the 1920s. While both

automobiles and electric streetcars shared the roadways of many U.S. cities during the decade, personal transport was on the rise. Between 1910 and 1930, the number of registered vehicles rose from 500,000 to 23 million (Muller1995). With the creation of new roads and highways, the automobile allowed development to spread beyond the confines of the existing rail network. Intra-urban dispersal reduced population densities making it impractical to further extend electric streetcar and trolley-lines into newly developing areas. During the 1920s, suburban areas grew faster than the central city for the first time in history (Muller1995). The beginning of the Great Depression in 1929, however, would slow growth considerably until the end of World War II.

Perhaps just as revolutionary as the mass adoption of the automobile in terms of its effect on American urban form, was the advent of zoning. Although the first zoning code was adopted by New York City in 1909, zoning was not legally validated until 1926 by the U.S. Supreme Court ruling in *Village of Euclid vs. Ambler Realty Co.* (272 U.S. 365). Zoning allowed local governments to have considerable control over private land by regulating how and for what purpose land may be used. Although cumulative zoning allows for some mixing of land uses, the more widely-adopted non-cumulative zoning fully separates each class and sub-class of land use. Single-family residential zones, for example, are excluded from other uses deemed incompatible, including industrial, commercial, and even multi-unit residential housing (Platt 2004). Zoning therefore provided a legal basis for separating land uses into segregated single-use enclaves, such as the single-family suburban subdivisions and commercial strip-malls that would proliferate in the post-war years.

By the 1940's, many planning professionals believed the traditional layout of grid-streets and mixed land uses that characterized the pre-automotive era were antiquated, incompatible, and outright dangerous. Saunders and Rabuck (1946) provide an insight into these views when describing an illustration of traditional town planning:

> Convenient street arrangement for giving directions – dangerous for automobiles and pedestrians. Every intersection can be the scene of a smash-up. Signals… prevent accidents and traffic jams, but interrupt flow of traffic. To reach this school, many pupils must cross two heavily traveled streets. No convenient, centralized shopping center. Stores next to homes. Value of homes destroyed.

Traditional town planning – with a mix of land uses and an interconnected street network – was clearly falling out of favor due the perceived ills of congestion and incompatible uses. The solution, it seemed, was to further stretch the fabric of the urban landscape to better accommodate the automobile, which now, as in a positive-feedback loop, was in ever more demand due to the expanding suburban realm.

While the suburbs expanded rapidly following World War II, the geometric configuration and composition of the urban landscape was changing as well. Not only were land uses increasingly segregated and compartmentalized, but the layout of the street network evolved from a rectilinear grid to a hierarchical, dendritic system of roads, arterials, and limited-access freeways. Residential subdivisions filled with cul-de-sacs and dead-end streets were designed to "let you into, but not across, the neighborhood" (Condon 2008). This system of development was designed to isolate (primarily single-family) residential areas from other land uses and from the noisy and congested arterial streets of suburbia. As a result of this isolation and lack of physical, functional, or

aesthetic cohesion among developments, residents often choose to drive even when amenities are within walking distance (Morris 2005). The hierarchical street network also meant that traffic was funneled into a limited number of multi-lane arterial roads and freeways, increasing congestion and focusing commercial demand along major corridors and points of intersection (Muller 1995; Condon 2008).

On a larger scale, the metropolitan region was taking on a new, expanded morphology following the introduction of the Interstate Highway Act of 1956. The new interstate highways corridors not only connected the growing suburbs to the central city as rail had nearly a century before, but increasingly they encircled the expanding city, providing a rapid means of moving across town from one suburb to another (Muller 1995). New nodes of concentrated development began to occur along these corridors, especially where circumferential beltways intersected major highways radiating outward from the urban core. These suburban business districts (SBDs), some of which would evolve into the Edge Cities described by Joel Garreau (1992), eventually came to challenge the economic dominance of the older central business districts (CBDs) (Platt 2004). No longer did the majority of suburbanites have to commute to the central city, as employment centers became spread throughout the metropolitan area (Muller 1995). Thus, even as the American city became more dispersed, centers of development coalesced forming an increasingly polycentric metropolitan patchwork.

Models of Urban Form

As the spatial structure of urban areas have evolved over the last century, a number of models have been developed to explain and conceptualize these changing intra-urban land use patterns. Models developed in the early 20th century emphasized a monocentric or core-periphery urban form. In the land use model developed by Burgess (1925), the city is conceptualized as a series of five concentric zones radiating out from the CBD. The first and most central zone, which includes the CBD, is considered the heart of the region both in terms of commerce and culture. This first zone is also where all major transportation lines converge. The second zone contains a mix of residential, commercial and industrial areas. According to the Burgess model, this zone is typically occupied by low-income residents and is likely to contain slums and other blighted areas. The three outer rings of the city are exclusively residential, with high-income residents most likely to live in the two outermost rings. All development in the Burgess model occurs from the central city outward (Rhind and Hudson 1980; Mandal 1990).

Building on the Burgess model, Hoyt (1939) developed a sectoral conceptualization of urban form that considered direction as well as distance from the CBD. Hoyt observed that rent levels throughout 25 U.S. cities did not typically vary by concentric ring, but rather by sections radiating out from the central city. The general pattern suggested that sections of the city, like slices of a pie, contained more homogenous rent levels (and, presumably, land values) than those found among concentric circles. Hoyt further postulated that urban growth must occur from the center outwards along particular corridors or wedges. High-income residential areas, for

example, move successively outward from their initial location within the central city in a direction that maximizes their access to major transportation routes and recreational or scenic amenities such as water fronts, open countryside and commercial centers. Directional growth resulted in the sectoral partitioning of the city not only in terms of rents and land values but also land uses. Areas with high property values effectively exclude undesirable uses such as heavy industry from developing within that sector (Rhind and Hudson 1980; Kaplan, Wheeler and Holloway 2003).

While both the Burgess and Hoyt model conceptualized the city in terms of a single, monocentric urban core, Harris and Ullman (1945) envisioned a polycentric, or polynucleated, intra-urban structure in their multiple nuclei model. According to the model, the city is composed of a number of sections, each with its own functional specialization. Different land uses and economic activities tend to coalesce around the city center in no universal concentric order or direction, but rather assemble according to the complex interaction of four primary variables. First, many land uses require access to specialized facilities or locational amenities. Large retail shopping centers, for example, require access to major transportation routes. Second, some activities, such as those associated with the financial, insurance, and real estate industries (FIRE), benefit from agglomeration, and tend to cluster together in central locations. Third, the incompatibility of certain land uses, such as heavy industry and high-income residential housing, assures a certain degree of regional differentiation. Lastly, high land values preclude the development of all but a few land uses in certain locations (e.g. office buildings in CBDs or large retail outlets at major highway intersections). These nodes of largely

homogenous economic activity form either as the expanding city envelops surrounding settlements, or when new nodes develop in accordance with the variables discussed above. Thus, according to Harris and Ullman's (1945) model, the city does not simply grow outward from the CBD, but rather evolves from the complex integration and development of separate functional nuclei (Rhind and Hudson 1980; Pacione 2001; Kaplan, Wheeler and Holloway 2003).

Expanding on the multi nuclei hypothesis, Vance (1964) proposed the urban realms model, in which the city is composed of autonomous nuclei (or urban realms) largely independent of the traditional CBD or central city. Polynucleated belts of urban development, argued Vance (1977), formed over the previous century primarily due to the extrodinary growth in population and areal extent of cities, as well as the introduction and mass adoption of the automobile. The size, character, and structure of urban realms depend on four primary factors. First is the topography of the landscape. Mountains, water bodies, and other natural features can both direct the spread of urbanization and influence the type of development within an urban realm. The second factor is the size the metropolitan region, with larger urban areas tending to have larger, more numerous, and more differentiated urban realms. Third is the level and character of economic activity within each realm, and fourth is the layout of infrastructure and overall accessibility within and between realms (Pacione 2001; Lang and Knox 2009). Particularly important to intra-urban realm accessibility is the presence of major circumferential highways and other transportation corridors. In addition, airport connections allow urban realms to connect with other cities, providing additional

economic independence from the central city. As urban realms become more powerful, the core-periphery relationship begins to weaken, resulting in what Vance (1964) described as a "sympolis" rather than a metropolis (Lang 2003).

Despite changes in urban growth patterns, Lang and Knox (2008) argue that Vance's urban realm concept is still useful in describing the early-21st century metropolis. They provide the example of Greater Los Angeles, which contains a number of urban realms each with their own "subregional identities." These realms include South Coast (or Orange County), the Inland Empire (Riverside and San Bernardino Counties), and central Los Angeles. Lang and Hall (2008) propose that there exist four major types of urban realms based on unique social characteristics, built densities, and development age. First is the urban core realm, which includes the original central city and older 19th and 20th century development. The second type of urban realm is the favored quarter. These areas, dominated by wealthy residential neighborhoods, luxury shopping outlets, and high-end business districts, contain the most affluent segment of the metropolitan population. Third is the maturing suburban realm with late 20th-century and early 21st-century development. Infill development within the maturing suburban realm is continually expanding the edge of the metropolis. Finally, the fourth type of urban realm is composed of emerging exurban communities along the very fringe of the city. Punctuated by low-density, leap-frog development, these realms are not expected to become fully integrated with the main metropolitan development for several decades to come (Lang and Knox 2009).

White (1987) provided a revised Burgess model to reflect new social, economic, and political forces influencing urban growth. White envisioned late-20th century urban form as a complex patchwork of concentric zones, corridors, epicenters (i.e. nuclei or nodes) and enclaves. The CBD, though having maintained its position as the economic and cultural heart of most large cities, had become more specialized in finance and management as retail and other activities migrated to the suburbs. Surrounding the CBD is the zone of stagnation, which White argued suffers not only from lack of investment, but also slum clearance, highway construction and relocation of industry to more peripheral locations (Pacione 2001). At one time it was expected that the CBD would expand and revitalize the zone of stagnation, but in most cities the CBD has expanded up rather than out (White 1987).

Most of the remainder of the city from the zone of stagnation outward is composed of a patchwork of wealthy enclaves and (mostly poor) immigrant pockets held together by a spatially diffuse realm dominated by the middle class. Dotting the urban landscape are clusters of specialized activity, such as industrial parks, universities, and hospitals that can exert significant influence on local land use patterns. Finally, as standard among polycentric models, there are epicenters and corridors of economic activity along major transportation routes, especially where radial and circumferential highways intersect. These nuclei and corridors "form a latticework that extends over the entire urban region," that increasingly "challenge the hegemony of downtown" (White 1987).

A new model of urban structure developed by Lang and Knox (2009) moves up in scale and beyond the single metropolis. They argue that the expansion of metropolitan areas, and the transportation linkages that bind them, have given rise to larger trans-metropolitan urban agglomerations, termed megapolitan regions. To be classified as a megapolitan region, neighboring metropolitan areas must share at least 15 percent of new commuters from 1995 onward. Using this criteria, Lang and Knox (2009) have identified nine megapolitan areas in the U.S. The concept of the megapolitan region borrows from Pickard's (1970) urban regions, described as areas with "high concentrations of urban activities and [an] urbanized population," and Lewis' (1983) 'galactic metropolis,' which contains "varying sized urban centers, subcenters, and satellites [that are] fragmented and multimodal, with mixed densities" (Lang and Knox 2009).

The "glue" that unites multiple metropolitan areas into a single megapolitan region is the mid-exurban realm, composed of low-density and scattered 'edgeless cities' (Lang 2003), and micropolitan areas with smaller central cities of 10,000 to 50,000 residents. These inter-metropolitan corridors are home to a growing number of "extreme commuters" who travel 90 miles or more to reach work, forming overlapping commuter sheds (Naughton 2006). Together, metropolitan and micropolitan areas now cover more than half the land area in the conterminous U.S. (Lang and Dhavale 2006). In addition to overlapping commuter sheds, megapolitan regions also exhibit "distinctive economic, political and cultural profiles," often with a singular dominate industry and strong regional economic interdependencies (Lang and Knox 2009).

Megapolitan regions take on a variety of spatial forms. The two main types identified by Lang and Knox (2009) are the corridor megapolitans and the galactic megapolitans. Corridor megapolitans, such as the Phoenix-Tucson region, contain two or more metropolitan areas with central "anchor" cities between 75 and 150 miles apart. Development occurs in a primarily linear fashion along one more interstate highways connecting anchor metropolitan areas. Corridor megapolitans are distinct from metroplexes, which are slightly less extensive urban areas, such as Dallas-Ft. Worth or Washington-Baltimore, that contain two anchor cities within about 30 miles of one another and suburban areas that physically overlap. The larger galactic megapolitan region contains three or more metropolitan areas with central anchor cities at least 150 miles apart. These urban regions are connected by a web of interstate highways and a number of micropolitan areas and mid-exurban realms. The Piedmont megapolitan, which runs from Raleigh-Durham in the north to Atlanta in the south along I-85, and the Great Lakes Crescent megapolitan, which includes the cities of Chicago, Detroit and Pittsburg among others, are each considered galactic megapolitan regions. When two or more megapolitan regions are in close proximity, share a similar cultural and physical climate, and have extensive business linkages (e.g. Megalopolis in the Northeast and the Great Lakes Crescent, Sun Corridor and SoCal) they combine to form a "Megaplex" (Lang and Knox 2009).

Each of the aforementioned models reflects to a certain degree the form and processes of urban development at the time in which they were conceived. Taken together, they provide a more complete understanding of both the successive changes that

have occurred over time, and the current state of the American metropolis. As Rhind and Hudson (1980) suggest, "one consequence of the changing character of the processes giving rise to land use patterns is that any given pattern, analyzed at any point in time, reflects the joint effect of these varying processes." The complex spatial lineage that characterizes the modern American city emphasizes the layered nature of urban areas, with new growth and new patterns of development building upon, and being influenced by, those of the past.

Measuring Urban Form

During the last half of the 20th century, the areal spread of many urban areas in the United States and elsewhere significantly outpaced population growth (Fulton et al. 2001; Sutton 2003). Although peripheral urban growth is not an exclusively modern phenomenon (Mumford 1961; Bruegmann 2006), the rapidity and magnitude of suburban and exurban expansion among cities of both the developed and developing world over the last several decades is unprecedented (Alig, Kline, and Lichtenstein 2004; Bruegmann 2006). Characterized by low density, auto-dependent, decentralized and non-contiguous "leap-frog" development, many view this urban sprawl as the source of numerous urban-related problems in the U.S., and elsewhere (Ewing 1997; Bruekner 2000; Frumpkin 2002; Stone 2008). Some of the more adverse effects associated with urban sprawl include an increase in the cost of municipal utilities and services (Carruthers and Ulfarsson 2003), increased vehicle travel, commute times, and traffic fatalities (Ewing, Pendall, and Chen 2003), elevated obesity rates in children and adults (Ewing et al. 2003; Ewing et al. 2006), increased stormwater runoff (Stone and Bullen 2006), loss of prime

agricultural land and natural areas (Nelson 1999; Bengston 2005; Brown et al. 2005), and a decrease in air quality (Ewing 2003; Borrego 2006; Stone 2008). The recognition of these adverse effects, and the desire to better understand the nature and causes of sprawl, has arguably provided much of the impetus for quantifying urban form in recent years.

Sprawl Indices

Several sprawl indices have been developed to quantitatively assess and compare the level of sprawl between multiple urban areas. Nasser and Overberg of USA Today (2001) developed a simple sprawl index ranking 271 U.S. metropolitan areas according to the percentage of the metropolitan population residing in census-defined urban areas (UAs). The U.S. Census Bureau defines UAs as census blocks or block groups that contain at least 1,000 people per square mile and adjacent census blocks with an overall population density of at least 500 people per square mile. Nasser and Overberg (2001) calculated percent urbanized population for 1990 and 1999, then ranked MSAs from 1 (least sprawling) to 271 for both years. The overall sprawl score, with a potential range of 2 to 542, was obtained by adding the two rankings.

Among large metropolitan areas with populations over 1 million, Nasser and Overberg (2001) observed that the top 5 most sprawling MSAs were located in the South: Nashville, TN, Charlotte, NC, Greensboro, NC, Austin, TX, and Atlanta, GA. Large MSAs were least sprawling in the West, with large cities such as Salt Lake City, UT, San Francisco, CA, San Diego, CA, and Los Angeles, CA all having scores below 80. The authors suggest that, in addition to differences in government policies and growth management efforts, natural landscape features such as topography and proximity to large

water bodies, significantly affect the tendency of MSAs to sprawl. Los Angeles, for example, is geographically constrained by the Pacific Ocean to the west and mountains to the east, causing outward development to slow. Similarly, Las Vegas has exhibited relatively compact, contiguous growth due in part to the area's arid climate, which has forced new development to stay within reach of the city's municipal water lines. Many other cities, such as Atlanta, GA and Charlotte, NC, lack these physical constraints on outward expansion and have seen a significant decrease in metropolitan population density between1990 and 1999 (Nasser and Overberg 2001).

Lopez and Hynes (2003) developed a similar sprawl index. They suggest that residential density is the most significant component of urban sprawl, noting that "other aspects of sprawl are…to a certain extent…dependent on and driven by how and where people live." Accordingly, Lopez and Hynes' (2003) sprawl index score is based on the percentage of metropolitan area population (from census 2000) in high-density tracts (i.e., those with more than 3,500 persons per square mile) versus low-density tracts (i.e., those with between 3,500 and 200 persons per square mile). Rural census tracts, or those with less than 200 persons per square mile, were excluded from the analysis. Lopez and Hynes (2003) computed sprawl index scores for 330 metropolitan areas. The potential range of the index was 0 to 100, with 100 indicating low population densities and high levels sprawl, and 0 indicating high population densities and low levels of sprawl across the entire metropolitan area.

The actual sprawl index scores ranged from 3.94 in Jersey City, NJ to 100 in thirteen metropolitan areas, including Anniston, AL, Clarksville, TN, Decatur, AL,

Goldsboro, NC, and Florence, SC. The average score for the entire U.S. was 49, with the majority of metropolitan areas scoring above 50 (indicating a tendency toward low-density). An analysis of regional variations in sprawl score indicated that the West had the least-sprawling metropolitan areas, with the highest number of MSAs scoring less than 25, the highest percentage of residents living in high-density census tracts, and the most residents living in MSAs with scores below 50. In accordance with Nasser and Overberg (2001), southern metropolitan areas were found to exhibit the highest levels of sprawl, with 42 percent of MSAs scoring above 75. All thirteen MSAs with the highest possible sprawl score of 100 were located in the South (Lopez and Hynes 2003).

In addition to regional variations in levels of sprawl, Lopez and Hynes (2003) observed that the size of the metropolitan area was significantly related to its sprawl score. Low sprawl scores were much more common among the largest MSAs. Seven out of nine metropolitan areas with a sprawl score below 25 had populations greater than 1 million, while smaller MSAs, with populations less than 250,000, represented 95 of the 135 metropolitan areas scoring above 75. When comparing sprawl scores based on 2000 census data with those obtained using 1990 data, Lopez and Hynes (2003) found that the residential density of U.S. metropolitan areas declined overall, indicating that urban sprawl increased over the decade.

Rather than using census-defined urban area boundaries or census tracts, Sutton (2003) systematically defined the extent of urban areas using nighttime satellite imagery. The radiance levels of urban areas at night were used to create two urban boundaries: a high threshold based on higher radiance levels and containing more compact urban core

areas, and a low threshold based on lower radiance levels and containing more extended conurbations. Two regressions, one for each threshold, described the relationships between the natural log (LN) of residential population and the natural log of urban area (in sq. km) for 300 urban clusters. When the data were displayed using scatterplots, the regression line (termed the "Sprawl Line") represented the average relationship between population and areal extent (i.e. the average per capita land use consumption) for urban clusters in the United States. Cities above the sprawl line had higher than expected populations and lower levels of sprawl, while those below the line had lower than expected populations and higher levels of sprawl.

For each of the 300 urban clusters, Sutton (2003) evaluated urban sprawl using the percent positive or negative deviation from the average population-areal extent relationship. The percent deviations ranged from -150 percent (more sprawling) to +70 percent (less sprawling). Several trends emerged from a geographic analysis of the data. First, most urban areas along the coast were above the "Sprawl Line," having below average per capita land consumption. Houston, TX, was a notable exception to this pattern at -40 percent. In addition to forming a physical barrier to outward development, as suggested by Nasser and Overberg (2001), Sutton (2003) hypothesized that higher land values along the coast encouraged relatively compact development, lowering the average per capita land consumption of coastal communities. In agreement with both Nasser and Overberg (2001) and Lopez and Hynes (2003), Sutton (2003) also found that western cities generally had low levels of land use consumption relative to cities in the Midwest and Northeast. The large west-coast metropolitan areas of Los Angeles, San Francisco,

San Diego, Portland, and Seattle all fell above the "Sprawl Line," while the mid-western and inland cities of Dallas-Ft. Worth, Oklahoma City, St. Louis, Minneapolis-St. Paul and Atlanta fell below the "Sprawl Line." Finally, most cities were found to have lower per capita land consumption using the low urban threshold relative to the high urban threshold. This was expected since the low urban threshold included outer-suburban and exurban areas characterized by low-density development (Sutton 2003).

In a different approach to assessing urban sprawl via urban residential distribution, Burchfield et al. (2006) used remotely sensed land cover data to determine the percentage of undeveloped land within one square kilometer around each 30 meter cell of residential development within the conterminous U.S. Burchfield et al. (2006) hypothesized that the leapfrog residential development characteristic of sprawl could be quantified by measuring the degree to which residential dwellings are spatially aggregated. A one-kilometer grid cell was deemed an appropriate scale for the analyses because less than one percent of residential developments were more than one kilometer away from other residential developments in 1992.

A sprawl index score was calculated for 40 metropolitan areas by averaging the percent of undeveloped land within one kilometer of all residential grid cells within the metropolitan area. For 1991, the sprawl index scores ranged from a low of 20.73 in Miami, FL to high of 55.57 in Atlanta, GA. Between 1976 and 1992, the index scores for most metropolitan areas changed by two percentage points or less. The percent of open space within 1 kilometer of the average residential development increased slightly from 44.72 percent in 1976 to 47.64 percent in 1992. According to Burchfield et al.'s index,

the top 5 most sprawling metropolitan areas in the U.S., averaged between 1976 and 1992, are: Pittsburgh, PA, Atlanta, GA, Greensboro, NC, Washington-Baltimore, VA/ MD, and Rochester, NY. Although residential development became more scattered between 1976 and 1992 in the majority of metropolitan areas, some of the most "sprawling" MSAs, including Atlanta and Washington-Baltimore, actually exhibited less scattered residential development, while a few of the least sprawling MSAs, such as Miami and Dallas, exhibited more scattered residential development over the 16-year period.

Recognizing that sprawl is a complex spatial phenomenon, additional sprawl indices have been developed that incorporate multiple measures of urban form. One of the most comprehensive attempts at defining and measuring sprawl was undertaken by Galster et al. (2001). They produced a sprawl index based on six measures of urban form: density, concentration, clustering, centrality, nuclearity and proximity. Density referred to the average number of residential units and employees per square mile of developable land within each U.S. Census-defined Urban Area (UA). Three methods were used to operationalize concentration, defined as the degree to which housing and employment are aggregated or dispersed throughout the UA: 1) percentage of high-density grids within the UA, 2) the coefficient of variation of employees or housing units among grids of particular size within the UA, and 3) the delta index, or the proportion of residential units (or other land use) that would need to be relocated throughout the UA in order to achieve a uniform distribution (Massey and Denton 1988; Galster et al. 2001). The degree of clustering was calculated by averaging over all one-miles-square grids within each UA,

the standard deviation of density (either of housing units or employees) for four equal parcels within each grid. Centrality, or the degree to which a particular land use is in proximity to a UA central business district (CBD), was evaluated by taking the average distance of a particular land use from the CBD and calculating a centralization index (Massey and Denton 1988). Assessing nuclearity first involved a multi-step process in which nodes or nuclei of development were identified according to the aggregation of high-density one-mile-square grids. Nuclearity was then determined based on the total number of nodes and the proportion of employees or housing units within all nodes relative to the CBD. Lastly, a measure of proximity was determined using the weighted average distance between land uses (Galster et al. 2001).

Using a GIS and 1990 U.S. census block data, these six measures of urban form were applied to the pattern of residential development in 13 large U.S. urban areas. To standardize the data and weigh each measure equally, Z scores were computed for each of the six measures across all 13 urban areas. The composite sprawl index score was then calculated as the sum of the six Z scores for each urban area. The scores ranged from a high of 8.9 for New York (indicating low levels of sprawl) to -4.83 for Atlanta (indicating high levels of sprawl). Interestingly, Miami was the next most sprawling area with an index score of -4.11. This contradicts the findings of the four previously mentioned sprawl indices, each of which indicated that Miami had among the lowest levels of sprawl in the nation. Although the small sample size precluded a full regional analysis, Galster et al. (2001) note that the top four least sprawling cities, New York, Philadelphia, Chicago and Boston, are all cities located in the Northeast or Midwest with

older, relatively dense pre-20th century urban cores. Los Angeles ranked as the fifth least sprawling city with a composite Z score of 0.8. The authors agree with previous interpretations (Nasser and Overberg 2001; Sutton 2003), and suggest that the outward growth of Los Angeles, although built around automotive transport, has been limited by the arid climate and topography of the surrounding area.

Expanding on Galster et al.'s (2001) analysis, Ewing et al. (2002) developed a multi-variable sprawl index composed of four primary sprawl factors: residential density, land use mix, street accessibility, and degree of centering. Derived using principal components analysis, each of these factors is a composite of multiple variables. The residential density measure incorporates the variables gross population density, the proportion of the population living at high urban densities, the estimated density at the center of the metropolitan area, and the weighted density of population centers within the metropolitan area. The land use mix factor included six variables measuring the proximity of residential development to businesses and institutions, and the job-resident balance. The degree of centering was calculated based on the density gradient (the decline in density from the center of the urban area outwards), the percentage of the population within close proximity to the CBD, and the proportion of the population residing in urban centers or sub centers within the metropolitan area. The fourth sprawl factor, street accessibility, was determined from the average block length, average block area, and percentage of small blocks. Larger average block sizes indicate less interconnected road networks, which are associated with sprawling development patterns within urban areas. To allow comparison between the 83 metropolitan areas included in

the analysis, Ewing et al. (2002) rescaled each of the four factors to have a mean of 100 and standard deviation of 25. An overall sprawl score was calculated for each metropolitan area by summing the four sprawl factors and applying a transformation to account for metropolitan area size.

According to the Ewing et al. (2002) index, the southern cities of Knoxville, TN, Greenville-Spartanburg, SC, Greensboro—Winston -Salem—High Point, NC, Columbia, SC and Raleigh-Durham, NC had the lowest residential density. Raleigh-Durham also topped the list of the most sprawling metropolitan areas in terms of mixed use development, indicating a high level of land-use segregation. Other measures, however, indicated characteristics of sprawl among cities of other regions. Two western cities, Vallejo—Fairfield—Napa, CA and Riverside—San Bernardino, CA, were most sprawling in terms of centrality, while the northern cities of Rochester, NY and Syracuse, NY had the least connected road networks. The composite sprawl index indicated that Riverside, CA, with a score of 14.22, was the most sprawling metropolitan area in the U.S. Part of the larger "Inland Empire" urban realm of Los Angeles, Riverside received a poor score on all four measures of urban sprawl. More than 66 percent of Riverside residents lived more than 10 miles from a CBD (low centrality), while only 28 percent lived within one-half mile of a non-residential land use. Furthermore, less than one percent of Riverside's population could be effectively served by transit, and seventy percent of city blocks were larger than average (low street connectivity). The next four most sprawling MSAs according to the Ewing et al. (2002) were all located in the Southeast: Greensboro—Winston-Salem—High Point, NC, Raleigh—Durham, NC,

Atlanta, GA, and Greenville—Spartanburg, SC. The top five least sprawling MSAs were New York City, NY Jersey City, NJ, Providence, RI, San Francisco, CA and Honolulu, HI.

Spatial Metrics

Spatial metrics, or landscape metrics, were first developed in the 1980s within the field of landscape ecology to assess the link between landscape patterns and ecological processes (O'Neill et al. 1988; Herold, Goldstein, and Clarke 2003). Spatial metrics are algorithms used to quantify particular spatial attributes of land use patches, classes of patches, or entire landscape configurations. They are generally divided into two main categories: those that quantify the composition of landscapes independent of spatial attributes (i.e., the variety and abundance of land uses), and those that quantify the spatial configuration of landscapes (i.e., the arrangement, orientation, and shape of land use patches) (McGarigal and Marks 1995). Bhatta et al.(2010) further classified spatial metrics into seven groups: 1) area/density/edge metrics (e.g. patch density, edge density, largest patch index, landscape shape index), 2) shape metrics (e.g. shape index, fractal dimension), 3) contagion/ interspersion metrics (e.g. contagion index, clumpiness index), 4) contrast metrics (e.g. edge contrast index), 5) isolation/ proximity metrics (proximity index, similarity index), 6) core area metrics (e.g. core area index), and 7) diversity metrics (e.g. Shannon's evenness index, patch richness). This dissertation utilizes the first three groups of metrics, all of which measure spatial configuration rather than spatial attributes.

Although spatial metrics were originally applied primarily to natural landscapes, they have been increasingly used to quantify urban form and to describe the spatiotemporal characteristics of urban land use change (Luck and Wu 2002; Herold et al. 2003; Wei et al. 2006; Bhatta et al. 2010). Luck and Wu (2002) used spatial metrics to analyze changes in landscape pattern along a 165-kilometer urban- rural gradient in Phoenix, AZ. Seven landscape metrics were calculated using a 15x15 km^2 moving window for four land use types along the gradient: agriculture, desert, urban and residential. Patches of urban (i.e. commercial and industrial areas) and residential land uses exhibited distinctive changes along the urban-rural gradient. Patch density, or the number of patches per unit area, was relatively low out to 75 kilometers. Beyond this distance, however, both "urban" and residential land use patches became more disaggregated as indicated by a rise in patch density, a decrease in mean patch size, and an increase in the landscape shape index. The dramatic change in the value of these metrics around 75 kilometers marks a recognizable transition between the urban realm of Phoenix and the surrounding rural countryside (Luck and Wu 2002).

Herold et al. (2003) used remote sensing, spatial metrics, and spatial modeling to analyze the urban growth of the Santa Barbara area from 1929 to 2001, and to project future growth through 2030. Six spatial metrics (class area, edge density, mean nearest neighbor distance, number of patches, largest patch index, and area-weighted mean patch fractal dimension) were calculated for each of the four subareas of Santa Barbara (Santa Barbara, Summerland, Goleta and Carpinteria) for eight separate years for which remotely sensed data was available. This data was then used to calibrate the Slope,

Landcover, Exclusion, Urbanization, Transportation, and Hillshade (SLEUTH) urban growth model, and simulate both the historic and future growth of the Santa Barbara urban area.

The six spatial metrics indicated dramatic changes in the spatial configuration of urban patches between 1929 and 2001. The class area (CA) metric, a direct measure of the total amount of urban area, increased significantly in all four Santa Barbara subareas, with the greatest rate of increase between the mid-1950s and mid-1980s. The Santa Barbara subarea alone grew by about 30 square kilometers. The edge density and fractal dimension metrics, both of which measure shape complexity, also exhibited an overall increase for each subarea over the 72-year period. From the late 1960s to mid-1970s onward, however, urban shape complexity either leveled off or began to decline throughout the Santa Barbara region. Herold et al. (2003) suggested that this decline in shape complexity was the result of infill development connecting once scattered development to the older urban cores. The total number of urban patches increased for each subarea, except central Santa Barbara, which showed a decline after 1965. The authors contend that by 2001 central Santa Barbara was "nearly completely urbanized and … highly structurally compact" (Herold et al. 2003). Located between the Pacific Ocean to the south and the foothills of the Santa Ynez Mountains to the north, outward growth in and around central Santa Barbara was geographically restricted by the early 1970's, leading to an increase in infill development.

In an analysis similar to Luck and Wu (2002), Weng (2007) used four spatial metrics (percentage of landscape, Shannon's evenness index, patch density, and mean

patch size) to describe spatial and temporal changes in landscape pattern along a west-east transect in Dane County, WI from 1968 to 2002. Seven equally spaced sample plots 2500 ha in area were selected along a 60 kilometer transect. Three plots, located within the vicinity of Madison, WI, had a mostly urban or suburban character, while the remaining four were predominately rural. Weng (2007) identified five classes of land use for analysis: open water, built-up (i.e. commercial, industrial, institutional land use), residential, agriculture, and open land.

The spatial metrics indicated a positive relationship between urbanization and landscape fragmentation and diversity both at different locations along the urban-to-rural gradient and at various points in time. Shannon's evenness index (SHEI), which measures the proportion of different land use types within a landscape, was significantly higher among the three urban and suburban plots. This indicates that urban areas tend to have a more even mix of different land uses relative to rural areas, which are more likely to be dominated by a single land use type such as agriculture, pasture, or forest. Furthermore, between 1968 and 2000, SHEI increased the most for a plot just west of the city of Madison, reflecting the area's transformation from predominately rural to suburban. A similar pattern was observed for patch density with highest values among the urban and suburban plots. Patch density (PD) also increased among plots along Madison's urban fringe over the 30-year period, indicating the outward growth of the city and the corresponding increase in land use fragmentation. Mean patch size (MPS) further indicated greater fragmentation toward the urban core, with the smallest patch size found near the center of the city.

Although overall patch size declined toward the central city, Weng (2007) found that residential MPS was highest in the urban and suburban plots. Weng suggested that while urban areas are often highly heterogeneous and may appear fragmented when using an overall measure of MPS or SHEI, the "urban center [of] the landscape is dominated by a well-connected matrix of built-up and residential lands," leading to less fragmentation among certain urban land uses. This also provides an explanation as to why the highest degree of landscape diversity, as indicated by Shannon's evenness index, was measured for a suburban plot rather than the city center. Areas along the suburban fringe also underwent the most extensive transformation in land use configuration and composition over the 30-year period. Differences in spatial metric signatures along the urban-rural gradient may facilitate the identification of urban fringe areas where future development is most likely (Weng 2007).

Huang and Sellers (2007) systematically investigated variations in urban form among 77 metropolitan areas throughout the world using a measure of population density and six spatial metrics: shape index, fractal dimension, centrality, compactness index, compactness index of the largest urban patch, and ratio of open space. Hierarchical cluster analysis was used to divide the cities into four groups based on similarities in urban form. The first cluster, characterized by moderate levels of density, compactness, complexity, centrality and open space, was comprised mostly of Asian and South American cities with a few from Europe as well. The second and third groups were composed almost entirely of cities in the developing world. They had the highest levels of density and centrality, and the lowest levels of complexity and open space. Cities in

the fourth group, located primarily in North American and Australia, exhibited the lowest density and centrality but an average amount of open space. Most European cities also fell into this fourth group, along with the Japanese city of Osaka. Huang and Sellers (2007) conclude that the greatest difference in urban form exists not between different geographic regions, but between urban areas of the developing and developed world. This study and others (Luck and Wu 2002; Herold et al. 2003; Dietzel et al. 2005; Weng 2007) collectively demonstrate that spatial metrics can be used effectively to describe and compare the spatial and temporal patterns of urban landscapes.

Urban Form and Air Quality

There are several mechanisms by which the morphology of urban landscapes can affect air quality at the local and regional scale. Stone (2008) divided these mechanisms into two main groups: vehicle tailpipe emissions and local meteorology. Vehicle emissions, however may be incorporated into a broader category that includes all energy use influenced by urban morphology (i.e., energy use by transportation systems, buildings, and other equipment). Taken together, the effects of urban form on energy use and local meteorological conditions, such as the urban heat island effect, can significantly affect the quantity of emissions, transport of pollutants, and formation of tropospheric ozone and photochemical smog.

Energy Consumption

The morphology of urban areas influences the per capita energy consumption of transportation systems and buildings. Larivi`ere and Lafrance (1999) developed a statistical model to determine the relationship between per capita annual energy

consumption and population density among the 45 most populous cities in Qu´ebec, Canada. They found that higher-density cities consume less electricity per capita than lower-density cities. According to the model, a three-fold increase in population density would reduce electricity consumption per capita in residential, commercial and miscellaneous sectors by 7 percent. In a related study, Ewing and Rong (2008) used regression analysis to investigate the relationship between urban sprawl at the county level and residential energy consumption. Urban sprawl was determined using Ewing et al.'s (2003) county sprawl index, which is comprised of six variables that quantify urban residential density, street accessibility, and the clustering of development. The authors found that the average household would annually consume about 20 percent less energy (17,900 fewer BTUs) living in a compact county (i.e., counties with a sprawl score one standard deviation below the mean) compared with a sprawling county (i.e., counties with a sprawl score one standard deviation above the mean).

Ewing and Rong (2008) also proposed that urban form can affect residential energy use directly through electric transmission and distribution losses (T&D), and indirectly through housing stock (i.e., type and size of dwellings) and the formation of urban heat islands (UHIs). The urban heat island effect, explored later in detail, refers to the tendency of compact urban environments to be 1ºC to 3 ºC warmer on average than the surrounding countryside (Rosenfield et al. 1995). As a result, more energy is needed to cool urban buildings during the summer, but less in the winter. Although the overall effect of UHIs on annual energy consumption depends on local climate and geography, Ewing and Rong concluded that nationwide, households living in compact counties

would consume approximately 1.4 million fewer BTUs of energy than those living in sprawling counties.

The effect of housing stock on residential energy use is typically greater and more uniform than that of the urban heat island effect. Regardless of location, and primarily due to a greater surface to volume ratio, larger houses consume more energy than smaller ones and detached houses consume more energy than attached, multi-unit housing (e.g., apartment buildings, condominiums). Households living in single-family detached housing, for example, consume 54 percent more energy for heating and 26 percent more energy for cooling than comparable households in attached dwellings (Ewing and Rong 2008). Compact urban areas typically contain more multi-unit housing, resulting in lower overall residential energy consumption per capita. Although electricity is typically generated outside urban areas, the resultant emissions from fossil-fuel-based power plants can influence the air quality of entire regions, including that of nearby cities (Hao et al. 2007). The result is that the energy efficiency of urban structures, which represent about half of a city's energy budget, holds significant implications for both regional air quality and global climate change (Steemers 2003).

The impact of urban form on intra-urban travel, vehicle emissions, and the energy consumption of transportation systems is well documented (Newman and Kenworthy 1989; Larivi`ere and Lafrance 1999; EPA 2001; Ewing, Pendall, and Chen 2003; Borrego et al. 2006). Newman and Kenworthy (1989) observed that among 32 large international cities, per capita gasoline consumption has an inverse exponential relationship with

population density. A less significant negative correlation existed between gasoline consumption and levels of urban centralization, as measured by the proportion of jobs located within the city center. The authors suggested that the low density, scattered urban patterns typical of urban sprawl influence gasoline consumption by increasing the distance of individual vehicle trips, and limiting the viability of alternative modes of transportation, such as rail, walking and biking. Similar studies have demonstrated significant associations between different aspects of urban form, including density, centrality, and mixed land use, and various transportation outcomes, such as vehicle miles traveled (VMT) per capita, use of public transportation, vehicle ownership rates, and commute times (Frank and Pivo 1994; Ewing 2003; Handy, Cao, and Mokhtarian 2005). Dense urban areas with high levels of urban centrality and mixed use development are generally less vehicle dependent.

Attempting to link urban form and tailpipe emissions directly, Frank et al. (2000) used travel survey data to assess the impact of different land use configurations on both travel behavior and estimated vehicle emissions of carbon monoxide (CO), nitrogen oxides (NOx), and volatile organic compounds (VOC) in the Central Puget Sound Region of Washington state. Five independent variables, including household density, work tract employment density, block density (representing street connectivity), home employment density (representing mixed use), and distance to work were incorporated into three regression models, one for each pollutant. While controlling for household size, number of vehicles, and household income, emissions of all three pollutants decreased significantly with increasing household density and employment density, but increased

significantly with increasing distance to work. In addition, a significant negative correlation was observed between block density and NOx emissions. A non-significant positive relationship was also found between home employment density and VOC emissions (Frank et al. 2000). Grazi et al. (2008) performed a similar analysis to determine the effect of urban density on transportation-related CO_2 emissions. While CO_2 emissions from public transport modes increased slightly with increasing density due to a greater number of trips and longer trip distances, emissions from private vehicles decreased appreciably. The authors determined that a 20 percent increase in residential density was associated with a 15 percent decrease in vehicular emissions. These data suggest that certain aspects of urban form, especially density, can have significant impacts on travel behavior and the emission of transportation-related pollutants.

Meteorology and the UHI

The structure and composition of urban environments can significantly influence local and regional meteorology, primarily through the well documented urban heat island (UHI) effect (Oke 1987; Yague and Zurita 1991; Kolokotroni and Giridharan 2008; Rajasekar and Weng 2009). Relative to rural landscapes, a significant proportion of most urban areas are covered by impervious surfaces, such as roads, buildings, and other structures that absorb and conduct heat more effectively than natural, vegetated surfaces (Oke 1987; Carnahan and Larson 1990; Weng 2001). The thermal property of urban surfaces coupled with waste heat generated by vehicles, buildings, industry, and various urban activities results in urban areas experiencing higher temperatures than the surrounding landscape, especially at night and during the summer months (Juaregui 1997;

Rosenzweig et al. 2005). Urban morphology can influence the distribution and formation of UHIs by affecting the amount of waste heat produced by vehicles and buildings (i.e., through vehicle travel and building energy efficiencies). In addition, urban development, particularly non-contiguous urban sprawl, increases the spatial variability of surface air temperatures by creating a complex patchwork of anthropogenic and natural surfaces with varying thermal properties (Weng 2003). While the magnitude of the urban heat island effect may be lower in low-density urban areas relative to more compact urban areas, the spatial extent and variability of the UHI is expected to be greater (Brazel 2000; Streuker 2003).

The formation and concentration of many atmospheric pollutants are sensitive to temperature variations and other urban meteorological conditions that are affected by UHIs. The formation of ground-level ozone is particularly sensitive to increasing temperature (Kuntasal and Chang 1987; Cox and Chu 1996; Stone 2005). Using a model to assess ozone formation in the Atlanta metropolitan area, Taha and Bornstein (1999) found that an increase in urban temperature of 1.5ºC increased average urban ozone concentrations by 10 percent. Such a relationship is expected given that the photochemical reaction that produces O_3 from the precursor emissions NOx and VOCs is temperature dependent (Taha and Bornstein 1999). Ozone levels may also be indirectly affected by temperature; the amount of NOx and VOCs produced by local fossil-fuel-based power plants is dependent on energy demand (Grand and Finster 1999). During the summer months, air conditioning systems can increase electricity demand significantly. It has been estimated that electric demand in large U.S. cities increases by 2 to 4 percent for

every 1 ºC rise in temperature (Akbari 1992). The emission of VOCs from certain species of vegetation also increases in response to rising temperatures (Cardelino and Chameides 1990). Assessing various heat island mitigation strategies in Los Angeles, Rosenfeld et al. (1998) concluded that increasing the reflectivity of urban surfaces using cool pavements and green roofs, and planting "low-emitting" trees for shade and evapotranspirative cooling could reduce annual ozone exceedances by 12 percent.

Directly Linking Urban Form and Air Quality

While ample research has demonstrated that a significant relationship exists between urban form and various mechanisms that affect air quality, few have attempted to link the morphology of urban landscapes with ambient measures of specific air pollutants. Ewing et al. (2003) developed a sprawl index (discussed later in detail) based on four primary measures of urban form: density, land use mix, centeredness, and connectivity. The index was used to assess the associations between urban sprawl and various travel and transportation variables, including daily VMT per capita, average vehicles per household, percentage of commuters using public transportation, percentage of commuters walking to work, and mean journey-to-work time among others. Using multiple regression analysis, Ewing (2003) found that metropolitan areas with higher levels of sprawl were generally associated with more vehicles per household, increased daily VMT per capita (inversely correlated with density only), less public transportation use, and less pedestrian commuting. Demonstrating a direct association between urban form and air quality, Ewing then conducted additional regressions analyzing daily

maximum 8-hour ozone levels between 1990 and 1999 using four measures of urban form. Average maximum 8-hour ozone levels had a significant negative correlation with urban density when controlling for the demographic variables metropolitan area population, average household size, percentage of the population of working age, and per capita income. A significant positive correlation was also found between land use mix and the control variable metropolitan population. These findings indicated that urban areas characterized by greater levels of sprawl (i.e., lower density, and less mixed-use, centered development) generally had higher maximum ozone levels due, in part, to auto-centric transportation habits that resulted in higher per capita vehicle emissions.

Stone (2008) used Ewing's sprawl index to investigate further the direct associations between urban form and air quality among 45 of the 50 most populous urban areas in the U.S. To measure air quality, the average number of annual ozone exceedances rather than the fourth highest 8-hour ozone concentration (the EPA standard for ozone) were used. Stone suggested that number of annual ozone exceedances is a more appropriate measure of overall air quality because it represents an annual trend rather than a single event. For each metropolitan area, the number of annual ozone exceedances was averaged over a 13-year period from 1990 to 2002. To address the impact of climate on regional ozone formation, average ozone season (May through September) temperature was included as a control variable. Stone also controlled for metropolitan population, though unlike Ewing, he did not include additional demographic variables. Using ordinary least squares regression analysis, three sets of models were created. The first set of models addressed the relationship between urban form (i.e., the

four main components of Ewing's sprawl index as well as the overall index) and mean annual emissions of the ozone precursors NOx and VOC. The regression models indicated that only density was significantly associated with precursor emissions. As metropolitan population density increased, annual emissions of NOx and VOC decreased.

The second set of models developed by Stone (2008) tested the association that existed between the average number of annual ozone exceedances and urban form. The connectivity and density sprawl index measures were significantly negatively associated with the number of ozone exceedances at the five percent level of significance. The overall sprawl index was also positively correlated with the number of ozone exceedances. Additionally, for every one standard deviation increase in the sprawl index, the number of high ozone days in large U.S. metro areas increased by 6.6 days.

The third set of models addressed the hypothesis that urban form influences ozone levels through various mechanisms independent of precursor emissions. To test this hypothesis, the average annual precursor emissions were incorporated into the models as control variables. Once more, Stone (2008) found a significant negative association between ozone exceedances and both urban density and connectivity, and a significant positive association between ozone exceedances and the overall sprawl index. Stone suggested that at least two non-emissions-based mechanisms could account for this observed relationship between urban form and ozone formation: the urban heat island effect and the distribution of ozone monitors. Stone also observed that the most sprawling metro areas (those ranking in the top 75^{th} percentile) had, on average, 62% more ozone exceedances than the least sprawling cities (25^{th} percentile). These results clearly support

Ewing's findings, and further indicate that certain aspects of urban morphology may influence tropospheric ozone levels at the metropolitan scale when controlling for select climatic and demographic variables.

Although Ewing (2003) and Stone (2008) provide evidence for a direct link between quantitative measures of urban form and air quality, their research is limited in scope in two primary ways: 1) both use a single, though multivariate, urban sprawl index to characterize urban form and 2) both use tropospheric ozone as the only air quality measure. To elucidate the complex relationship that exists between urban form and air quality further, this dissertation will incorporate multiple measures of urban form and assess their association with several criteria air pollutants. In addition to sprawl indices, such as the one developed by Ewing, spatial metrics derived entirely from remotely sensed land use data will also be used to characterize urban form and relate urban form to multiple air pollutants at the metropolitan and megapolitan scale.

CHAPTER III

METHODOLOGY

Research Hypotheses

This dissertation research assesses the relationships between specific aspects of urban form and levels of air pollution among large urban areas in the United States. Evidence provided by Ewing et al. (2003), Stone (2008) and others (Newman and Kenworthy 1989; Rosenfeld et al. 1998; Larivi`ere and Lafrance 1999; Frank et al. 2000) suggest that cities characterized by more sprawl-like land use patterns (i.e. low density, discontiguous development) will exhibit higher levels of air pollution, primarily due to enhanced automotive dependency, reductions in building energy efficiencies, and effects on local meteorology such as the urban heat island effect. These studies indicate that strong and positive relationships exist between levels of tropospheric ozone and urban sprawl. Previously discussed mechanisms, including the notable link between urban form and the consumption of fossil fuels, suggest that similar significant associations may also exist for additional air pollutants. This serves as the basis for the first two hypotheses:

> H1: Urban areas with morphological features indicative of higher levels of sprawl will exhibit elevated emissions of the ozone (O_3) precursors volatile organic compounds (VOCs) and nitrogen oxides (NO_x), fine particulate matter ($PM_{2.5}$),

coarse particulate matter (PM_{10}), and the greenhouse gas carbon dioxide (CO_2).

H2: Urban areas with morphological features indicative of higher levels of sprawl will exhibit higher ambient concentrations of ozone (O_3), fine particulate matter ($PM_{2.5}$), and coarse particulate matter (PM_{10}).

Although the overall relationship between urban sprawl and levels of air pollution is expected to be strong and positive, it is likely that the degree of association between individual measures of urban form and levels of air pollution will vary considerably. Composite sprawl indices that incorporate multiple measures of urban form provide a more complete picture of the complex spatial configuration of urban areas, and should therefore exhibit a more significant degree of association with measures of air quality. Therefore, the third hypothesis states that:

H3: Composite sprawl indices, such as the one developed by Ewing et al. (2003), that incorporate multiple measures of urban form will have a higher degree of association with levels of air pollutants than either sprawl indices that incorporate a single measure or individual spatial metrics.

Under the assumption that urban sprawl always increases air pollution, all other factors being equal, this analysis can also be loosely interpreted as a rough test of how well a particular sprawl index or measure of urban form is able to capture one of the expected consequences of urban sprawl.

The degree of association between measures of urban form and air quality are also expected to vary due to the differing physical and chemical properties of air pollutants

and their relative susceptibility to changes in urban land use configurations. Fine particulates ($PM_{2.5}$) and coarse particulates (PM_{10}), for example, are both associated with vehicular traffic, which may be influenced by various aspects of urban form. Fine particulates from mobile sources, however, are primarily released in tailpipe exhaust as a product of fossil fuel combustion, whereas much of PM_{10} consists of non-exhaust mineral particles resuspended by moving vehicles and other activities (Duering et al. 2002). At the metropolitan scale, it is expected that exhaust and non-exhaust particulates will exhibit different patterns of dispersal with smaller exhaust particulates forming a wider and more homogenous distribution (Gehrig and Buchmann 2003). A large fraction of $PM_{10,}$ by contrast, is expected to exhibit heightened sensitivity to site-specific conditions rather than large-scale urban spatial patterns. Therefore, it is anticipated at the metropolitan scale that the associations between urban sprawl and levels of $PM_{2.5}$ will be greater than for PM_{10}.

The third and fourth hypotheses addressed by this investigation are that the scale (megapolitan vs. metropolitan) and extent (high vs. low threshold) of urban areas will significantly affect the degree of association between urban form measured using spatial metrics and levels of air pollutants. More specifically, it is expected that:

> H4: Measures of urban form calculated at the low urban threshold will exhibit a higher degree of association with levels of air pollution than those calculated at the high urban threshold.

The high urban threshold, which includes mostly contiguous urban and suburban development, represents a more conservative estimate of urban extent, while the low urban threshold includes a larger area that extends beyond most suburbs into the exurban and peri-urban realm. The outer rings of urban development with less street connectivity, greater distances between services, and fewer mass transit options (i.e. characteristics of sprawl), typically promote greater vehicle usage, resulting in higher emissions per capita. Therefore, the more comprehensive and inclusive model of urban form provided by the low urban threshold should exhibit stronger relationships with both emissions and ambient levels of air pollutants.

The effect of scale on the strength of association between urban form and air pollution is less certain. However, the spatial signature of megapolitan urban agglomerations are expected to vary significantly from metropolitan statistical areas (MSAs) and combined statistical areas (CSAs), both classified herein as "metropolitan-scale." Megapolitan areas are composed of more than one MSA or CSA and typically include micropolitan areas, a number of smaller urban cores, and substantial tracts of exurban and rural areas. The existence of multiple large urban cores makes megapolitan areas inherently polycentric. The functional connections between these nodes, including the degree to which commuter sheds overlap, are likely to be weaker than those within a single metropolitan area where either one urban core dominates (e.g. Miami, FL) or multiple cores are within close proximity (e.g. Dallas – Ft. Worth, TX). Diffusion of functional interdependency may undermine the effect of urban form on air quality at the megapolitan scale. Therefore, if a discernable difference does exist among spatial scales:

H5: Associations between levels of air pollution and urban form at the metropolitan scale will be greater than those observed at the megapolitan scale.

Study Area

Urban form and air quality were assessed for 86 metropolitan-scale areas (Figure 1) and 19 megapolitan areas (Figure 2) within the conterminous United States. The metropolitan-scale areas included 23 metropolitan statistical areas (MSAs) and 63 combined statistical areas (CSAs). According to the U.S. Office of Management and Budget (OMB), an MSA contains "at least one urbanized area of 50,000 or more population, plus adjacent territory that has a high degree of social and economic integration with the core as measured by commuting ties" (OMB 2008). Outlying counties are included in an MSA if 25 percent or more commuters commute to a central county (i.e. counties with a UA of 50,000 or more residents). Combined statistical areas include any combination of multiple adjacent metropolitan and micropolitan statistical areas (urban clusters with 10,000 to less than 50,000 residents) with an employment interchange of at least 15 percent. As of 2000, the 366 MSAs and 127 CSAs in the U.S. covered approximately 34 percent of the conterminous land area and contained about 83 percent of the population (GAO 2004).

Combined within a single list and ranked according to 2000 population, MSAs and CSAs with a population greater than 500,000 were selected for use in this study. Population ranged from a high of 21,361,797 in New York City, NY to 512,720 in Lafayette, LA. The total number of MSAs and CSAs was limited to 86 for two reasons.

First, this subset represents a relatively homogenous cohort of "large" metropolitan areas both in terms of population (i.e. > 500k pop.) and geographic area. As Ewing et al. (2003) observed, "Smaller metropolitan areas appear to be fundamentally different from large ones… They are more likely to be monocentric, for example, while large metropolitan areas are likely to be polycentric." Second, air quality data is more limited among smaller metropolitan areas. Even among large metropolitan areas, some air quality data – especially for PM_{10} – were not available for each year between 1998 and 2002.

To test the hypothesis that associations between urban form and air quality are more significant at the metropolitan level than at a larger regional scale, urban form and air quality data were also gathered for the 19 megapolitan areas identified by Lang (2006). Lang (2006) envisioned a hierarchy of urban areas based on scale that, listed from smallest to largest, included 1) metropolitan statistical areas (MSAs), 2) combined statistical areas (CSAs), 3) megapolitan areas, and 4) mega-regions. It should be noted that many large MSAs that are independent of CSAs (e.g. Phoenix, AZ and Miami, FL) are of roughly the same size and population as the average CSA. Megapolitan areas are defined by Lang (2006) as "Two or more metropolitan areas with principal anchor cities between 50 and 200 miles apart that will have an EIM of 15% by 2040 based on projection." EIM refers to employment interchange measure. Megapolitan areas are therefore differentiated from CSAs primarily in terms of scale (i.e. principal cities are generally < 50 miles apart within CSAs and > 50 miles apart within megapolitan areas) and degree of employment interchange (i.e. CSAs reached a 15 percent interchange in 2000 while megapolitan areas are projected to by 2040).

The size of megapolitan areas, while larger in population and area than most CSAs, vary considerably. Megapolitan areas range in size from 19,495 km^2 to 126,944 km^2, contain four to 70 counties, and are home to between 3.9 and 33.5 million residents (Lang 2006). As of 2005, about 61 percent of the U.S. population lived within megapolitan areas, which covered approximately 12 percent of the conterminous U.S. land area. Megapolitan areas have been further classified into 7 "mega-regions" based on spatial proximity and shared cultural, environmental, and economic linkages. Mega-regions currently represent the largest scale of urban agglomeration in the U.S. (Lang 2006).

Air Quality Data

Data regarding O_3, the O_3 precursors VOCs and NOx, $PM_{2.5}$, and PM_{10} were obtained from the U.S. Environmental Protection Agency's (EPA) online AirData database. The database includes air quality data from both the Air Quality System (AQS) and the National Emissions Inventory (NEI). The AQS provides annual summaries of ambient concentrations of seven criteria air pollutants (CO, NO_2, SO_2, O_3, $PM_{2.5}$, PM_{10}, Pb) and 188 hazardous air pollutants (HAPs) measured at thousands of monitoring stations across the U.S. The AQS also indicates the number of days per year ambient concentrations of criteria air pollutants are above EPA standards (i.e. number of exceedances). AQS data are available for the current year and ten previous years. The NEI includes estimates of annual emissions of five criteria air pollutants (CO, NO_x, SO_2, $PM_{2.5}$, and PM_{10}) and two criteria air pollutant precursors (VOCs and NH_3) from point, nonpoint, and mobile sources. Nonpoint and mobile emissions data are available at the

county level for the years 1990 through 2002, and point source emissions are available for the years 1996, 1999, and 2002. AirData allows users to query the AQS and NEI databases through a simple geographic interface at: http://www.epa.gov/oar/data/geosel.html.

Air quality data downloaded from the AirData database were imported into a GIS for processing. Annual ambient concentrations and number of annual exceedances were averaged for all monitoring stations within each metropolitan and megapolitan area over the 5-year period 1998 to 2002. Averaging the ambient concentration of air pollutants over multiple years should reduce the impact of annual fluctuations. In addition, this five-year period was specifically chosen to coincide with the majority of the urban form data, which were collected on or around the year 2000. Non-point emissions of VOCs, NOx, $PM_{2.5}$ and PM_{10} were averaged for all counties within each metropolitan and megapolitan area for the year 2000. A 5-year average was deemed unnecessary for emissions data due to minimal annual fluctuations. Point-emissions were consciously excluded from analysis as dependent variables because the sources of these emissions, mainly power generating facilities and large industrial operations, are not expected to be as strongly affected by urban form.

To investigate the potential impact of urban sprawl on climate change, estimations of county-level emissions of carbon dioxide for 2002 were obtained from the Vulcan Project (http://www.purdue.edu/eas/carbon/vulcan) at Purdue University. The Vulcan Project provides estimates of CO_2 emissions from both point and non-point sources at a

10x10 km resolution and by county. Total CO_2 emissions and on-road (i.e. mobile) CO_2 emissions were calculated for each metropolitan and megapolitan area by summing county-level emissions.

Urban Form Data

Sprawl Indices

Measures of urban form were obtained from two sources: 1) existing sprawl indices and 2) spatial metrics applied to remotely sensed landcover data. Sprawl indices have been developed to compare the level of urban sprawl among multiple urban areas based on quantitative measures of urban form. Six sprawl indices were originally selected for use in this dissertation. However, because Galster et al.'s (2001) index was applied to only 13 metropolitan areas, it was not possible to obtain statistically significant results using this index. Of the remaining five sprawl indices, three are based primarily on residential population density: Nasser and Overberg 2001; Lopez and Hynes 2003; and Sutton 2003. Sutton (2003) calculated two separate datasets, one measuring sprawl based on a high urban threshold and the other based on a low urban threshold, which are essentially two separate sprawl indices. The sprawl index developed by Burchfield et al. (2006), which measures the percentage of undeveloped land within one square kilometer of each 30 meter cell of residential development, is both a measure of urban contiguity and density of residential development. The sprawl index developed by Ewing et al. (2003) is a composite index that incorporates four dimensions of urban form: residential density, land use mix, degree of centering, and street accessibility. In addition to the overall sprawl index score, Ewing et al. (2003) provided a score for each of the four

dimensions of urban sprawl so that they may also be assessed separately. Among the many measures of urban sprawl that have been developed, the aforementioned indices were chosen for use in this investigation because they have each quantified urban sprawl for multiple metropolitan-scale urban areas in the U.S., providing a direct means of comparison.

The use of three sprawl indices that measure residential density may appear redundant or unnecessary. Each index, however, uses a different method of measuring this fundamental aspect of urban form. Nasser and Overberg (2001), for example, measured residential density as the percentage of the metropolitan population residing in census-defined urban areas (UAs), while Lopez and Hynes' sprawl index is based on the percentage of metropolitan area population in high-density tracts versus low-density tracts with rural tracts excluded. Sutton (2003) calculated residential density by first using nighttime satellite imagery to delineate two separate spatial extents for each urban area. By comparing the degree of association between these indices and measures of air quality, it is not only possible to assess the magnitude of these relationships, but also how sensitive they are to methodological differences. If residential density is indeed a powerful predictor of air quality when controlling for complicating factors, significant associations should exist for each measure of residential density. However, significant differences in association between indices and measures of air quality may also be indicative of a certain degree of methodological "inequity" in terms of each measure's ability to anticipate one of the expected real-world consequences of sprawl-like land use patterns. The sprawl index developed by Sutton (2003) has additional utility in discerning

whether differences in urban threshold affect the degree of association between metropolitan-scale population density and levels of air pollution.

Spatial Metrics: An Overview

In addition to pre-existing sprawl indices, nine spatial metrics were used to quantify urban form for 86 metropolitan-scale areas and 19 megapolitan regions in the U.S. Spatial metrics are particularly useful within the context of this investigation because they 1) provide a systematic and quantitative means of assessing various aspects of urban form among multiple urban areas, 2) can be used to assess and compare urban form among larger-scale megapolitan regions for which no other measure of urban form or urban sprawl have yet been developed, 3) provide a means of determining the effect of both scale and urban extent on measures of urban form and the relationships between urban form and air quality, and 4) are relatively easy to calculate and interpret.

Nine spatial metrics are used in this investigation: edge density (ED), largest patch index (LPI), area-weighted mean shape index (AWMSI), landscape shape index (LSI), area-weighted mean patch fractal dimension (AWMPFD), contagion (CONTAG), clumpiness index (CLUMPY), contiguity (CONTIG), and percentage of like adjacencies (PLADJ). Edge density measures the length of the border between urban and non-urban patches on a per hectare basis. As ED increases, urban patches become increasingly irregular and complex. A long urban-rural boundary may be indicative of abundant greenfield development along specific transportation corridors, as is typically observed among sprawling exurban areas (Herold et al. 2003).

$$ED = \frac{\sum_{k=1}^{m} e_{ik}}{A}(10{,}000) \quad (5)$$

Where e_{ik} is the total edge length (m) of class i (urban) in the landscape, and A is the total landscape area. The result is multiplied by 10,000 to convert to hectares.

Ranging in value from 0 to 100, the largest patch index (LPI) equals the proportion of the urban landscape that is comprised by the largest patch. LPI is commonly used as measure of fragmentation, however in urban landscapes it may also serve as basic proxy of urban nuclearity or polycentrism. A greater degree of polycentrism (and more fragmentation) should result in lower LPI values. This metric may be least indicative of urban sprawl, as neither monocentrism nor polycentrism is inherently more sprawl-like. The degree of polycentrism, however, is expected to affect inter- and intra-urban travel and other functional linkages that may in turn impact air quality. Furthermore, as a basic measure of urban fragmentation, LPI is expected to exhibit a strong positive correlation with PD.

$$LPI = \frac{\max_{j=1}^{n}(a_{ij})}{A}(100) \quad (6)$$

Where $\max(a_{ij})$ is the area (m^2) of the largest urban patch and A is the total landscape area (m^2). The result is multiplied by 100 to convert to a percentage.

The shape index (SHAPE) measures the shape complexity of urban patches by dividing total urban patch perimeter by the minimum perimeter needed to form a

maximally compact (i.e. circular) urban patch. The area-weighted mean shape index (AWMSI) provides a means of quantifying and comparing patch shape across multiple spatial scales by averaging the shape complexity (i.e. SHAPE) of all urban patches in the landscape and weighing patches according to size. This improves the accuracy of the overall measurement because the perimeter and areas of very small patches are highly influenced by image pixel size. AWMSI equals one for a maximally compact patch, and increases without limit as patches become more complex (McGarigal et al. 2002).

$$AWMSI = \sum_{i=1}^{m} \sum_{j=1}^{n} \left[\left(\frac{p_{ij}}{\min p_{ij}} \right) \left(\frac{a_{ij}}{A} \right) \right] \quad (7)$$

Where m is the number of patch types (2: urban and non-urban), n is the number of patches of a class, p_{ij} is the perimeter of patch ij (urban) measured in number of cell surfaces, min p_{ij} is the minimum perimeter possible for patch ij, and A is the total landscape area (m^2) (Gustafson 1998; McGarigal et al. 2002).

Similar to AWMSI, the area weighted mean patch fractal dimension (AWMPFD) measures the complexity of urban patch shape using a perimeter to area ratio that does not vary with size. Fractal dimension ranges between 1 and 2, with lower values associated with simple compact shapes like squares and rectangles, and higher values associated with complex, convoluted shapes (McGarigal et al. 2002). Urban areas often start as fairly compact, simple areas but spread outward over time creating complex and fragmented shapes as development sprawls across the available landscape. When infill development begins to occur, however, the shape of urban patches may become more

continuous and increasingly less complex, leading to lower AWMSI and AWMPFD values (Herold et al. 2003).

$$AWMPFD = \sum_{i=1}^{m} \sum_{j=1}^{n} \left[\left(\frac{2ln(0.25p_{ij})}{ln(a_{ij})} \right) \left(\frac{a_{ij}}{A} \right) \right] \quad (8)$$

Where m is the number of patch types (2: urban and non-urban), n is the number of patches of a class, p_{ij} is the perimeter (m) of patch ij (urban), a_{ij} is the area (m) of patch ij, and A is the total landscape area (m^2) (McGarigal et al. 2002; Herold et al. 2003).

The landscape shape index (LSI) equals the total length of urban patch edges divided by the minimum edge length possible for a single, maximally compact urban patch of the same size. The LSI is very similar to AWMSI, but is calculated at the class level (i.e. urban vs. non-urban landcover) over the entire landscape at once. AWMSI calculates a separate score for each urban patch and then averages these scores for the entire landscape. Like AWMSI, LSI equals zero for a maximally compact urban patch and increases without limit as urban patches become more disaggregated. A high degree of correlation is expected between AWMSI and LSI, although the two metrics may vary considerably for highly complex urban landscapes. High values of both AWMSI and LSI are expected to indicate higher levels of urban sprawl.

$$\text{LSI} = \frac{e_i}{\min e_i} \quad (9)$$

Where e_i is the total length of edge of class i (urban) measured in of number of cell surfaces, including all landscape boundary and background edge segments involving patch type I, and min e_i minimum total length of edge of class i measured in number of cell surfaces (McGarigal et al. 2002).

The clumpiness index (CLUMPY) provides a measure of urban patch aggregation. CLUMPY equals -1 when patches are maximally separated (i.e. a regular or uniform distribution), zero when patches are randomly distributed, and 1 when patches are maximally aggregated or clumped. Higher values of CLUMPY are likely to be associated with more compact, contiguous urban areas and lower levels of urban sprawl.

$$Given\ G_i = \left(\frac{g_{ii}}{(\sum_{k=1}^{m} g_{ik}) - \min e_i}\right)$$

$$CLUMPY = \left[\left[\frac{G_i - P_i}{P_i}\right]\right] for\ G_i < P_i < 0.5;\ else$$

$$CLUMPY = \left[\left[\frac{G_i - P_i}{1 - P_i}\right]\right] \quad (10)$$

Where g_{ii} is the number of like adjacencies between pixels of class i (urban) determined using the double-count method, g_{ik} is the number of adjacencies between pixels of class i and class k (non-urban), determined using the double-count method, min e_i is the minimum perimeter of a patch type i for a maximally

aggregated patch type, and P_i is the proportion of the landscape occupied by patch type i (McGarigal et al. 2002).

The contagion index is calculated at the landscape level (i.e. calculated from an average or aggregate of all landcover classes over the entire landscape, rather than a single class type). Contagion measures the fragmentation and heterogeneity of the urban landscape by determining the probability that a given urban pixel (30x30 meters) will share a border with another urban pixel. The contagion index therefore, is based on the adjacency of urban pixels rather than urban patches. Ranging in value from 0 to 100, CONTAG approaches zero when urban patches are highly disaggregated, and 100 when urban units are maximally aggregated. Urban landscapes are therefore more contiguous and homogenous when the contagion index is high, and more dispersed and heterogeneous when the contagion index is low (McGarigal et al. 2002; Herold et al. 2003). In a landscape composed solely of urban and non-urban patches, high CONTAG values should represent greater contiguity between urban patches and lower levels of urban sprawl.

$$CONTAG = \left[\frac{\sum_{i=1}^{m}\sum_{k=1}^{m}\left[(P_i)\left[\frac{g_{ik}}{\sum_{k=1}^{m} g_{ik}}\right]\right]*\left[ln(P_i)\left[\frac{g_{ik}}{\sum_{k=1}^{m} g_{ik}}\right]\right]}{2\ln(m)}\right](100) \quad (11)$$

Where P_i is the proportion of the landscape occupied by class i (urban), g_{ik} is the number of adjacencies between pixels of classes i and k (non-urban) determined

using the double-count method, and m is the number of patch types present in the landscape (m = 2) (McGarigal et al. 2002).

As its name implies, the contiguity index (CONTIG) is a measure of the average contiguity or spatial connectedness of urban pixels within an urban patch. A 3x3 pixel moving window is used to calculate a contiguity value for each pixel in which orthogonally contiguous pixels are weighted more heavily than diagonally contiguous pixels. The contiguity index is standardized to range from 0 to 1, with higher values corresponding to larger, more contiguous urban patches. As with CLUMPY and CONTAG, an increase in urban sprawl is expected to correlate with lower values of CONTIG.

$$CONTIG = \frac{\left[\frac{\sum_{r=1}^{x} c_{ijr}}{a_{ij}}\right] - 1}{v - 1} \quad (12)$$

Where c_{ijr} is the contiguity value for pixel r in patch ij, v is the sum of the values in a 3x3 moving window, and a_{ij} is the area of patch ij in terms of number of cells.

Finally, the percentage of like adjacencies (PLADJ) index measures the proportion of total pixel adjacencies that are between pixels of the same class (i.e. between urban pixels). Like CONTAG, PLADJ is calculated at the landscape level. The number of internal pixel adjacencies is tallied using the double-count method; adjacencies involving the landscape boundary, however, are counted once. PLADJ ranges from 0 to 100 with 0 corresponding to a landscape in which urban patches are maximally

disaggregated. This can only occur when each urban pixel constitutes a separate urban patch forming a checkerboard pattern in which there are no orthogonal like adjacencies. Given the tendency of urban land use to form contiguous "clumps," values of PLADJ are expected to be high (i.e. closer to the maximum value of 100) for all urban landscapes. This is also expected of other measures of urban "continuity" that use a similar value scale, most notably CONTIG and CLUMPY.

$$PLADJ = \left(\frac{g_{ii}}{\sum_{k=1}^{m} g_{ik}}\right)(100) \qquad (13)$$

Where g_{ii} is the number of like adjacencies between pixels of class i (urban) and g_{ik} is the number of adjacencies between pixels of class i and class k (non-urban), both determined using the double-count method.

Together, these nine spatial metrics characterize several important spatial attributes of urban sprawl, including urban fragmentation, contiguity, nuclearity, and shape complexity. Although some spatial metrics may measure similar spatial attributes, they each do so in a unique way (e.g. AMWSI and AWMPFD). While no single metric can quantify overall landscape pattern, combined they should provide a diverse, quantitative view of the urban sprawl phenomenon. The proceeding section outlines the procedure involved in calculating spatial metrics.

Calculating Spatial Metrics

The landcover dataset to which the spatial metrics were applied was produced by the Multi-Resolution Land Characteristics Consortium (MRLC). A joint initiative of the

EPA, USGS, NOAA and other federal agencies, the MRLC produces several Landsat-based landcover databases, including the National Land Cover Database (NLCD) used in this study. The NLCD, available for the years 1992 and 2001, is a 30-meter resolution dataset comprised of three primary layers: land cover, impervious surface and canopy density. The land cover data contains 16 land cover types classified using the Anderson Level II classification scheme (Anderson et al. 1976). Landcover data for all 50 states is available for download in 16 separate sections through the MRLC website: http://www.mrlc.gov/nlcd_multizone_map.php.

A GIS was used to first append the landcover data from 2001, creating a seamless landcover map of the conterminous U.S. The original 16 land cover types were reclassified into two categories: urban and non-urban. The urban category included four different land uses originally designated under the Anderson Level II classification scheme as developed: developed open space, low-intensity development, medium intensity development, and high intensity development. Urban classes were based on percent impervious surface area (e.g. urban open space contained less than 20 percent impervious surface area while urban high intensity contained greater than 80 impervious surface area). The non-urban land use category included all other classes (e.g. forest, wetlands, cropland, pasture land, open water). The reclassified data was then extracted into separate files using the metropolitan and county boundaries of each MSA/ CSA or megapolitan area. Metropolitan-scale and megapolitan areas were used to investigate potential differences in urban form that may exist at these two scales, and to determine how scale influences the relationships between urban form and air quality.

Within the county-based boundaries of most metropolitan and megapolitan areas is a considerable portion of rural land. To obtain a more accurate assessment of urban form, the extent of developed areas within these larger urban boundaries were systematically delineated. The use of administrative boundaries, such as the U.S. Census-defined Urban Areas (UAs), to determine the extent of urban development can be problematic. There are inconsistencies between census UAs and landcover maps derived from remotely sensed imagery, causing significant portions of developed land to extend beyond UA boundaries in some cases, while large tracts of rural land are included in others (Vogelmann, Sohl, and Howard 1998; Herold et al. 2003; Sutton 2003). As an alternative to UAs and other administrative boundaries, nighttime satellite imagery from the Defense Meteorological Satellite Program's Operational Linescan System (DMSP OLS) was used to determine the areal extent of urban areas within existing metropolitan and megapolitan area boundaries.

The DMSP OLS city lights data product depicts the intensity of city lights at night on a scale ranging from 0 to 63 (Figure 3). At the center of most large U.S. cities, the light intensity reaches the maximum value of 63, indicating a high concentration of bright lights. Toward the urban periphery, the light intensity value diminishes to a value between approximately 5 and 20. The challenge was to determine a light intensity threshold that would separate urban from non-urban (i.e. rural) areas. Due to the uncertainty involved in determining what is and is not urban, it was decided that two urban threshold should be used: a high threshold that includes a more limited urban extent composed of relatively continuous urban and suburban areas, and a low intensity

threshold that contains more extensive conurbations with intermittent exurban and peri-urban areas. The city lights data, the NLCD landcover product and other Landsat satellite imagery were layered within a GIS to determine by visual inspection the light intensity values that would best encapsulate the two urban thresholds. To make this determination at the appropriate scale, the Greensboro—Winston-Salem—High Point CSA (i.e. "The Triad") served as a case study (Figure 4). A light intensity value of 13 was chosen to demarcate the low urban threshold (i.e. light intensity values ≥ 13 were considered urban), while a light intensity value of 44 was chosen to demarcate the high urban threshold (i.e. light intensity values ≥ 44 were considered urban). Therefore, values less than 13 represent rural areas, values between 13 and 44 represent exurban and peri-urban areas, and values greater than 44 represent suburban and urban areas. The two urban thresholds were applied to the reclassified (i.e. urban and non-urban) NLCD landcover data to produce two separate urban landcover datasets for each metropolitan and megapolitan area. Figure 5 illustrates these two datasets for the Greensboro—Winston-Salem—High Point CSA. Nine spatial metrics were calculated for the two urban thresholds separately using the public domain software FRAGSTATS v. 3.3 (McGarigal et al. 2002).

Urban Form Factors

A correlation analysis revealed several significant correlations between the nine individual spatial metrics (Tables 1-4). Due to the high potential for multicollinearity among the spatial metric variables, principal component analysis (PCA) was used to

extract two separate sets of urban form factors: one set derived from the spatial metrics calculated at the high urban threshold, and one set derived from the spatial metrics calculated at the low urban threshold. PCA yielded two urban form factors at both the high urban threshold (Table 5) and low urban threshold (Table 6). With acceptably low levels of correlation among factors, the orthogonal Varimax rotation method was used on both sets to maximize the variance between loadings and improve interpretation.

The two urban form factors derived from PCA of the spatial metrics were classified as "continuity" and "shape complexity." The continuity factor appears to represent the spatial connectedness of urban land use, while shape complexity provides a measure of the "jaggedness" of the urban boundary (Longley and Mesev 2000; McGarigal et al. 2002; Huang, Lu and Sellers 2007). Spatial metrics that loaded high on the "continuity" factor included contagion, contiguity, percentage of like adjacencies, largest patch index, and the clumpiness index (Tables 5 and 6). Spatial metrics that loaded high on the "shape complexity" factor included area-weighted mean shape index, landscape shape index, area-weighted mean patch fractal dimension, and to lesser extent, edge density (Tables 5 and 6). Contagion loaded negatively under the factor "continuity" at the low urban threshold, but positively at the high urban threshold. Contagion represents the spatial continuity of both urban and non-urban patches in the landscape. Thus, overall landscape contagion may be low if either landcover class has low continuity. At the high urban threshold, contagion is largely determined by the urban landcover, but at the low urban threshold non-urban landcover exerts a much greater influence. This may explain the unexpected negative loading of contagion under urban

"continuity." Explaining 87 percent of the total variance found among the nine original spatial metrics calculated at the high urban threshold and 79.7 percent of the total variance at the low urban threshold, the urban continuity and shape complexity factors represent two vital spatial characteristics of urban landscapes that are expected to significantly affect transportation behaviors and thus vehicle emissions.

The procedure described above was repeated for spatial metrics calculated at the megapolitan scale. Principal component analysis yielded the two urban form factors "shape complexity" and "continuity" at both the high (Table 7) and low urban threshold (Table 8). Varimax rotation was again used to maximize the variance between loadings and improve interpretation. The two urban form factors accounted for 91.3 percent of the variance among the nine original spatial metrics at the high urban threshold and 75.3 percent of the variance at the low urban threshold. At both the high and low urban thresholds, the spatial metrics clumpiness index, contiguity, and percent of like adjacencies loaded high under the urban form factor "continuity," while area-weighted mean shape index and area-weighted mean patch fractal dimension loaded high under "shape complexity." Three additional spatial metrics loaded high at either the high or low urban threshold. At the high urban threshold, largest patch index loaded high under "continuity," while landscape shape index loaded high under "shape complexity." At the low urban threshold, edge density loaded high under "shape complexity." This indicates that the largest patch index, landscape shape index, and edge density are especially sensitive to changes in urban extent at the megapolitan scale.

Control Variables

Regional air quality is influenced by a number of factors not directly related to urban form. To more accurately assess the relationships between measures of urban form and air quality, it was necessary to control for confounding variables. Although the list of potential influences is extensive, seven control variables were selected as having strong theoretical or empirically-informed ties to air quality (Fitz-Simmons 2003; Elminir 2005; Camalier et al. 2007; Jacob and Winner 2009; Lai and Cheng 2009). These variables include population, population within 500 kilometers, point-source industrial emissions, metropolitan area (km^2), wind speed, and the two primary climatic variables temperature and moisture.

The relationship between the population of an urban area and air pollutant emissions is straight-forward: more people results in more cars, more buildings, greater energy use, and more pollution. However, because air pollution can disperse over great distances, it is also important to consider the population of the surrounding multi-state region. New York City, for example, is located near the center of the east coast Megalopolis; the largest near-continuous urban agglomeration in the U.S., stretching from Washington, D.C. to Boston, MA. New York is also due-east of the Great Lakes manufacturing belt. In this position, New York readily receives air pollution from surrounding population centers. By contrast, cities such as Denver, CO and Minneapolis-Saint Paul are relatively isolated, and thus less affected by external sources of urban air pollution. Therefore, to account for the influence of both local and regional population on local air pollution levels, local area population and population within a 500 kilometer

radius of each metropolitan and megapolitan area boundary were used as separate control variables. The 500 kilometer radii regional delineation is based on the observation that ozone concentrations are generally spatially coherent out to about 400 to 600 km, depending on the time scale (Porter et al. 1996; Rao et al. 1997). A similar pattern of spatial variation exists for PM_{10} and $PM_{2.5}$ (Fitz-Simmons 2003).

The area (km^2) of a metropolitan or megapolitan area can also influence the emission of air pollutants. All other factors equal, urban areas that extend over a larger geographic area are expected to produce more air pollution. It should be noted that some metropolitan and megapolitan areas are over- or under-bounded. Under-bounded cities are most common in the West (e.g. Los Angeles and Las Vegas) where counties are typically much larger than in the East. This limitation, however, is not expected to significantly undermine the utility of area as a control variable, as the effect of over- and under-bounding will likely mitigate one another at the national scale. While larger urban areas can be expected to produce more emissions in total, the geographic extent should not affect ambient pollutant concentrations at any specific location. Area will therefore be used as a control variable for pollutant emissions but not ambient concentrations.

Local climate and meteorological conditions can have a significant effect on the production, abundance, and distribution of air pollutants. The meteorological parameters wind speed, air temperature, relative humidity, precipitation, and synoptic weather events are all known to significantly affect air quality. While most meteorological parameters are measured directly, synoptic weather systems can be indirectly evaluated in part by measuring precipitation and cloud cover (Elminir 2005; Camalier, Cox and Dolwick

2007). Of particular relevance to this investigation are the impacts of meteorological parameters on levels of O_3 and PM. Studies have consistently shown that O_3 levels exhibit significant positive associations with temperature and significant negative associations with relative humidity (Elminir 2005; Ordonez et al. 2005; Camalier et al. 2007). In fact, Camalier et al. (2007) observed that up to 80 percent of the variance in O_3 levels in the eastern U.S. could be explained using only temperature and humidity as predictor variables. Abundant sunlight, high temperatures, and low humidity are conducive to the photochemical processes involved in the production of ozone. Temperature and humidity, however, may affect other pollutants differently. The ambient concentrations of PM_{10}, CO and SO_2, for example, all tend to decrease with increasing temperature, and increase with increasing humidity (Elminir 2005). Unlike temperature and humidity, wind speed tends affect all air pollutants similarly; an increase in wind speed generally results in greater dispersal and lower concentrations of air pollutants (Jacob and Winner 2009). Although wind direction can also affect air quality, its affect varies from place to place due to site-specific conditions. Precipitation events can have an immediate and significant effect on ambient air pollutant concentrations. As particles of rain, snow and sleet fall through the atmosphere they pick up a wide variety of gases and particulates through a process of "precipitation scavenging," resulting in the wet deposition of these materials (Davenport and Peters 1978; Naresh et al. 2007). Precipitation, cloud cover, and wind speed vary under the influence of cyclonic (low-pressure) and anti-cyclonic (high-pressure) weather systems, and can therefore provide

some measure of synoptic-scale weather patterns (Camalier et al. 2007; Lai and Cheng 2009).

To account for differences in climate and meteorology among metropolitan and megapolitan areas, PCA was used to create the two climate factors "temperature" and "moisture" from seven original meteorological parameters: average annual temperature, average maximum temperature, average annual precipitation, number of cloudy days, cooling degree days, heating degree days, and relative humidity (Tables 9 and 10). These parameters were specifically chosen for having either known direct or indirect influences on air quality. PCA was used in order to address the significant correlations between meteorological parameters at both the metropolitan and megapolitan scales. Average annual wind speed was not well represented by either the temperature or moisture factor, and was retained as a separate meteorological control variable at both scales.

Meteorological data was obtained from the National Oceanic and Atmospheric Administration's (NOAA) National Environmental Satellite, Data, and Information Service (http://ols.nndc.noaa.gov). All data are multi-year (or multi-decade) averages or "climatological normals." Data were averaged for all cities within each metropolitan or megapolitan area for which data were available. Heating degree days and cooling degree days are "used to estimate [the] amount of energy required to maintain comfortable indoor temperature levels [(65 F)]" and serve to account for the effect of fluctuating diurnal temperatures on energy use.

The seventh and final control variable accounts for variations in point-source industrial emissions of $PM_{2.5}$ and the O_3 precursors VOCs + NOx among urban areas.

Cities in the Northeast and Midwest regions (i.e. the "Frost Belt" and "Rust Belt") have historically had a larger industrial base than those in the South or West. While emissions from industrial point-sources reflect the economic character of urban areas, they are not expected to be significantly affected by urban form. Emissions from these sources must therefore be controlled for. Emissions from non-industrial point-sources, such as power plants, may be indirectly affected by urban form, and are therefore not included within this control variable. Descriptive statistics for all control variables are presented in Table 11.

Regression Models

Metropolitan Scale

Six sets of regression models, and 63 total models, were used to assess the degree of association between urban form (independent variable) and air quality (dependent variable) at the metropolitan scale. In the first two sets of regression models, the independent variables are urban form factors derived from the PCA of nine spatial metrics. The last four sets of regression models incorporate sprawl indices or sprawl index components (i.e. Ewing et al.'s four urban sprawl components: residential density, land use mix, street accessibility and degree of centering) as independent variables. Each set of regression models is described in detail below.

Urban Form Factor Models

1) In the first set of regression models, the independent variables are the urban form

factors “continuity” and “shape complexity,” derived from the nine spatial metrics calculated at the high and low urban threshold. The dependent variables include the ambient concentration of the three air pollutants $O_{3,}$ $PM_{2.5,}$ and PM_{10}. Six separate regression models were used to test the hypothesis that cities that exhibit greater continuity and lower levels of shape complexity among urban patches have lower ambient concentrations of $O_{3,}$ $PM_{2.5,}$ and PM_{10}. A separate model was developed for each of the three air pollutants and each of the two sets of urban form factors. Thus, in three models urban form factors 1 and 2 are derived from spatial metrics calculated at the high urban threshold, and in the other three they are derived from spatial metrics calculated at the low urban threshold. By comparing the results of these two model subsets, it is also possible to evaluate the third research hypothesis (H3) that the relationship between levels of air pollution and urban form are stronger when assessing urban form at the low urban threshold. All control variables except area are included in this set of regression models, as climate, wind speed, metropolitan population, regional population, and point-source industrial emissions can all impact the ground-level concentration of air pollutants.

$$Y = \beta_0 + \beta_1 X_1 + \beta_2 X_2 + \beta_3 X_3 + \beta_4 X_4 + \beta_5 X_5 + \beta_6 X_6 + \beta_7 X_7 + \beta_8 X_8 + e \quad (14)$$

Where:

Y = ambient concentration of O_3 or

= ambient concentration of $PM_{2.5}$ or

= ambient concentration of PM_{10};

X_1 = climate factor 1 (“temperature”);

X_2 = climate factor 2 (“moisture”);

X_3 = average annual wind speed (mph);

X_4 = population;

X_5 = population within 500 km;

X_6 = for O_3: point-source industrial emissions of VOCs and NOx or

= for $PM_{2.5}$: point-source industrial emissions of $PM_{2.5}$ or

= for PM_{10}: point-source industrial emissions of PM_{10};

X_7 = urban form factor 1 (“continuity”) and

X_8 = urban form factor 2 (“shape complexity”)

2) The second set of regression models tests the hypothesis that metropolitan areas with greater urban “continuity” and lower urban “shape complexity” (independent variables) are associated with lower non-point source emissions of the O_3 precursors NOx and VOCs, $PM_{2.5}$, PM_{10}, and “on-road” CO_2 (dependent variables). Non-point emissions are primarily from mobile sources, including automobiles, and should therefore be strongly affected by travel behavior and variables that affect travel behavior such as urban form. A total of eight regression models were used to assess these associations, two for each dependent variable. For each dependent variable, one model includes as independent variables the two urban form factors urban “continuity” and urban “shape complexity” calculated at the high urban threshold, and one model includes the two urban form factors

calculated at the low urban threshold. Because non-point source emissions are not expected to be significantly affected by wind speed, regional population, or point-source emissions, these control variables were not included in this set of regression models. Climate, metropolitan population, and metropolitan area size (km^2) however, affect energy use and both point- and non-point emissions, and are therefore included as control variables.

$$Y = \beta_0 + \beta_1 X_1 + \beta_2 X_2 + \beta_3 X_3 + \beta_4 X_4 + \beta_5 X_5 + \beta_6 X_6 + e \quad (15)$$

Where:

Y = non-point source VOCs + NOx emissions or
= non-point source $PM_{2.5}$ emissions or
= non-point source PM_{10} emissions or
= non-point source CO_2 "on-road" mobile emissions;

X_1 = climate factor 1 ("temperature");

X_2 = climate factor 2 ("moisture");

X_3 = population;

X_4 = geographic area (km^2);

X_5 = urban form factor 1 ("continuity") and

X_6 = urban form factor 2 ("shape complexity")

Urban Sprawl Index Models

3) Regression model sets three through six all contain as independent variables sprawl indices or sprawl index components. The third set of regression models test the degree of association between individual sprawl indices and the ambient concentrations of $O_{3,}$ $PM_{2.5,}$ and PM_{10}. As stated in the first research hypothesis, metropolitan areas with higher levels of sprawl should exhibit higher concentrations of air pollutants. Regression models in sets five and seven are also used to test the second research hypothesis (H2) that composite sprawl indices (i.e. Ewing et al. (2003)) that incorporate multiple measures of urban form are better predictors of air pollutant levels than sprawl indices that incorporate a single measure of urban form. Higher values indicate higher levels of urban sprawl for the sprawl indices Burchfield (2006), Lopez and Hynes (2003), and Nasser and Overberg (2001), while lower values indicate higher levels of urban sprawl for Ewing et al. (2003) and Sutton (2003). Due to high levels of collinearity, a separate regression model is run for each of the six sprawl indices.

$$Y = \beta_0 + \beta_1 X_1 + \beta_2 X_2 + \beta_3 X_3 + \beta_4 X_4 + \beta_5 X_5 + \beta_6 X_6 + \beta_7 X_7 + e \qquad (16)$$

Where:

Y = ambient concentration of O_3 or
= ambient concentration of $PM_{2.5}$ or
= ambient concentration of PM_{10};

X_1 = climate factor 1 (“temperature”);

X_2 = climate factor 2 (“moisture”);

X_3 = average annual wind speed (mph);

X_4 = population;

X_5 = population within 500 km;

X_6 = for O_3: point-source industrial emissions of VOCs and NOx or

= for $PM_{2.5}$: point-source industrial emissions of $PM_{2.5}$ or

= for PM_{10}: point-source industrial emissions of PM_{10} and

X_7 = sprawl index: Burchfield et al. (2006) or

= sprawl index: Ewing et al. (2003) or

= sprawl index: Lopez and Hynes (2003) or

= sprawl index: Nasser and Overberg (2001) or

= sprawl index: Sutton (2003) “high threshold” or

= sprawl index: Sutton (2003) “low threshold”

4) The fourth set of regression models incorporate as independent variables the four component urban sprawl measures of the Ewing et al. (2003) sprawl index. The three regression models in this set are used to assess the degree of association between the ambient concentration of O_3, $PM_{2.5}$, and PM_{10} and four specific spatial attributes of urban sprawl: residential density, land use mix, street accessibility, and degree of centering. By incorporating all four measures of urban sprawl within each of three regression models (one for each dependent variable), it is possible to evaluate the relative contribution of each attribute of urban form to changes in air pollutant concentrations. In a similar analysis, Stone (2008) used

separate regression models for each of the four components and found that residential density was most significantly associated with both O_3 precursor emissions and number of annual O_3 exceedances. With acceptable levels of collinearity among variables, however, it is appropriate to run these components together in a single model to a gain a more accurate picture of their specific relationships with air pollutant levels.

$$Y = \beta_0 + \beta_1 X_1 + \beta_2 X_2 + \beta_3 X_3 + \beta_4 X_4 + \beta_5 X_5 + \beta_6 X_6 + \beta_7 X_7 + \beta_8 X_8 + \beta_9 X_9 + \beta_{10} X_{10} + e \quad (17)$$

Where

Y = ambient concentration of O_3 or
= ambient concentration of $PM_{2.5}$ or
= ambient concentration of PM_{10};

X_1 = climate factor 1 (“temperature”);

X_2 = climate factor 2 (“moisture”);

X_3 = average annual wind speed (mph);

X_4 = population;

X_5 = population within 500 km;

X_6 = for O_3: point-source industrial emissions of VOCs and NOx or
= for $PM_{2.5}$: point-source industrial emissions of $PM_{2.5}$ or
= for PM_{10}: point-source industrial emissions of $PM_{10;}$

X_7 = residential density;

X_8 = land use mix;

X_9 = street accessibility; and

X_{10} = degree of centering

5) The fifth set of regression models tests the hypothesis that urban sprawl influences local air quality primarily by affecting non-point emissions. While non-point emissions are directly related to population, they are less influenced by meteorology, topography, and other environmental factors that significantly affect ambient concentrations. Therefore, a greater degree of association is expected between urban sprawl indices and air pollutant emissions than between sprawl indices and the ambient concentrations of air pollutants (regression set five).

$$Y = \beta_0 + \beta_1 X_1 + \beta_2 X_2 + \beta_3 X_3 + \beta_4 X_4 + \beta_5 X_5 + e \quad (18)$$

Where:

Y = non-point source VOCs + NOx emissions or

= non-point source $PM_{2.5}$ emissions or

= non-point source PM_{10} emissions or

= non-point source CO2 “on-road” mobile emissions;

X_1 = climate factor 1 (“temperature”);

X_2 = climate factor 2 (“moisture”);

X_3 = population;

X_4 = geographic area (km^2) and

X_5 = sprawl index: Burchfield et al. (2006) or

= sprawl index: Ewing et al. (2003) or

= sprawl index: Lopez and Hynes (2003) or

= sprawl index: Nasser and Overberg (2001) or

= sprawl index: Sutton (2003) "high threshold" or

= sprawl index: Sutton (2003) "low threshold"

6) The sixth and final set of regression models at the metropolitan scale are used to assess the degree of association between the four component urban sprawl measures of the Ewing et al. (2003) sprawl index and the non-point source emission of the O_3 precursors NOx and VOCs, $PM_{2.5}$, PM_{10}, and "on-road" CO_2. As with the composite Ewing et al. (2003) sprawl index, an increase in urban sprawl (i.e. lower sprawl scores) are expected to result in both higher emissions and higher ambient concentrations of air pollutants.

$$Y = \beta_0 + \beta_1 X_1 + \beta_2 X_2 + \beta_3 X_3 + \beta_4 X_4 + \beta_5 X_5 + \beta_6 X_6 + \beta_7 X_7 + \beta_8 X_8 + e \quad (19)$$

Where

Y = non-point source VOCs + NOx emissions or

= non-point source $PM_{2.5}$ emissions or

= non-point source PM_{10} emissions or

= non-point source CO_2 "on-road" mobile emissions;

X_1 = climate factor 1 ("temperature");

X_2 = climate factor 2 ("moisture");

X_3 = population;

X_4 = geographic area (km^2);

X_5 = residential density;

X_6 = land use mix;

X_7 = street accessibility; and

X_8 = degree of centering

Megapolitan Scale

Four sets of regression models, and 14 total models, were used to assess the degree of association between urban form (independent variable) and air quality (dependent variable) at the megapolitan scale. Only half the number of model sets was needed at the megapolitan scale because urban form was assessed solely using urban form factors derived from the PCA of nine spatial metrics. No sprawl indices have yet been calculated at the megapolitan scale. The regression models used at the megapolitan scale are identical in form to the first two sets of regression models described above at the metropolitan scale. Note that while the form of the models is the same, each variable was calculated anew at the megapolitan scale.

Study Limitations and Considerations

In accordance with Ewing (2003) and Stone (2008), this research will be limited in geographic scope to the United States. This is done in order to achieve a high level of consistency among both the air quality data and urban form data across multiple urban areas. In addition, the sprawl indices included in this dissertation have only been applied to American cities, and most are based on data only available through U.S. government agencies. Similar sources of data describing both urban attributes and air quality are

available in many other countries. An analysis of urban form and air quality involving urban areas of multiple countries is thus a possibility for future research, provided that limitations regarding data availability and consistency are overcome.

Several issues arise when using remote sensing and spatial metrics to quantify urban form. The NLCD landcover data does not differentiate between different types of urban landcover, such as residential, commercial, industrial, highways, roads, or public buildings. The lack of differentiation, especially between roads and buildings, may add considerable error to certain spatial metric calculations. For example, two spatially independent clusters of urban development may be counted as a single contiguous urban patch if connected by a road. This phenomenon is problematic in exurban and rural areas where roads connect independent patches. In urban areas, however, roads comprise an important and highly-integrated component of the urban fabric and should not be discounted. Therefore, the differentiation and elimination of roads would reduce error in exurban areas, but introduce new error in urban areas. In future studies, total error may be reduced by differentiating rural roads from urban roads and eliminating or designating rural roads as a non-urban land use. This could be achieved in future studies by abandoning the NLCD and performing an independent landcover classification for each metropolitan area under study. Note that the use of nighttime satellite imagery to delineate urban extent, as opposed to using metropolitan county-based boundaries only, should help minimize the "rural road" influence.

Another potential drawback of using the NLCD is that the land cover data was produced by seven mapping consortium partners over 66 individual mapping zones. Although standardized, a few mapping zones do appear to exhibit some differences. Urban patches, including roads, appeared especially fragmented among urban areas in mapping zones 47 and 60. Elevated fragmentation was reflected in abnormally high patch densities (PD) among cities in these two mapping zones, including New York, Philadelphia, Richmond, Norfolk and Washington-Baltimore in zone 60, and Cincinnati, Lexington, and Louisville in zone 47. Outliers beyond three standard deviations from the mean were not observed for any other spatial metrics, suggesting that PD alone was significantly affected. To reduce the error introduced by differences in urban patch fragmentation among mapping zones, PD was excluded from the analysis.

All spatial metrics are to some degree dependent upon the extent of the landscape. This issue is an example of the modifiable aerial unit problem (MAUP). The results of metric calculations can be dramatically altered by simply resizing or reshaping the landscape under study. It is therefore necessary to identify the scale most appropriate for this analysis. Wei (2007) observed that the landscape response to urbanization, as measured using spatial metrics, could be moderately identified at the county level, but only weakly at the city level. This indicates that similar analyses should be carried out at the metropolitan scale or higher for best results. Accordingly, nighttime satellite imagery in conjunction with county boundaries is used to systematically delineate urban areas at scales (metropolitan and megapolitan) appropriate for this analysis.

Although multiple control variables are used in each regression model, several confounding factors that can affect the ambient concentration and emission of air pollutants have not been accounted for. One notable factor is the influence of topography on the transportation and dispersal of air pollutants. Mountains can act as barriers to the movement of air pollutants, either "shielding" an urban area from external sources of pollution upwind, or trapping pollution over an urban area that would have otherwise dispersed downwind. In either scenario, the ambient concentration of airborne pollutants will be significantly affected by the elevation, orientation, and spatial extent of nearby mountain ranges. In order to effectively control for topography, each of these characteristics must be estimated for each urban area in close proximity of a mountain range. The addition of multiple topographic control variables to each regression model, however, was deemed unfavorable or unnecessary because 1) the vast majority of metropolitan areas are not in close proximity to a mountain range, 2) air pollutant levels are averaged over a wide area, which would include both the upwind and downwind sections of urban areas such as Los Angeles, and 3) additional variables would reduce the statistical power of the regression models.

CHAPTER IV

RESULTS AND DISCUSSION

Geographic Overview: Air Quality

Non-Point Source Emissions

Estimates of the non-point source emissions of the O_3 precursors VOCs and NOx, $PM_{2.5}$, PM_{10} and CO_2 are reported here by county and by MSA/ CSA. First, a county-level analysis provides an overview of non-point source emissions throughout the U.S. The four air pollutants exhibit a similar geographic pattern, with the greatest total non-point source emissions in either populated counties or those that are especially large in area (i.e. Western counties) (Figures 6-9). This demonstrates the need to control for population and geographic area when assessing the relationships between urban form and air quality. The spatial distribution of emissions can also be evaluated by controlling for either geographic area ("emission density") or population (emissions per capita).

When controlling for geographic area (km^2), non-point source emissions were highest among populated counties (Figures 10-13). New York County, the most populous county in the U.S., had the highest non-point source emission density of the O_3 precursors VOCs and NOx (1,070 tons/ km^2), $PM_{2.5}$ (47.8 tons/ km^2) and on-road CO_2 (23,089 tons/ km^2), and the second highest emission density of PM_{10} (102 tons/ km^2).

In contrast to emission density, less populated counties generally had the highest non-point source emissions per capita (Figures 14-17). This may reflect in part the use of agricultural machinery and other equipment found primarily in rural areas. Urban residents are also expected to drive less and use less energy per capita relative to their rural and suburban/ exurban counterparts, reducing fossil-fuel based emissions per capita (Frank and Pivo 1994; Frank et al. 2000).

At the metropolitan scale, total non-point source emissions were also highest among the most populated MSAs and CSAs, where anthropogenic activity is most highly concentrated. The greatest quantity of O_3 precursors (VOCs + NOx) (1,290,381 tons) and $PM_{2.5}$ (110,608 tons) from non-point sources, for example, originated from the New York-Newark-Bridgeport CSA, the most populous urban agglomeration in the U.S. Known for its dense network of interstate highways and pervasive car culture, the Los Angeles-Long Beach-Riverside CSA had the highest on-road emission of CO_2 (≈ 37 million tons). The Dallas-Ft. Worth CSA, the ninth most populous metro area in the U.S. in 2000, emitted the greatest quantity of PM_{10} (374,034 tons) from non-point sources.

Emission density was significantly lower for metropolitan-scale areas, which typically include both rural and urban counties. In addition, some of the most populous metropolitan-scale areas, including Los Angeles, contain significant tracts of rural land, reducing emission density significantly. Due to its moderate geographic area and large population, the New York-Newark-Bridgeport CSA had the highest non-point source emission density of O_3 precursors (VOCs + NOx) (39.4 tons/ km^2), $PM_{2.5}$ (3.37 tons/ km^2) and on-road CO_2 (801 tons/ km^2). McAllen-Edinburg-Pharr, TX had the highest

non-point source emission density of PM_{10} (15.7 tons/ km^2), followed by three other Texas metros: Houston, Dallas-Ft. Worth, and Austin.

Similar to the county level, non-point source emissions per capita were generally lowest among the most populous metropolitan-scale areas. The per capita emission of air pollutants from non-point sources also exhibited some regional variation. Three of the four metropolitan-scale areas with the highest non-point source emissions of O_3 precursors were located along the Gulf Coast: Baton Rouge, LA (155 tons), Mobile, AL (144 tons), and New Orleans, LA (121 tons). The per capita non-point source emission of $PM_{2.5}$ and PM_{10} also exhibited limited regional clustering, with the highest values occurring generally in the South and Midwest. In addition, six of the top 10 metropolitan-scale areas in terms of per capita on-road CO_2 emissions were located in the South. An analysis of variance (ANOVA) confirmed that out of four major U.S. regions (Northeast, Midwest, South, West) (Figure 18), metropolitan-scale areas in the South had higher O_3 precursor emissions per capita ($\bar{x}$ = 98.6 tons) than any other region, and significantly higher emissions relative to the Northeast ($\bar{x}$ = 79.4 tons). Furthermore, per capita PM_{10} emissions were highest among metropolitan-scale areas in the Midwest ($\bar{x}$ = 58.4 tons), and were significantly higher in the Midwest than the Northeast ($\bar{x}$ = 28.9 tons).

Point v. Non-Point Source Emissions

Although this investigation focuses specifically on the relationships between urban form and the non-point source emission of air pollutants, both point and non-point source emissions can contribute significantly to ambient concentrations, and therefore the magnitude and spatial distribution of point sources must also be considered. Some point-

sources may be affected indirectly by urban form (e.g. fossil-fuel-based power plants), while others may have a very weak connection to urban form or none at all (e.g. industrial operations). The ratio of point source to non-point (primarily mobile) source emissions can therefore provide some indication as to the degree to which urban form is capable of affecting air quality within each metropolitan area. The ambient concentration of air pollutants may be less attributable to differences in urban form among metropolitan areas with a significant proportion of total emissions from point sources relative to those with emissions primarily from non-point sources.

For all but one of the 86 metropolitan-scale areas included in this study, the majority of O_3 precursor (VOCs + NOx), $PM_{2.5}$ and PM_{10} emissions originated from non-point sources. The proportion of total emissions from non-point sources ranged from 53 percent in San Diego, CA to about 90 percent in Albany, NY for O_3 precursors ($\bar{x}$ = 81 percent), from 47 percent in Pittsburgh, PA to 99 percent in Albuquerque, NM for $PM_{2.5}$ ($\bar{x}$ = 82 percent), and from 56 percent in Jacksonville, FL to near 100 percent in Albuquerque, NM for PM_{10} ($\bar{x}$ = 91 percent). In general, cities with high levels of industrial activity, such as Pittsburgh, PA, Cincinnati, OH, Chicago, IL, Birmingham, AL, and Houston, TX had a lower proportion of total emissions from non-point sources. Likewise, cities with less heavy industry (and fewer industrial emissions), such as Albuquerque, NM, McAllen, TX, San Diego, CA, Syracuse, NY, and Fresno, CA, had a higher percentage of total emissions from non-point sources. The ambient concentration of air pollutants in cities with less heavy industry may therefore be influenced to a greater extent by urban morphology than those with more. In the regression models used to

evaluate the association between urban form and air quality (results presented later in the chapter), the control variable "industrial emissions" helps to account for this variation among metropolitan and megapolitan areas.

A similar relationship was also observed for CO_2, which was evaluated in terms of on-road sources; a sub-group of non-point sources emissions that do not include buildings and non-vehicular modes of transportation (i.e. airplanes, ships, rail, etc.). The proportion of total CO_2 emissions from non-point on-road sources ranged from five percent in Baton Rouge, LA to 53 percent in Jackson, MS ($\bar{x}$ = 33 percent). The top five metros with the highest proportion of total CO_2 emissions from on-road (primarily vehicular) sources also included Seattle, WA (53 percent), Harrisburg, PA (53 percent), Phoenix, AZ (53 percent), and Albuquerque, NM (49 percent). The five metros with the lowest proportion of total CO_2 emissions from on-road sources also included Allentown, PA (9 percent), New Orleans, LA (9 percent), Mobile, AL (13 percent), and Birmingham, AL. Interestingly, New York, NY (36 percent) had a greater proportion of total CO_2 emissions from on-road sources than cities such as Atlanta, GA (33 percent) and Washington-Baltimore (35 percent), well known for having extensive auto-centric suburbs.

Ambient Concentrations

The ambient concentration of both O_3 (Figure 19 and 20) and $PM_{2.5}$ (Figure 21 and 22) exhibited a strong regional pattern with the highest concentrations of both pollutants generally occurring within central and southern California and across the eastern portion of the United States. The concentration of PM_{10}, however, was much less regionalized, with both high and low concentrations scattered throughout the country

(Figure 23 and 24). Furthermore, while the concentrations of O_3 and $PM_{2.5}$ were highest in and around major urban centers, elevated levels of PM_{10} were found in many rural locations as well. The weaker spatial correlation between PM_{10} concentrations and urbanity reflects the nature of coarse particulates, a substantial portion of which is produced by non-urban activities such as agriculture and natural processes (e.g. soot from forest fires, suspension of soil and mineral matter) (Laden 2000). Descriptive statistics for both pollutant concentrations and emissions are reported in Table 12.

Ozone concentrations averaged between 1998 and 2002 were highest within four regional clusters: Southern California and the Central Valley, the Southeastern U.S. (excluding Florida), the Ohio Valley/ Great Lakes manufacturing corridor, and the East Coast Megalopolis from Washington D.C. in the south to Boston in the north (i.e. "BosWash") (Figure 19 and 20). The lowest concentrations of O_3 over the 5-year period were generally found in five regions: the west coast of California, the Northwest, the upper Midwest, Florida, and the Southwest. Levels of $PM_{2.5}$ exhibited a similar spatial distribution, with the highest concentrations found in Southern California and the Central Valley, the Ohio Valley/ Great Lakes manufacturing corridor, and the Southeast including the Atlanta, GA, Knoxville, TN and Birmingham, AL metro areas (Figure 21 and 22). The lowest concentrations of $PM_{2.5}$ were recorded in the Southwest, the Mountain and Great Plains states and the Northwest. PM_{10} concentrations were highest in the Southwest including Southern California and the Phoenix, AZ metropolitan area (Figure 23 and 24).

An analysis of variance (ANOVA) was performed to determine if the concentration of O_3, $PM_{2.5}$ and PM_{10} in 86 MSAs and CSAs varied significantly among

four major U.S. regions: Northeast, Southeast, Midwest, and West (Figure 18). Ozone concentration did not vary significantly between metros in the Northeast ($\bar{x}$ = 88.4 ppb), South ($\bar{x}$ = 85.7 ppb) or Midwest ($\bar{x}$ = 82.7 ppb). Metropolitan areas located in the West, however, had significantly lower average O_3 concentrations ($\bar{x}$ = 75.3 ppb). $PM_{2.5}$ concentration was significantly lower among metros in the West ($\bar{x}$ = 11.7 μg/m^3) relative to those in the Midwest ($\bar{x}$ = 14.2 μg/m^3). $PM_{2.5}$ concentration in the Northeast ($\bar{x}$ = 12.8 μg/m^3) and the South ($\bar{x}$ = 13.6 μg/m^3) did not vary significantly from other regions. The concentration of coarse particulates (PM_{10}) was significantly higher among metropolitan areas in the West ($\bar{x}$ = 29.6 μg/m^3) relative to those in the Northeast ($\bar{x}$ = 20.5 μg/m^3). Nearly equal, PM_{10} concentration in the Midwest ($\bar{x}$ = 25.7 μg/m^3) and the South ($\bar{x}$ = 25.1 μg/m^3) did not vary significantly from other regions.

The top 10 MSAs and CSAs with the highest and lowest air pollutant concentrations are reported in Table 13 and Table 14, respectively. The two metro areas with the highest ambient (4th maximum 8 hour) concentration of O_3 between 1998 and 2002 were both located in California's Central Valley: Bakersfield and Fresno. Despite the relatively high concentrations of O_3 in Southern and Central California, the West region maintained the lowest average O_3 concentrations (reported above) of any region. Therefore, California, as the most populous and arguably the most urbanized state in the West, appears to be an exception among western states in terms of high O_3 levels. While the highest concentrations were recorded in the West, six of the top 10 metros were located in the South. Four of the six Southern metropolitan areas, including Knoxville,

TN, Chattanooga, TN, Atlanta, GA, and Columbia, SC, form a cluster of urban areas all within approximately 300 kilometers of one another. The top 10 list also contains one metro area in the Midwest (Youngstown, OH-PA), and one in the Northeast (Philadelphia, PA). All 10 metro areas experienced O_3 concentrations well above the EPA standard of 75 ppb. The two metropolitan –scale areas with the lowest ambient concentrations of O_3 are both located in the Northwest: Seattle, WA and Portland, OR. With the exception of San Francisco, CA, the remaining metros with the 10 lowest O_3 concentrations were generally located in the Upper Midwest or South/ Southwest.

The two metro areas with the highest $PM_{2.5}$ concentrations were located in the West region: Fresno, CA and Los Angeles, CA. Three Southern cities with the highest concentrations of O_3 also made the top 10 list for $PM_{2.5}$: Atlanta, GA, Knoxville, TN, and Chattanooga, TN. Bakersfield, CA, with the highest concentration of O_3, also had the 8^{th} highest concentration of $PM_{2.5}$. The three largest urban areas in Ohio also made the $PM_{2.5}$ top 10 list: Columbus, Cincinnati and Cleveland. The average annual mean concentration of $PM_{2.5}$ for all top 10 metropolitan-scale areas was above the current EPA standard of 15 $\mu g/m^3$. While the West region contained three metropolitan areas with the highest $PM_{2.5}$ concentrations, eight of the 10 metros with the lowest concentrations of $PM_{2.5}$ were also located in the West. With the exception of Miami, FL and the two Northwestern cities, Portland, OR and Seattle, WA, the metros with the lowest concentrations of $PM_{2.5}$ all have arid or semi-arid climates.

Five of the top 10 metropolitan-scale areas with the highest concentration of PM_{10} were located in the West. Three metros were located in the South, two in the Midwest, and none in the Northeast. With a maximum PM_{10} average of 42 $\mu g/m^3$ in Phoenix, AZ, all ten metros were below the EPAs standard of 50 $\mu g/m^3$. Five of the top 10 metropolitan-scale areas with the lowest concentration of PM_{10} were located in the Northeast, including the metro with the lowest concentration of PM_{10} (16 $\mu g/m^3$): Hartford, CT. Only Fresno, CA and Bakersfield, CA, both located within California's Central Valley, made the top 10 list of all three air pollutants, while the two major metropolitan centers in the Northwest, Portland, OR and Seattle, WA were the only metropolitan-scale areas among those with the 10 lowest concentrations of O_3, $PM_{2.5}$ and PM_{10}.

Geographic Overview: Urban Form

Urban Sprawl Indices

The metropolitan-scale areas with the highest levels of urban sprawl according to the six sprawl indices used in this investigation were generally clustered around the Mid-South region within the states of Arkansas, Tennessee, Georgia, North Carolina and South Carolina (Figure 25). In this descriptive analysis, relative levels of sprawl were evaluated by summing the number of sprawl indices indicating that an MSA/ CSA was among the top 10 most/ least sprawling large (500k+ pop.) metropolitan-scale areas in the country. Both Knoxville, TN and Charlotte, NC were ranked among the top 10 most sprawling metros in five of six sprawl indices (Table 15). The two cities, however, were only evaluated for five of the six sprawl indices, and therefore may have ranked within the top

10 of all six. Two additional metros within the Southeast, Greensboro—Winston-Salem—High-Point, NC, and Atlanta, GA made the top 10 list of four sprawl indices. Nashville, TN, Little Rock, AR, and Knoxville, TN were each ranked within the top 10 most sprawling metros by three sprawl indices. Only Nashville, TN was ranked as the most sprawling metropolitan-scale area by more than one sprawl index: Nasser and Overberg (2001), Sutton (2003) High Threshold and Sutton (2003) Low Threshold. The three additional metropolitan areas ranked as most sprawling by urban sprawl indices included Greensboro—Winston-Salem—High-Point, NC (Ewing et al. 2003), Greenville, SC (Lopez and Hynes 2003) and Phoenix, AZ (Burchfield et al. 2006). Interestingly, Phoenix, AZ was not listed within the top 10 most sprawling metros by any of the other five sprawl indices. The Burchfield et al. index rankings were the least cohesive, with several metro areas appearing only on their top 10 list, including Washington-Baltimore, Richmond, VA, Boston, MA, San Francisco, CA, San Antonio, TX and Pittsburg, PA. Three of these cities, including the top-ranked Phoenix, AZ, were ranked among the top 10 least sprawling large metros by other sprawl indices.

The metropolitan-scale areas ranked as having the least urban sprawl were distributed throughout the U.S., with two clusters occurring in the Northeast and the West, particularly California (Figure 26). The New York metro area, the most populous urban area in the country, was ranked as having the least urban sprawl by four sprawl indices, and was ranked the sixth least sprawling metro by a fifth index (Table 16). Well known for its auto-centricity, the Los Angeles area was ranked among the 10 least sprawling large metros by four sprawl indices, and was ranked the second least sprawling

metro by three. Just south of the Los Angeles area, San Diego was also one of the 10 least sprawling metros according to four separate indices, as was San Antonio, TX and Miami, FL. In addition to Los Angeles and San Diego, five other MSA/ CSAs in California were considered least sprawling by one or more indices. In California's Central Valley, Sacramento and Stockton were each ranked among the 10 least sprawling metros by three indices, while Fresno and Bakersfield were ranked as such by two indices. Also in California, the San-Francisco area was ranked the third least sprawling large metro by the Ewing et al. (2003) composite sprawl index. This contradicts the Burchfield et al. (2006) sprawl index, which ranked the San Francisco area as the eighth most sprawling out of 40 large metro areas. In the central portion of the country, the least sprawling metros included Denver, CO, El Paso, TX and New Orleans, LA with three "votes," (i.e. ranked least sprawling by three indices), and Omaha, NE and Chicago, IL with two "votes." Along the BosWash megapolitan corridor in the Northeast, Philadelphia had two "votes," New York five, Springfield, MA one, Providence, RI one, Boston, MA one, and Portland, ME one. Metros located in the Ohio Valley/ Steel Corridor and Mid-Southeast were generally not ranked among the least sprawling by any index. Descriptive statistics for the six sprawl indices and the four Ewing et al. (2003) urban sprawl components are provided in Table 17.

Spatial Metrics

Nine spatial metrics were calculated for each of the 86 most populous MSAs/CSAs and the 19 megapolitan areas in the U.S. Descriptive statistics for spatial metrics calculated at the metropolitan and megapolitan scale are presented in Table 18

and Table 19, respectively. For each metropolitan and megapolitan area, spatial metrics were calculated at a high and low urban threshold. Using a paired t-test, the means of all nine spatial metrics were found to vary significantly between the high and low urban thresholds at the metropolitan scale (Table 20). Edge density (ED), largest patch index (LPI), contiguity (CONTIG), percentage of like adjacencies (PLADJ), and the clumpiness index (CLUMPY) were significantly greater at the high urban threshold, while landscape shape index (LSI), area-weighted mean shape index (AWMSI), area-weighted mean patch fractal dimension (AWMPFD), and contagion (CONTAG) were significantly greater at the low urban threshold. A similar pattern was observed at the megapolitan scale, although ED, CONTAG, and CLUMPY did not vary significantly between the high and low urban threshold (Table 21). Four of the five spatial metrics that were significantly higher at the high urban threshold at the metropolitan scale, LPI, CONTIG, PLADJ, and CLUMPY, all loaded highly on the "continuity" urban form factor (Table 5). These four spatial metrics generally measure the degree to which urban patches are aggregated within the landscape. As expected, the urban landscape captured within the high threshold (i.e. primarily the urban core and surrounding suburbs) exhibited a more aggregated, continuous and compact distribution relative to the urban landscape modeled using the low urban threshold, which contained a more extended urban realm with exurban/ periurban areas as well as the suburban and urban core. Further reflecting the spatial differences between urban landscapes at the high and low urban threshold, three of the four spatial metrics that were significantly higher at the low urban threshold at the metropolitan scale, LSI, AWMSI and AWMPFD loaded highest on the "shape

complexity" urban form factor. This suggests that the urban landscape at the low urban threshold exhibited a more complex shape, as well as a less continuous or aggregated distribution than at the high urban threshold. More fully included within the low urban threshold, the exurban/ periurban realm typically exhibits to a greater extent than any other part of the urban landscape sprawl-like characteristics such as patchy, dispersed and discontiguous development. Although edge density was unexpectedly higher at the high urban threshold, it did not load particularly high on "shape complexity" (Table 5), and was not significantly different at the megapolitan scale. It may therefore be a relatively "weak" measure of shape complexity at the high urban threshold. Furthermore, the majority of urban—non-urban edge (i.e. urban-rural boundary) was found within the high urban threshold, which was significantly smaller in area among most metros, potentially leading to the higher edge density (i.e. urban—non-urban edge per hectare) at the high urban threshold.

In addition to urban extent, scale (i.e. metropolitan vs. megapolitan) had a significant effect on the mean value of three spatial metrics: AWMSI, LPI, and LSI (Table 22). AWMSI, a weighted measure of urban perimeter-area ratio, was 22.6 units (32 percent) greater at the megapolitan scale than at the metropolitan scale. Another measure of shape complexity, LSI, was 92.3 units (87 percent) greater at the megapolitan scale. The urban landscape therefore appears more complex at the megapolitan scale, perhaps in part due to the enhanced presence of complex inter-urban space and inter-urban as well as intra-urban polycentricism. Megapolitan regions also tend to be much less consolidated than metropolitan (MSA or CSA) areas, and therefore often exhibit highly complex linear

(e.g. the Carolina Piedmont megapolitan area, Figure 27) or "galactic" (e.g. the Georgia Piedmont megapolitan area, Figure 28) shapes (Figure 29). It is important to note that an urban region's "shape" is dependent upon scale, and a megapolitan area with a linear shape may be part of a larger galactic mega-region (Lang and Dhavale 2005). The significantly lower LPI among megapolitan areas also reflects the less consolidated, polycentric nature of these larger urban regions. LPI, the percent of the total urban area within the largest urban patch, was 5.22 percent (17 percent difference) higher at the metropolitan scale.

The nationwide distribution of spatial metric values calculated at the metropolitan scale with the high and low thresholds averaged are illustrated in Figures 30-38. Because most spatial metrics appeared to exhibit some regional clustering, a hot spot analysis using the Getis-Ord Gi* statistic was performed to highlight clusters of high and low values for each spatial metric among the 86 metropolitan-scale areas (Figures 39-47). As expected, all spatial metrics exhibited some degree of high and low clustering across the U.S. High values of ED, a basic measure of urban shape complexity, were most intensely clustered around the mid-Southeast and mid-Atlantic regions (Figure 39). High values of ED are expected to be indicative of more sprawl-like conditions. Several metro areas within this area had the highest urban edge densities in the nation, including Norfolk, VA (78 m/ha), Atlanta, GA (74 m/ha), Greenville, SC (72 m/ha), Philadelphia, PA (71 m/ha), and Richmond, VA (69 m/ha). The largest cluster of metro areas with low values of ED was located along a linear corridor from Louisiana to Iowa. Within this corridor, the cities

of New Orleans, LA (29 m/ha), Memphis, TN (32 m/ha) and Omaha, NE (34 m/ha) had the lowest values of ED.

A single large, intense cluster of metropolitan areas with high values of landscape shape index (LSI) was located along the east coast from Georgia to New Hampshire (Figure 40). Like ED, LSI is expected to rise as the spatial morphologies of urban areas become increasingly sprawl-like. The cluster of metros with high values of LSI is very similar to the one observed for ED (Figure 39). At the southern end of the cluster is Atlanta, GA with the highest LSI in the nation (278). The other four metros with the highest LSI scores included New York, NY (271), Washington-Baltimore (271), Philadelphia, PA (264), and Boston, MA (243). Although many low values of LSI were found among metros in the West and Midwest (Figure 31), there was no discernable high-intensity cluster of low LSI values according to the Getis-Ord Gi* statistic (Figure 40). The five metros with the lowest LSI were Stockton, CA (46), Wichita, KS (48), Salt Lake City, UT (54), Las Vegas, NV (54), AND El Paso, TX (54).

A cluster of metros with relatively low values of largest patch index (LPI) were located along the east coast; two clusters of metros with high LPI were located in the Northwest and Southwest (Figure 41). Lower LPI indicates that less of the urban landcover composes the largest urban patch in the landscape, which may reflect greater urban decentralization and discontinuity. Metros with the lowest LPI included Portland, ME (17 percent), Norfolk, VA (18 percent), Washington-Baltimore (19 percent), Lexington, KY (20 percent), and Madison, WI (20 percent). In addition to having two separate large urban cores (i.e. Washington, D.C. and Baltimore, MA) and thus inter-

urban polynucleation, the Washington-Baltimore CSA also exhibits considerable intra-urban polynucleation, particularly around Washington with 23+ "edge cities" (Garreau 1991). This reduces the proportion of urban land contained within the largest urban patch (i.e. central Washington, D.C.). The low LPI in Norfolk, VA is primarily the result of geographic position; the metropolitan area is split into two primary urban cores (i.e. Newport-News—Hampton and Norfolk—Portsmouth) by the Hampton Roads waterway. Metros with the highest LPI were Miami, FL (64 percent), San Diego, CA (61 percent), Chicago, IL (53 percent), Los Angeles, CA (53 percent), and Detroit, MI (51 percent). Miami's high LPI is due to its unique geographic situation between the Atlantic Ocean to the east and the Everglades to the west, which has restricted its outward urban growth. The San Diego and Los Angeles areas are similarly constrained by the local topography with the Pacific Ocean to the west and coastal mountain ranges to the east.

High and low values of the two remaining measures of urban shape complexity, area-weighted mean shape index (AWMSI) and area-weighted mean patch fractal dimension (AWMPFD), exhibited similar geographic distributions, with an intense clustering of high values in the Northeast and Southwest, and a clustering of low values around Northern California-Nevada and Louisiana-Arkansas (Figure 42 and 43). Like ED and LSI, high values of AWMSI and AWMPFD indicate greater urban complexity characteristic of the jagged, irregular land use patterns found in "sprawling" areas (Longley and Mesev 2000; McGarigal et al. 2002; Huang, Lu and Sellers 2007). The five metros with the highest AMMSI and AWMPFD included Atlanta, GA (218; 1.48), Boston, MA (207; 1.47), New York, NY (179; 1.45), Pittsburgh, PA (142; 1.45), and

Greenville-Spartanburg, SC (122; 1.45). Atlanta, GA stands out as having particularly high levels of urban shape complexity, with the highest level of landscape shape index (LSI) and third highest edge density (ED) as well. While central Boston and New York have compact shapes and high population densities, their surrounding suburban and exurban areas appear to be among the most spatially complex in the nation. The metros with the lowest levels of AWMSI and AWMPFD were also nearly congruent: New Orleans, LA (22; 1.31), Lafayette, LA (25; 1.32), Wichita, KS (31; 1.34) and Sacramento, CA (31; 1.33), and Bakersfield, CA (32; 1.35) and Fresno, CA (32; 1.34). While New Orleans and Lafayette are both found in southern Louisiana, Sacramento, Bakersfield and Fresno are all located within California's Central Valley. Each of these urban areas is relatively spatially compact with either limited or regular (i.e. grid-like) suburban/ exurban expansion. Like Miami, FL, the outward expansion of New Orleans, LA has been limited by its geographic position between a large body of open water (i.e. Lake Pontchartrain) and extensive wetlands.

The spatial metrics contiguity (CONTIG), percentage of like adjacencies (PLADJ) and clumpiness index (CLUMPY), which measure particular aspects of urban continuity, exhibited similar high and low clusters. A large, intense cluster of metropolitan-scale areas with low values of CONTIG, PLADJ and CLUMPY was found along the east coast from Alabama to Massachusetts (Figures 44-46). This cluster is similar to the low-value cluster of LPI and the high value cluster(s) of the shape complexity metrics LSI, AWMSI, and AWMPFD. This area of the eastern U.S. therefore appears to have a disproportionately high number of metros with relatively low values of

urban continuity and high values of urban shape complexity. In addition to the large, low-value cluster along the east coast, three discernable high-value clusters of CONTIG, PLADJ and CLUMPY were also identified by the Getis-Ord Gi* statistic: the far west including metros in California, Nevada and Utah, the central U.S. from Louisiana and Texas to Oklahoma, Kansas, and Missouri (roughly encompassing the I-35 corridor), and the Great Lakes region. Higher values of each of these three metrics is expected to indicate more cohesive, less fragmented urban landscapes and lower levels of sprawl. Greenville-Spartanburg, SC had the lowest value of CONTIG (0.831) and PLADJ (77), and the second lowest value of CLUMPY (0.750). Also among the ten metros with the lowest values of all three metrics were Richmond, VA (0.839; 85; 0.766), Philadelphia, PA (0.839; 85; 0.761), Norfolk, VA (0.843; 85; 0.748), Washington-Baltimore (0.848; 86; 0.779), and Atlanta, GA (0.851; 86; 0.761). Several of these cities also scored relatively high on measures of shape complexity, suggesting that urban areas with high levels of urban shape complexity are also likely to have low levels of urban continuity. Metros with the highest values of CONTIG, PLADJ and CLUMPY were a less homogenous group than those with the lowest values. Denver, CO, for example, had the highest CONTIG (0.952), but ranked 6th highest for CLUMPY (0.889) and 22nd highest for PLADJ (92). Miami, FL was ranked first among 86 metros in terms of PLADJ (95), second in terms of CONTG (0.948) and 28th for CLUMPY (0.860). San Francisco, CA (0.944; 95; 0.918) and Salt Lake City, UT (0.942; 95; 0.914) were the only two metros that ranked within the top five for all three metrics. Salt Lake City in particular scored

low on nearly every measure of urban shape complexity, providing further evidence that these two components of urban morphology are negatively related.

The ninth and final spatial metric, contagion (CONTAG), is a measure of urban continuity or fragmentation similar to PLADJ. It determines the probability that a given urban pixel (30x30 meters) will share a border with another urban pixel. Also like PLADJ, CONTAG is calculated at the landscape level rather than by class. Although CONTAG is a measure of urban continuity like PLADJ, CONTIG, and CLUMPY, the Getis-Ord Gi* hotspot analysis revealed a slightly different clustering pattern for high and low values. A cluster of metros with low values of CONTAG were found in the Southeast, most notably the Atlanta, GA (27.6) and Greenville-Spartanburg, SC (30.4) areas. While a map of CONTAG values (Figure 47) indicates that several metros in the Northeast, especially Norfolk, VA (27.4) and Philadelphia, PA (30.1) had moderate to high values of CONTAG, the Getis-Ord GI* statistic did not identify this area as a low-value hotspot. This is likely due to a number of metros in the Northeast and Ohio Valley with relatively high CONTAG values. The metropolitan-scale areas with the highest CONTAG also included two in the southeast: Tucson, AZ (27.4) and Albuquerque, NM. The five metros with the lowest CONTAG included Lafayette, LA (44.8), Madison, WI (44.6), Salt Lake City, UT (42.8), Syracuse, NY (41.5) and Des Moines, IA (41.3). Furthermore, two additional cities in Louisiana, Baton Rouge (41.3) and New Orleans (41.0) were ranked 6th and 7th respectively, and compose a cluster of metros with high contagion identified by the Getis-Ord Gi* hotspot analysis.

In addition to performing the Getis-Ord Gi* hotspot analysis, which identified specific clusters of metropolitan-scale areas with especially high and low levels of each spatial metric, an ANOVA was conducted to determine whether statistically significant differences in spatial metrics existed between metros in four major U.S. regions: Northeast, Midwest, South and West (Figure 18). As with the Getis-Ord Gi* analysis, spatial metrics calculated at the high and low threshold were averaged for each metro. A statistically significant difference in the mean value of all spatial metrics except largest patch index (LPI) was found between the four regions (Table 23; Figure 48). Although the ANOVA indicated a significant difference in landscape shape index (LSI) between regions ($p = 0.041$), post hoc tests (equal variances not assumed) could not identify a significant difference between any two regions (Figure 49).

Among the seven spatial metrics for which statistically significant differences between individual regions were found, a few discernable patterns were identified. First, for each spatial metric there were at most two regions that varied significantly from one another. Second, metros in the Northeast and South exhibited greater shape complexity as measured in terms of edge density (ED), LSI, area-weighted mean shape index (AWMSI) and area-weighted mean patch fractal dimension (AWMPFD). Metros in the Northeast ($p = 0.027$) and South ($p = 0.014$) regions had significantly higher ED than those in the Midwest (Figure 50). Metros in the Northeast also had significantly higher AWMSI than those in the West ($p = 0.047$) (Figure 51), and significantly higher AWMPFD than metros in both the Midwest ($p = 0.009$) and West ($p = 0.024$) (Figure 52). Third, metros in the Northeast and South had lower average contiguity (CONTIG) (Figure 53), contagion

(CONTAG) (Figure 54), percentage of like adjacencies (PLADJ) (Figure 55), and clumpiness index (CLUMPY) (Figure 56) than metros in the Midwest or West. Specifically, metros in the Northeast had significantly lower CONTIG than those in the Midwest ($p = 0.003$) and West ($p = 0.013$), and significantly lower PLADJ than those in the Midwest ($p = 0.001$) and West ($p = 0.019$). Both the Northeast ($p = 0.006$) and South ($p = 0.041$) had significantly lower CLUMPY than the Midwest, while the Midwest had significantly higher CONTAG than the South ($p = 0.019$).

Metros with extreme values of spatial metrics for each of the four U.S. regions were also identified using boxplots (Figures 48-56). Philadelphia, PA, for example, had unusually high levels of edge density (ED) for the Northeast, while Cincinnati, OH and Louisville, KY were above the normal range of ED among metros in the Midwest (Figure 50). Philadelphia was also a statistical outlier in terms of high levels of landscape shape index (LSI) (Figure 49), and low levels of contiguity (Figure 53), percentage of like adjacencies (PLADJ) (Figure 55) and the clumpiness index (Figure 56). Among metros in the Northeast, New York, NY had extreme high values of LSI and AWMSI (i.e. measures of "shape complexity"), Boston, MA had extreme high values of AWMSI, and Buffalo, NY had extreme high values of the urban "continuity" metrics CONTIG, PLADJ and CLUMPY. New York, Philadelphia and Boston, the three most populous urban areas in the Northeast, appear to have very complex and discontiguous urban "footprints" at the MSA/ CSA scale despite having relatively compact and dense urban cores. In contrast, Buffalo has a relatively simple and compact urban footprint, with much of the suburban development contiguous with the urban core.

The Midwestern outliers included Cincinnati, OH, Louisville, KY, Chicago, IL, Lexington, KY, and Madison, WI. Cincinnati had unusually high ED and low contagion indicating high shape complexity and low continuity (Figure 50). The spatial morphology of urban development throughout the Cincinnati area is more scattered than in many other Midwestern cities in part due to the area's undulating topography. Central Cincinnati is punctuated by hilly terrain and split north-south by the Ohio River, reducing measures of urban cohesion. Madison, WI was an outlier among Midwestern cities for three spatial metrics: low largest patch index (LPI), low contiguity (CONTIG) and high contagion (CONTAG). While low values of LPI usually indicate more polynucleated or less centralized urban forms, this may not be the case for either Madison, WI or Lexington, KY. Among the most populous 86 metropolitan-scale areas used in this study, the two cities are among the smallest with a 2000 population of 556,999 and 602,773, respectively. As smaller "large" urban areas, their urban cores are relatively centralized and contiguous. The low LPI therefore is a result of numerous neighboring communities and municipalities within each city's multi-county CSA boundary. Chicago, IL, the largest urban area in the Midwest region, had the highest LPI, indicating a high level of spatial continuity among the area's suburban realms.

Madison, WI had extreme low values of CONTIG, but extreme high values of CONTAG, despite a significant positive correlation between the two metrics when high and low threshold values are averaged ($r^2 = 0.463$, $p < 0.001$). The contagion metric, however, exhibited a significant negative correlation with both CONTIG and PLADJ at the low urban threshold. A possible explanation is that the CONTAG metric calculates

both dispersion and interspersion, and is therefore affected not only by the proportion of like-adjacencies between pixels, but also the proportion of the landscape occupied by a single landcover class (i.e. either urban or non-urban). The greater the percentage of the landscape occupied by a single landcover class, the higher the CONTAG. Within the Madison-Baraboo, WI CSA boundary, the non-urban landcover class composes 84 percent of the landscape at the low urban threshold, but only 59 percent of the landscape at the high urban threshold. This pattern is similar among other metros, explaining why CONTAG is generally higher at the low urban threshold (i.e. due to greater contagion, primarily among non-urban pixels), and why CONTAG is the only metric in which values calculated at the high and low urban threshold are uncorrelated ($r^2 = 0.010$, $p = 0.925$) (Table 4). The Madison area therefore had unusually high CONTAG due to the large proportion of non-urban land within the urban region's CSA boundary, rather than abundant urban-urban pixel adjacencies.

Among metros in the South region, Atlanta, GA exhibited unusually high levels of shape complexity as measured by the urban form factors LSI, AWMSI and AWMPFD. As suggested earlier, Atlanta appears to have the most complex urban morphology of any large urban area in the U.S. Atlanta, however, was not an outlier among the urban "continuity" metrics, which did not have a single extreme measure in the South. The Washington-Baltimore CSA, at the northeastern fringe of the South region, also exhibited unusually high LSI, only slightly lower than Atlanta. The two metros were ranked first and third in terms of LSI, with New York City second. The Washington-Baltimore area has a high degree of both intra- and inter-urban polynucleation leading to high levels of

shape complexity. Miami, FL had an extreme high value of LPI, primarily due to the area's geographic constraints. Greenville-Spartanburg, SC had unusually low PLADJ, indicating low urban continuity, while Lafayette, LA and New Orleans, LA exhibited extreme low values of AWMPFD, indicating low shape complexity.

Finally, two metros in the West region exhibited extreme values, both with unusually high landscape shape index (LSI): Los Angeles, CA and Seattle, WA. The Los Angeles area had the sixth highest LSI in the nation; Seattle had the 11th highest. Los Angeles also scored within the top 20 percent in terms of area-weighted mean shape index (AWMSI) and area-weighted mean patch fractal dimension (AWMPFD). The Los Angeles region therefore had relatively high levels of urban shape complexity, particularly when compared to other metros in the West, which on average had lower AWMSI and AWMPFD than metros in the Northeast. While the central portion of Los Angeles and Seattle are mostly contiguous and shape-filling (i.e. low shape complexity), both cities have adjacent urban realms with complex suburban development patterns, elevating the shape complexity of the two regions.

Urban Form Factors

Two urban form factors, urban "continuity" and urban "shape complexity," were derived from the nine spatial metrics using principal component analysis (PCA). At both the metropolitan and megapolitan scale, a separate set of factors were produced from spatial metrics calculated at the high and low urban threshold. The two uncorrelated factors represent the majority of variation among the original nine spatial metrics (Tables 5-8). Although component loadings varied by spatial extent and scale, the spatial metrics

edge density (ED), area-weighted mean shape index (AWMSI), area-weighted mean patch fractal dimension (AWMPFD), and landscape shape index (LSI) generally loaded high under urban "continuity," while largest patch index (LPI), clumpiness index (CLUMPY), contiguity (CONTIG) and percentage of like adjacencies (PLADJ) generally loaded high under urban "shape complexity." Contagion (CONTAG) loaded high under urban "continuity" only when calculated at the high urban threshold (Tables 5-8). The urban form factors provide a means of summarizing the more detailed morphological information contained within the nine spatial metrics discussed above.

The top 10 MSAs and CSAs with the highest and lowest urban "continuity" and urban "shape complexity" are presented in Table 24 (high threshold) and Table 25 (low threshold); all 19 megapolitan areas are ranked similarly in Table 26 (continuity) and Table 27 (shape complexity). The urban form factor "scores" are a linear combination of all nine spatial metrics weighted by their associated factor loadings (DeCoster 1998). All factor scores have an average of 0 and a range of approximately -3.0 to 3.0, with values less than -1 representing low levels of urban "continuity" and urban "shape complexity," and values greater than 1 representing high levels of urban "continuity" and urban "shape complexity." Values around 0 (i.e. approximately -1 to 1) represent moderate or average levels of the two urban form factors. All other morphological features equal, lower levels of urban "continuity" and higher levels of urban "shape complexity" are expected to indicate higher levels of urban sprawl.

At the metropolitan scale, high urban threshold, urban "continuity" ranged from a high of 1.56 in Sacramento, CA to a low of -2.64 in Philadelphia, PA; urban "shape

complexity" ranged from a high of 2.49 in New York City to a low of -1.16 in Mobile, AL (Table 24). At the low urban threshold, urban "continuity" ranged from a high of 1.92 in Salt Lake City, UT to a low of -1.15 in Tucson, AZ; urban "shape complexity" ranged from a high of 1.96 in Atlanta, GA to a low of -1.03 in Scranton, PA (Table 25). The majority of cities with the highest urban "continuity" at the high urban threshold were located in the West and Midwest regions; three of the top 10 were located in California. By contrast, the majority of cities with the lowest urban "continuity" at the high urban threshold were located in the South or Northeast regions. This general regional pattern was also observed at the low urban threshold, although three cities in the South made the top 10 list in terms of high urban "continuity": New Orleans, LA, Miami, FL and Memphis, TN. As mentioned earlier, the outward urban growth of both New Orleans and Miami has been highly constrained by local geography due to their position between extensive wetlands and large bodies of water. The relative urban "continuity" of the two cities increases from the high to low urban threshold because their outer suburban-exurban areas are more dramatically affected by geographic constraints; their inner urban-suburban cores may not – in terms of urban "continuity" – appear much different from other relatively contiguous cities.

The metropolitan-scale areas with the lowest urban "continuity" included four cities ranked among the most sprawling according to one or more sprawl indices: Atlanta, GA, Greenville-Spartanburg, SC, Washington-Baltimore, and Richmond, VA. Interestingly, the list also contains Philadelphia, PA, which is ranked among the 10 least sprawling metros by both Lopez and Hynes (2003) and Burchfield (2006), and New York,

NY, which is ranked among the 10 least sprawling metros by five of the six sprawl indices (Table 16). It is important to consider, however, that urban "continuity" is only one potential measure of urban form, and that it is measured primarily among combined statistical areas (CSAs), rather than MSAs, and therefore addresses urban form at a broader scale than most sprawl indices. New York City, Boston and Philadelphia all have relatively compact urban cores, but complex and discontinuous urban morphologies at the CSA scale. For cities whose urban form changes dramatically from urban core to urban periphery, both urban extent and scale can significantly affect measures of urban form and the evaluation of urban sprawl.

Urban extent clearly affects both urban "continuity" and urban "shape complexity" in most large metros. Only four cities, for example, made the top 10 list in terms of highest urban "continuity" when calculated at the both the high and low urban threshold. Several Midwestern cities, including Tulsa, OK, Detroit, MI, Dayton, OH, and Toledo, OH were listed as having the highest urban continuity at the high urban threshold, but were displaced by the Western and Southern cities of Las Vegas, NV, New Orleans, LA, Denver, CO, Miami, FL and Memphis TN at the low urban threshold. Detroit in particular fell from sixth to 20th place in terms of highest urban continuity, presumably due to a significant drop in urban continuity between the high and low urban thresholds. Like many large U.S. cities, Detroit appears to have a relatively continuous or contiguous urban core that becomes increasingly discontiguous and fragmented toward the urban periphery. The Detroit-Warren-Flint, MI CSA includes not only Detroit proper but also many satellite communities with primarily fragmented, suburban-exurban

morphologies. These satellite communities, as well as the exurban-rural realms in between, are more completely included in the low urban threshold, reducing the area's overall urban "continuity," and increasing its "shape complexity."

The 10 metros with the highest urban "shape complexity" were located in all four regions of the U.S. (Table 24 and 25). However, as with the lowest urban "continuity," more cities were located in the South (4) than any other region. Half the metros on the top10 list of lowest urban "shape complexity" were also located in the South; only Scranton, PA, (low urban threshold) was located in the Northeast. Seven metros made the top 10 list in terms of highest urban "shape complexity" when calculated at both the high and low urban threshold. This indicates that these cities likely exhibited complex urban shapes throughout the urban realm; from the inner suburbs to the outer exurban-rural fringe. The top 10 list also includes several of the most populous metros in the country, including New York City, Los Angeles, Chicago, Boston, Dallas-Ft. Worth, and Detroit. Several cities with the lowest populations among the 86 metros exhibited the lowest urban "shape complexity," such as Lafayette, LA, Mobile, AL, and Scranton, PA. The apparent positive correlation between population and urban "shape complexity," at both the high and low urban threshold, was statistically significant (high threshold: $r^2 = 0.655$, $p < 0.001$; low threshold: $r^2 = 0.579$, $p < 0.001$). A significant correlation, however, was not found between metro population and urban "continuity" (high threshold: $r^2 = -0.254$, $p < 0.001$; low threshold: $r^2 = 0.579$, $p < 0.001$).

The correlation between population and urban "shape complexity" does not necessarily suggest that larger metropolitan-scale areas will have more complex urban

shapes, or that shape complexity is simply a product of city size. The relationship may in part be the result of variations in the relative proportion of urban area included by the high and low urban thresholds. The area of the low urban threshold always exceeds the area of the high urban threshold, though the exact ratio of the two landscapes varies by metro. This ratio tends to be larger for large metros and smaller for smaller metros. For example, in Bakersfield, CA (pop. 690,000) the high urban threshold covers 585 km^2, approximately 23% of the 2,517 km^2 covered by the low urban threshold. In nearby Los Angeles, CA (pop. 16,950,000), however, the 9,396 km^2 covered by the high urban threshold also represents 62 percent of the 15,097 km^2 covered by the low urban threshold. Thus, in the much larger Los Angeles area, the high urban threshold represents a larger portion of the total urban landscape, and may therefore include a greater proportion of urban periphery than in Bakersfield. The urban periphery is expected to more complex than the urban core due the increased density of urban—non-urban boundary. Urban "shape complexity" is therefore likely influenced not only by the size of the urban area directly, but also indirectly through the relative size of the two urban extents.

Figures 57 through 60 depict urban "continuity" and urban "shape complexity" by metropolitan-scale area. At both the high and low urban threshold, urban "continuity" is more spatially clustered than urban "shape complexity." As was performed for each individual spatial metric, the Getis-Ord Gi cluster analysis was employed to highlight clusters of metros high and low values of urban "continuity" and urban "shape complexity." (Figures 61-64). A separate cluster analysis was conducted for high and low

urban thresholds. Although high and low clusters of urban "continuity" and urban "shape complexity" were similar at the two urban thresholds, there were noticeable differences. A cluster of metros with high urban "continuity" calculated at the high urban threshold was found in the Great Lakes region (Figure 61). Three cities in this region were among the top 10 metros with the highest urban "continuity" calculated at the high urban threshold: Detroit, MI, Dayton, OH and Toledo, OH (Table 24). This cluster, however, was not observed when the low urban threshold was used (Figure 62). Indeed, the three cities no longer made the top 10 list (Table 25). Similarly, a cluster of metros in California with high urban "continuity" at the high urban threshold exhibited a reduction in intensity at the low urban threshold. It may be inferred then that urban development across multiple cities in these two regions had relatively high urban "continuity" up to the suburban-exurban boundary. At the suburban-exurban transition zone and beyond, urban development may have become much less continuous, reducing the continuity of the urban landscape.

Metros with low levels of urban "continuity" at both the high and low urban threshold were found along the East coast from Georgia to Massachusetts (Figure 61 and 62). This broad region constituted the only significant cluster of metros with low urban "continuity" at both high and low urban thresholds. Among the metros with the lowest urban "continuity" in this region were Philadelphia, PA, Atlanta, GA, Greenville-Spartanburg, SC, Washington-Baltimore, Norfolk, VA, Richmond, VA, Boston, MA and New York, NY (eight of the top 10) (Table 24 and 25). This cluster is very similar to the cluster of metros with low CONTIG (Figure 44), PLADJ, and CLUMPY; three spatial

metrics that loaded high under urban "continuity" (Tables 5-8). Unlike the clusters of metros with high levels of urban "continuity," the distribution and intensity of this low "continuity" cluster changes little between the high and low urban thresholds. This is supported by the top 10 lists; four metros are listed as having among the 10 highest urban "continuity" at both the high and low urban threshold, while six metros are among those with the 10 lowest urban "continuity" at both thresholds (Table 24 and 25). The opposite was observed for urban "shape complexity"; seven metros had among the 10 highest "shape complexity" at both the high and low urban thresholds, while five are listed among the top 10 with the lowest "shape complexity" at both thresholds. This suggests that less sprawl-like morphological features, such as high urban "continuity" and low urban "shape complexity," are more sensitive to changes in urban extent than more sprawl-like features (i.e. low "continuity, high "shape complexity). Urban areas generally exhibit more sprawl-like spatial tendencies toward their urban periphery, which may not be fully represented by the high urban threshold. The more complete inclusion of peripheral suburban-exurban development by the low urban threshold significantly reduces the urban "continuity," and increases the "shape complexity," of many metros, thereby affecting their ranking in terms of the two measurements. Thus, for metros with high continuity and low shape complexity at the high urban threshold (i.e. less sprawl-like spatial patterns throughout their urban-suburban core), it is more likely that their ranking will decrease, rather than increase, when the urban form factors are calculated at the low urban threshold. In contrast, metros with low "continuity" and high "shape complexity" at the high urban threshold have "less to lose," as their urban-suburban cores

already exhibit the spatial morphology of many suburban-exurban areas in terms of urban "continuity" (e.g. Atlanta, GA) or urban "shape complexity" (e.g. New York, NY). Their rankings are therefore less likely to change between high and low urban thresholds. Note that although New York has the highest "shape complexity," this measure does not pertain to the city of New York alone, but rather the entire New York-Newark-Bridgeport CSA, which covers 30 counties over four states.

Urban "shape complexity" exhibited less clustering than urban "continuity" (Figures 63 and 64). At both high and low urban thresholds, clusters of metros with relatively low urban "shape complexity" were small and scattered throughout the country. Larger clusters of metros with high "shape complexity" were located in the Southeast at the high urban threshold, and the lower Mississippi Valley at the low urban threshold. The lack of clustering indicates greater spatial variability in urban "shape complexity" relative to urban "continuity." Whereas cities in the eastern U.S. generally exhibited lower levels of urban "continuity" at both urban thresholds, a similar statement regarding broad regional differences cannot be made for urban "shape complexity."

The conclusion drawn from the Getis-Ord Gi cluster analysis that metros exhibited greater regional variability in urban "continuity" relative to urban "shape complexity" was further supported by an ANOVA of four U.S. regions: Northeast, Midwest, South, West (Table 28). Measured at the high urban threshold, urban "continuity" was significantly higher among metros in the Midwest than those in the Northeast and South (Figure 65). At the low urban threshold, urban "continuity" was significantly higher among metros in Midwest and West than those in the Northeast

(Figure 66). There was, however, no significant difference in urban "shape complexity" among metros in the four regions (Figure 67 and 68).

Regional outliers in terms of both urban "continuity" and urban "shape complexity" were found only at the high urban threshold. Two metros had unusually low urban "continuity" relative to other cities in their regions: Philadelphia in the Northeast and Cincinnati in the Midwest (Figure x). There were seven statistical outliers in terms of urban "shape complexity"; five high and two low. Metros with high levels of "shape complexity" included New York, NY and Boston, MA in the Northeast, Chicago, IL in the Midwest, and Atlanta, GA and Miami, FL in the South. Metros with low levels of "shape complexity" included Portland, ME in the Northeast and Lexington, KY in the Midwest. Each of these metros was also an outlier for one or more individual spatial metrics.

In terms of urban morphology, urban sprawl may be partially described by urban "continuity" and urban "shape complexity;" high levels of urban "continuity" and low levels of "shape complexity" generally represent lower levels of sprawl. In Figure 69 (high threshold) and Figure 70 (low threshold), each of the 86 metropolitan-scale areas are plotted in terms of urban "continuity" and urban "shape complexity;" metros in the bottom right quadrant may be described as least-sprawling; metros in the top left, most-sprawling. Figures 71 and 72 convey the same information for the 19 megapolitan-scale areas. Note that several metropolitan (e.g. Madison, WI, Tucson, AZ) and megapolitan-scale areas (e.g. Carolina Piedmont, Lake Front) are in different quadrants depending on whether the high or low urban threshold is used.

Correlation Analysis

Air Pollution vs. Urban Sprawl Indices

Pearson correlations were performed prior to the regression analyses to determine if significant associations were likely to be found between measures of urban form and air quality, and whether there exists multicollinearity among independent (including control) variables. The first set of correlations were used to examine the relationships between urban sprawl, as assessed using urban sprawl indices, and both air pollutant concentrations and per capita non-point source emissions (Table 29). Emissions per capita were used in addition to gross emissions to control for the significant positive affect of metropolitan population on non-point source emissions. Ambient concentrations were averaged between 1998 and 2002; non-point source emissions were estimated for the year 2000. Correlations were calculated at the metropolitan scale unless otherwise specified. The associations between urban form and air quality were more fully explored at both the metropolitan and megapolitan scale using regression analysis (section 4.4).

An increase in the Ewing et al. (2003) sprawl index (indicating a *decrease* in urban sprawl) was associated with a significant reduction in the concentration of O_3, number of annual O3 exceedances (days per year O_3 concentration exceeded 0.075 ppm over an 8-hour average), and concentration of $PM_{2.5}$ (Table 29a). An increase in the Ewing et al. index was also significantly correlated with an increase in O_3 non-point source emissions, and a decrease in O_3 non-point source emissions per capita, and the per capita emission of CO_2 from on-road sources (Table 29b). A decrease in the Ewing et al. sprawl index was not significantly correlated with a change in $PM_{2.5}$ emissions nor the

concentration or emission of PM_{10}. Metropolitan-scale areas with higher levels of urban sprawl according to the Ewing et al. sprawl index were more likely to experience higher emissions of O_3 precursors from non-point sources, but fewer emissions per individual.

The four components of the Ewing et al. sprawl index, street connectivity, degree of centeredness (or centrality), mixed use development, and residential density, were each associated with a significant change in one or more air pollutants. An increase in street connectivity (indicated by higher values) was significantly correlated with a decrease in the concentration and number of annual exceedances of O_3, the per capita emission of O_3 and $PM_{2.5}$, and the on-road emission of CO_2 (Table 29a). Street connectivity was also positively correlated with O_3 and $PM_{2.5}$ non-point source emissions (Table 29b). An increase in degree of centeredness was significantly correlated with a decrease in the number of annual O3 exceedances and the concentration of $PM_{2.5,}$ while an increase in mixed use was significantly associated with an increase in the per capita non-point source emission of O_3 precursors only. Residential density was positively correlated with the non-point source emission O_3 precursors, $PM_{2.5}$ and PM_{10} emissions, and negatively correlated with the per capita non-point source emission of O_3 precursors, PM_{10} and on-road CO_2. Of the four components of urban sprawl, street connectivity and residential density are most likely to influence levels of O_3, PM, and on-road emission of CO_2 at the metropolitan scale.

As with the composite Ewing et al. (2003) sprawl index, the significant correlations between urban sprawl components and non-point source emissions were positive, while the significant correlations between urban sprawl components and per

capita non-point source emissions were negative. Larger metropolitan areas, which typically produce more total emissions from non-point sources, are also likely to have greater street connectivity and higher population densities, resulting in a positive correlation between these variables. Due to higher residential densities, however, the residents of larger cities (i.e. New York, Chicago, San Francisco, Washington, D.C.), are more likely to use public transit and other alternative modes of transportation, reducing the emission of O_3 precursors, PM and CO_2 per individual. These relationships are also apparent using the sprawl indices developed by Sutton (2003), Lopez and Hynes (2003), and Nasser and Overberg (2001), each of which are based primarily on residential density.

An increase in urban sprawl according to the Sutton (2003) sprawl index was significantly correlated with a reduction in the number of annual exceedances of O_3, the concentration of $PM_{2.5}$, and the on-road emission of CO_2 when calculated at a low urban threshold (Table 29). At the high urban threshold, the Sutton sprawl index was significantly correlated with a reduction in the concentration and per capita emission of O_3 precursors $PM_{2.5}$ PM_{10} and on-road CO_2, and an increase in the non-point source emission of O_3 precursors. The only measure of air pollution significantly correlated with an increase in urban sprawl at both the high and low urban threshold, according to the Sutton sprawl index, was the per capita emission of CO_2 from on-road sources; all other significant correlations were found only at the high or low urban threshold. With six significant correlations at the high urban threshold and only two significant correlations at the low urban threshold, urban extent appears to have played a significant role in

determining the degree of correlation between urban sprawl (i.e. relative levels of residential density) and both the concentration and non-point source emission of air pollutants.

Based on relatively simple measures of metropolitan population density, the sprawl indices developed by Lopez and Hynes (2003) and Nasser and Overberg (2001), were also significantly correlated with the concentration and non-point source emission of multiple air pollutants. An increase in urban sprawl according to the Lopez and Hynes sprawl index was significantly correlated with an increase in the concentration, number of annual exceedances of O_3, the per capita non-point source emission of O_3 precursors, the per capita emission of $PM_{2.5}$ and PM_{10}, and the on-road emission of CO_2. The Lopez and Hynes index was negatively correlated with the non-point source emission of O_3 precursors, $PM_{2.5}$ and PM_{10}. Unexpectedly, the Lopez and Hynes sprawl index also exhibited a marginally significant ($r^2 = -0.240$; $p = 0.045$) negative correlation with the concentration of PM_{10}, suggesting that an increase in metropolitan population density was significantly related to an increase in the ambient concentration of coarse particulates at the metropolitan scale. This result, however, may be spurious given that the Lopez and Hynes index was significantly correlated with an increase in the per capita emission of PM_{10}, and because no other index was significantly correlated with a change in PM_{10} concentration. The Nasser and Overberg index exhibited a similar pattern of correlations, with significant associations with all air pollutant variables except the ambient concentration and per capita non-point source emission of PM_{10}.

The Burchfield et al. (2006) sprawl index, based on the spatial continuity of residential development, was not correlated with a significant change in the ambient concentration or non-point source emission of any air pollutant. The lack of correlation between the Burchfield index (2006) and levels of air pollution may have resulted partially from the limited sample size (n = 40) relative to the other indices (n = 63-86), and a misalignment between the date associated with the urban form data (1992) and the air quality data (1998-2002). The index may also simply fail to represent a measure of urban sprawl (amount open space surrounding each residential pixel) that is significantly related to air quality at the metropolitan scale. In either case, the Burchfield et al. index is not likely to be a significant predictor of air pollutant levels in the regression models that follow.

The set of correlations above between urban sprawl indices and air pollutant levels support three important conclusions. First, there exist significant and predominately positive relationships between multiple measures of urban sprawl and multiple air pollutants. Second, both complex composite urban sprawl indices (i.e. Ewing et al. (2003)) and relatively simple population-density-based urban sprawl indices, such as Lopez and Hynes (2003) and Nasser and Overberg (2001), were significantly correlated with multiple air pollutants, and are likely to be significant predictors of air quality. Third, the limited number of significant correlations found between urban sprawl indices and the concentration and non-point source emission of PM_{10} suggest that coarse particulates may exhibit less association with urban sprawl and specific measures of urban form compared with O_3, $PM_{2.5}$ and CO_2.

Air Pollution vs. Spatial Metrics

The second set of correlations involved nine spatial metrics calculated at the metropolitan scale, high urban threshold (Table 30). Each spatial metric was significantly correlated with a change in the concentration or non-point source emission of one or more air pollutants. An increase in the urban "shape complexity" metrics edge density (ED), landscape shape index (LSI), and area-weighted mean shape index (AWMSI), were significantly correlated with a rise in O_3 concentration, while a increase in the urban "continuity" metrics largest patch index (LPI), contagion (CONTAG), clumpiness index (CLUMPY) and contiguity (CONTIG) were significantly correlated with a decrease in O_3 concentration (Table 30a). Additionally, percentage of like adjacencies (PLADJ) was significantly correlated with a decrease in number of annual O_3 exceedances. No spatial metrics were significantly correlated with the ambient concentration of either $PM_{2.5}$ or PM_{10}.

Four spatial metrics, calculated at the high urban threshold, were also significantly correlated with the non-point source emission of air pollutants (Table 30b). An increase in LPI was significantly correlated with a decrease in the per capita non-point source emission of O_3 precursors, and an increase in the non-point source emission of $PM_{2.5}$ and PM_{10}. The three "shape complexity" metrics, AWMSI, AWMPFD, and LSI were each negatively correlated with the per capita emission, and positively correlated with the total non-point source emission, of O_3 precursors, $PM_{2.5}$ and PM_{10}. Initially, these results appear to contradict expectations. Urban areas with more urban sprawl are expected to exhibit greater shape complexity, and, as supported by the previous set of

correlations, urban areas with more sprawl-like urban morphologies tend to have higher levels of air pollution. Therefore, urban shape complexity was expected to be positively, rather than negatively, correlated with air pollutant levels. The reason for this unexpected relationship is that strong negative correlations exist between metropolitan population and per capita non-point source emissions (Table 31), and strong positive correlations exist between metropolitan population and urban shape complexity at both the high (r^2 = 0.655; $p < 0.001$) and low ($r^2 = 0.579$; $p < 0.001$) urban threshold (Table 32a). As urban areas become larger, urban shape complexity and total non-point source emissions increase, while per capita non-point source emissions decrease. Thus, metropolitan areas with greater urban complexity may exhibit greater total emissions, but lower emissions per capita. Among urban areas of the same size and equivalent metropolitan population, greater urban shape complexity is expected to result in higher non-point source emissions per capita. Interestingly, the significant relationship between residential population and urban "shape complexity" does not exist at the megapolitan scale (Table 32b), indicating that larger, more populous urban regions do not have more complex urban footprints than those with less population.

Fifty five significant correlations were found between spatial metrics calculated at the low urban threshold and levels of air pollutants (Table 33), compared with 35 significant correlations at the high urban threshold (Table 30b). A rise in O_3 concentration was significantly correlated with an increase in the urban "shape complexity" metrics ED, AWMSI, AWMPFD, and LSI, and a decrease in the urban "continuity" metrics LPI (O_3 concentration only), CLUMPY, CONTIG and PLADJ (Table 33a). As observed at the

high urban threshold, an increase in the "shape complexity" metrics was generally correlated with an increase in non-point source emissions, and a decrease in per capita non-point source emissions (Table 33b). As previously mentioned, this relationship likely exists due to the strong positive correlations between shape complexity, metropolitan population, and total non-point source emissions, and the strong negative correlation between metropolitan population and non-point source emissions per capita.

Several significant correlations were found only when spatial metrics were calculated at the low urban threshold. Most notable were the additional significant correlations between non-point emissions (total and per capita) and the urban "continuity" spatial metrics CONTAG, CONTIG and PLADJ. The three metrics did not have a single significant correlation with air pollutant emissions when calculated at the high urban threshold. While the relationships between air pollutant emissions and CONTIG and PLADJ followed the established pattern of positive correlations with total non-point source emissions and negative correlations with non-point source emissions per capita, CONTAG was positively correlated with emissions and negatively correlated with emissions per capita (Table 33b). Urban areas with lower levels of sprawl are expected to have lower per capita emissions and higher levels of contagion, which is a measure of urban-urban pixel adjacency and thus overall urban continuity. Significant positive correlations between CONTAG and the per capita emission of O_3 precursors and $PM_{2.5}$ were therefore unexpected. At the low urban threshold, however, CONTAG is highly influenced by the proportion of non-urban space, which is generally expected to be higher for more scattered, less centralized, and generally more sprawl-like urban areas.

Increasing levels of CONTAG may therefore actually represent more, rather than less, sprawl-like conditions. As suggested, this may also explain why, at the low threshold only, CONTAG exhibits a significant negative correlation with CONTIG and PLADJ. Also at the low threshold only, LPI, CONTIG and PLADJ were significantly correlated with a reduction in on-road CO_2 emissions. As urban areas become more continuous and less fragmented, fewer and shorter vehicle trips result in lower per capita CO_2 emissions from on-road sources. Finally, an increase in landscape shape index (LSI) was positively correlated with $PM_{2.5}$ concentration at the low urban threshold.

In summary, the correlations above suggest that 1) there likely exists significant associations between the concentration and non-point source emission of air pollutants and specific measures of urban form calculated using spatial metrics, 2) a greater number of significant correlations exist between O_3 levels and spatial metrics than between PM and spatial metrics, 3) there exist unexpected significant negative correlations between measures of urban "shape complexity" and the per capita emission of both O_3 precursors and PM, and 4) more correlations exist between air pollutant levels and spatial metrics calculated at the low urban threshold relative those calculated at the high urban threshold.

Air Pollution vs. Urban Form Factors

Calculated at both the high and low urban thresholds, the urban form factor urban "continuity" was significantly correlated with a decrease in O_3 concentration and number of ozone exceedances at the metropolitan scale (Table 34a). At the low urban threshold only, an increase in urban "continuity" was also correlated with a significant decrease in $PM_{2.5}$ concentration. At both the high and low urban thresholds, the non-point source

emission of O_3 precursors, $PM_{2.5}$, and PM_{10} were positively correlated with an increase in urban "shape complexity." In accordance with the results presented above for individual spatial metrics, however, an increase in urban "shape complexity" was significantly correlated with a decrease in the per capita non-point source emission of O_3 precursors, PM and on-road CO_2 (Table 34b) Thus, metros with higher levels of "shape complexity" generally had higher non-point source emissions, but lower emissions per individual. As previously mentioned, larger metros tend to have higher levels of shape complexity, but lower per capita emissions. The higher "shape complexity" likely arises in part due to the complex suburban and exurban realms surrounding many large cities (e.g. Atlanta, Los Angeles, Boston), while the relatively low non-point source emissions per capita is likely due to the large urban cores and dense inner suburban realms of the largest metros, which encourage alternative modes of transportation and support more energy-efficient lifestyles (e.g. New York City, Chicago, San Francisco). Furthermore, the significant positive correlations between "shape complexity" and non-point source emissions suggest that cities with more complex urban morphologies also produce more total emissions from non-point (primarily mobile) sources. Due to the significant correlation between "shape complexity" and metropolitan population, however, this correlation may also be due primarily to city size rather than the direct influence of "shape complexity" on emissions. Regardless of the cause of these correlations, it does not appear that urban "shape complexity" is directly related to changes in the actual concentration of air pollutants, possibly indicating a relative weak relationship between this particular measure of urban form and air quality.

Unlike urban "shape complexity," urban "continuity" was not significantly correlated with metropolitan population. The significant negative correlations between urban "continuity" and the ambient concentrations of O_3 and $PM_{2.5}$ may therefore be more indicative of a direct relationship between urban form and air pollutant levels. They suggest that urban areas with more continuous urban development experience lower levels of both ozone and fine particulate matter. Urban "continuity," however, was not significantly correlated with non-point source emissions, indicating that urban "continuity" may affect the concentrations of O_3 and $PM_{2.5}$ through non-emissions based mechanisms.

Correlations between urban form factors and air pollutant levels were also carried out at the megapolitan scale. A single significant correlation was found between O_3 concentration and urban "continuity" calculated at the low urban threshold (Table 35a). Higher urban "continuity" was associated with lower concentrations of O_3. No significant correlations were found between urban form factors and air pollutant emissions (Table 35b). From this preliminary analysis it appears that any measurable relationship between urban form and air pollution is more likely to be observed at the metropolitan, rather than megapolitan, scale. One possible explanation is that most vehicular trips are taken within, rather than between, metropolitan areas, making the metropolitan area the more relevant scale at which to assess the influence of urban morphology on air quality.

Air Pollution vs. Control Variables

Multiple significant correlations were found between air pollutants and control variables at the metropolitan scale (Table 36). A single significant positive correlation

was found between the climate factor "temperature" and PM_{10} concentration. The second climate factor, "moisture," was significantly correlated with an increase in O_3 and $PM_{2.5}$ concentration and the emission of O_3 precursors, and a decrease in PM_{10} concentration. These correlations more likely reflect a regional bias rather than a direct link between climate and air pollution. O_3 and $PM_{2.5}$ were found in highest concentration in "moist" metros with varying temperatures, while PM_{10} concentration warm generally higher among metros with warm, dry climates. The negative correlation between PM_{10} concentration and "moisture" may in part be due to the enhanced sensitivity of PM_{10} to precipitation events relative to O_3 and $PM_{2.5}$. The on-road emission of CO_2 was not significantly correlated with either climate factor. In addition to the two climate factors, wind speed was retained as an independent meteorological variable. Correlations between air pollutant concentrations and wind speed were negative – and significant for PM – while air pollutant emissions were unchanged. As wind speed increases, air pollutants are more readily dispersed, lowering their concentration.

Metropolitan population was significantly correlated with a reduction in the per capita non-point source emission of O_3 precursors, $PM_{2.5}$, PM_{10}, and on-road CO_2. While total non-point source emissions generally rise with increasing metropolitan population, emissions per capita decrease significantly in large part due to a reduction in personal transportation and per capita tailpipe emissions (Frank et al. 2000; Grazi et al. 2008). Regional population within 500 kilometers was significantly correlated with an increase in O_3 and $PM_{2.5}$ concentration, and a decrease in $PM_{2.5}$ emissions, PM_{10} concentration and PM_{10} emissions. Because air pollution commonly disperses over hundreds of kilometers,

the region surrounding each metropolitan area can significantly affect that area's air quality. The Inter-urban transport of O_3 and $PM_{2.5}$ within densely populated regions, such as East Coast Megalopolis, can be significant, leading to elevated concentrations among cities in these regions. With less dependency on human activities, however, the concentration of PM_{10} was negatively correlated with regional population, suggesting that the highest PM_{10} levels were located in less-populated regions of the country.

Although an increase in metropolitan area (km^2) generally results in higher total emissions, a moderately significant ($r^2 = -0.214$; $p = 0.48$) negative correlation was found between area and the per capita non-point source emission of O_3 precursors. This result was unexpected given that larger counties are predominately rural, and that areas with lower population densities typically exhibit higher emissions per capita. A scatterplot of the data revealed that the Los Angeles CSA, with a relatively high population density and low per capita emissions, also had the greatest area. The metro with the second greatest area was Las Vegas, which also had relatively low per capita O_3 precursor emission. The two metros skew the relationship such that the overall correlation between metropolitan area (km^2) and per capita O_3 precursor emissions is significant and negative. Additionally, a significant positive correlation was observed between metropolitan area and PM_{10} concentration. The highest concentrations of PM_{10} were located in some of the largest metropolitan areas in terms of geographic size, such as Phoenix, Los Angeles, and Las Vegas.

The final three control variables, industrial emissions of O_3 precursors, $PM_{2.5}$ and PM_{10}, are each used in a particular subset of regression models to control for differences

in point-source manufacturing emissions, which are not expected to be influenced by urban form. Because industrial emissions represent only a limited portion of total emissions, their correlation with ambient concentrations were expected to be minimal and pollutant-specific (i.e. between VOC + NOx emissions and O_3 concentration or between $PM_{2.5}$ emissions and $PM_{2.5}$ concentration). A significant positive correlation was observed between O_3 precursor industrial emissions and O_3 concentration, as anticipated. Significant positive correlations, however, were also found between $PM_{2.5}$ concentration and the industrial emission of O_3 precursors and PM_{10}, in addition to $PM_{2.5}$. Thus, metros with higher industrial emissions of O_3 precursors and PM_{10} also tended to experience higher concentrations of $PM_{2.5}$.

Evaluating Collinearity

A series of correlations were performed to assess the potential for collinearity among independent variables. The first set of correlations included the six urban sprawl indices and the four Ewing et al. (2003) sprawl index components (Table 37). Significant correlations were found between every sprawl index, except Burchfield et al. (2006), which was significantly correlated with Nasser and Overberg (2001) (i.e. USA Today) only. Three of the four sprawl components, with urban centrality as the exception, were also significantly correlated with one another as well as with each sprawl index. Urban centrality, or degree of centeredness, was not significantly correlated with any sprawl index or sprawl component. Centrality, like each of the four sprawl components, is a composite measure of multiple (6) operational variables. These variables included, for example, variation in population density, population within a certain distance of the CBD,

and the dominance of metropolitan sub-centers relative to the CBD. The lack of significant correlation between urban centrality and the other urban sprawl indices and components suggests that centrality offers unique information about urban form not captured by the other measures. Similarly, Burchfield et al. (2006) is the only sprawl index to rely solely on remotely-sensed data. The index provides unique spatial information about the density of residential development and open space across the urban landscape. The high degree of correlation between urban sprawl indices suggests that running all six (with or without the four Ewing sprawl index components) within a single regression model would result in an undesirable level of multicollinearity. Including the four sprawl components within a single, separate model, however, should be acceptable; not only are there fewer correlations among sprawl components, but they each measure unique aspects of urban form.

Significant correlations were also found among most spatial metrics calculated at both the high (Table 1) and low (Table 2) urban thresholds. At the high urban threshold, all spatial metrics were significantly correlated with one another, with the exception of largest patch index (LPI) and the urban "shape complexity" metrics area-weighted mean shape index (AWMSI), area-weighted mean patch fractal dimension (AWMPFD) and landscape shape index (LSI). LPI measures the proportion of the landscape composed of by the largest urban patch. It may be considered a measure of urban continuity as urban areas with a greater proportion of urban landcover within a single, large urban patch typically contain more urban-urban pixel adjacencies. Indeed, when deriving the urban form factors using PCA, LPI loaded high under urban "continuity" at both the high

(Table 5) and low (Table 6) urban threshold. LPI differs from the other measures of urban "continuity," however, in that it does not directly measure urban pixel or patch adjacencies. This may explain why significant negative correlations were not found between LPI and the three urban "shape complexity" metrics. With the exception of LPI, the urban "continuity" metrics, including CONTAG, CLUMPY, CONTIG, and PLADJ were positively correlated with one another and negatively correlated with the urban "shape complexity" metrics ED, AWMSI, AWMPFD, and LSI (Table 1). A similar pattern of correlations was observed for the low urban threshold (Table 2). When high and low thresholds were averaged, significant correlations were observed between all spatial metrics except LSI and AWMPFD (Table 3).

In the regression analyses that follow, the two urban form factors urban "continuity" and urban "shape complexity" were run as independent variables aside a set of control variables. Due to the nature of PCA, the two urban form factors are uncorrelated, but correlations may have existed between urban form factors and control variables. An additional set of correlations between control variables and urban form factors were examined at both the metropolitan and megapolitan scale to assess the potential for multicollinearity. Although significant correlations were found between the urban form factors and controls, they were not strong or numerous enough to warrant concern (Table 38). As already discussed throughout this section, however, the results did yield important insights. At the metropolitan scale, for example, an increase in population was significantly correlated with an increase in urban "shape complexity." A similar pattern was not observed at the megapolitan scale. While urban "shape complexity" was

positively correlated with metropolitan population, urban "continuity" was negatively correlated with regional population (within 500 km) at both the high and low urban threshold at the metropolitan scale, and at the low urban threshold at the megapolitan scale. This reflects the greater degree of regional clustering among high and low values of urban "continuity" relative to high and low values of urban "shape complexity." Metros with low urban "continuity" were clustered along the east coast and mid-south regions of the U.S., which have numerous urban centers and relatively high populations. Finally, urban "shape complexity" exhibited a significant positive correlation with metropolitan area (km^2) and the industrial emission of O_3 precursors, $PM_{2.5}$, and PM_{10} at the metropolitan scale. As measures of urban form, neither urban "continuity" nor urban "shape complexity" are expected to influence industrial emissions directly. Rather, both variables are similarly correlated with metropolitan size; larger metropolitan areas in terms of both population and area tend to exhibit more complex urban shapes, and produce more total emissions from point and non-point sources.

Spatial Metrics: High vs. Low Threshold

A final set of correlations was performed to assess the impact of urban extent on each of the nine spatial metrics at the metropolitan scale. High and low threshold "versions" of all spatial metrics were significantly and positively correlated (along the diagonal) with the exception of contagion (CONTAG) (Table 4). Contagion for any given metro may vary significantly between high and low urban thresholds, and CONTAG calculated at one threshold is not a significant predictor of CONTAG at the other threshold. Unlike the other urban "continuity" metrics, CONTAG was on average higher

when calculated at the low urban threshold due to the presence of large, continuous patches of non-urban land (Table 18). Contagion is a measure of overall landscape continuity and not the continuity of urban patches alone. While urban continuity generally decreased from the high to low urban threshold, the continuity of non-urban lands increased, resulting in an overall increase in CONTAG. Thus, an urban area may have low CONTAG at the high urban threshold, and much higher CONTAG at the low urban threshold, despite a negative or negligible change in the continuity of urban landcover between the two thresholds.

Summary of Correlations

The correlation analysis revealed several important relationships between measures of urban form and air quality. Firstly, there exist significant correlations between levels of multiple air pollutants and sprawl indices, individual spatial metrics, and urban form factors derived from spatial metrics. Although there was some variation in the direction of association, most statistically significant correlations suggested that an increase in urban sprawl or urban sprawl-like morphologies was associated with an increase in both the ambient concentration and per capita non-point source emission of O_3, PM and CO_2. While correlation does not suggest causation, these results do support the hypothesis that urban form may have a measurable effect on regional air quality. Regression analysis is used in the following section to more accurately assess the strength and direction of these relationships by controlling for a number of confounding factors such as variations in climate, population, and industrial emissions.

Secondly, the relationships between measures of urban form and air pollutant levels are influenced by both urban extent (i.e. high and low urban thresholds) and scale (i.e. metropolitan vs. megapolitan). More significant correlations were found between spatial metrics and air pollutant levels at the low urban threshold and at the metropolitan scale. The low urban threshold captures more completely the morphology of the urban area, including that of the outer suburban and exurban realms, potentially resulting in more accurate or comprehensive measures of urban form. The comparison of scale is confounded by the limited number (19) of megapolitan-scale areas available for analysis. Furthermore, sprawl indices have not yet been developed at the megapolitan scale. Calculated for both metropolitan and megapolitan areas, however, the urban form factors urban "continuity" and urban "shape complexity" were clearly affected by scale; 18 significant correlations were found between air pollutants and urban form factors at the metropolitan scale (Table 34), and only one at the megapolitan scale (Table 35)

Thirdly, there exist several significant correlations between independent variables: both spatial metrics and urban sprawl indices. The high potential for multicollinearity between multiple urban sprawl indices justifies running them individually, and with the appropriate control variables, within separate regression models. To address the collinearity among the nine spatial metrics, PCA was used to produce the two uncorrelated urban form factors urban "continuity" and urban "shape complexity," to be run together, with the appropriate control variables, within a single regression model.

Regression Analysis: Metropolitan Scale

Regression Model Set 1

Eight separate regression models (four that include urban form factors calculated at the high urban threshold, and four that include urban form factors calculated at the low urban threshold) were used in regression set 1 to assess the degree of association between the two urban for factors "continuity" and "shape complexity," and four measures of ambient air pollution: O_3 concentration, number of O_3 exceedances, $PM_{2.5}$ concentration and PM_{10} concentration. No significant association ($p < 0.05$) was found between the ambient concentration of air pollutants and urban form factors calculated at either the high (Table 38) or low (Table 39) urban threshold. If a decrease in urban "continuity" and an increase in urban "shape complexity" represent higher levels of urban sprawl, this first set of results do not support the hypothesis that urban areas with morphological features indicative of higher levels of sprawl will exhibit higher ambient concentrations of O_3 and PM. It important to consider, however, that the urban form factors "continuity" and "shape complexity" are limited and very specific spatial attributes of urban form and therefore cannot represent fully the complex nature of urban sprawl.

Several significant associations were found between air pollutant concentrations and control variables. At both the high and low urban threshold a significant positive association was observed between the moisture factor and the concentration of $PM_{2.5}$, and a significant negative association between the moisture factor and the concentration of PM_{10}. The relationship was highly significant for PM_{10} ($p < 0.001$), and moderately significant for $PM_{2.5}$ ($p = 0.046$; $p = 0.037$). One standard deviation increase in the

"moisture" factor resulted in a 0.584 μg/m^3 (4.4 percent) increase in $PM_{2.5}$ concentration and a 2.77 μg/m^3 (10.7 percent) decrease in PM_{10} concentration. Although Elminir (2005) observed that PM_{10} concentration increased with increasing humidity, the "moisture" factor represents additional meteorological variables including annual average precipitation and number of cloudy days. The negative association between PM_{10} and moisture may have therefore resulted from the minimizing effects of precipitation scavenging and vertical mixing associated with cyclonic weather systems, outweighing any positive effect from an increase in relative humidity. The moderate positive association found between moisture and $PM_{2.5}$ may indicate that fine particulate matter is less sensitive to these meteorological processes. However, it may also reflect regional inequities if "moist" regions of the U.S. (i.e. the East vs. the West) are associated with higher $PM_{2.5}$ emissions, resulting in higher $PM_{2.5}$ concentrations.

A significant negative relationship was found between average annual wind speed and the number of O_3 exceedances, concentration of $PM_{2.5}$ and concentration of PM_{10} at both the high and low urban threshold. For every one mph decrease in wind speed at the high urban threshold, the number of annual O_3 exceedances increased by approximately 1.8 days, $PM_{2.5}$ concentration decreased by 0.851 μg/m3 (6.4 percent) and PM_{10} concentration decreased by 1.136 μg/m3 (4.4 percent) (Table 38). Similar associations were observed among models with urban form factors calculated at the low urban threshold (Table 39). An increase in wind speed generally aids the dispersal of locally produced air pollutants, resulting in lower concentrations (Jacob and Winner 2009). With

a wide spatial distribution, however, ozone may be less sensitive to changes in wind speed relative to airborne particulates.

Regional population within 500 km of each metropolitan area was significantly associated with an increase in O_3 concentration, number of O_3 exceedances, and $PM_{2.5}$ concentration. Combining results from high and low threshold models, for each additional ten million residents within 500 km, O_3 concentration increased by 2.87 ppb (3.4 percent) to 2.95 ppb (3.5 percent), number of O_3 exceedances increased between 1.82 days and 1.89 days, and $PM_{2.5}$ concentration increased by 0.61 μg/m3 (4.6 percent) to 0.64 μg/m3 (4.8 percent). PM_{10} concentration was not significantly related to regional population, potentially indicating minimal inter-urban transport. The significance of regional population as a predictor variable of the ambient concentration of O_3 and PM is apparent in this and subsequent regression model sets. If regional population were included in the regression models developed by Ewing et al. (2003) and Stone (2008), it is possible that the associations they observed between components of the Ewing et al. (2003) sprawl index (i.e. residential density, street connectivity, mixed use, and degree of centeredness) and levels of O_3 may have been altered significantly.

A potentially significant ($p = 0.052$) positive association at the high urban threshold and a significant association ($p = 0.043$) at the low urban threshold was found between point-source industrial emissions of the O_3 precursors VOC + NOx, and O_3 concentration. Ozone concentration increased by 0.072 ppb (0.09 percent) for every 1000 ton (5.9 percent) increase in industrial point-source emissions at the high urban threshold, and by 0.075 ppb at the low urban threshold. Industrial emissions represent a limited

portion of total emissions, explaining their weak association with most ambient measures of air pollution. However, having little or no direct link to urban form, industrial emissions represent an important control variable. No significant associations were observed between air pollutant concentrations and the remaining control variables "temperature" and metropolitan population. The latter suggests that ambient levels of O_3 and PM do not vary significantly by population among large metropolitan areas (i.e. > 500,000 population).

Regression Model Set 2

In the second set of regression models, the dependent variables included the annual non-point source emission of the O_3 precursors VOCs + NOx, $PM_{2.5}$, PM_{10}, and CO_2. Four regression models were used to assess the degree of association between air pollutant emissions and the urban form factors "continuity" and "shape complexity" calculated using the high urban threshold (Table 40), and four were used to assess the degree of association between air pollutant emissions and the urban form factors calculated using the low urban threshold (Table 41). The combined non-point emission of the O_3 precursors VOCs and NOx decreased significantly with increasing urban "continuity," as calculated at both the high and low urban threshold. One standard deviation increase in urban "continuity" resulted in an 11,685 ton (6.2 percent) reduction in O_3 precursor emissions at the high urban threshold, and a 10,331 ton (5.4 percent) reduction at the low urban threshold. Changes in urban "continuity" did not significantly affect the emission of PM or CO_2. An increase in urban "shape complexity," as calculated at both the high and low urban threshold, resulted in a significant increase in the emission

of O_3 precursors, $PM_{2.5}$ and PM_{10}. For every one standard deviation increase in urban "shape complexity" at the high urban threshold, O_3 precursor emissions increased by 15,837 tons (8.4 percent), $PM_{2.5}$ emissions increased by 4,402 tons (18 percent), and PM_{10} emissions increased by 26,707 tons (30.6 percent) (Table 40). At the low urban threshold, one standard deviation increase in urban "shape complexity" was associated with a 14,913 ton (7.9 percent) increase in O_3 precursor emissions, a 3,055 ton (12.4 percent) increase in $PM_{2.5}$ emissions, and a 22,096 ton (25.3) increase in PM_{10} emissions (Table 41).

These data support the second research hypothesis that urban areas with morphological features indicative of higher levels of sprawl (i.e. greater urban "continuity" and lower urban "shape complexity") will exhibit higher non-point source emissions of O_3 precursors, PM, and CO2, all other factors equal. Interestingly, however, this effect does not appear to translate into higher ambient concentrations of O_3, $PM_{2.5}$ or PM_{10} (regression model set 1). Thus, although urban "continuity" and "shape complexity" may affect non-point (primarily mobile) source emissions, presumably by altering the length and duration of automotive trips, the large number of non-emissions based mechanisms and confounding variables affecting ambient air quality significantly reduces their influence on the concentration of O_3 and PM as measured at the metropolitan scale.

Variation in urban "continuity" and urban "shape complexity" at the low urban threshold had a slightly weaker effect on the emission of O_3 precursors than at the high urban threshold, as indicated by lower regression coefficients. A single standard deviation increase in urban "continuity," for example, resulted in a 0.8 percent (6.2 - 5.4) greater

decrease in O_3 precursor emissions at the high urban threshold. Similarly, a single standard deviation increase in urban "shape complexity" resulted in a 0.5 percent greater increase in O_3 precursor emissions, a 5.6 percent greater increase in $PM_{2.5}$ emissions, and a 5.3 percent greater increase in PM_{10} emissions at the high urban threshold relative to the low urban threshold. These findings are not in support of the fourth research hypothesis that measures of urban form calculated at the low urban threshold will exhibit a higher degree of association with levels of air pollution. Although the degree of association between urban form factors and air pollutant emissions were similar at both the high and low urban extent, there exists a minimal but discernable trend toward greater association when urban form factors are derived from spatial metrics calculated at the high urban threshold.

Significant positive associations were observed between both metropolitan population and metropolitan area and the emission of all four air pollutants at both the high and low urban threshold. Among models with urban form factors calculated at the high urban threshold, an increase of one million residents was associated with an increase in the non-point emission of 52,835 tons of O_3 precursors (28 percent), 3,616 tons of $PM_{2.5}$ (14.7 percent), 6,374 tons of PM_{10} (7.3 percent), and 1.375 million tons of CO_2 (26.7 percent) (Table 40). Also at the high urban threshold, each standard deviation increase in geographic area (12,969 km^2) was associated with a 23,980 ton (12.7 percent) increase in O_3 precursor emissions, a 4,785 ton (19.5 percent) increase in $PM_{2.5}$ emissions, a 22,397 ton (25.6 percent) increase in PM_{10} emissions, and an 86.062 ton (21.7 percent) increase in CO_2 on-road emissions (Table 40). Similar increases in

pollutant emissions associated with an increase in metropolitan population and area were observed among "low threshold" models (Table 41). As expected, larger metropolitan areas in terms of both population and geographic size were associated with higher non-point emissions of O_3 precursors, PM and CO_2.

In the first set of regression models, the "moisture" factor was associated with a significant increase in the ambient concentration of $PM_{2.5}$, and a significant reduction in the concentration of PM_{10}. In this second set of regression models, the "moisture" factor was positively related to the emission of O_3 precursors and $PM_{2.5}$ at the high threshold (Table 40), and O_3 precursors, $PM_{2.5}$, and PM_{10} at the low threshold (Table 41). These results suggest that metropolitan areas that exhibit relatively high levels of "moisture" (i.e. abundant rainfall, high humidity) tend to be associated with higher O_3 precursor and PM emissions. While this may have resulted in a higher ambient concentration of $PM_{2.5}$, as observed in regression model set 1, the ambient concentration of O_3 was unaffected. Most surprisingly, the ambient concentration of PM_{10} decreased significantly with increasing "moisture," despite a significant reduction in PM_{10} non-point source emissions with increasing "moisture." Any increase in PM_{10} concentration that may have resulted from the elevated non-point emission of PM_{10} among "moist" metropolitan areas therefore appears to have been offset by rain scavenging and other meteorologically-related mechanisms. The result is that an increase in "moisture" is significantly associated with a decrease in the ambient concentration of PM_{10}.

Regression Model Set 3

Regression model set 3 contains 24 regression models used to evaluate the degree of association between pollutant concentration and urban sprawl as measured using six separate urban sprawl indices. The first four regression models include as the independent variable the Ewing et al. (2003) composite sprawl index (Table 42). When controlling for other factors, a significant negative association was found between the Ewing et al. sprawl index and the ambient concentration of O_3, $PM_{2.5}$, and the number of annual O_3 exceedances. Because larger values of the Ewing et al. sprawl index indicate lower levels of urban sprawl, higher levels of sprawl were associated with significantly higher ambient concentrations of O_3 and $PM_{2.5}$. A significant relationship was not found between the Ewing et al. sprawl index and the ambient concentration of PM_{10}. Given that the standard deviation in the urban sprawl score among Ewing et al.'s original sample of 83 metropolitan areas was 25 units, a single standard deviation increase in urban sprawl (i.e. a decrease of 25 units) was associated with a 2.625 (-25*-0.105) ppb (3.2 percent) rise in O_3 concentration, an increase of 3.9 high ozone days, and an increase in $PM_{2.5}$ concentration of 1.025 $\mu g/m^3$ (7.8 percent).

Using the 45 most populous metropolitan areas in the U.S., Stone (2008) found that one standard deviation increase in the Ewing et al. sprawl index was associated with an increase of 6.6 high ozone days. Despite variations in the number and type of control variables, the number of metropolitan areas analyzed, and the range of years for which air quality data were collected, the results presented here and those of Stone (2008) are quite similar. Stone (2008) reported that the average number of ozone exceedances for 45

metropolitan areas between 1990 and 2002 was 15.1 days. An increase of 6.6 days was therefore equivalent to a 43.7 percent increase in the number of high ozone days per year. This is nearly equal to the 44.7 percent increase reported here.

In the second group of regression models (Table 43), urban sprawl was assessed using the Sutton (2003) sprawl index calculated at a high urban threshold. The Sutton index, like the Ewing et al. index, uses an inverse scale; lower sprawl scores indicate higher levels of sprawl. Among the 84 metropolitan areas included in this study for which Sutton (high threshold) urban sprawl scores were available, a decrease of approximately 26 units represents a single standard deviation increase in urban sprawl. Degree of urban sprawl is evaluated by the Sutton sprawl indices using the percent deviation of a given urban area from the average or "expected" population density of 300 urban areas in the U.S. It is therefore a relative measure of population density for U.S. cities. One standard deviation increase in urban sprawl according to the Sutton (high threshold) index was associated with a 1.65 ppb (2 percent) increase in ambient O_3 concentration and an additional 3.22 high ozone days per annum. The Sutton (high threshold) sprawl index was not significantly associated with the ambient concentration of either $PM_{2.5}$ or PM_{10}.

Similar significant associations were found between the Sutton sprawl index calculated at a low urban threshold and levels of O_3 (Table 44). For every one standard deviation increase in urban sprawl (equal to approximately -32 units at the low urban threshold), ambient ozone concentration rose by 2.24 ppb (2.7 percent), and number of annual ozone exceedances increased by 3.37 days. Significant associations were not observed between the Sutton (low threshold) sprawl index and the concentrations of

$PM_{2.5}$ and PM_{10}. Thus, urban areas that exhibit higher levels of urban sprawl, as defined as having lower than average population densities, can expect to experience slightly higher O_3 concentrations and similar levels of PM compared with cities with lower levels of urban sprawl. As also observed with urban form factors in regression model set 1, urban extent does not appear to have significantly affected the degree of association between urban form and the ambient concentrations of O_3 and PM.

The Lopez and Hynes (2003) sprawl index was also significantly associated with the ambient concentration and number of annual exceedances of O_3 (Table 45), but not the ambient concentration of $PM_{2.5}$ or PM_{10}. In the Lopez and Hynes (2003) index, increasing levels of urban sprawl are represented by larger index values. For the 85 metropolitan areas included in this study for which Lopez and Hynes' sprawl scores were available, a single standard deviation increase in urban sprawl is equal to 21 units. One standard deviation increase in urban sprawl according to the Lopez and Hynes sprawl index was associated with a 2.184 ppb (2.6 percent) rise in O_3 concentration, and an additional 3.44 ozone exceedances per year.

The sprawl index developed by Nasser and Overberg (2001) was significantly associated with O_3 concentration only (Table 46). With a standard deviation of 112.7 units, as calculated using the 86 metropolitan areas included in this study, a single standard deviation increase in urban sprawl was associated with a 1.803 ppb (2.1 percent) rise in O_3 concentration. While the methodologies vary, the indices developed by Nasser and Overberg (2001), Lopez and Hynes (2003), and Sutton (2003) are all based on population density. The results collectively indicate that residential population density

calculated at the metropolitan scale is an important predictor of ozone concentration, but is not significantly related to the concentration of either fine (PM2.5) or course (PM10) particulates. Population density, although a key component of urban sprawl, may therefore have a unique – if not singular – effect on ozone.

The Burchfield et al. (2006) index was the only one of six urban sprawl indices not significantly associated with the ambient concentration of O_3 or PM (Table 47). The Burchfield et al. (2006) index differs from the proceeding four indices in that it measures the density of residential land use rather than residential population. Furthermore, it is based on remotely-sensed land cover data rather than census-derived demographic data. In addition to these fundamental methodological differences, the Burchfield et al. sprawl index was applied to only 40 metropolitan areas, which limits the statistical power of the regression models. The data used in the Burchfield et al. sprawl index, from 1992, is also temporally removed from the air quality data (1998 – 2002) by 6 to 10 years. Each of these factors may have contributed to the index's poor predictive power in this analysis.

To summarize, five of the six sprawl indices indicated a significant rise in O_3 concentration (average 8-hour 4^{th} maximum) of between 1.65 ppb (2 percent) and 2.625 ppb (3.1 percent) for every one standard deviation increase in urban sprawl. Four sprawl indices were also significantly associated with the number of annual O_3 exceedances, indicating that an increase of one standard deviation in urban sprawl may result in an additional 3.22 to 3.9 ozone exceedances (i.e. O_3 concentration > 75 ppb) per year. Only the Ewing et al. (2003) composite sprawl index was significantly associated with $PM_{2.5}$ concentration. As the only sprawl index derived from multiple independent measures of

urban sprawl, the significant associations between the Ewing et al. sprawl index and the ambient concentrations of both O_3 and $PM_{2.5}$ provides evidence in support of the third research hypothesis that composite sprawl indices that incorporate multiple measures of urban form will have a higher degree of association with levels of air pollutants that sprawl indices that incorporate only a single measure (e.g. residential density).

All six control variables were significantly associated with the ambient concentration of O_3 and/or PM in at least one regression model of this set. In four out of six regression models in which O_3 concentration was the dependent variable, an increase in the "temperature" factor was significantly ($p < 0.05$) associated with an increase in ambient O_3 concentration. Specifically, for each one standard deviation increase in the "temperature" factor, O_3 concentration rose between 1.815 ppb (2.2 percent) and 2.364 ppb (2.8 percent). To provide perspective, a single standard deviation in the "temperature" factor is equivalent to the difference in "temperature" between Greensboro, NC (+0.06 sd) and Dallas, TX (+1.08 sd).

All other factors equal, an increase in temperature is expected to increase ambient levels of O_3 by accelerating the photochemical reaction that produces the secondary air pollutant. The lack of significant association between temperature and O_3 concentration among regression models in set 1 was unexpected. The "temperature" factor, however, is not equivalent to a simple measure of average temperature, as it also takes into account variability among the meteorological variables maximum temperature, heating degree days, and cooling degree days. Temperature and temperature-related parameters have less

effect on the ambient concentration of PM, which is released directly into the atmosphere as a primary air pollutant.

The second climate factor, "moisture," was significantly associated with a reduction in PM_{10} concentration in all six regression models with PM_{10} concentration as the dependent variable. The "temperature" factor was not significantly associated with either $PM_{2.5}$ or O_3 concentration. For every standard deviation increase in the "moisture" factor, PM_{10} concentration declined between 2.61 $\mu g/m^3$ (10 percent) and 4.12 $\mu g/m^3$ (16 percent). Presumably, the negative association between PM_{10} and the "moisture" factor is attributable primarily to heightened precipitation scavenging and wet deposition of coarse particulates in "moist" metropolitan areas (i.e. areas with abundant rainfall, high humidity).

Where significant associations were found, wind speed was consistently negatively related to air pollutant concentrations. Although no significant association was found between wind speed and O_3 levels as measured in terms of ambient concentration, a significant relationship was found between wind speed and number of annual O_3 exceedances in four out of six regression models. For every 1 mph increase in average annual wind speed, the number of annual O_3 exceedances declined between 1.335 and 1.861 days. The ambient concentration of PM_{25} declined in all six regression models by a magnitude of 0.606 $\mu g/m^3$ (4.6 percent) to 0.884 $\mu g/m^3$ (6.7 percent), and PM_{10} declined in three of six regression models by 1.005 $\mu g/m^3$ (3.9 percent) to 1.139 $\mu g/m^3$ (4.4 percent) in response to every 1 mph increase in wind speed.

Metropolitan area population was significantly associated with a rise in $PM_{2.5}$ concentration in a single model involving the Ewing et al. sprawl index (Table 42). For every 1 million person increase in metropolitan population, $PM_{2.5}$ concentration increased by 0.245 $\mu g/m^3$ (1.8 percent). Likewise, in a single regression model involving the Sutton (high) sprawl index (Table 43), a 1 million person increase in metropolitan population was associated with an additional 0.561 O_3 exceedances per annum.

Regional population within 500 km was significantly associated with an increase in O_3 concentration, number of annual O_3 exceedances, and $PM_{2.5}$ across all six groups of regression models in Set 3 (Tables 42-47). Regional population within 500 km was not significantly associated with PM_{10} concentration in any model. For every 10 million person increase in regional population – approximately the difference in regional population between Las Vegas, NV (45 million) and Lexington, KY (55 million) – O_3 concentration increased between 2.92 ppb (3.5 percent) and 3.61 ppb (4.3 percent), number of annual O_3 exceedances rose between 1.57 to 2.41 days, and PM_{25} increased between 0.48 $\mu g/m^3$ (3.6 percent) and 0.63 $\mu g/m^3$ (4.8 percent).

Finally, point-source industrial emissions were positively associated with O_3 concentration in two regression models within this set: one involving the Lopez and Hynes sprawl index (Table 45); the other the Nasser and Overberg sprawl index (Table 46). The point-source industrial emissions control variable differs depending on the dependent variable; in these two models, the variable refers to the combined emission of the O_3 precursors VOCs and NOx by industrial point-sources. Thus, for every 10,000 ton ($\approx$ 60 percent of the mean) increase in the combined industrial point-source emission of

VOCs and NOx, ambient O_3 concentration is expected to rise between 0.16 ppb (0.2 percent) and 0.80 ppb (1.0 percent).

Regression Model Set 4

The fourth set of regression models assess the strength of association between the ambient concentration of air pollutants and the four components of the Ewing et al. (2003) urban sprawl index: street connectivity, centrality, mixed use, and residential density (Table 48). As with the composite sprawl index, each of the four components is scaled with a mean of 100 and a standard deviation of 25 units. For all four components, an increase in value indicates a reduction in "sprawl-like" conditions. Out of the four components of urban sprawl, only residential density was a significant predictor variable, and only in association with O_3 concentration and number of annual O_3 exceedances. One standard deviation increase in residential density was associated with a decrease in average annual (4^{th} maximum, 8 hour) O_3 concentration of 5.725 (25*-0.229) ppb (6.8 percent), and a reduction of 8.125 high ozone days (>75 ppb) per year.

Using the same modeling procedure, but with a different set of control variables, Ewing et al. (2003) found that both a decrease in residential density and an increase in mixed use development were significantly associated with an increase in O_3 concentration as measured in 1999. Specifically, Ewing et al. (2003) calculated a 15 ppb decrease in O_3 concentration per standard deviation increase in residential density, and a 3 ppb increase in O_3 concentration per standard deviation increase in mixed use development. The discrepancy in the strength of association between residential density and O_3 concentration found by Ewing et al. (2003) and those of the current study may be

attributed to differences in the number of metropolitan areas used, the range of years the air quality data was taken (i.e. 1999 in Ewing et al. vs. 1998 – 2002 here), and the control variables used. The only control variable used in both Ewing et al. (2003) and the current study is metropolitan population. While metropolitan population is a significant predictor of O_3 concentration in both studies, Ewing et al.'s models did not contain additional significant control variables. In the current study, both the "temperature" factor and regional population within 500 km were significant predictors of O_3 concentration. Under the influence of these additional significant control variables, the strength of association between residential density and O_3 concentration may have been reduced. Furthermore, the relationship between residential density and O_3 concentration may not have been as accurately assessed when using air pollutant data from a single year (1999), due to the potential for significant annual fluctuations (Bereitschaft 2008).

Expecting a decrease rather than an increase in O_3 concentration with increasing mixed use development, Ewing et al. (2003) suggested that an increase in the fine-grain mix of urban land uses could contribute to a rise in air pollution by encouraging "more short vehicle trips and hence more cold starts and hot soaks." Given that the positive relationship between mixed use and O_3 concentration was "barely significant," Ewing et al. further postulated that the mixed use measure may not have been "successfully operationalized," or the results may simply be spurious. While in the current study the mixed use component was not found to be significantly associated with O_3 or PM concentration, it is interesting to note that, in accordance with Ewing et al.'s findings, all such associations are positive (Table 48).

Stone (2008) conducted a similar analysis, choosing to run each of Ewing et al.'s four sprawl components (as well as the composite sprawl index) in separate regression models, along with the two control variables average annual O_3 season temperature and metropolitan population. Running each component separately, Stone (2008) found a significant negative association between number of annual ozone exceedances and both residential density and street connectivity. According to Stone (2008), a single standard deviation increase in residential density is associated with 14.8 additional ozone exceedances per year, while a single standard deviation increase in street connectivity is associated with 5.4 additional ozone exceedances. This is nearly double the 8.125 additional ozone exceedances associated with a 25-unit increase in residential density found in this study. The discrepancy in the number of predicted ozone exceedances between studies appears to be primarily the result of averaging the air quality data over two different sets of years (i.e. 1990-2002 in Stone (2008), 1998-2002 here). Between 1990 and 2002, annual ozone exceedances averaged approximately 15.1 days per year (Stone 2008). An additional 14.8 ozone exceedances therefore represents a 98 percent increase from the mean. Due to a decline in ozone levels throughout the 1990s, the average number of ozone exceedances between 1998 and 2002 was 8.72 days. Thus, an additional 8.125 ozone exceedances per year represents a 93 percent increase from the mean; within only 5 percent of Stone's (2008) estimate of a 98 percent increase. Additionally, Stone (2008) ran each of the four sprawl components in separate regression models, whereas in the current study all four components were run together within a single model. If the four sprawl components were run in separate models, as per Stone

(2008), the results of this study would have also indicated a significant ($p = 0.008$) decrease in ozone exceedances per 25-unit increase in street connectivity.

The results of regression model set 4, in conjunction with the findings of Ewing et al. (2003) and Stone (2008), indicate that residential density is an important – if not the most important – component of urban form in regard to air pollution. However, since a significant association between residential density and PM concentration was not found, this statement may only apply to the ambient concentration of O_3. From regression model set 3 (Table 42), the concentration of fine particulate matter ($PM_{2.5}$) is negatively associated with the composite Ewing et al. (2003) sprawl index, suggesting that $PM_{2.5}$ may be significantly affected by urban form, but less sensitive than O_3 to residential density and the three other sprawl components in the Ewing et al. (2003) sprawl index.

In addition to the four components of urban sprawl, all control variables except point-source industrial emissions were significant in at least one of four models (Table 48). Consistent with previous models, the "temperature" factor was significantly associated with O_3 concentration only. For each standard deviation increase in "temperature," O_3 concentration increased by 2.592 ppb (3.1 percent). The "moisture" factor was significantly associated with PM_{10} concentration only, with one standard deviation rise in "moisture" associated with a 2.876 $\mu g/m^3$ (11.1 percent) decrease in PM_{10} concentration. A significant reduction in $PM_{2.5}$ concentration of 0.640 $\mu g/m^3$ (1.3 percent) was also found per 1 mph increase in wind speed. Both metropolitan population and regional population within 500 km were significantly associated with a increase in O_3 concentration, number of annual O_3 exceedances, and $PM_{2.5}$ concentration. Each

additional 1 million residents was associated with a rise in O_3 concentration of 1.372 ppb (1.6 percent), an additional 2.426 O_3 exceedances per year, and a 0.569 μg/m^3 (4.3 percent) increase in $PM_{2.5}$ concentration. Finally, an increase of 10 million residents within 500 km was associated with a 2.72 ppb (3.2 percent) increase in O3 concentration, an additional 1.46 ozone exceedances per year, and a 0.43 μg/m^3 (3.2 percent) increase in $PM_{2.5}$ concentration.

Regression Model Set 5

The relationships between urban sprawl and the non-point source emission of the O_3 precursors VOCs and NOx, $PM_{2.5}$, PM_{10}, and "on-road" CO_2 in 2000 were explored in the fifth set of regression models. In each regression model, the independent variables included one of six urban sprawl indices and four control variables: the climate variables "temperature" factor and "moisture" factor, metropolitan population, and geographic area (km^2). Two significant ($p < 0.05$) associations were found between air pollutant emissions and urban sprawl indices: a significant negative relationship between the Sutton (low threshold) sprawl index and the non-point emission of $PM_{2.5}$ and PM_{10} (Tables 49-54). For every standard deviation decrease in urban sprawl, according to the Sutton (low threshold) sprawl index (i.e. +32 units), the non-point emission of $PM_{2.5}$ decreased by 106 tons and PM_{10} decreased by 558 tons. The average non-point emission of $PM_{2.5}$ for the 76 metropolitan areas included in this model (i.e. the 76 metropolitan areas for which Sutton (low threshold) sprawl index scores were available) was 24,500 tons. The average non-point source emission of PM_{10} was 87,300 tons. Thus, for the average metropolitan area, a single standard deviation increase in urban sprawl according to the Sutton (low

threshold) sprawl index is associated with a 0.41 percent rise in non-point $PM_{2.5}$ emissions and a 0.63 percent rise in PM_{10} emissions.

The lack of significant association between five of the six sprawl indices and the non-point emission of O_3 precursors, $PM_{2.5}$, PM_{10}, and CO_2 was unexpected. Although Stone (2008) also did not find a significant association between urban sprawl, as measured using the Ewing sprawl index, and the emission of the ozone precursors VOCs + NOx, he used total emissions rather than non-point source emissions only. Because total emissions include point-sources such as power plants and large industrial operations that are not expected to be as significantly affected by urban form as non-point (primarily mobile) sources, a lower degree of association between emissions and urban form may be expected when using total emissions rather non-point source emissions only. This rational provides a partial explanation as to why the p-value found here ($p = 0.169$) regarding the relationship between the Ewing et al. (2003) sprawl index and non-point O_3 precursor emissions is substantially lower than that found by Stone (2008) ($p = 0.300$) when assessing the relationship between the Ewing et al. (2003) sprawl index and total O_3 precursor emissions.

In regression model set 3, several significant associations were found between urban sprawl indices and the ambient concentration of air pollutants, primarily O_3 (also measured in terms of mean annual exceedances). The largely non-significant associations found between the non-point emission of air pollutants and urban sprawl indices therefore suggests, as hypothesized by Stone (2008), that the ambient concentration of O_3 and $PM_{2.5}$ may be affected by urban form through non-emissions-based mechanisms. Stone

(2008) hypothesized that these non-emissions-based mechanisms may include the effect of urban form on the UHI phenomenon, and differences in the spatial arrangement of air quality monitoring stations in low-density, scattered cities relative to high-density, centralized cities. Because only non-point source emissions were included in this study, however, there exists the possibility that some point-source emissions (e.g. those from power plants) may be more strongly affected by urban form than anticipated. This may help explain why sprawl indices like Ewing et al. (2003) are significant "predictors" of O_3 and $PM_{2.5}$ concentration, but not of O_3 precursor and $PM_{2.5}$ non-point source emissions.

Among the four control variables included in this set of regression models, metropolitan population was the most significant predictor of air pollutant emissions. Metropolitan population was highly significant ($p \leq 0.001$) in 23 of 24 regression models, accounting for much of the model's predictive power. The adjusted R^2 of the first regression model of the set (Table 49), for example, would decline from 0.946 to 0.484 if metropolitan population were eliminated. A similar pattern was observed for regression models in sets 2 and 6, both with air pollutant emissions as the dependent variable. An increase of one million residents per metropolitan area was associated with an increase in the non-point emission of between 53,928 (28.5 percent) and 57,788 tons (30.6 percent) of the O_3 precursors VOCs and NOx, 3,990 (16.3 percent) and 4,570 tons (18.6 percent) of $PM_{2.5}$, 8,162 (9.3 percent) and 13,001 tons (14.9 percent) of PM_{10}, and between 1.239 million (36 percent) and 1.435 million tons (41 percent) of on-road CO_2.

Statistically significant ($p < 0.05$) in 23 of 24 regression models, geographic area was also a strong predictor of air pollutant emissions. Larger metropolitan areas in terms of area, as well as population, are expected to produce and emit a greater quantity of O_3 precursors, PM, and on-road CO_2, all other factors equal. One standard deviation increase in geographic area (12,969 km^2) was associated with an increase of between approximately 18,714 (9.9 percent) and 29,270 tons (15.5 percent) of O_3 precursors, 4,773 (19.5 percent) and 6,381 tons (26 percent) of $PM_{2.5}$, 22,825 (26 percent) and 31,385 tons (36 percent) of PM_{10}, and between 0.954 (27 percent) and 1.883 million tons (54 percent) of on-road CO_2 emissions. For comparison, a single standard deviation in geographic area among the 86 largest MSAs and CSAs in the U.S. (12,969 km^2) is equivalent in size to the Greensboro—Winston-Salem—High Point, NC CSA.

Of the two climatic control variables "temperature" factor and "moisture" factor, only "moisture" was significantly associated with air pollutant emissions in regression model set 5. The "moisture" factor was significantly associated with an increase in the non-point emission of O_3 precursors in five of six models, and an increase in the non-point emission of $PM_{2.5}$ in a single model that included the Lopez and Hynes (2003) sprawl index. An increase in one standard deviation of the "moisture" factor was associated with a 15,007 (7.9 percent) to 18,391ton (9.7 percent) rise in the non-point emission of O_3 precursors, and a 2,993 ton (12.2 percent) increase in the non-point emission of $PM_{2.5}$ when the Lopez and Hynes (2003) sprawl index was included as an independent variable (Table 52).

Regression Model Set 6

The sixth and final set of regression models at the metropolitan scale was used to assess the degree of association between the non-point emission (year 2000) of the O_3 precursors VOCs and NOx, $PM_{2.5}$, PM_{10} and on-road CO_2, and the four components of the Ewing et al. (2003) urban sprawl index: street connectivity, centrality, mixed use, and residential density (Table 55). Each of the four components represents a separate measure of urban form and a unique way of evaluating specific attributes of urban sprawl. As previously mentioned, the components have a mean value of 100 and a standard deviation of 25. Higher values represent less sprawl-like conditions (i.e. higher residential density, greater centrality, more mixed use, and greater street connectivity).

Residential density was the only significant urban sprawl component when all four components were run together in one model (Table 55). A single significant relationship was found between residential density and the on-road emission of CO_2. One standard deviation increase in residential density was associated with a 2.5 million ton reduction in on-road CO_2 emissions in 2000. That is, for every standard deviation increase in residential density, the average large (i.e. 500,000+ population) metropolitan area could expect to produce approximately 2.5 million tons fewer on-road-related (i.e. primarily automotive) CO_2 emissions, equivalent to a 49 percent reduction from the mean. Although no significant association between the four urban sprawl components and the non-point emission of O_3 precursors and PM were found when running all four sprawl components in a single model, Stone (2008) reported a significant ($p = 0.02$) negative association between residential density and O_3 precursor emissions when running each

sprawl component in a separate model. Attempting to recreate this result, residential density was run in a separate regression model, yielding a potentially significant ($p = 0.074$) negative association. Only when the geographic area (km^2) control variable was eliminated from the model was a similar significant ($p = 0.01$) relationship found between residential density and O_3 precursor emissions. It should be noted, however, that in this dissertation only non-point emissions were used, whereas Stone (2008) used total O_3 precursor emissions. This exercise demonstrates the potential for misleading results when significant confounding factors are omitted. The additional confounding factors controlled for in this set of regression models, relative to Stone (2008), include the "moisture" factor, geographic area, and the individual sprawl components themselves. The addition of these variables should provide a more accurate assessment of the relationships between sprawl components and air pollutant emissions.

The non-significant relationships between the four sprawl components and the emission of O_3 and PM lend further support to the hypothesis proposed by Stone (2008) that urban form affects air quality through additional mechanisms other than air pollutant emissions. Mentioned earlier in regression set 5, it is also possible that these components fail to operationalize the aspects of urban form that have the greatest or most direct impacts on the non-point emission of O_3 precursors and PM. This competing hypothesis seems unlikely at this juncture, however, given that 1) it is improbable that all four distinct components of Ewing et al.'s urban sprawl index would fail to operationalize in a meaningful way the spatial configurations that affect the non-point emission of O_3 precursors and PM, and 2) Ewing et al. found significant associations between all four

components and multiple travel and transportation outcomes, including a significant positive association between residential density and average vehicle ownership, VMT per capita, and use of public transportation, all of which suggest that these components of urban form directly impact the non-point source emission of air pollutants associated with tailpipe exhaust, including O_3 precursors and PM. The incongruity between the significant associations found earlier between urban sprawl and air pollutant concentrations (particularly O_3) and the lack of significant association between urban sprawl (and urban sprawl components) and air pollutant non-point emissions therefore remains unresolved. Interestingly, the reverse situation was observed for the urban form factors "continuity" and "shape complexity," which, if considered at once, were significantly related to the non-point emission of O_3 precursors, $PM_{2.5}$ and PM_{10}, but not their ambient concentrations.

Similar to regression model set 5, metropolitan population and geographic area were the two most significant control variables (Table 55). A highly significant ($p < 0.001$) positive association was found between metropolitan population and the non-point emission of O_3 precursors, $PM_{2.5}$ and CO_2. An increase of one million people per metropolitan area was associated with a 61,841 ton (32.7 percent) increase in the non-point emission of O_3 precursors, a 4,441 ton (33.6 percent) increase in $PM_{2.5}$ non-point emissions, and a 1.975 million ton (38.4 percent) increase in on-road CO_2 emissions. Despite the non-significant ($p = 0.152$) relationship between metropolitan population and the non-point emission of PM_{10}, the associated increase in PM_{10} of 9,654tons (11 percent) per 1 million increase in population is similar to other models in which metropolitan

population was a significant predictor of PM_{10} emissions. Geographic area was significant across all four models. For each standard deviation increase in geographic area (12,969 km^2), non-point O_3 precursor emissions increased by 18,105 tons (9.6 percent), $PM_{2.5}$ by 4,786 tons (19.5 percent), PM_{10} by 25,873 tons (29.6 percent), and on-road CO_2 by 729,117 tons (14.2 percent). Finally, one standard deviation increase in the "moisture" factor was significantly associated with a rise in the non-point emission of O_3 precursors equal to 17,402 tons (9.2 percent). The "temperature" factor was not significantly related to the emission of air pollutants within this set of regression models.

Metropolitan Scale Summary

At the metropolitan scale, several significant associations were found between urban form/ urban sprawl and the ambient concentration and non-point emission of air pollutants. The two urban form factors urban "continuity" and "shape complexity," while not significant predictors of ambient pollutant concentration (set 1), were significantly related to the non-point emission of O_3 precursors and PM (set 2). Urban "continuity" was significantly associated with a decrease in O_3 precursor emissions, while "shape complexity" was significantly associated with an increase in O_3 precursors, $PM_{2.5}$, and PM_{10}. Thus, the non-point (largely automotive-based) emission of O_3 precursors and PM, but not their ambient concentrations, generally increased as large metropolitan areas exhibited less continuous, more complex spatial patterns.

The relationships between the two urban form factors "continuity" and "shape complexity," and both the ambient concentration and non-point emission of air pollutants was not significantly affected by differences in urban threshold. No significant

association was found between urban form factors and the ambient concentration of air pollutants at either the high or low urban threshold (Table 38 and 39), and the same four significant associations were found among urban form factors and the emission of air pollutants at both urban thresholds (Table 40 and 41). Differences in urban threshold may therefore have a significant effect on the value of individual spatial metrics (e.g. edge density, landscape shape index), but represented as urban form factors, their overall association with air pollutant levels appears largely unchanged.

The relationships between individual sprawl indices and the ambient concentration (set 3) and non-point emission (set 5) of air pollutants exhibited a different pattern. While spatial-metric-derived urban form factors were more strongly related to non-point emissions, sprawl indices were more strongly associated with ambient concentration. Although an increase in urban sprawl, as measured by five of the six sprawl indices, was associated with an increase in the ambient concentration of at least one of three air pollutants, only two significant relationships were found between sprawl indices and non-point emissions. Among the six sprawl indices, the Ewing et al. (2003) composite sprawl index appeared to be the best overall predictor of air pollutant concentrations, with a significant negative relationship (lower scores represent higher levels of sprawl) with O_3 concentration, number of annual O3 exceedances, and $PM_{2.5}$ concentration. Three sprawl indices, including Sutton (high threshold) (2003), Sutton (low threshold) (2003), and Lopez and Hynes (2003) indicated a significant positive relationship between increasing levels of sprawl and O_3 concentration and number of annual O_3 exceedances. The sprawl index developed by Nasser and Overberg (2001) was

significantly associated with O_3 concentration only, while Burchfield et al.'s (2006) index was not significant. Out of the four components of the Ewing et al. (2003) sprawl index, only residential density was significantly related to air pollutant levels, including the concentration and number of annual exceedances of O_3 (Table 48) and the on-road emission of CO_2 (Table 55).

At least one control variable was found significant in each model at the metropolitan scale. Among models in which the ambient concentration of air pollutants was the dependent variable (sets 1, 3, and 4), regional population within 500 km was the most consistently significant control variable. Among models in which the non-point source emission of air pollutants was the dependent variable (sets 2, 5, and 6), metropolitan population and geographic area (km^2) were the two most consistently significant control variables. Among all models in which the control variables were present and significant, an increase in population within 500 km, metropolitan population, and metropolitan geographic area was associated with a significant increase in air pollution. In regression model set 3 and 4, the "temperature" factor was also significantly associated with an increase in O3 concentration, while an increase in the "moisture factor" was consistently negatively associated with PM_{10} concentration in regression model sets 1, 3 and 4. Across regression model sets 1, 3 and 4, wind speed was regularly associated with a significant reduction in the ambient concentration of multiple air pollutants, but most consistently $PM_{2.5}$.

Together, the results of regression model sets 1 through 6 generally support the first three research hypotheses. Regarding the first hypothesis (H1), urban areas with

morphological features indicative of higher levels of sprawl, as evaluated in terms of urban form factors or urban sprawl indices, either exhibited a significant increase or no significant change in the ambient concentration of O_3 or PM. Among 36 regression models in which ambient concentration was the dependent variable, not a single model indicated a significant decrease in air pollutant concentration with increasing urban sprawl, while 12 models indicated a significant increase. In support of the second hypothesis (H2), urban areas with morphological features indicative of higher levels of sprawl either exhibited a significant increase or no significant change in the non-point source emission of the O_3 precursors VOCs and NOx, $PM_{2.5}$, PM_{10} and on-road CO_2. Once again, no regression models indicated a decrease in air pollutant emissions with increasing urban sprawl, while 9 of 36 models indicated an increase.

The Ewing et al. (2003) composite sprawl index, which includes the four urban sprawl components residential density, street connectivity, mixed used, and degree of centeredness, was the only index significantly associated with the concentration of both O_3 and $PM_{2.5}$ (Table 42). However, the Sutton (low threshold) index was the only urban sprawl index significantly associated with air pollutant emissions (Table 51). Furthermore, the urban form factor urban "shape complexity" was significantly associated with a rise in O_3 precursor emissions, $PM_{2.5}$ and PM_{10} emissions at both the high and low urban threshold. The Ewing et al. index therefore preformed best at predicting air pollutant concentrations, but not air pollutant emissions. These results lend only partial support to the third research hypothesis (H3) that composite sprawl indices

(i.e. Ewing et al.) will exhibit a stronger association with levels of air pollutants than indices that incorporate a single measure of urban form.

The fourth research hypothesis (H4) that measures of urban form (i.e. urban form factors) calculated at the low urban threshold will exhibit a higher degree of association with levels of air pollutants than those calculated at the high urban threshold was not supported by these results. In regression model sets 1 and 2, urban extent (i.e. high vs. low urban threshold) did not significantly affect the degree of association between urban form factors and the ambient concentration or non-point source emission of air pollutants. The fifth research hypothesis (H5) will be addressed following the megapolitan scale results (below).

Regression Analysis: Megapolitan Scale

Regression Model Set 1

Regression model sets 1 and 2 at the megapolitan scale are identical in form to sets 1 and 2 at the metropolitan scale. The regression models in set 1 were used to assess the degree of association between urban form as measured using the two urban form factors urban "continuity" and urban "shape complexity," and the ambient concentration of O_3, $PM_{2.5}$ and PM_{10} (Table 56 and 57) Out of eight regression models, only a single potentially significant association ($p = 0.052$) was observed between urban form factors and air pollutant concentrations (Table 56). One standard deviation increase in urban "shape complexity" calculated at the high urban threshold was associated with a 1.441 $\mu g/m^3$ increase in $PM_{2.5}$ concentration. This represents an 11 percent increase from the mean concentration of 13.0 $\mu g/m^3$. No significant associations were observed between

urban form factors calculated at the low urban threshold and the ambient concentration of air pollutants. As expected, however, a positive trend was observed between air pollutant concentration and urban "shape complexity" in all eight regression models (both high and low threshold). The relationships between urban "continuity" and air pollutant concentrations were mixed with negative associations for O_3, and positive associations for $PM_{2.5}$ and PM_{10}. That is, as urban "continuity" increased at both the high and low urban threshold, O_3 concentration and number of O_3 exceedances trended downward, while the concentrations of $PM_{2.5}$ and PM_{10} trended upward. The concentration of all three air pollutants were expected to decrease with increasing urban "continuity."

Regional population within 500 km was significantly associated with an increase in air pollutant concentration in all but a single model. Among the regression models with urban form factors calculated at the high urban threshold (Table 56), O_3 concentration increased by 3.12 ppb (2.7 percent), O_3 exceedances by about 3 days per year (20 percent), $PM_{2.5}$ by 1.11$\mu g/m^3$ (8.5 percent), and PM_{10} by 1.08 $\mu g/m^3$ (4.3 percent), for every 10 million person increase in regional population. Similarly, at the low urban threshold (Table 57), an increase of 10 million residents within 500 km was associated with a 2.64 ppb (3.1 percent) increase in O_3 concentration, a 1.21 $\mu g/m^3$ (9.3 percent) increase in $PM_{2.5}$ concentration, and a 1.21 $\mu g/m^3$ (4.8 percent) increase in PM_{10} concentration. The "moisture" factor was significantly associated with PM_{10} concentration in both the "high threshold" and "low threshold" models. A single standard deviation increase in the "moisture" factor was associated with approximately a 4.0 $\mu g/m^3$ (15.4 percent) to 4.3 $\mu g/m^3$ (16.6 percent) decrease in PM_{10} concentration. Finally,

wind speed was significantly associated with a decrease in $PM_{2.5}$ concentration at the high threshold only, with a 1 mph reduction in average annual wind speed average wind speed associated with a 1.317 $\mu g/m^3$ (10 percent) reduction.

Regression Model Set 2

The final set of regression models relate the two urban form factors urban "continuity" and urban "shape complexity" with the non-point emission of O_3 precursors (VOCs and NOx), $PM_{2.5}$, PM_{10}, and on-road CO_2. As in regression model set 1, the first four regression models include urban form factors calculated at the high urban threshold (Table 58), while the final four regression models contain urban form factors calculated at the low urban threshold (Table 59). No significant ($p \leq 0.05$) associations were found between urban form factors and air pollutant emissions. However, one potentially significant ($p = 0.062$) association was observed between urban "continuity" calculated at the low urban threshold and the emission of on-road CO_2. A single standard deviation increase in urban "continuity" was associated with a 996,629 ton (12 percent) decrease in CO_2 emissions from on-road sources.

Among the four control variables, megapolitan population was the only consistently significant predictor of non-point emissions. An increase in megapolitan population was associated with a significant rise in the non-point emission of O_3 precursors, $PM_{2.5}$, and on-road CO_2, and a potentially significant increase in the non-point emission of PM_{10} in both "high threshold" and "low threshold" models. In the four "high threshold" models (Table 58), each additional 1 million residents per megapolitan

area was associated with a 54,790 ton (7.7 percent from the mean) increase in the non-point source emission of O_3 precursors, a 5,022 ton (5.7 percent) increase in $PM_{2.5}$, a 12,915 ton (4.1 percent) rise in PM_{10}, and an increase of 1.223 million tons (14.7 percent) of on-road CO_2. Among the "low threshold" models (Table 59), an increase in population of 1 million residents was associated with 55,906 ton (7.8 percent) increase in O_3 precursor non-point source emissions, a 5,133 ton (5.8 percent) increase in $PM_{2.5}$ emissions, a 12,368 (4.0 percent) increase in PM_{10} emissions, and a 1.224 million ton (14.7 percent) rise in on-road CO_2 emissions. The "moisture" factor was the only other significant control variable in this set of regression models, with a significant positive association with O_3 precursor emissions. One standard deviation increase in the "moisture" factor was associated with a 103,695 ton (14.6 percent) increase in non-point source O_3 precursor emissions in the "high threshold" model (Table 58), and a101,012 tons (14.2 percent) increase in non-point source O_3 precursor emissions in the "low threshold" model (Table 59).

Megapolitan Scale Summary

At the 95 percent confidence level, no significant association was found between the two spatial-metrics-based urban form factors urban "continuity" and urban "shape complexity" and either the ambient concentration or non-point source emission of O_3, O_3 precursors, PM, and CO_2. There were, however, two potentially significant ($p \leq 0.062$) associations between these variables. First, an increase in "shape complexity" calculated at the high threshold was associated with a rise in $PM_{2.5}$ concentration. Second, an increase in urban "continuity" calculated at the low urban threshold was associated with a

decrease in the on-road emission of CO2. Among control variables, regional population within 500 km was the only consistently significant predictor of the ambient concentration of air pollutants, while megapolitan area population was the only consistently significant predictor of non-point source emissions.

The megapolitan-scale analysis was performed primarily to assess the effect of scale on the relationships between measures of urban form (i.e. urban form factors) and the ambient concentration and non-point source emission of air pollutants. It was hypothesized (H5) that associations between levels of air pollution and urban form would be most significant at the metropolitan scale. In brief, the rational is that urban form at the metropolitan scale is "more relevant" to, and affects to a greater degree, the majority of vehicular trips, which are intra-urban rather than inter-urban. Given the relationships between urban form, transportation outcomes and tailpipe emissions (Newman and Kenworthy 1989; Frank and Pivo 1994; Ewing 2003; Handy, Cao, and Mokhtarian 2005), the greater the connection between urban form and the number and duration of vehicular trips, the greater the influence urban form can have on the non-point source emission and ambient concentration of air pollutants produced from the combustion of fossil fuels. Although the results of this study suggest that the associations between urban form and air quality are more significant at the metropolitan scale as hypothesized, the limited number of megapolitan scale areas (19 total) severely limits the power of the megapolitan scale regression models, and precludes a definitive assessment.

Case Studies

Los Angeles and the Inland Empire

The ten highest O_3 concentrations (mean annual 4th maximum 8-hour concentration) and seven of the ten highest $PM_{2.5}$ concentrations (mean annual concentration) recorded at individual monitoring stations were within the state of California. Eight of the top ten O_3 concentrations occurred in the Riverside-San Bernardino-Ontario MSA (Figure 73). Often referred to as the "Inland Empire" due to its inland position east of central Los Angeles, the Riverside-San Bernardino-Ontario MSA is one of Los Angeles' largest urban realms, stretching approximately 70 kilometers from east to west. The highest O_3 concentration (183 ppb) was recorded in Crestline, CA, located in a mountainous portion of San Bernardino County approximately 15 kilometers northeast of San Bernardino. The annual 4th maximum 8-hour O_3 concentration averaged over the years 1998 to 2002 was 140 ppb at the Crestline monitoring station. This is nearly twice the current ozone standard set by the U.S. Environmental Protection Agency (EPA) of 75 ppb. Ozone levels above the 75 ppb standard are considered unhealthy; levels above 100 ppb are considered "very unhealthy," and may cause severe respiratory impairments among sensitive groups. The fourth (22.11 µg/m^3) and tenth (21.94 µg/m^3) highest $PM_{2.5}$ concentrations were found within Los Angeles proper, while the ninth (21.95 µg/m^3) highest concentration was located in the city of Riverside (Figure 74). These concentrations are also well above the EPA standard of 15 µg/m^3 and the national average (1998-2002) of 12.62 µg/m^3).

The high concentration of air pollutants, most notably tropospheric O_3, throughout the Inland Empire may be partly attributable to unique geographic and climatic conditions. The area is situated to receive significant quantities air pollutants transported eastward from the Los Angeles Basin by the prevailing winds. Gaps in the coastal mountain range between central Los Angeles and the Inland Empire further facilitates the intra-urban transport of air pollution between the two realms. The Inland Empire is itself a large urban agglomeration consisting of approximately four million residents and serviced by four interstate highways: I-10, I-15, I-210 and I-215. The area is therefore capable of producing significant quantities of the O_3 precursors (NOx and VOCs), PM, CO_2, and other airborne pollutants *in situ*.

In this analysis, the Riverside-San Bernardino-Ontario MSA was included within the larger Los Angeles-Long Beach-Riverside Combined Statistical Area, which as a whole exhibited lower O_3 concentrations. The Inland Empire had an average O_3 concentration of 107 ppb, while the Los Angeles-Long Beach-Riverside CSA had an average O_3 concentration of about 92 ppb, and the Los Angeles-Long-Beach-Santa Ana MSA (exclusive of the Inland Empire) had an average O_3 concentration of only 82 ppb; less than the average O_3 concentration of 83.6 ppb found among the 86 MSAs and CSAs included in this study (Table 12). The Los Angeles-Long Beach-Riverside CSA, however, had the second highest $PM_{2.5}$ concentration. Although 4th in terms of total $PM_{2.5}$ emissions, the Los Angeles area ranked second in non-point source emissions in 2000. The CSA was also second in terms of the non-point source emission of the O_3 precursors VOCs and NOx. The greater variation in the concentration of O_3 throughout the Greater

Los Angeles area was likely due the heightened sensitivity of O_3 to site-specific conditions. The Los Angeles-Long Beach-Riverside CSA also had the ninth highest average annual mean PM_{10} concentration and was the source of more on-road CO_2 (174,883,523 tons) than any other MSA or CSA except New York, NY. The amount of CO_2 emitted by on-road sources, however, is highly correlated with metropolitan population ($r^2 = 0.737$). At 2.51 tons per person, per year, the per capita emission of CO_2 from on-road sources in the Los Angeles-Long Beach-Riverside CSA was the sixth lowest among the 86 metropolitan-scale areas.

The topography and climate of Inland Empire likely contributed to the area's elevated air pollutant levels, particularly that of tropospheric ozone. The Inland Empire is almost entirely surrounded by mountainous terrain, which limits the outward dispersal of locally-produced air pollutants and presents a physical barrier to the cool, "clean" sea breeze from the Pacific Ocean. Due to its distance from the sea and the influence of the coastal mountain range, the average maximum summer temperature is generally higher in the Inland Empire compared with central Los Angeles. The slightly higher summer temperatures may help facilitate the chemical reactions that produce O_3 from precursor emissions, including nitrogen oxides (NOx) and volatile organic compounds (VOCs). Furthermore, the topography of the area is conducive to the formation of thermal inversions that can further trap air pollutants near ground level.

The local production of air pollutants, primarily by non-point sources, may have been exacerbated by the Inland Empire's "sprawl-like" urban morphology. According to the Ewing et al. (2003) sprawl index, the Riverside-San Bernardino-Ontario MSA was

the most sprawling metropolitan area in the United States in 2000. The four components of the Ewing et al. index indicated that the Riverside area had relatively low centrality with greater than 66 percent of the population living more than 10 miles from their place of employment, lower than average mixing of land uses (i.e. only 20 percent of residents lived within a half block of a business or institution), residential density too low to readily support mass transit, and poor street connectivity with 70 percent of blocks larger than expected in a traditional urban street pattern (Ewing et al. 2002). This portion of Los Angeles is especially auto-centric with longer commute times (31 vs. 29 minutes) and a lower transit ridership (1.72 vs. 6.82 percent) than the central Los Angeles basin (Ewing et al. 2002).

The Inland Empire was not evaluated separately in this study from the encompassing Los Angeles-Long Beach-Riverside CSA, making any quantitative assessment of the urban "continuity" or urban "shape complexity" of the Riverside-San Bernardino-Ontario the subject of future research. Evaluating the area at a broader scale, the entire Los Angeles-Long Beach-Riverside CSA had high urban "shape complexity" and average urban "continuity" (Figure 69 and 70). A visual inspection of the region suggests that the Los Angeles basin is relatively contiguous and compact with the majority of development either "high intensity" or "medium intensity" according to the National Landcover Dataset (NLCD 2001) (Figure 75). The intensity of development is based on the amount of impervious surface per unit area. Adjacent urban realms including the Inland Empire to the west and the San Fernando Valley the north had higher proportions of low intensity development, reflecting the more suburban-like

character of these areas. Population density was also substantially lower in the Riverside-San Bernardino PMSA (199 persons/ sq. mile) compared with the more central Los-Angeles-Long Beach PMSA (2,344 persons/ sq. miles) (Census 2000). Thus, although other factors likely contributed to the high concentrations of air pollutants found in the western LA basin, such as inter-urban transport, topography and meteorology, it is probable that the area's "sprawl-like" spatial structure, most notably the dominance of auto-dependent development, was also a significant contributor.

California's Central Valley

Outside the Inland Empire, several of the highest O_3 and $PM_{2.5}$ concentrations were recorded throughout California's Central Valley (Figure 76 and 77). Three of the ten highest single concentrations of PM_{10} were also in California; however, they were outside the Central Valley near Modesto, CA along the coast and Calexico, CA in the southeastern portion of the state. The two highest O_3 concentrations outside the Inland Empire were in close proximity to the two metropolitan-scale urban areas with the highest average O_3 concentrations between 1998 and 2002: Bakersfield, CA (110 ppb avg., 114 ppb max) and Fresno, CA (109.6 ppb avg., 122 ppb max). The two highest $PM_{2.5}$ concentrations outside of Riverside, CA were also recorded in the Central Valley: one near Fresno, CA (27.67 $\mu g/m^3$) and the other near Visalia, CA (27.60 $\mu g/m^3$) about 60 km south of Fresno (Figure 77). A visual analysis of O_3 concentrations throughout the Central Valley yields a distinct pattern in which values generally rise from west to east, and reach their peak near the base of the Sierra Nevada Mountain Range (Figure 76). The highest concentration of O_3 near Sacramento, CA, for example, was located northeast of

the city along the lower slope of the mountain range. With peak elevations in excess of 4,000 meters, the Sierra Mountain Range provides an effective barrier to the dispersal of air pollutants that form within California's Central Valley.

An examination of urban form among the major cities in the Central Valley suggests that topography, rather than urban sprawl, is the primary factor in the area's high levels of air pollution. Although the Fresno-Madera, CA CSA had the highest average concentration of O_3 and $PM_{2.5}$ between 1998 and 2002, it was rated as having moderate-to-low levels of sprawl according to the Nasser and Overberg (2001), Ewing et al. (2002), Sutton (2003), and Lopez and Hynes (2003) sprawl indices. In fact, the Sutton (2003) sprawl index, calculated at a low urban threshold, rated Fresno, CA as the least sprawling metro in the U.S. (Table 16). Likewise, the Bakersfield, CA MSA, with the second highest concentration of O_3 and the sixth highest concentration of $PM_{2.5}$, was rated as having relatively low levels of sprawl by the Nasser and Overberg (2001) and Lopez and Hynes (2003) indices and the metro with the third lowest sprawl according to the Sutton (2003) urban sprawl index, low urban threshold. The largest urban area in the California's Central Valley, the Sacramento—Arden-Arcade—Truckee, CA-NV CSA exhibited higher than average levels of O_3 but below average levels of both PM2.5 and PM10. The Sacramento area also exhibited some of the lowest levels of urban sprawl according to multiple sprawl indices (Table 16).

In agreement with the urban sprawl indices, the metros in California's Central valley generally had high urban "continuity" and low urban "shape complexity." The Sacramento area had the highest urban "continuity;" Stockton, CA had the eighth highest

urban "continuity" and eighth lowest "shape complexity;" and Bakersfield, CA had the ninth lowest urban "shape complexity" at the high urban threshold (Table 24). Furthermore, Fresno, CA had above average urban "continuity" and below average urban "shape complexity." Thus, both the sprawl indices and urban form factors suggest that the major cities of California's Central Valley exhibited relatively low levels of urban sprawl. Combined, the four metros did however produce significant quantities of air pollution from non-point sources, including approximately 815,000 tons of VOCs+NOx (O_3 precursors), or slightly less the Los Angeles, CA area; 71,000 tons of $PM_{2.5}$, or nearly equal to Atlanta, GA; and 8.7 million tons of CO_2 from on-road sources, or slightly more than Atlanta, GA. Therefore, while urban sprawl may not yet be a major concern within this region, the substantial release of anthropogenically-produced air pollution into an area in which dispersal is highly constrained by mountainous topography has resulted in some of the worst air quality in the nation. Given that approximately 90 percent of total O3 precursor and PM25 emissions within the Central Valley originated from non-point sources, any measure to increase the use of transit and reduce automotive travel is likely to be of benefit to regional air quality. One such measure is currently underway. As of 2011, an 800-mile long $43 billion high-speed rail line is planned for California that would connect all major cities in the Central Valley, including Bakersfield, Visalia, Fresno, Modesto, Stockton and Sacramento to Los Angeles and San Francisco along the coast (CA High-Speed Rail Authority 2011). Expected to travel at a speed of 354 km/ hour (220 miles/ hour), the rail line would likely offset airline as well as automotive travel throughout California.

Giants of the South: Atlanta, GA and Houston, TX

Largely unconstrained by natural topography and lacking strong urban containment policies, Atlanta, GA has exemplified – perhaps more than any other city in the U.S. – the rapid, low-density urban expansion that characterizes urban sprawl both in terms of pattern and process. From 1973 to 1999, urban landcover within the Atlanta MSA increased by 247 percent, while the area's population grew only 96 percent (Yang 2002). As in many large metropolitan areas, the majority of growth occurred along Atlanta's urban periphery, expanding the area's low density suburban and exurban realms. While the population density of the entire Atlanta MSA actually increased by 6.4 percent between 1990 and 2000, the amount of land classified as exurban within the area's metropolitan boundary increased by 54.2 percent (Nelson and Sanchez 2005). Among 35 of the largest MSAs in the U.S., Atlanta's exurban growth outpaced all but three cities: Charlotte, NC (55.9 percent), Houston, TX (58.8 percent) and Las Vegas, NV (110.9 percent). Only slightly larger than Atlanta, GA in terms of population (i.e. 4.1 vs. 4.6 million in 2000), the Houston, TX area also underwent substantial growth during the last three decades of the 20th century. Between 1990 and 2000, the population of Houston area grew from 3.73 to 4.67 million, an increase of 25 percent (Census 2000). Also like Atlanta, Houston is largely unconstrained by physical barriers; the Gulf of Mexico to the south has not restricted the outward growth of the greater Houston area to a significant degree.

The sprawl-like morphology of the Atlanta area was captured in this analysis by spatial metrics and urban form factors. Calculated at the high urban threshold, the

Atlanta—Sandy-Springs--Gainesville, GA-AL CSA had the second lowest urban "continuity" and the second highest urban "shape complexity" of the 86 metropolitan-scale areas (Table 24, Figure 69). Atlanta also had the second lowest urban "continuity" and highest urban "shape complexity" when spatial metrics were calculated at the low urban threshold (Figure 70). At the megapolitan scale, with Atlanta as the dominant urban core of the Georgia Piedmont, the area had the lowest urban "continuity" at the high urban threshold and the highest urban "shape complexity" at the low urban threshold (Figure 70). Thus, when including within the urban extent Atlanta's highly complex suburban-exurban fringe, the area is potentially the most complex metropolitan- and megapolitan-scale urban agglomeration in the United States. Four of the six sprawl indices also ranked the Atlanta area as among the ten most sprawling large (500k+ population) metropolitan-scale areas in the U.S (Figure 25). Ranked 3rd in terms of urban sprawl by the Ewing et al. (2003) index, and 2nd according to the Burchfield (2006) index, Atlanta had particularly low levels of street connectivity, reflecting the metro's primarily suburban character.

With a residential population 12 percent greater than Atlanta, yet covering only 4 percent more land, Houston's urban morphology is markedly different. Most obviously, Houston has a higher population density. In 2000, the population density of Houston was about 1393 persons/ sq. mi. (36 percent) greater than in Atlanta (Nelson and Sanchez 2005). Furthermore, the population density of Houston grew faster than in Atlanta between 1990 and 2000 (8.0 vs. 6.4 percent). As mentioned, the percent increase in exurban land in Houston was 58.8 percent between 1990 and 2000, slightly higher than

the 54.2 percent increase in Atlanta. However, in 2000, Atlanta had 1,397.4 square miles classified as exurban, whereas Houston only had 681.7, a 51 percent difference. The greater urban density and lower proportion of exurban landcover in Houston is reflected in the urban sprawl indices and urban form factors. In terms of urban sprawl indices, Houston is ranked consistently as having lower levels of sprawl than Atlanta. Although Houston is ranked 10th in urban sprawl according to the Sutton (2003) sprawl index (low urban threshold), no other index ranks Houston within the top 10 (Table 15). The urban form factors suggest that Houston exhibits average urban "shape complexity," but above average urban "continuity," similar to nearby Dallas-Ft. Worth, TX (Figure 69 and 70).

Given the rapid growth of the area, and sprawl-like nature of Atlanta's urban structure, it is not surprising that the Atlanta region exhibited among the highest air pollutant concentrations at both the metropolitan and megapolitan scale between 1998 and 2002. A monitoring station in Atlanta recorded an average annual O_3 concentration of 109.4 ppb, the highest concentration outside of California (Figure 78). At the metropolitan level, the Atlanta-Sandy Springs-Gainesville, GA-AL CSA had the 7th highest average O_3 concentration at 98.36 ppb, and the third highest average $PM_{2.5}$ concentration at 17.83 µg/m^3. Houston also experienced high levels of O_3; the Houston-Baytown-Huntsville, TX CSA had the 6th highest average O_3 concentration at 99.51 ppb, slightly higher than Atlanta. Houston, however, had a substantially lower average $PM_{2.5}$ concentration at 12.86 µg/m^3; lower in fact than the average 13.23 µg/m^3 among all 86 metropolitan-scale areas.

The relatively high concentration of O_3 in Houston is likely the result of substantial O_3 precursor emissions within the CSA. Three times the amount of O_3 precursors (VOCs and NOx) were emitted from industrial sources in Houston than in Atlanta. A total of 151,000 tons of VOCs and NOx were emitted from industrial sources in and around Houston TX in the year 2000, about 30,000 tons more than in Chicago, ILL, the MSA/CSA with the second highest industry-based O_3 precursor emissions. The Greater Houston-Galveston area contains a large number of industrial facilities, including some of the largest petrochemical complexes in the world. These facilities are a major source of industrial pollution, including VOCs, NOx, SO_2 and CO_2 (Washenfelder et al. *in press*). Non-point sources likely contribute significantly to O_3 levels throughout the Houston area. While Houston emitted three times more industrial-source VOCs and NOx than Atlanta, both urban areas produced about 467,000 tons of non-point source emissions in 2000. Finally, the per capita emission of both O_3 precursors and $PM_{2.5}$ in Atlanta and Houston were nearly equal. The last two findings were unexpected given that non-point source emissions are believed to be influenced by urban morphology, which appears to vary significantly between the two urban areas.

The Northeast Megalopolis

Covering some 173 counties, 12 MSAs, 9 CSAs, and 3 megapolitan areas (i.e. New England, Core Megalopolis, and Chesapeake Megalopolis), and home to about 48.3 million people in 2000 (51.2 million in 2009), the East Coast "Megalopolis" that stretches from Washington, D.C. in the south to Boston, MA in the north (also known as "BosWash") is the largest urban agglomeration in the United States. As such, the region

produces substantial quantities of air pollution from both point and non-point sources. Due to the close proximity of major industrial and population centers, the inter-urban transport of air pollution between neighboring – and often overlapping – airsheds results in elevated air pollutant levels throughout the Megalopolis corridor (Slade 1967). In December 2008, nearly every county in the region was in nonattainment for $O_{3,}$ and the majority of counties from Washington, D.C. to New Haven, CT were in nonattainment for $PM_{2.5}$ (EPA 2011). Counties in nonattainment have exceeded the EPAs standard for a particular air pollutant. No counties were in nonattainment for PM_{10}, which is less associated with urban activity.

During the study period from 1998 to 2002, high levels of O_3 were found throughout Megalopolis, including multiple locations in New Jersey, Maryland (especially around the Washington-Baltimore, MA-VA CSA), Pennsylvania, and New York (Figure 79). New York City, NY, however, reported several relatively low O_3 concentrations between 1998 and 2002, including an average of 58 ppb in central Manhattan. It is not uncommon for O_3 levels to be lower in the central city than in the surrounding suburbs due to the reaction of O_3 with nitrogen oxide (NO), which is typically abundant in dense urban centers, to form nitrogen dioxide (NO_2) and oxygen (O_2). $PM_{2.5}$ was found in highest concentration within the urban centers of New York City, Philadelphia, Baltimore and Washington, D.C (Figure 80).

Although several single concentrations of both O_3 and $PM_{2.5}$ were among the highest in the nation, the Philadelphia-Camden-Vineland, PA-NJ-DE-MD was the only metropolitan-scale area within Megalopolis to have one of the top 10 highest average

concentrations of O_3; none made the top 10 list for $PM_{2.5}$ (Table 13). Furthermore, while total emissions of O_3 precursors, $PM_{2.5}$, and CO_2 from on-road sources in the New York metro were the highest in the nation, the city also had among the lowest per capita emission of all three pollutants. The high population densities and large urban cores of New York City, Boston, and Philadelphia facilitate more energy-efficient lifestyles that typically include smaller living spaces and regular use of transit, walking and biking. As a result, the per capita emission of air pollutants and CO_2 throughout the region is relatively low.

The urban sprawl indices generally agree that the metro areas of New York, Philadelphia and Boston have relatively low levels of urban sprawl (Table 16). New York is ranked the least-sprawling large metropolitan-scale area by three separate sprawl indices: Ewing et al. (2003), Lopez and Hynes (2003) and Sutton (2003) (high threshold). According to the four components of the Ewing et al. sprawl index, the New York area is "in a class by itself," particularly in regard to population density (Ewing et al. 2003). It is important to note, however, that Ewing et al. used the New York primary metropolitan statistical area (PMSA), which is only a component of the larger New York MSA and CSA, and includes New York City and three surrounding counties. Compared with the 35 counties included in the New York-Newark-Bridgeport, NY-NJ-CT-PA, Ewing's PMSA-based assessment of the New York area is much more limited to the urban core and inner suburbs. Had Ewing et al. used CSA, rather than PMSA, boundaries it is likely that New York, as well as the other large urban centers of the Megalopolis region, would have been ranked higher in terms of urban sprawl. Urban extent can also significantly affect

measures of urban sprawl. When evaluated at the MSA level by the Sutton (2003) sprawl indices, the New York area was ranked the least sprawling metro at the high urban threshold; at the low urban threshold, however, New York was ranked as having an average level of urban sprawl. Similarly, Boston was ranked the 11th least-sprawling large metropolitan area at the high urban threshold, but the 13th most-sprawling metropolitan area at the low urban threshold, just behind Greensboro—Winston-Salem—High-Point, NC. The extensive suburban and exurban areas detected at the MSA scale, and particularly at the low urban threshold, around New York, Boston, Philadelphia, and Washington-Baltimore are all the more evident at the CSA level. Spatial metrics calculated at the CSA level, at both a high and low urban threshold, describe the extended spatial morphologies of these large urban areas.

Even at the high urban threshold, which does not typically include the exurban realm, the four major urban centers of the Northeast Megalopolis – New York, Boston, Philadelphia, and Washington-Baltimore – had among the lowest urban "continuity" of any large MSA or CSA (Table 24). Philadelphia had the lowest urban "continuity" of the 86 metropolitan-scale areas, followed by Washington-Baltimore (ranked 4th), Boston (ranked 8th) and New York (ranked 10th). New York was also found to have the highest "shape complexity" at the high urban threshold, while Boston was ranked 4th. At the low urban threshold, the discontinuity among Boston's suburban and exurban areas becomes more evident as the metro is ranked 3rd in terms of least urban "continuity," behind Greenville, SC and Atlanta, GA. The relative urban "continuity" of Philadelphia, now ranked 5th, and Washington-Baltimore, now ranked 8th, increase slightly. At the low

urban threshold, New York was no longer ranked among the top 10 least "continuous" urban areas, suggesting that the area's exurban realm may have been more continuous than that of the other three cities. The New York-Newark-Bridgeport, NY-NJ-CT-PA CSA, however, fell only to second-place in terms of urban "shape complexity," behind first-ranked Atlanta, GA. Boston maintained its rank as the 4th most complex urban area. Philadelphia and Washington, D.C. each had slightly lower than average urban "shape complexity." The urban form factors indicate that the major urban centers of the Northeast Megalopolis generally have very complex urban morphologies, owing to extensive suburban and exurban areas that extend well beyond PMSA – and to some extent MSA – boundaries. Air quality within the Northeast Megalopolis is affected by the structure of these extended conurbations that, beyond the dense central urban cores, reflect the complex and often fragmented morphologies typical of other large cities consistently described as sprawling, such as Atlanta, GA.

The Southeast "Sprawl Belt"

A cluster of metros in the Southeastern United States have consistently been ranked as among the most sprawling in the nation. Within this "Sprawl Belt" (Figure 81) are 13 MSA/CSAs, including Charlotte-Gastonia-Salisbury, NC-SC, Knoxville-Sevierville-La Follette, TN CSA, Greensboro--Winston-Salem--High Point, NC, Atlanta-Sandy Springs-Gainesville, GA-AL, Greenville-Spartanburg-Anderson, SC, Nashville-Davidson--Murfreesboro--Columbia, TN, and Little Rock-North Little Rock-Pine Bluff, AR, each ranked by three or more sprawl indices as among the 10 most sprawling large metropolitan-scale areas in the U.S. (Figure 25). Metros in this region also had generally

low urban "continuity" and average urban "shape complexity." Atlanta, GA, discussed in greater detail in the following section, exhibited an exceptionally complex and fragmented urban morphology, with the second lowest urban "continuity" and highest urban "shape complexity" at the low urban threshold. While three other cities in the region, Greenville-Spartanburg-Anderson, SC, Knoxville-Sevierville-La Follette, TN, and Columbia-Newberry, SC, also had some of the lowest levels of urban "continuity," only Atlanta, GA made the top 10 list for urban "shape complexity" at both the high and low urban threshold. Charleston-North Charleston, SC was the only metro in the "Sprawl Belt" listed among the top 10 least complex urban areas, while Memphis, TN was the only metro listed among the top 10 most continuous. In regard to individual spatial metrics, metros within the "Sprawl Belt" generally appeared most similar to those in the Northeast, with relatively high urban edge density (ED) (Figure 30) and fractal dimension (AWMPFD) (Figure 34), and low continuity (CONTIG) (Figure 35), contagion and largest patch index (LPI) (Figure 32).

Air quality within the "Sprawl Belt" was relatively poor between 1998 and 2002; the region constituted one of the three main clusters of high concentrations of O_3 and $PM_{2.5}$ in the Eastern U.S. The two additional regions included the previously discussed Northeast Megalopolis and the "Rust Belt" around the Great Lakes and Ohio River Valley. Portions of the region, particularly around Birmingham, AL and Mobile, AL, also recorded some of the highest single concentrations of PM_{10} (Figure 23). When averaged over the entire metropolitan-scale area, four "Sprawl Belt" cities had among the top 10 highest concentrations of O_3: Knoxville, Chattanooga, Atlanta and Columbia (Table 13).

Four cities in the region also had among the top 10 highest concentrations of $PM_{2.5}$: Atlanta, Birmingham, Knoxville and Chattanooga. Furthermore, the average per capita emission of CO_2 from on-road sources among metros in the "Sprawl Belt" was 1.86 tons/ person; significantly greater ($p = 0.007$) than the 1.55 tons/ person among metros outside the region. The per capita emission of O_3 precursors from non-point sources was also significantly higher ($p = 0.003$) among metros of the "Sprawl Belt." The per capita emissions of $PM_{2.5}$ and PM_{10} from non-point sources were higher, but not significantly greater, among metros in the "Sprawl Belt." The two megapolitan areas within the region, the Georgia Piedmont and the Carolina Piedmont,

The poor air quality suffered by several cities within the Southeastern "Sprawl Belt" may in part be the result of substantial population growth and the rapid expansion of low-density, auto-dependent suburban and exurban areas within the region. Outside the Southwest, the fastest growing region in the U.S., metros with the highest percent increase in population between 1990 and 2000 included several in the "Sprawl Belt," including Atlanta, GA (38.9 percent), Raleigh-Durham, NC (38.9 percent), Charlotte, NC (29 percent), and Nashville, TN (25 percent) (U.S. Census 2001). At 20.6 percent, the average growth rate among the 14 metropolitan-scale areas in the "Sprawl Belt" was considerably greater than the average 13.5 percent growth rate for all MSAs between 1990 and 2000. The rapid growth of cities in the Southeast and Southwest is partially a result of a general shift in population from the North and Midwest to the South and West that has seen the South's share of U.S. population increase from 31 to 36 percent and the West's share of population increase from 13 to 22 percent between 1950 and 2000. The

South also added 14.8 million new residents over the 1990's, more than any other region (U.S. Census Bureau 2001b).

As urban areas of the Southeast have grown in population, so too have they swelled in size. An analysis of city lights at night provided an estimate of urban growth between 1990 and 2008 (Bereitschaft 2010). Atlanta grew the most in terms of absolute number of square miles added (3,653 km^2; 44 percent), while Raleigh-Durham grew the most in terms of percent change in area (53 percent; 1,131 km^2). Growth of the urban area outpaced population growth in at least two metros within the "Sprawl Belt": Birmingham, AL and Memphis, TN. Overall population growth in Birmingham and Memphis was a modest 17 and 20 percent, respectively. The two metros therefore likely experienced a significant urban-to-suburban shift in population in addition to a moderate increase in total population.

Low-density development along the urban periphery has been especially pronounced in several "Sprawl Belt" cities. Among 49 large U.S. metropolitan areas, Atlanta, GA and Charlotte, NC had the lowest urban-to-exurban population density ratio (6 percent), indicating that the population density of the exurban realm, relative to the urban core, was much lower than average (Sutton 2006). For comparison, the urban-to-exurban population density ratio in New York was 14 percent, Chicago 18 percent, Minneapolis-St. Paul 23 percent, and Las Vegas 28 percent. Furthermore, a relatively high proportion of the total land area of "Sprawl Belt" cities was determined exurban. As of 2000, exurban areas accounted for 44.7 percent of all urban land cover in Memphis, 55.8 percent in Atlanta, 59.9 percent in Nashville, 65.5 percent in Birmingham and 80.3

percent in Charlotte (Sutton 2006). Cities outside the "Sprawl Belt" generally had lower proportions of exurban landcover: New York had16.4 percent, Chicago 18.5 percent, Phoenix 20.2 percent and Washington-Baltimore 36.6 percent (Sutton 2006) (Table 60). The relatively high proportion of exurban development among cities in the "Sprawl Belt" was reflected in the low urban "continuity" found in the region (Figure 57 and 58). Growth in exurban landcover was also especially high in Atlanta and Charlotte between 1990 and 2000; exurban landcover grew by 54.2 percent in Atlanta and 55.9 percent in Charlotte (Nelson and Sanchez 2005). Among 35 large metropolitan areas, only Houston (58.8 percent) and Las Vegas (110 percent) underwent greater exurban growth between 1990 and 2000 (Nelson and Sanchez 2005). The rapid growth of low density, auto-dependent exurbia within the "Sprawl Belt," and across the South and Southwest, was likely due in part to a lack of "strong" urban containment policies, such as urban growth boundaries (UGBs) and urban service limits. "Weak" urban containment, such as minimum lot size restrictions, and "natural" urban containment, referring to limitations on growth imposed by the surrounding landscape, does not appear to have been as effective at limiting exurban expansion (Nelson and Sanchez 2005).

Cascadia

The case studies presented thus far have focused primarily on cities and regions of the U.S. that have experienced high levels of O_3 and PM, particularly during the 5-year (1998 to 2002) study period. The high levels of air pollution experienced in these areas can be explained, in varying degrees, by geographic situation, local topography, point and non-point source emissions, and – as suggested in this dissertation – urban form.

Although it would be difficult, if not impossible, to fully disentangle all the factors that influence regional air quality, it appears that the right combination of factors have conspired in the Northwestern U.S. to produce some of the lowest average concentrations of O_3 and PM of any urbanized region in the nation.

Bounded by the Pacific Ocean to the west and the Cascade Range the east, Cascadia refers to the megapolitan area in the Pacific Northwest that encompasses the two combined statistical areas of Seattle-Tacoma-Olympia, WA and Portland-Vancouver-Beaverton, OR-WA. Although the region has experienced peak concentrations of O_3 and PM that have exceeded EPA standards (Snow et al. 2003), between 1998 and 2002 Cascadia as a region had the lowest average O_3 and PM_{10} concentrations, and the third lowest average $PM_{2.5}$ concentration, of the 19 megapolitan areas (Table 61 and 62). Furthermore, among the 86 metropolitan-scale areas, Seattle-Tacoma-Olympia, WA had the lowest average concentration of O_3, the second lowest concentration of $PM_{2.5}$, and the 10^{th} lowest concentration of $PM_{2.5}$. Likewise, Portland-Vancouver-Beaverton, OR-WA had the second lowest average concentration of O_3, the 4^{th} lowest concentration of PM_{10}, and the 6^{th} lowest concentration of $PM_{2.5}$ (Table 14).

Key to the region's relatively healthy air quality are a number of factors that likely include 1) significant distance from other population and industrial centers, thus limiting inter-regional transport, 2) local meteorology that is generally unfavorable to the photochemical production of air pollutants (i.e. abundant and frequent rainfall, well below-average sunshine, moderate temperatures), and 3) below average per capita emission of O_3 precursors and PM in the Seattle and Portland areas. The per capita

emission of O_3 precursors, $PM_{2.5}$, and PM_{10} from all sources (point and non-point) were well below average in Seattle, and below average in Portland. The per capita emission of O_3 precursors from non-point (primarily mobile) sources was slightly above average in Portland, but below average for Seattle, while the per capita emission of $PM_{2.5}$ and PM_{10} from non-point sources was below average for both Portland and Seattle. The per capita emission of CO_2 from on-road sources was 1.257 tons/ person in Seattle and 1.155 tons/ person in Portland; substantially less than the 1.599 tons/ person average for all 86 metropolitan-scale areas.

Although Ewing et al. (2003) ranked Portland as the 6th least-sprawling large metro in the nation, neither Portland nor Seattle were among the top 10 least-sprawling metros according to the five other sprawl indices. The two metros, however, were generally ranked as having average or below average levels of sprawl. Interestingly, Seattle was ranked among the 20 most-sprawling metros according to the Sutton (2003) sprawl index when expected population density was calculated using a high urban threshold. At the low urban threshold, however, the Sutton (2003) index ranked Seattle among the 20 least-sprawling metros. This suggests that the population density of Seattle was higher than expected when exurban areas were included in the calculation, but lower than expected when they were excluded. According to the Ewing et al. (2003) sprawl components ($\bar{x}$ = 100), residential density (103.6) and degree of centeredness (98) in the Seattle area was near average, while street connectivity (117.1) was above average and degree of mixed uses (79.4) was below average. In Portland, residential density (101.3) and degree of mixed uses (102.3) were average, while street connectivity (128) and

degree of centeredness (121.8) were above average (Ewing et al. 2003). Together, the six sprawl indices and four sprawl components suggest that that the two largest urban centers in the Cascadia region, Portland, OR and Seattle, WA, exhibited approximately average levels of urban sprawl. It is worth noting, however, that the street connectivity in both Portland and Seattle was well above average, indicating a more cohesive, traditional urban street layout.

The spatial structure of urban landcover within Portland, OR, Seattle, WA and the encompassing Cascadia megapolitan area is also indicative of low-to-moderate levels of urban sprawl. Seattle-Tacoma-Olympia CSA had the 7th highest urban "shape complexity" when calculated at the high urban threshold (Table 24), and the 11th highest urban "shape complexity" at the low urban threshold (Table 25). Portland-Vancouver-Beaverton, OR-WA also exhibited above average urban "shape complexity," though only less than one standard deviation from the mean. In terms of urban "continuity," Seattle was slightly below average at the low urban threshold and average at the high urban threshold. Urban "continuity" in the Portland area was about one standard deviation above average at both the high and low urban threshold. The lower urban "continuity" observed in Seattle may be partly the result of natural topography; the local terrain is punctuated by hills, mountains, lakes, and the several bays and inlets of Puget Sound. Among19 megapolitan areas, Cascadia had the 6th highest urban "continuity" at the high urban threshold, and the 7th highest urban "continuity" at the low urban threshold (Table 26). Urban "shape complexity" for the entire Cascadia region was about average at the high urban threshold and slightly above average at the low urban threshold (Table 27).

Thus, the urban form factors urban "continuity" and urban "shape complexity" support the conclusion drawn from the sprawl indices: the Cascadia region in not exceptional in terms of either high or low levels of urban sprawl.

It is somewhat unexpected that the Cascadia region did not exhibit particularly low levels of urban sprawl given the growth management policies enacted by the states of Washington and Oregon. While Washington's Growth Management Act (GMA), adopted in 1990, was only in place approximately 10 years prior to the study period (1998-2002), Oregon's growth management legislation was enacted two decades earlier in 1973. Proposed in 1977, and accepted by the state in 1980, Portland's metropolitan regional government, Metro, developed the region's first urban growth boundary (UGB). The UGB, required of all municipalities or metropolitan areas in Oregon, is designed to restrict urban growth outside a designated area in order to preserve prime agricultural lands and natural areas, promote the efficient use of public services (i.e. water, sewer, roads, transit), and retain existing businesses and attract new economic development within the urban core (Metro 2011). Washington's GMA also mandated long-term urban growth boundaries on a county-wide basis. King County, which includes much of the Seattle area, established urban growth boundaries in 1994 (Robinson, Newell and Marzluff 2005).

Although there is little doubt UGBs have played an important part in the recent evolution of urban form within the Cascadia region, there is some uncertainty as to their effectiveness as a growth management strategy. In support of the UGB, and the other growth management efforts in Washington and Oregon, Nelson and Sanchez (2005)

found that Seattle had the 4th highest increase in population density (9.1 percent), and Portland the 6th highest percent increase (8.0 percent), among the 35 largest metropolitan areas in the U.S. between 1990 and 2000. Furthermore, Portland was among only three metropolitan areas to have a decline (-3 percent) in exurban land area between 1990 and 2000 (Nelson and Sanchez 2005). The other two metropolitan areas were Miami, FL (-31.9 percent) and New Orleans, LA (-2.9 percent), both of which were mentioned previously for having substantial natural barriers to urban expansion. Exurban area in Seattle increased by 12.5 percent, less than all but seven other metropolitan areas. In Portland, population growth (54.3 percent) outpaced the increase in urbanized land (35.8 percent) between 1980 and 2000, resulting in a 13.6 percent increase in population density over the 20 year period (Jun 2004). Jun (2004), however, claims the increase in population density is merely average among 32 (unidentified) metropolitan areas. Additionally, Jun (2004) found that employment within Portland's urban core grew by 70.8 percent (ranked 6th out of 32), housing units within the urbanized area increased by 54.4 percent (ranked 16th), auto users increased by 69.9 percent (ranked 12th), public transit users grew by 26.1 percent (ranked 11th) and mean commuting time increased by 14.5 percent (ranked 15th) between 1980 and 2000. Therefore, among 32 metropolitan areas, Portland had higher than average employment growth in the central city, slightly above average increase in auto and transit users, and an average increase in housing units and mean commuting time. Jun (2004) also performed an analysis of new housing stock in Portland and found that, as in most metropolitan areas, new housing in Portland was more likely to be built away from the urban core in low-density suburban areas.

However, new housing was also more likely to be built in areas with pre-existing housing stock, suggesting that new development occurred in a mostly contiguous fashion, thus meeting one of the objectives of the UGB. The urban form factor urban "continuity" establishes further support for this conjecture, as the Seattle-Tacoma-Olympia CSA had the 14th highest urban "continuity" at the high urban threshold and the 17th highest urban "continuity" at the low urban threshold among the 86 MSAs and CSAs included in this analysis. Finally, Jun (2004) observed that about 40 percent of all new housing units in Portland were constructed to the north of the city in Clark County, Washington, which is outside the UGB. Jun (2004) contends that Clark County has likely absorbed much of the suburban and exurban growth in Portland, acting as a kind of "safety valve for growth outside the UGB." Indeed, substantially fragmented, low-intensity suburban development can be seen north of the city using a map of urban landcover (Figure 82). As Jun (2004) suggests, inter-state cooperation is necessary to support UGBs and other strong urban containment policies in metropolitan areas like Portland that transcend state boundaries.

While the effectiveness of the UGB and other growth management strategies in Washington and Oregon remain a subject of debate, the relationship between low levels of air pollution and relatively low levels of urban sprawl throughout Cascadia was mirrored in other regions of the U.S. As identified by megapolitan area, these regions include most notably the Treasure Coast (i.e. Miami, FL), the Front Range (i.e. Denver and Colorado Springs, CO) and Northern California (i.e. San Francisco, San Jose and Sacramento, CA). Each of these megapolitan areas experienced moderate-to-low concentrations of O_3 and PM between 1998 and 2002, and exhibited below average urban

"shape complexity" and above average urban "continuity" (Figure 71 and 72). Thus, Portland, OR, Seattle, WA, and the encompassing Cascadia megapolitan area fit the compelling trend suggested by the results of this dissertation that a discernable relationship exists between urban form and regional air quality, and that urban areas with lower levels of urban sprawl or less sprawl-like urban morphologies are more likely to experience better air quality, all other factors equal.

CHAPTER V

CONCLUSION

Summary of Major Findings

The primary objectives of this dissertation research were threefold: 1) To evaluate the degree of association between multiple air pollutants (O_3, $PM_{2.5}$, PM_{10}, CO_2) and multiple measures of urban form among the 86 largest MSAs/CSAs and 19 megapolitan areas in the U.S., 2) to compare and evaluate the relative predictive capability of a multi-variable composite urban sprawl index (i.e. Ewing et al. 2003), single-variable urban sprawl indices (e.g. Lopez and Hynes 2003) and the two spatial metric-derived measurements of urban morphology, urban "continuity" and urban "shape complexity," and 3) to determine the effect of scale and urban extent on the potential associations between air pollutant levels and both individual spatial metrics and the urban form factors urban "continuity" and urban "shape complexity."

Using multiple linear regression, significant associations were observed between multiple measures of urban form and both the ambient concentration and non-point emission of multiple air pollutants. Those urban areas that exhibited more sprawl-like urban morphologies generally experienced higher levels of air pollution and/ or greater non-point source emissions. At the metropolitan scale, an increase in urban sprawl as

assessed using urban sprawl indices was primarily associated with an increase in the ambient concentration of ozone (O_3) and fine particulate matter ($PM_{2.5}$), while an increase in sprawl-like spatial patterns as measured using spatial metrics-based urban form factors (i.e. urban "continuity" and urban "shape complexity"), was primarily associated with an increase in the non-point source emission of O_3, $PM_{2.5}$ and course particulate matter (PM_{10}). An increase in the emission of CO_2 from on-road sources was significantly associated with a reduction in residential density, one of the four sprawl components of the Ewing et al. (2003) urban sprawl index (Table 55).

The significant associations identified here between levels of O_3 (both O_3 concentration and number of annual O_3 exceedances) and both the Ewing et al. composite sprawl index and the sprawl index component residential density, were also observed by Ewing et al. (2003) and Stone (2008). Ewing et al. (2003), however, also found a significant positive association between degree of mixed use development and O_3 concentration, while Stone (2008) found significant associations between both street network connectivity and the overall composite sprawl index, and number of annual O_3 exceedances. As discussed in Chapter 4, both Ewing et al. (2003) and Stone (2008) ran each of the four sprawl index components within separate regression models, whereas in this dissertation they were included within a single model. When run together using the current data, only residential density is a significant predictor of O_3; when run separately, an increase in both residential density and street connectivity are significantly associated with a decrease in O_3 levels.

The composite index developed by Ewing et al. (2003) was the only one among six urban sprawl indices significantly associated with the concentration of both O_3 and $PM_{2.5}$ (Table 42). No sprawl index was significantly associated with air pollutant emissions or the concentration of PM_{10}. In terms of total number of significant associations with air pollutant levels, the Ewing et al. index performed "best" among the individual sprawl indices, though all but the Burchfield et al. (2005) index were significantly associated with either the concentration or number of annual exceedances of O_3. Every significant association between urban sprawl indices and air pollution was positive, indicating that an increase in air pollution was related to an increase in urban sprawl. The Ewing et al. index is unique among the six sprawl indices in that it incorporates multiple measures of urban form, whereas the remaining indices, with the exception of Burchfield et al. (2005), are based primarily on residential density. Although the Ewing et al. composite sprawl index alone was significantly associated with $PM_{2.5}$ concentration, the residential population-based sprawl indices were nearly equally associated with O_3 concentration. Thus, if this analysis had focused solely on O_3, as both Ewing et al. (2003) and Stone (2008) did, no discernable difference in predictive capability between the indices could be made. Furthermore, the significant associations between O_3 concentration and the residential population density-based sprawl indices Sutton (2003), Lopez and Hynes (2003), and Nasser and Overberg (2001), support the notion that residential density was the most influential of the four Ewing et al. (2003) sprawl components. The common significance of residential density within this dissertation and among previous studies solidifies the importance of this factor in any

urban design, plan, or policy concerned with air quality, particularly at the metropolitan or regional scale.

Derived from nine spatial metrics that measure specific spatial attributes of urban morphology, the two urban form factors, "continuity" and "shape complexity", exhibited several significant associations with the non-point source emission of air pollutants, rather than their ambient concentrations. An increase in urban "continuity" was significantly associated with a decrease in the non-point source emission of O_3 precursors (VOCs + NOx) at the metropolitan scale, while urban "shape complexity" was significantly associated with an increase in the non-point source emission of O_3, $PM_{2.5}$, and PM_{10}. Urban "continuity" represents the degree to which the urban landscape is fragmented; greater urban "continuity" is expected among urban areas that are less fragmented, with more contiguous and less "leap-frog" development. Less open space between urban developments should result in shorter automotive trips and fewer emissions from non-point (primarily mobile) sources. Urban "shape complexity" provides a composite measure of urban area-to-perimeter ratio or the "jaggedness" of the urban boundary. Less compact urban landscapes with highly convoluted, plane-filling perimeters, common among suburban and exurban areas, are also expected to increase the number and duration of automotive trips. The results therefore support the theoretical linkages between urban morphology and non-point (primarily automotive) emissions. It is interesting, however, that significant associations were not also found between urban "continuity," urban "shape complexity," and ambient concentrations. This "disconnect" between non-point source emissions and ambient concentrations suggests that the

concentration of O3 and PM are not significantly influenced by non-point source emissions alone, even when confounding factors such as precipitation, temperature, population, and geographic area are controlled for. This is not to say, however, that non-point source emissions are irrelevant to air quality. For O_3 precursors, $PM_{2.5}$ and PM_{10}, non-point source emissions constitute the majority of total emissions within most urban areas. Furthermore, non-point source emissions from vehicles likely have a more fine-grained effect on air quality, with emissions and ambient concentrations highest along busy roadways and other transportation corridors. Depending on where air quality monitors are located, these "spikes" in air pollutant concentrations may or may not be included in metropolitan averages.

While the Ewing et al. (2003) urban sprawl index was the most consistently significant predictor of air pollutant concentrations among all urban form variables, these associations appear to have existed independently of non-point source emissions. Five of the six urban sprawl indices, including Ewing et al., were significant predictors of the ambient concentration, but not the non-point source emission, of O_3 and/ or $PM_{2.5}$. Stone (2008) also found no significant association between the Ewing et al. sprawl index and the total emission of O_3 precursors (NOx + VOCs) among 45 of the largest metropolitan areas in the U.S. Stone (2008), however, observed that the Ewing et al. sprawl component residential density, when run separate of the three other sprawl components, and with the control variables average O_3 season temperature and metropolitan population, was associated with a significant reduction in O_3 precursor emissions. The same result was obtained using the data and control variables of this dissertation ($p = 0.014$), but only if

residential density is run within a separate regression model; if residential density is combined with the three other Ewing et al. (2003) sprawl index components within a single regression model, residential density is no longer a significant predictor of total O_3 precursor emissions ($p = 0.094$). Thus, there are likely non-emissions-based mechanisms, as well as emissions-based mechanisms, through which urban form may affect air pollutant concentrations. Stone (2008) hypothesized that the heat island effect and the geographic distribution of ozone monitors could account for two such non-emissions-based mechanisms. The spatial extent of the heat island effect may be enhanced by low-density, decentralized urban land use patterns, thereby promoting the formation of photochemical air pollution. Furthermore, a dispersed pattern of air quality monitors, more likely to be found in low-density, decentralized urban regions, may be able to detect downwind plumes of air pollution more readily than in a more compact region with monitors centered around the urban core (Stone 2008). This effect would likely be most significant for O_3, which is typically found in highest concentration in suburban and exurban areas well beyond the central city. Further research is needed to address these and other potential mechanisms.

Urban extent did not significantly affect the relationships between the two urban form factors urban "continuity" and urban "shape complexity," and non-point source emissions. Five significant associations were observed at the high urban threshold and four at the low urban threshold. Individual spatial metrics, however, were significantly affected by urban extent. At the metropolitan scale, three of the four "shape complexity" metrics were significantly higher when calculated at the low urban threshold, reflecting

the higher proportion of geometrically complex suburban and exurban areas included within the low urban threshold. Likewise, four of the five urban "continuity" metrics were significantly lower at the low urban threshold, indicating less continuity among urban developments at the urban fringe. Although the absolute value of each spatial metric changed significantly between the high and low urban thresholds, the variability in the data remained largely unchanged. With the exception of contagion (CONTAG), all spatial metrics calculated at the two urban extents were significantly correlated (Table 4). Therefore, the urban morphology of the 86 metropolitan-scale areas became more complex and less continuous between the high and low urban thresholds by roughly the same amount.

Associations between urban form factors and non-point source emissions were most significant at the metropolitan scale, perhaps in part due to a substantially larger sample size (i.e. 86 metropolitan-scale areas vs. 19 megapolitan-scale areas), but also likely due to the disproportionally influential effect of metropolitan-scale urban form on the majority of vehicular trips. With major urban centers within megapolitan areas typically anywhere from 75 to 150 miles apart, the vast majority of daily trips occur within, rather than between, metropolitan areas. Although urban form at the megapolitan scale may not be as pertinent to air quality as urban form at the metropolitan scale, the inter-urban transport of air pollution assures that air quality is a truly regional issue that is best addressed by inter-metropolitan, if not inter-state, cooperation.

Future Research

During the completion of this dissertation research, a number of additional avenues of investigation were identified regarding the relationships between urban form and air quality. First, the scope of the investigation may be widened to include additional urban areas. The metropolitan-scale areas used in this dissertation were limited to the 86 most populous MSAs and CSAs in the United States. This group of "large" metropolitan-scale areas each had a population of 500,000 or more. Future studies may focus on the relationships between urban form and air quality among "medium-sized" MSAs/ CSAs (e.g. populations between 500,000 and 250,000) or small MSAs/ CSAs (e.g. populations < 250,000). A comparison of these groups may also reveal differences in urban form and air quality among MSA/CSAs of varying sizes. For example, in this dissertation larger metropolitan-scale areas tended to have greater urban "shape complexity." It is unknown whether this trend exists only among large MSAs/ CSAs or metros of all sizes. More generally it may be asked whether larger urban areas are more or less sprawl-like according to various metrics and indices, and whether their populations are on average exposed to higher or lower levels of air pollution.

The scope of study could also be broadened to include urban areas from countries and continents other than the U.S. and North America to provide a comparative assessment of urban form, air quality, and the strength of association between urban form and air quality among different regions and under varying cultural, political, economic and social conditions. An international analysis of urban form using spatial metrics has

already been carried out by Huang, Lu and Sellers (2007). This investigation, however, may be expanded to include not only additional cities, regions, and measures of urban form, but also to assess variations in the relationships between urban form, air quality, and other environmental parameters. It is likely that the dynamic between urban form and environmental quality will be markedly different, for example, between cities of the developed and developing world and those with a western versus a non-western character.

In addition to expanding the geographic scope of the investigation, additional air pollutants and other measures of air quality (e.g. AQI, non-attainment areas) may be used to determine whether the significant associations observed here between measures of urban form and O_3, PM, and CO_2 are similar for other common air pollutants and toxins. In this dissertation, a significant difference was observed in the number and strength of associations between urban form and the concentration of O_3, $PM_{2.5}$, and PM_{10}. In the regression analysis, the largest number of significant associations were found between measures of urban form and the concentration of O_3 (six, not including O_3 exceedances), followed by $PM_{2.5}$ (two), and PM_{10} (none). Furthermore, four significant associations were found between urban form and the non-point source emission of O_3 precursors and $PM_{2.5}$, two significant associations between urban form and the non-point source emission of PM_{10}, and one significant association between urban form and the emission of CO2 from on-road sources. It is reasonable to expect that other air pollutants will also exhibit a range of associations with urban form. This knowledge may be useful in

identifying what air pollutants are most likely to be influenced significantly by changes in urban form, and may therefore be most readily affected by planning policy.

The case studies presented in this dissertation provide additional detail regarding the complex relationships between urban form and air quality, as well as the multitude of confounding factors, such as topography and meteorology, which are unique to each individual city or urban region. It may be fruitful, however, to perform a more thorough examination of urban form and air quality for a limited number of urban areas. The National Landcover Dataset (NLCD 2001) was chosen for use in this dissertation because it provides data for the entire United States, allowing a quick assessment and comparison of urban landcover among a large number (86) of metropolitan-scale areas. A more detailed, custom landcover classification could be performed for a limited number of urban areas, providing additional quantitative measures of urban form that may affect air quality. Furthermore, it may be possible to fully differentiate rural roads from urban roads, thereby reducing the error introduced when two urban patches are connected by a rural road and incorrectly classified as a single patch.

Finally, one of the challenges of this study was to account for a variety of confounding variables that affect air quality, but have no discernable connections with urban form. Although a number of control variables were identified and included within the multiple linear regression models, additional factors exist. Topography, for example, clearly had a significant impact on regional air quality among a few metropolitan areas. As observed in California's Central Valley, high mountain ranges such as the Sierra Nevada's can impede the dispersal of air pollutants, causing a spike in concentration

within the adjacent valley, particularly on the windward side. It may be possible to create a dummy variable to represent metropolitan areas within close proximity to a mountain range with some pre-defined minimum elevation (e.g. 3,000 m). The model could be enhanced by specifying whether a metropolitan area is on the windward or leeward side of the mountain range. Including such a "mountain" variable in the multiple linear regression models may be particularly useful if the study were expanded to include a larger number (> 86) of metropolitan areas.

Policy Implications

The major findings of this dissertation suggest that urban areas that exhibit more sprawl-like urban morphologies are more likely to experience higher levels of air pollution. Among the measures of urban form examined, residential density was most strongly associated with air pollution, suggesting that a significant increase in residential density could result in a detectable reduction in the ambient concentration of O_3, $PM_{2.5}$, and the emission of CO_2 from on-road sources. An increase in residential density is beneficial in regard to air quality primarily because it encourages alternative modes of transportation, such as walking, biking and transit, reducing tailpipe emissions per capita (Frank et al. 2000; Ewing 2003; Grazi et al. 2008). Urban areas with high residential densities were found to share additional characteristics potentially of benefit to air quality, including a greater degree of mixed-use development and improved street network connectivity (Table 37). There are currently a variety of planning policies used to encourage compact development as a means of providing healthier, more livable communities (Geller 2003; Ewing 2003)

Several cities and metropolitan areas throughout the U.S. have in recent decades adopted a number of urban planning policies, often termed smart growth, growth management, or sustainable development, to promote compact communities and reduce low-density suburban sprawl. One strategy for limiting the growth of low-density development along the urban periphery is the formation of urban growth boundaries (UGBs) or urban service limits. Urban growth boundaries restrict urban development beyond a designated line by 1) preventing the extension of public services, such as water, sewer and fire protection beyond the UGB, 2) imposing large minimum lot size restrictions (e.g. 40+ acres) and/ or land use restrictions (e.g. agriculture only) outside the UGB to discourage suburban or exurban land uses, and 3) forbidding new development outside the UGB, such as in Portland, Oregon (Nelson and Sanchez 2005; Stone 2008). Although UGBs and other strong urban containment strategies have been in place for a relatively short period of time (e.g. since 1980 in Oregon, 1994 in Washington, and 1998 in Tennessee), evidence suggests they can be effective at encouraging compact development. Four of the five metropolitan areas identified by Nelson and Sanchez (2005) as having "strong" urban containment policies, including Portland, OR, Miami, FL, San Diego, CA, and Sacramento, CA were ranked among the least sprawling metros by at least one urban sprawl index (Table 16). Miami and Sacramento also had among the highest urban "continuity" at the low urban threshold (Table 25). Furthermore, Nelson and Sanchez (2005) reported that all five metros with "strong" urban containment policies, including Seattle, WA, experienced an increase in population density between 1990 and 2000, whereas cities that decreased in population density had either "weak" or

no urban containment policy. As reported in the Cascadia case study (section 4.6.6), Miami and Portland were among three of the 35 largest metropolitan areas to exhibit a decrease in total exurban area between 1990 and 2000 (Nelson and Sanchez 2005).

In addition to urban containment policies such as UGBs, other smart growth efforts are being implemented to reduce greenhouse gas emissions, improve air quality, and meet other sustainability goals. Transit-oriented development (TOD), for example, focuses moderate-to-high density residential and commercial development around public transit depots. In addition to transit accessibility, TOD projects often aim to provide compact, mixed-use centers with open space and public areas to encourage pedestrianism (Ewing et al. 2007). Ideally, residents of TODs should be able to make most daily trips by walking or biking, while longer inter-urban trips are accommodated by public transit. Transit oriented developments are expected to reduce average vehicle trip length, vehicle miles traveled (VMT), and ease traffic congestion throughout the metropolitan region (Zhang 2010). Other alternatives to low-density sprawl include neotraditional or new urbanist developments, which incorporate "traditional" (i.e. pre-WWII) urban design elements. According to the Congress for the New Urbanism, traditional design elements may include a town center, often with a park or other open space, streets arranged in compact, "walkable" blocks, availability of affordable housing, schools and retail stores within walking distance (i.e. horizontal mixed-use development), and a "human-scaled public realm" (Congress for the New Urbanism 2010). Together, these design elements are meant to encourage a pedestrian-oriented lifestyle, though it is critical that new

urbanist developments are connected, through transit, to the larger urban environment to reduce automotive trips beyond the neighborhood.

The urban morphology of most large cities in the United States has, over the last century, undergone a major transformation. The relatively compact, centralized cities of the pre-automotive, pre-interstate era have given way to ever more diffuse, decentralized, suburban and exurban morphologies. Having now recognized the deleterious effects of largely unplanned and ineffective land use patterns, it is possible to intentionally guide urban development along a more sustainable course. Whether based on traditional neighborhoods or new high-rise developments, compact communities combined with high-frequency, high-capacity public transit offers the most promising alterative to automotive-based suburban sprawl. Although technological innovations, such as the electric car, will likely do much to reduce air pollutant emissions over the coming decades, it is important to consider at once all the benefits sustainable design practices may have to offer: cleaner air, cleaner water, fewer greenhouse emissions, and a healthier, more stimulating living environment.

REFERENCES

Akbari, H. 1992. Cooling Our Communities. U.S. Environmental Protection Agency, Office of Policy, Planning, and Evaluation, Climate Change Division.

Alig, R.J., J.D. Kline, and M. Lichtenstein. 2004. Urbanization on the US landscape: looking ahead in the 21st century. *Landscape and Urban Planning*. 69:219-234.

Aneja, V.P., R.G. Oommen, A.J. Riordan, S.P Arya, R.J. Wayland, and G.C. Murray. 1999. Ozone patterns for three metropolitan statistical areas in North Carolina, USA. *Atmospheric Environment*. 33:5081-5093.

Aneja, V., A.A. Andrea, and S.P. Arya. 2000. An observational based analysis of ozone trends and production for urban areas in North Carolina. *Chemosphere – Global Change Science*. 2:157-165.

Bacon, E.N. 1974. Design of Cities. Revised Ed. New York, NY: Penguin Books.

Bhatta, B., S. Saraswati and D. Bandyopadhyay. 2010. Urban sprawl measurement from remote sensing data. *Applied Geography*. Article in Press.

Bengston, D.N., R.S. Potts, D.P. Fan, and E.G. Goetz. 2005. An analysis of the public discourse about urban sprawl in the United States: Monitoring concern about a major threat to forests. *Forest Policy and Economics*. 7: 745– 756.

Boden, T.A., G. Marland, and R.J. Andres. 2009. Global, Regional, and National Fossil-Fuel CO_2 Emissions. Carbon Dioxide Information Analysis Center, Oak Ridge National Laboratory, U.S. Department of Energy, Oak Ridge, Tenn., U.S.A. doi 10.3334/CDIAC/00001

Bereitschaft, B. 2008. Spatial-temporal distribution of tropospheric ozone in the Carolina Piedmont megapolitan area. *The North Carolina Geographer*. 16:49-59.

Bereitschaft, B. 2010. Estimating urban growth in the Southeastern U.S. (1990 – 2008) using nighttime satellite imagery. Unpublished Manuscript.

Borrego, C., H. Martins, O. Tchepel., L. Salmim, A. Monteiro, and A.I. Miranda. 2006. How urban structure can affect city sustainability from an air quality perspective. *Environmental Modelling and Software*. 21:461-46

Brazel, A., N. Selover, R. Vose, and G. Heisler. 2000. The tale of two climates – Baltimore and Phoenix urban LTER sites. *Climate Research*. 15:123-135.

Brown, D.G., K.M. Johnson, T.R. Loveland, D.M. Theobald. 2005. Rural land-use trends in the conterminous United States. *Ecological Applications*. 15:1851–1863.

Bruekner, J.K. 2000. Urban Sprawl: Diagnosis and Remedies. *International Regional Science Review*. 23(2):160-171.

Bruegmann, R. 2006. *Sprawl: A Compact History*. Chicago, Ill: University of Chicago Press.

Burchfield, M., H.G. Overman, D. Puga, and M.A. Turner. 2006. Causes of sprawl: A portrait from space. *Quarterly Journal of Economics*. 121(2):587-633.

Burgess, E.W. 1925. The growth of the city: an introduction to a research project. In Park, R.E. and Burgess, E.W. (eds) The City, pp. 47-62.

Camalier, L., W. Cox, and P. Dolwick. 2007. The effects of meteorology on ozone in urban areas and their use in assessing ozone trends. *Atmospheric Environment*. 41:7127-7137.

Cardelino, R., and W. Chameides. 1990. Natural hydrocarbons, urbanization, and urban ozone. *Journal of Geophysical Research*. 95:13971-13979.

Carnahan, W.H., and R.C. Larson. 1990. An analysis of an urban heatsink. *Remote Sensing of Environment*. 33:65–71.

Carruthers, J.I., and G.F. Ulfarsson. 2003. Urban sprawl and the cost of public services. *Environment and Planning B: Planning and Design*. 30:503-522.

Condon, P.M. 2008. Design Charrettes for Sustainable Communities. Washington, D.C.: Island Press.

Cline, W.R. 2007. Global Warming and Agriculture. Washington, D.C.: Peterson Institute.

Cuhadaroglu, B. and E. Demirci. 1997. Influence of some meteorological factors on air pollution in Trabzon city. *Energy and Buildings*. 25:179-184.

Dasgupta, S., B. Laplante, C. Meisner, D. Wheeler, and J. Yan. The impact of sea level rise on developing countries: A comparative analysis. World Bank Policy Research Working Paper 4136, February 2007. Washington, D.C.

DeCoster, J. 1998. *Overview of Factor Analysis.* Online: http://www.stat-help.com/notes.html

Devenport, H.M. and L.K. Peters. 1978. Field studies of atmospheric particulate concentration changes during precipitation. *Atmospheric Environment*. 12:997–1008.

Dietzel, C., M. Herold, J.J. Hemphill, and K.C. Clarke. 2005. Spatio-temporal dynamics in California's Central Valley: Empirical links to urban theory. *International Journal of Geographical Information Science*. 19:175-195.

Duany, A., E. Plater-Zyberk, and J. Speck. 2000. Suburban Nation: The Rise of Sprawl and the Decline of the American Dream. New York, NY: North Point Press.

Duering, I., J. Jacob, A. Lohmeyer, M. Lutz, and W. Reichenbacher. 2002. Estimation of the ''non-exhaust pipe'' PM10 emissions of roads for practical traffic air pollution modelling, Proceedings of the 11th International Symposium Transport and Air Pollution, June 2002, Graz, Austria, 19.21.

Elminir, H. 2005. Dependence of urban air pollutants on meteorology. *Science of the Total Environment*. 350:225-237.

EIA. 2010. Annual Energy Outlook 2010. U.S. United States Energy Information Administration, Department of Energy, Washington D.C.

EPA. 2001. Our Built and Natural Environments: A Technical review of the interactions between land use, transportation and environmental quality (EPA 231-R-01–002). Washington, D.C.

EPA. 2007. "What is Acid Rain?" Environmental Protection Agency, Washington, D.C. Available online: http://www.epa.gov/acidrain/what/index.html

EPA. 2008. "Particulate Matter: National Summary of Particulate Matter Emissions." Environmental Protection Agency, Washington, D.C. Available online: http://www.epa.gov/air/emissions/pm.htm

EPA. 2009. “Air Trends: Particulate Matter.” Environmental Protection Agency, Washington, D.C. Available online: http://www.epa.gov/airtrends/pm.html

EPA. 2009b. Air Quality Index: A Guide to Air Quality and Your Health. Environmental Protection Agency, Office of Air Quality Planning and Standards, Outreach and Information Division. Research Triangle Park, NC.

EPA. 2010. “Ground-Level Ozone: Basic Information.” Environmental Protection Agency, Washington, D.C. Available online: http://www.epa.gov/air/ozonepollution/basic.html

EPA. 2010b. “Particulate Matter: Basic Information.” Environmental Protection Agency, Washington, D.C. Available online: http://www.epa.gov/oar/particlepollution/basic.html
Ewing, R. 1997. Is Los Angeles-style sprawl desirable? *Journal of the American Planning Association*. 63(1):107-126.

Ewing, R., K Bartholomew, S. Winkelman, J. Walters and D. Chen. 2007. Growing Cooler: The Evidence on Urban Development and Climate Change.

Ewing, R., R.C. Brownson, and D. Berrigan. 2006. Relationship between urban sprawl and weight of United States youth. *American Journal of Preventative Medicine*. 31(6):464-474.

Ewing, R., R. Pendall, and D. Chen. 2002. Measuring sprawl and its impacts. Smart Growth of America Report. Available Online: http://www.smartgrowthamerica.org/sprawlindex/sprawlindex.html

Ewing, R., R. Pendall, and D. Chen. 2003. Measuring sprawl and its transportation impacts. *Transportation Research Record*. 1831:175-183.

Ewing, R. and F. Rong. 2008. The impact of urban form on U.S. residential energy use. *Housing Policy Debate*. 19(1):1-30.

Ewing, R., T. Schmid, R. Killingsworth, A. Zlot, and S. Raudenbush. 2003. Relationship between urban sprawl and physical activity, obesity, and morbidity. *American Journal of Health Promotion*. 18:47–57.

Felzer, B., D. Kicklighter, J. Melillo, C. Wang, Q. Zhuang, and R. Prinn. 2004. Effects of ozone on net primary production and carbon sequestration in the conterminous United States using a biogeochemistry model. *Tellus B*. 56(3):230-248.

Frank, L., B. Stone, and W. Bachman. 2000. Linking land use with household vehicle emissions in the central Puget Sound: methodological framework and findings. *Transportation Research D*. 5:173-196.
Frank, L.D. and G. Pivo. 1994. Impacts of mixed use and density on utilization of three modes of travel: single-occupant vehicle, transit, and walking. *Transportation Research Record*. 1466:44-52.

Frumpkin, H. 2002. Urban sprawl and public health. *Public Health Reports*. 117(3): 201-217.

Fulton, W., R. Pendall, M. Nguyen, and A. Harrison. 2001. Who sprawls the most? How growth patterns differ across the united states. Washington, DC: The Brookings Institution.

Gallion, A.B., and S. Eisner. 1986. The Urban Pattern: City Planning and Design. 5th Ed. New York, NY: Van Nostrand Reinhold Company.

Galster, G., R. Hanson, M.R. Ratcliffe, H. Wolman, S. Coleman and J. Freihage. 2001. Wrestling Sprawl to the Ground: Defining and Measuring an Elusive Concept. *Housing Policy Debate*. 12(4):681-717.

Galvez, O. 2007. Synoptic-scale transport of ozone in Southern Ontario. *Atmospheric Environment*. 41:8579-8995.

GAO. 2004. Metropolitan Statistical Areas: New Standards and Their Impact on Selected Federal Programs. Report to the Subcommittee on Technology, Information Policy, Intergovernmental Relations and the Census, Committee on Government Reform, House of Representatives. United States General Accounting Office. Washington, D.C. Available Online: http://www.gao.gov/new.items/d04758.pdf

Gao, H.O. and D.A. Niemeier. 2008. Using functional data analysis and diurnal ozone and NOx cycles to inform transportation emissions control. *Transportation Research Part D*. 13:221-238.

Gehrig, R. and B. Buchmann. 2003. Characterising seasonal variations and spatial distribution of ambient PM10 and PM2.5 concentrations based on long-term Swiss monitoring data. *Atmospheric Environment*. 37(19):2571-2580.

Geller, A.L. 2003. Smart growth: a prescription for livable cities. *American Journal of Public Health*. 93(9):1410-1415.

Gray, K. A. and M.E. Finster. 1999. The Urban Heat Island, Photochemical Smog, and Chicago: Local Features of the Problem and Solution. U.S. Environmental Protection Agency, Atmospheric Pollution Prevention Division.

Grazi, F., J.C. Van der Bergh, and J.N. Van Ommeren. 2008. An empirical analysis of urban form, transport, and global warming. *Energy Journal*. 29(4):97-122.

Grimm, N.B., S.H. Faeth, N.E. Golubiewski, C.L Redman, J. Wu, X. Bai, and J.M. Briggs. 2008. Global change and the ecology of cities. *Science*. 319:756-760.

Gustafson, E. J. 1998. Quantifying landscape spatial pattern: what is the state of the art? *Ecosystems*. 1:143–156.

Haines, M. 2002. Vital Statistics. In S. Carter, M. Haines, A. Olmstead, R. Sutch, and G. Wright (Eds.), *Historical Statistics of the United States: Millennial Edition*. New York, NY: Cambridge University Press.

Handy, S., X. Cao, and P. Mokhtarian. 2005. Correlation or causality between the built environment and travel behavior? Evidence from Northern California. *Transportation Research Part D*. 10:427-444.

Hao, J., L. Wang, M. Shen, L. Li, and J. Hu. 2007. Air quality impacts of power plant emissions in Beijing. *Environmental Pollution*. 147(2):401-408.

Harris, C.D. and E.L. Ullman. 1945. The nature of cities. *Annals of the American Academy of Political and Social Science.* 242:7-17.

Harrison, R.M., A.R. Deacon, M.R. Jones, and R.S. Appleby. 1997. Sources and processes affecting concentrations of PM10 and PM2.5 particulate matter in Birmingham (U.K.). *Atmospheric Environment*. 31(24):4103-4117.

Herold, M., N.C. Goldstein, and K.C. Clarke. 2003. The spatiotemporal form of urban growth: measurement, analysis and modeling. *Remote Sensing of Environment*. 86:286-302.

Hillier, B.1996. Cities as movement economies. *Urban Design International*. 1:41-60.

Hofmann, D.J., J.H. Butler, and P.P. Tans. 2009. A new look at atmospheric carbon dioxide. *Atmospheric Environment*. 43:2084-2086.

Hoyt, H. 1939. The Structure and Growth of Residential Neighborhoods in American Cities. Washington, D.C.: US Federal Housing Administration.

Huang, J., X.X. Lu, and J.M. Sellers. A global comparative analysis of urban form: Applying spatial metrics and remote sensing. *Landscape and Urban Planning*. 82:184-197.

Hubbard, M.C., and W.G. Cobourn. 1999. An enhanced ozone forecasting model using air mass trajectory analysis. *Atmospheric Environment*. 33:4663-4674

Imhoff, M. L., W.T. Lawrence, D.C. Stutzer, and C.D. Elvidge. 1997. A technique for using composite DMSP/OLS "city lights" satellite data to map urban area. *Remote Sensing of Environment*. 61:361-370.

Intergovernmental Panel on Climate Change (IPCC). 2007. Climate Change 2007: Synthesis Report.

Intergovernmental Panel on Climate Change (IPCC). 2009. "Carbon Dioxide: Projected emissions and concentrations." Available Online: http://www.ipcc-data.org/ddc_co2.html

Jacob, D.J. and D.A. Winner. 2009. Effect of climate change on air quality. *Atmospheric Environment*. 43:51-63.

Jenkin, M.E. and K.C. Clemitshaw. 2000. Ozone and other secondary photochemical pollutants: chemical processes governing their formation in the planetary boundary layers. *Atmospheric Environment*. 34:2499-2527.

Jensen, J. R. and D.C. Cowen.1999. Remote sensing of urban/suburban infrastructure and socio-economic attributes. *Photogrammetric Engineering and Remote Sensing*. 65(5):611–622.

Jerrett, M. et al. 2009. Long-term ozone exposure and mortality. *The New England Journal of Medicine*. 360:1085-1095.

Jun, M-J. 2004. The effects of Portland's urban growth boundary on urban development patterns and commuting. *Urban Studies*. 41(7):1333-1348.

Kansal, A. 2009. Sources of reactivity of NMHCs and VOCs in the atmosphere: A review. *J. of Hazardous Materials*. 166:17-26.

Kaplan, D.H., J.O. Wheeler, and S. Holloway. 2003. Urban Geography. Hoboken, NJ: Wiley, John & Sons, Incorporated.

Keeling, C.D., R.B. Bacastow, A.E. Bainbridge, C.A. Ekdahl, P.R. Guenther, L.S. Waterman, and J.F.S. Chin. 1976. Atmospheric carbon dioxide variations at Mauna Loa observatory, Hawaii. *Tellus*. 28(6):538-551.

Khasnis, A.A. and M.D. Nettleman. 2005. Global warming and infectious disease. *Archives of Medical Research*. 36(6):689-696.
Laden, F., L.M. Neas, D.W. Dockery, and J. Schwartz. 2000. Association of fine particulate matter from different sources with daily mortality in six U.S. cities. *Environmental Health Perspectives*. 108(10):941-947.

Lai, L. and W. Cheng. Air quality influenced by urban heat island synoptic weather patterns. *Science of the Total Environment*. 407:2724-2733.

Lang, R. 2003. Edgeless cities: exploring the elusive metropolis. Washington, D.C.: The Brookings Institution.

Lang, R. 2006. Megapolitan America. New Metropolis Lecture Series. September 6, Alexandria, VA.

Lang, R.E. and D. Dhavale. 2006. Micropolitan America: a brand new geography in Berube, A., B. Katz and R.E. Lang (Eds) *Redefining Cities and Suburbs: Evidence from Census 2000*, Vol. 3, pp. 237-258. Washington, D.C.: Brookings Institution Press.

Lang, R.E. and J. S. Hall. 2008. The Sun Corridor: Planning Arizona's Megapolitan Area. Morrison Institute of Public Policy, Tempe, AZ.

Lang, R.E. and P.L. Knox. 2009. The New Metropolis: Rethinking Megalopolis. *Regional Studies*. 43(6):789-802.

Latza, U., S. Gerdes, and X. Baur. 2009. Effects of nitrogen dioxide on human health: systematic review of experimental and epidemiological studies conducted between 2002 and 2006. *International Journal of Hygiene and Environmental Health*. 212(3):271-287.

Larivi`ere, I. and G. Lafrance. 1999. Modelling the electricity consumption of cities: effect of urban density. *Energy Economics*. 21(1):53-66.

Lewis, P.E. 1983. The galactic metropolis, in Pratt, R.H. and G. Macinko (Eds) *Beyond the Urban Fringe*, pp. 60-91. Minneapolis, MN: University of Minnesota Press.

Likens, G.E., C.T. Driscoll, and D.C. Buso. 1996. Long term effects of acid rain: Response and recovery of a forest ecosystem. *Science, New Series*. 272(5259):244-246.

Liu, J., C. Chan, and F.T. Jeng. 1994. Pr edicting personal exposure levels to carbon monoxide (CO) in Taipei, based on actual CO measurements in microenvironments and a Monte Carlo simulation method. *Atmospheric Environment*. 28(14):2361 -2368.

Liu, L.S. and A.J. Rossini. 1996. Use of kriging models to predict 12-hour mean ozone concentrations in Metropolitan Toronto – A pilot study. *Environment International*. 22(6):677-692.

Lopez, R. and H.P. Hynes. 2003. Sprawl in the 1990s: measurement, distribution and trends. *Urban Aff. Rev*. 38(3):325–355.

Lu, H-C and G-C Fang. 2002. Estimating the frequency distributions of PM10 and PM2.5 by the statistics of wind speed at Sha-Lu, Taiwan. *The Science of the Total Environment*. 298:119-130.

Lu, R., and R.P. Turco. 1995. Air pollutant transport in a coastal environment—II. Three-dimensional simulations over Los Angeles basin. *Atmospheric Environment*. 29(13):1499-1518.

Luck, M.A., G.D. Jenerette, J. Wu, and N.B. Grimm. 2001. The urban funnel model and the spatially heterogeneous ecological footprint. *Ecosystems*. 4:782–796.

Luck, M. and J. Wu. 2002. A gradient analysis of urban landscape pattern: a case study from the Phoenix metropolitan region, Arizona, USA. *Landscape Ecology*. 17:327–339.

Mandal, R.B. 1990. Land Utilization: Theory and Practice. New Delhi, India: Concept Publishing Company.

Massachusetts v. Environmental Protection Agency, 549 U.S. 497 (2007).

Massey, D.S. and N. Denton. 1988. The dimensions of residential segregation. *Social Forces*. 67:281-313.

McConnell et al. 1999. Air pollution and bronchitic symptoms in southern California children with asthma. *Environmental Health Perspectives*. 107(9):757-760.

McGarigal, K., and B.J. Marks. 1995. FRAGSTATS: spatial pattern analysis program for quantifying landscape structure. USDA Forest Service, Pacific Northwest Research Station. General Technical Report PNW-GTR-351.

McGarigal, K., S.A. Cushman, M.C. Neel, and E. Ene. 2002. FRAGSTATS: Spatial Pattern Analysis Program for Categorical Maps. Computer software program produced

by the authors at the University of Massachusetts, Amherst. Available online: www.umass.edu/landeco/research/fragstats/fragstats.html

Morris, D.E. 2003. It's a Sprawl World After All. Gabriola Island, BC, Canada: New Society Publishers.

Muller, E.K. 2001. Industrial suburbs and the growth of metropolitan Pittsburgh. Journal of *Historical Geography*. 27(1):58-73.

Muller, P.O. 1995. "Transportation and Urban Form: Stages in the Spatial Evolution of the American Metropolis." In Hanson, S. (ed.) The Geography of Urban Transportation, 2nd Edition. New York: Guilford, p. 29.

Mumford, L. 1961. The City in History: Its Origins, its Transformation, and its Prospects. New York, NY: Harcourt, Brace & World, Inc.

Murphy, J.J., M.A. Delucchi, D.R. McCubbin, and H.J. Kim. 1999. The cost of crop damage caused by ozone air pollution from motor vehicles. *Journal of Environmental Management*. 55: 273–289.

Naresh, R., S. Sundar, and J.B. Shukla. 2007. Modeling the removal of gaseous pollutants and particulate matters from the atmosphere of a city. *Nonlinear Analysis*. 8:337-344.

Nasser, H.E. and P. Overberg. 2001. What you don't know about sprawl. USA Today, 22 February, 1A, 6A–9A.

Naughton, K. 2006. The long and grinding road. *Newsweek*. 1 May, 41-44.

Nelson, A.C. 1999. Comparing states with and without growth management: analysis based on indicators with policy implications. *Land Use Policy*. 16:121–127.

Nelson, A.C. and T.W. Sanchez. 2005. The effectiveness of urban containment regimes in reducing exurban sprawl. DISP 160:42–47.

Newman P. and J. Kenworthy. 1989. Cities and automobile dependence. An international sourcebook. Gower Technical, Aldershot.

Newton, P. 1997. Reshaping cities for a more sustainable future: exploring the link between urban form, air quality, energy and greenhouse gas emissions. Report of the Australian Academy of Technological Sciences and Engineering, Melbourne, Australia.

Nguyen, H.T., and K.H. Kim. 2006. Comparison of spatiotemporal distribution patterns of NO_2 between four different types of air quality monitoring station. *Chemosphere*. 65:201-212.

Nicholls, R.J., and N. Mimura. 1998. Regional issues raised by sea-level rise and their policy implications. *Climate Research*. 11:5-18.

Olivier, J.G., A. F. Bouwman, K. W. Van der Hoek, and J.M. Berdowski. 1998. Global air emission inventories for anthropogenic sources of NO_x, NH_3 and N_2O in 1990. *Environmental Pollution*. 102(1):135-148.

Oltmans, S.J., A.S. Lefohn, J.M. Harris, and D.S. Shadwick. 2008. Background ozone levels of air entering the west coast of the US and assessment of longer-term changes. *Atmospheric Environment*. 42:6020-6038.

Oke, T.R., 1987. Boundary Layer Climates. Methen, London, second ed. 435pp.

OMB. 2008. OMB Bulletin No. 09-01. Executive Office of the President, Office of Management and Budget. Washington, D.C. Available Online: http://www.whitehouse.gov/sites/default/files/omb/assets/omb/bulletins/fy2009/09-01.pdf

O'Meara, M. 1999. Reinventing cities for people and the planet. Worldwatch Paper. 149:4-94.

O'Neill, R. V., J. R. Krummel, R.H. Gardner, G. Sugihara, B. Jackson, D.L. Deangelis, B.T. Milne, M.G. Turner, B. Zygmunt, S.W. Christensen, V.H. Dale, and R.L. Graham. 1988. Indices of landscape pattern. *Landscape Ecology*. 1:153-162.

Pacione, M. 2001. Urban Geography, a global perspective. New York, NY: Routledge.

Pataki, D.E., R.J. Alig, A.S. Fung, N.E. Golubiewski, C.A. Kennedy, E.G. McPherson, D.J. Nowak, R.V. Pouyat, and P. Romero Lankao. 2006. Urban ecosystems and the North American carbon cycle. *Global Change Biology*. 12(11): 2092-2102.

Pickard, J.P. 1970. Is megalopolis inevitable? *The Futurist*. October, 151-156.

Porter, P. S., S.T. Rao, I.G. Zurbenko, E. Zalewsky, R.F. Henry, and J.Y. Ku.1996. Statistical characteristics of spectrally-decomposed ambient ozone time series data. Report to the OTAG Air Quality Analysis Workgroup.

Rajasekar, U. and Q. Weng. 2009. Spatio-temporal modeling and analysis of urban heat islands using Landsat TM and ETM+ imagery. *International Journal of Remote Sensing*. 30(13):3531-3548.

Rao, S. T., I. G. Zurbenko, R. Neagu, P. S. Porter, J. Y. Ku, and R. F. Henry. 1997. Space and Time Scales in Ambient Ozone Data. *Bull. Amer. Meteor. Soc.* 78:2153–2166.

Raupach, M.R., G. Marland, P. Ciais, C. Quere, J.G. Candell, G. Klepper, and C.B. Field. 2007. Global and regional drivers of accelerating CO_2 emissions. *Proceedings of the National Academy of Sciences*. 104(24):10288-10293.

Platt, R.H. 2004. Land Use and Society: Geography, Law, and Public Policy. Revised Edition. Washington, D.C.: Island Press.

Reps, J.W. 1965. The Making of Urban America: A History of City Planning in the United States. Princeton, NJ: Princeton University Press.

Rhind, D. and R. Hudson. 1980. Land Use. New York, NY: Methuen & Co.

Rimetz-Planchon, J., E. Perdix, S. Sobanska, and C. Bremard. 2008. PM10 air quality variations in an urbanized and industrialized harbor. *Atmospheric Environment*. 42:7274-7283.

Robinson, L., J.P. Newell, J.M. Marzluff. 2005. Twenty-five years of sprawl in the Seattle region: growth management responses and implications for conservation. *Landscape and Urban Planning*. 71:51-72.

Rosenfeld, A., H. Akbari, S. Bretz, B. Fishman, D. Kurn, D. Sailor, and H. Taha. 1995. Mitigation of urban heat islands: materials, utility programs, updates. *Energy and Buildings* 22:255-65.

Rosenzweig, C., W.D. Solecki, L. Parshall, M. Chopping, G. Pope, and R. Goldberg. 2005. Characterizing the urban heat island in current and future climates in New Jersey. *Environmental Hazards*. 6:51-62.

Samet, J.M. et al. 2000. Fine particulate air pollution and mortality in 20 U.S. cities, 1897-1994. The New England Journal of Medicine. 343:1742-1749.

Sanders, S.E., and A.J. Rabuck. 1946. New City Patterns: The Analysis of and a Technique for Urban Reintegration. New York, NY: Reinhold Publishing Corp.

Scholze, M., W. Knorr, N.W. Arnell, and I.C. Prentice. 2006. A climate-change risk analysis for world ecosystems. *Proceedings of the National Academy of Sciences of the United States*. 103(35):13116-13120.

Seinfeld, J.H. and S.N. Pandis. 1997. Atmospheric Chemistry and Physics, from Air Pollution to Climate Change. New York, NY: John Wiley & Sons.

Shepherd, J.M., and S.J. Burian. 2003. Detection of urban-induced rainfall anomalies in a major coastal city. *Earth Interactions*. 7(4):1-17.

Slade, D.H. 1967. Modeling air pollution in the Washington, D.C., to Boston Megalopolis. *Science*. 157(3794):1304-1307.

Steemers, K. 2003. Energy and the city: density, buildings and transport. *Energy and Buildings*. 35(1):3-14.

Schindler, D.W. 1988. Effects of acid rain of freshwater ecosystems. *Science*. 239(4836):149 – 157.

Smith, Z.A. 2009. The Environmental Policy Paradox. 5th Ed. Upper Saddle River, NJ: Pearson Education, Inc.

Snow, J.A., J.B. Dennison, D.A. Jaffe, H.U. Price, J.K. Vaughan, and B. Lamb. 2003. Aircraft and surface observations of air quality in Puget Sound and a comparison to a regional model. *Atmospheric Environment*. 37:4019-4032.

Southworth , M. and E.B. Joseph. 2003. Streets and the Shaping of Towns and Cities. Washington, D.C.: Island Press.

Stone, B. 2008. Urban sprawl and air quality in large US cities. *Journal of Environmental Management*. 86:688-698.

Stone, B., and J. Bullen. 2006. Urban form and watershed management: how zoning influences residential stormwater volumes. *Environment and Planning*. 33:21-37.

Streuker, D. 2003. Satellite-measured growth of the urban heat island of Houston, Texas. *Remote Sensing of Environment*. 85(3):282-289.

Sushira, H.S., T.V. Ramachandra, and K.S. Jagadish. 2004. Urban sprawl: metrics, dynamics and modelling using GIS. *International Journal of Applied Earth Observation and Geoinformation*. 5:29–39

Sutton, P.C. 2003. A scale-adjusted measure of "urban sprawl" using nighttime satellite imagery. *Remote Sensing of Environment*. 86:353-369.

Taha, H. and R. Bornstein.1999. Urbanization of meteorological models: Implications on simulated heat islands and air quality. Invited paper, *International Congress of Biometeorology and International Conference on Urban Climatology*, 8-12 November, 1999, Sydney, Australia.

Tans, P. 2010. "Trends in Atmospheric Carbon Dioxide." NOAA/ESRL. Available Online: http://www.esrl.noaa.gov/gmd/ccgg/trends/#mlo_full

Taseiko, O.V., S.V. Mikhailuta, A. Pitt, A.A. Lezhenin, and Y.V. Zakharov. 2009. Air pollution dispersion within urban street canyons. *Atmospheric Environment*. 43:245-252.

United Nations. 2006. State of the World's Cities 2006/2007. United Nations Centre for Human Settlements. Nairobi, Kenya.

U.S. Census Bureau. 2001. Metropolitan areas ranked by percent population change: 1990 to 2000. U.S. Department of Commerce. Economics and Statistics Administration. U.S. Census Bureau, Washington, D.C.

U.S. Census Bureau. 2001b. Census 2000 Brief: Population Change and Distribution 1990 to 2000. U.S. Department of Commerce. Economics and Statistics Administration. U.S. Census Bureau, Washington, D.C.

USDA. 2009. "Effects of Ozone Air Pollution on Plants." United States Department of Agriculture, Agricultural Research Service. Available online: http://www.ars.usda.gov/Main/docs.htm?docid=12462

Van Metre, P., Mahler, B., and E. Furlong. 2000. Urban sprawl leaves its PAH signature. *Environmental Science Technology*. 34: 4064-4070.

Vance, J. E., Jr. 1964. Geography and Urban Evolution in the San Francisco Bay Area. Berkeley, CA: Institute of Governmental Studies.

Vardoulakis, S. and P. Kassomenos. 2008. Sources and factors affecting PM10 levels in two European cities: Implications for local air quality management. *Atmospheric Environment*. 42:3949-3963.

Vingarzan, R. 2004. A review of surface ozone background levels and trends. *Atmospheric Environment*. 38:3431-3442.

Vogelmann, J. E., T. Sohl, and S.M. Howard.1998. Regional characterization of land cover using multiple sources of data. *Photogrammetric Engineering and Remote Sensing*. 64(1):45-57.
Volz,, A. and D. Kley. 1988. Evaluation of the Montsouris series of ozone measurements in the 19th century. *Nature*. (332):240–242.

Wallace, J. and P. Kanaroglou. 2009. The effect of temperature inversions on ground-level nitrogen dioxide (NO2) and fine particulate matter (PM2.5) using temperature profiles from the Atmospheric Infrared Sounder (AIRS). *Science of the Total Environment*. 407:5085-5095.

Warneck, P. (Ed.). 1988. Chemistry of the Natural Atmosphere. New York, NY: Academic Press.

Warner, S.B. 1978. Streetcar Suburbs: The Process of Growth in Boston, 1870 – 1900. Cambridge, MA: Harvard U. Press.

Washenfelder, R.A. 2010. Characterization of NO_x, SO_2, ethene, and propene from industrial emission sources in Houston, Texas. *Journal of Geophysical Research*. 115, D16311. 14 pp.

Wei, J., J. Ma, R. W. Twibell, and K. Underhill. Characterizing urban sprawl using multi-stage remote sensing images and landscape metrics. *Computers, Environment and Urban Systems*. 30:861-879.

Weng, Q. 2001. A remote sensing-GIS evaluation of urban expansion and its impact on surface temperature in the Zhujiang Delta, China. *International Journal of Remote Sensing*. 22:1999– 2014.

Weng, Q. 2003. Fractal analysis of satellite-detected urban heat island effect. *Photogrammetric Engineering & Remote Sensing*. 69(5):555-566.

White, M. 1987. American Neighborhoods and Residential Differentiation. New York, NY: Russell Sage Foundation.

World Health Organization. 2007. Estimated deaths & DALYs environmental risk factors, by WHO Member State, 2002. Available online: www.who.int/quantifying_ehimpacts/countryprofilesebd.xls

Yang, X. 2002. Satellite monitoring of urban spatial growth in the Atlanta metropolitan area. *Photogrammetric Engineering & Remote Sensing*. 68(7):725-734.

Zhang, M. 2010. Can transit-oriented development reduce peak-hour congestion? *Transportation Research Record*. 2174:148-155

APPENDIX A

TABLES AND FIGURES

Table 1. Pearson correlations among spatial metrics calculated at the high urban threshold.

		ED	LPI	AWMSI	AWMPFD	CONTAG	CLUMPY	LSI	CONTIG	PLADJ
	r^2	-.486**	1							
LPI	Sig.	.000								
	N	86	86							
	r^2	.531**	.048	1						
AWMSI	Sig.	.000	.663							
	N	86	86	86						
	r^2	.689**	-.007	.880**	1					
AWMPFD	Sig.	.000	.951	.000						
	N	86	86	86	86					
	r^2	-.904**	.661**	-.414**	-.596**	1				
CONTAG	Sig.	.000	.000	.000	.000					
	N	86	86	86	86	86				
	r^2	-.959**	.379**	-.553**	-.700**	.826**	1			
CLUMPY	Sig.	.000	.000	.000	.000	.000				
	N	86	86	86	86	86	86			
	r^2	.642**	-.205	.888**	.766**	-.504**	-.652**	1		
LSI	Sig.	.000	.058	.000	.000	.000	.000			
	N	86	86	86	86	86	86	86		
	r^2	-.901**	.648**	-.415**	-.570**	.916**	.834**	-.553**	1	
CONTIG	Sig.	.000	.000	.000	.000	.000	.000	.000		
	N	86	86	86	86	86	86	86	86	
	r^2	-.814**	.536**	-.367**	-.514**	.803**	.759**	-.479**	.862**	1
PLADJ	Sig.	.000	.000	.001	.000	.000	.000	.000	.000	
	N	86	86	86	86	86	86	86	86	86

**Correlation is significant at the 0.01 level. *Correlation is significant at the 0.05 level.

Table 2. Pearson correlations among spatial metrics calculated at the low urban threshold.

		ED	LPI	AWMSI	AWMPFD	CONTAG	CLUMPY	LSI	CONTIG	PLADJ
LPI	r^2	.010	1							
	Sig.	.927								
	N	86	86							
AWMSI	r^2	.459**	.350**	1						
	Sig.	.000	.001							
	N	86	86	86						
AWMPFD	r^2	.530**	.293**	.860**	1					
	Sig.	.000	.006	.000						
	N	86	86	86	86					
CONTAG	r^2	-.563**	-.727**	-.435**	-.379**	1				
	Sig.	.000	.000	.000	.000					
	N	86	86	86	86	86				
CLUMPY	r^2	-.822**	.469**	-.261*	-.392**	.012	1			
	Sig.	.000	.000	.015	.000	.910				
	N	86	86	86	86	86	86			
LSI	r^2	.588**	-.011	.792**	.581**	-.309**	-.510**	1		
	Sig.	.000	.918	.000	.000	.004	.000			
	N	86	86	86	86	86	86	86		
CONTIG	r^2	-.559**	.734**	-.093	-.249*	-.345**	.917**	-.353**	1	
	Sig.	.000	.000	.395	.021	.001	.000	.001		
	N	86	86	86	86	86	86	86	86	
PLADJ	r^2	-.595**	.714**	-.112	-.260*	-.309**	.939**	-.382**	.992**	1
	Sig.	.000	.000	.305	.016	.004	.000	.000	.000	
	N	86	86	86	86	86	86	86	86	86

**Correlation is significant at the 0.01 level (2-tailed). *Correlation is significant at the 0.05 level.

Table 3. Pearson correlations among spatial metrics with the high and low threshold values averaged.

		ED	LPI	AWMSI	AWMPFD	CONTAG	CLUMPY	LSI	CONTIG	PLADJ
	r^2	-.295**	1							
LPI	Sig.	.006								
	N	86	86							
	r^2	.462**	.221*	1						
AWMSI	Sig.	.000	.041							
	N	86	86	86						
	r^2	.633**	.167	.887**	1					
AWMPFD	Sig.	.000	.123	.000						
	N	86	86	86	86					
	r^2	-.884**	-.019	-.562**	-.704**	1				
CONTAG	Sig.	.000	.860	.000	.000					
	N	86	86	86	86	86				
	r^2	-.961**	.423**	-.392**	-.567**	.753**	1			
CLUMPY	Sig.	.000	.000	.000	.000	.000				
	N	86	86	86	86	86	86			
	r^2	.628**	-.111	.832**	.704**	-.605**	-.586**	1		
LSI	Sig.	.000	.308	.000	.000	.000	.000			
	N	86	86	86	86	86	86	86		
	r^2	-.776**	.734**	-.187	-.355**	.463**	.873**	-.415**	1	
CONTIG	Sig.	.000	.000	.085	.001	.000	.000	.000		
	N	86	86	86	86	86	86	86	86	
	r^2	-.786**	.667**	-.221*	-.383**	.494**	.873**	-.432**	.957**	1
PLADJ	Sig.	.000	.000	.040	.000	.000	.000	.000	.000	
	N	86	86	86	86	86	86	86	86	86

**Correlation is significant at the 0.01 level (2-tailed). *Correlation is significant at the 0.05 level.

Table 4. Pearson correlations among spatial metrics calculated at the high and low urban threshold.

		ED H	LPI H	AWMSI H	AWMPFD H	CONTAG H	CLUMPY H	LSI H	CONTIG H	PLADJ H
ED L	r^2	.846**	-.224*	.533**	.649**	-.688**	-.869**	.575**	-.692**	-.669**
	Sig.	.000	.038	.000	.000	.000	.000	.000	.000	.000
	N	86	86	86	86	86	86	86	86	86
LPI L	r^2	-.240*	.796**	.335**	.286**	.478**	.122	.100	.455**	.359**
	Sig.	.026	.000	.002	.008	.000	.264	.357	.000	.001
	N	86	86	86	86	86	86	86	86	86
AWMSI L	r^2	.305**	.089	.840**	.711**	-.238*	-.358**	.671**	-.204	-.248*
	Sig.	.004	.415	.000	.000	.027	.001	.000	.059	.021
	N	86	86	86	86	86	86	86	86	86
AWMPFD L	r^2	.330**	.037	.610**	.631**	-.302**	-.370**	.409**	-.218*	-.262*
	Sig.	.002	.738	.000	.000	.005	.000	.000	.044	.015
	N	86	86	86	86	86	86	86	86	86
CONTAG L	r^2	-.289**	-.461**	-.507**	-.503**	.010	.375**	-.427**	.010	.060
	Sig.	.007	.000	.000	.000	.925	.000	.000	.927	.583
	N	86	86	86	86	86	86	86	86	86
CLUMPY L	r^2	-.818**	.568**	-.290**	-.432**	.801**	.792**	-.398**	.815**	.771**
	Sig.	.000	.000	.007	.000	.000	.000	.000	.000	.000
	N	86	86	86	86	86	86	86	86	86
LSI L	r^2	.564**	-.245*	.830**	.689**	-.468**	-.582**	.914**	-.478**	-.465**
	Sig.	.000	.023	.000	.000	.000	.000	.000	.000	.000
	N	86	86	86	86	86	86	86	86	86
CONTIG L	r^2	-.649**	.714**	-.071	-.201	.758**	.584**	-.195	.755**	.684**
	Sig.	.000	.000	.515	.063	.000	.000	.072	.000	.000
	N	86	86	86	86	86	86	86	86	86
PLADJ L	r^2	-.690**	.715**	-.104	-.241*	.787**	.625**	-.234*	.783**	.724**
	Sig.	.000	.000	.342	.025	.000	.000	.030	.000	.000
	N	86	86	86	86	86	86	86	86	86

**Correlation is significant at the 0.01 level (2-tailed). *Correlation is significant at the 0.05 level

Table 5. Principal component analysis of spatial metrics calculated at the metropolitan scale, high urban threshold. PCA yielded two factors: “continuity” and “shape complexity.”

Spatial Metric	Continuity	Shape Complexity
ED	-0.803	0.532
LPI	0.843	0.215
AWMSI	-0.079	0.962
AWMPFD	-0.264	0.912
CONTAG	0.889	-0.353
CLUMPY	0.717	-0.582
LSI	-0.286	0.855
CONTIG	0.897	-0.361
PLADJ	0.829	-0.325
% of variance	67.6	19.4

Table 6. Principal component analysis of spatial metrics calculated at the metropolitan scale, low urban threshold. PCA yielded two factors: “continuity” and “shape complexity.”

Spatial Metric	Continuity	Shape Complexity
ED	-0.375	0.809
LPI	0.834	0.417
AWMSI	0.049	0.902
AWMPFD	-0.107	0.896
CONTAG	-0.537	-0.671
CLUMPY	0.830	-0.507
LSI	-0.218	0.837
CONTIG	0.960	-0.216
PLADJ	0.959	-0.248
% of variance	47	32.7

Table 7. Principal component analysis of spatial metrics calculated at the megapolitan scale, high urban threshold. PCA yielded two factors: “continuity” and “shape complexity.”

Spatial Metric	Continuity	Shape Complexity
ED	-0.814	0.471
LPI	0.789	0.543
AWMSI	-0.317	0.906
AWMPFD	-0.369	0.897
CONTAG	0.903	-0.294
CLUMPY	0.851	-0.358
LSI	-0.317	0.906
CONTIG	0.927	-0.337
PLADJ	0.917	-0.371
% of variance	73.4	17.9

Table 8. Principal component analysis of spatial metrics calculated at the megapolitan scale, low urban threshold. PCA yielded two factors: “continuity” and “shape complexity.”

Spatial Metric	Continuity	Shape Complexity
ED	-0.370	0.851
LPI	0.438	0.143
AWMSI	-0.334	0.738
AWMPFD	-0.117	0.862
CONTAG	-0.521	-0.713
CLUMPY	0.753	-0.565
LSI	-0.797	0.317
CONTIG	0.948	-0.258
PLADJ	0.893	-0.358
% of variance	54.2	21.1

Table 9. Principal component analysis of meteorological/climatic variables at the metropolitan scale yielded two climate factors: “temperature” and “moisture.”

	Temperature	Moisture
Avg. Temp.	0.985	-0.062
Avg. Max. Temp.	0.968	-0.189
Avg. Precipitation	0.145	0.911
Cloudy Days	-0.620	0.697
Cooling Degree Days	0.944	-0.034
Heating Degree Days	-0.958	0.075
Relative Humidity	-0.188	0.872
% of variance	63.5	26.3

Table 10. Principal component analysis of meteorological/climatic variables at the megapolitan scale yielded two climate factors: “temperature” and “moisture.”

	Temperature	Moisture
Avg. Temp.	0.991	0.052
Avg. Max. Temp.	0.990	-0.047
Avg. Precipitation	0.087	0.935
Cloudy Days	-0.582	0.717
Cooling Degree Days	-0.970	0.016
Heating Degree Days	-0.582	0.717
Relative Humidity	0.060	0.864
% of variance	55.5	27.3

Table 11. Descriptive statistics for control variables at the metropolitan scale (Metro.) and megapolitan scale (Mega.).

Pollutant	Scale	Mean	Maximum	Minimum	Range	Standard Deviation
Temperature Factor	Metro.	0	2.54	-1.49	4.04	1.0
(standard deviations)	Mega.	0	1.65	-1.31	2.96	1.0
Moisture Factor	Metro.	0	1.48	-3.01	4.49	1.0
(standard deviations)	Mega.	0	1.34	-2.60	3.94	1.0
Average Wind Speed	Metro.	8.93	12.3	6.0	6.3	1.48
(mph)	Mega.	9.01	12.3	6.53	5.77	1.39
Population	Metro.	2.24	21.4	0.513	20.8	3.15
(millions)	Mega.	8.78	31.1	3.52	27.5	6.62
Population within 500 km	Metro.	38.3	80.7	5.69	74.9	19.6
(millions)	Mega.	47.8	92.1	8.08	84.1	25.6
Geographic Area	Metro.	15.9	88.5	2.63	85.8	12.9
(10^3 km^2)	Mega.	58.2	128	21.8	106	23.0
Industrial Emissions	Metro.	16.9	151	0.41	150	23.0
VOCs + NOx (10^3 tons)	Mega.	61.5	236	12.5	223	55.2
Industrial Emissions	Metro.	2.70	30.5	0.09	30.4	4.39
$PM_{2.5}$ (10^3 tons)	Mega.	9.07	33.0	0.592	32.4	8.80
Industrial Emissions	Metro.	3.46	37.2	0.13	37.1	5.39
PM_{10} (10^3 tons)	Mega.	11.7	40.2	1.37	38.8	11.1

Table 12. Descriptive statistics for air pollutants calculated at the metropolitan scale (Metro.) and megapolitan scale (Mega.).

Pollutant	Scale	Mean	Maximum	Minimum	Range	Standard Deviation
O_3 Concentration	Metro.	83.6	98.4	61.1	37.3	8.76
(ppb)	Mega.	84.0	96.9	60.0	36.9	9.40
O_3 Exceedances	Metro.	8.72	38.9	0.5	38.4	8.58
(# days)	Mega.	15.8	30.6	0.85	29.7	9.16
VOC+NO_x Non-pt.	Metro.	189	1,290	36.0	1,254	197
Emissions (thousand tons)	Mega.	708	2,099	269	1,830	426
$PM_{2.5}$ Concentration	Metro.	13.2	21.3	5.71	15.6	2.96
(µg/m3)	Mega.	13.0	18.7	8.0	10.7	3.13
$PM_{2.5}$ Non-pt. Emissions	Metro.	24.5	111	4.36	106	20.3
(thousand tons)	Mega.	88.1	209	37.2	172	38.9
PM_{10} Concentration	Metro.	25.9	50.1	14.7	35.4	6.17
(µg/m3)	Mega.	25.0	40.1	19.5	20.5	5.09
PM_{10} Non-pt. Emissions	Metro.	87.3	374	7.56	367	76.7
(thousand tons)	Mega.	311	604	96.0	50.7	130
CO_2 On-road Emissions	Metro.	3.461	36.99	0.547	36.44	5.142
(million tons)	Mega.	12.79	41.02	4.927	36.09	8.307

Table 13. Top 10 MSAs and CSAs with the highest ambient concentrations of O_3, $PM_{2.5}$ and PM_{10}.

MSA or CSA	Region	Conc. (ppb)
Average annual 4th maximum 8-hour O3 (ppb)		
Bakersfield, CA	West	110.13
Fresno-Madera, CA	West	109.57
Youngstown-Warren-East Liverpool, OH-PA	Midwest	103.00
Knoxville-Sevierville-La Follette, TN CSA	South	101.33
Chattanooga-Cleveland-Athens, TN-GA	South	100.00
Houston-Baytown-Huntsville, TX	South	99.51
Atlanta-Sandy Springs-Gainesville, GA-AL	South	98.36
Columbia-Newberry, SC	South	98.00
Mobile-Daphne-Fairhope, AL	South	98.00
Philadelphia-Camden-Vineland, PA-NJ-DE-MD	Northeast	96.05
Average annual mean PM2.5 (µg/m^3)		
Fresno-Madera, CA CSA	West	21.28
Los Angeles-Long Beach-Riverside, CA	West	20.30
Atlanta-Sandy Springs-Gainesville, GA-AL	South	17.83
Birmingham-Hoover-Cullman, AL	South	17.82
Knoxville-Sevierville-La Follette, TN	South	17.81
Chattanooga-Cleveland-Athens, TN-GA	South	17.38
Columbus-Marion-Chillicothe, OH	Midwest	17.13
Bakersfield, CA	West	16.88
Cincinnati-Middletown-Wilmington, OH-KY-IN	Midwest	16.76
Cleveland-Akron-Elyria, OH	South	16.64
Average annual mean PM10 (µg/m^3)		
Phoenix-Mesa-Scottsdale, AZ	West	42.35
Omaha-Council Bluffs-Fremont, NE-IA	Midwest	40.07
Fresno-Madera, CA	West	34.80
Las Vegas-Paradise-Pahrump, NV	West	34.37
Little Rock-North Little Rock-Pine Bluff, AR	South	34.00
St. Louis-St. Charles-Farmington, MO-IL	Midwest	32.68
Bakersfield, CA	West	32.25
El Paso, TX	South	32.07
Los Angeles-Long Beach-Riverside, CA	West	31.44
Mobile-Daphne-Fairhope, AL	South	30.47

Table 14. Top 10 MSAs and CSAs with the lowest ambient concentrations of O_3, $PM_{2.5}$ and PM_{10}.

MSA or CSA	Region	Conc. (ppb)
Average annual 4th maximum 8-hour O3 (ppb)		
Seattle-Tacoma-Olympia, WA	West	61.18
Portland-Vancouver-Beaverton, OR-WA	West	62.73
Des Moines-Newton-Pella, IA	Midwest	63.00
San Francisco-San-Jose-Oakland, CA	West	64.13
McAllen-Edinburg-Pharr, TX	South	68.00
Omaha-Council Bluffs-Fremont, NE-IA	Midwest	68.00
Albuquerque, NM	West	70.75
Miami-Fort Lauderdale-Miami Beach, FL	South	70.83
Tucson, AZ	West	70.83
Minneapolis-St. Paul-St. Cloud, MN-WI	Midwest	71.64
Average annual mean PM2.5 (µg/m^3)		
Albuquerque, NM	West	5.71
Colorado Springs, CO	West	7.17
Tucson, AZ	West	7.55
Denver-Aurora-Boulder, CO	West	8.07
Las Vegas-Paradise-Pahrump, NV	West	8.16
Portland-Vancouver-Beaverton, OR-WA	West	8.69
Miami-Fort Lauderdale-Miami Beach, FL	South	8.83
El Paso, TX	South	9.50
Phoenix-Mesa-Scottsdale, AZ	West	9.67
Seattle-Tacoma-Olympia, WA	West	10.04
Average annual mean PM10 (µg/m^3)		
Hartford-West Hartford-Willimantic, CT	Northeast	16.00
Seattle-Tacoma-Olympia, WA	West	17.06
Grand Rapids-Muskegon-Holland, MI	Midwest	18.40
Portland-Vancouver-Beaverton, OR-WA	West	18.43
Boston-Worcester-Manchester, MA-NH	Northeast	18.66
Portland-Lewiston-South Portland, ME	West	18.75
Francisco- San Jose-Oakland, CA	West	18.83
Providence-New Bedford-Fall River, RI-MA	Northeast	18.90
Albany-Schenectady-Amsterdam, NY	Northeast	19.33
Rochester, NY	Northeast	20.00

Table 15. Top 10 most sprawling MSAs and CSAs by sprawl index*

MSA or CSA	Region	Score
Ewing et al. (2003) Index		
Greensboro--Winston-Salem--High Point, NC	South	46.78
Raleigh-Durham-Cary, NC	South	54.2
Atlanta-Sandy Springs-Gainesville, GA-AL	South	57.66
Greenville-Spartanburg-Anderson, SC	South	58.56
Knoxville-Sevierville-La Follette, TN	South	68.68
Rochester, NY	Northeast	77.93
Dallas-Fort Worth, TX	South	78.26
Detroit-Warren-Flint, MI	Midwest	79.47
Syracuse-Auburn, NY	Northeast	80.27
Little Rock-North Little Rock-Pine Bluff, AR	South	82.27
Lopez and Hynes (2003) Index		
Greenville-Spartanburg-Anderson, SC	South	98.76
Chattanooga-Cleveland-Athens, TN-GA	South	95.86
Knoxville-Sevierville-La Follette, TN	South	94.17
Greensboro--Winston-Salem--High Point, NC	South	91.77
Lafayette-Acadiana, LA	South	91.6
Charlotte-Gastonia-Salisbury, NC-SC	South	88.06
McAllen-Edinburg-Pharr, TX	South	87.31
Columbia-Newberry, SC	South	87.02
Little Rock-North Little Rock-Pine Bluff, AR	South	85.93
Charleston-North Charleston, SC	South	85.64
Nasser and Overberg (2001) -- USA Today Index		
Nashville-Davidson--Murfreesboro--Columbia, TN	South	478
Little Rock-North Little Rock-Pine Bluff, AR	South	474
Knoxville-Sevierville-La Follette, TN	South	464
Portland-Lewiston-South Portland, ME	Northeast	457
Charlotte-Gastonia-Salisbury, NC-SC	South	454
Fort Wayne-Huntington-Auburn, IN	Midwest	452
Lexington-Fayette-Frankfort-Richmond, KY	Midwest	446
Greensboro-Winston-Salem-High Point, NC	South	437
Mobile-Daphne-Fairhope, AL	South	433
Austin-Round Rock, TX	South	413
Sutton (2003) High Threshold Index		
Nashville-Davidson-Murfreesboro-Columbia, TN	South	-95
Oklahoma City-Shawnee, OK	South	-47

Chattanooga-Cleveland-Athens, TN-GA	South	-47
Indianapolis-Anderson-Columbus, IN	Midwest	-45
Charlotte-Gastonia-Salisbury, NC-SC	South	-36
Knoxville-Sevierville-La Follette, TN	South	-34
Atlanta-Sandy Springs-Gainesville, GA-AL	South	-32
Birmingham-Hoover-Cullman, AL	South	-31
Minneapolis-St. Paul-St. Cloud, MN-WI	Midwest	-28
Youngstown-Warren-East Liverpool, OH-PA	Midwest	-28
Sutton (2003) Low Threshold Index		
Nashville-Davidson--Murfreesboro--Columbia, TN	South	-118
Knoxville-Sevierville-La Follette, TN	South	-88
Indianapolis-Anderson-Columbus, IN	Midwest	-70
Charlotte-Gastonia-Salisbury, NC-SC	South	-69
Greenville-Spartanburg-Anderson, SC	South	-60
Minneapolis-St. Paul-St. Cloud, MN-WI	Midwest	-57
Youngstown-Warren-East Liverpool, OH-PA	Midwest	-51
St. Louis-St. Charles-Farmington, MO-IL	Midwest	-48
Atlanta-Sandy Springs-Gainesville, GA-AL	South	-47
Houston-Baytown-Huntsville, TX	South	-44
Burchfield et al. (2006) Index		
Phoenix-Mesa-Scottsdale, AZ	West	57.7
Atlanta-Sandy Springs-Gainesville, GA-AL	South	55.6
Greensboro--Winston-Salem--High Point, NC	South	52.9
Charlotte-Gastonia-Salisbury, NC-SC	South	52.7
Washington-Baltimore-Northern Virginia, DC-MD-VA-WV	Northeast	49.8
Richmond, VA	South	48.8
Boston-Worcester-Manchester, MA-NH	Northeast	47.6
San Francisco--San-Jose--Oakland, CA	West	46.9
San Antonio, TX	South	45.6
Pittsburgh-New Castle, PA	Northeast	44.9

*Among MSAs and CSAs with populations > 500,000.

Table 16. Top 10 least sprawling MSAs and CSAs by sprawl index*

MSA or CSA	Region	Score
Ewing et al. (2003) Index		
New York-Newark-Bridgeport, NY-NJ-CT-PA	Northeast	177.78
Providence-New Bedford-Fall River, RI-MA	Northeast	153.71
San Francisco-San-Jose-Oakland, CA	West	146.83
Omaha-Council Bluffs-Fremont, NE-IA	Midwest	128.35
Boston-Worcester-Manchester, MA-NH	Northeast	126.93
Portland-Vancouver-Beaverton, OR-WA	West	126.12
Miami-Fort Lauderdale-Miami Beach, FL	South	125.68
New Orleans-Metairie-Bogalusa, LA	South	125.39
Denver-Aurora-Boulder, CO	West	125.22
Albuquerque, NM	West	124.45
Lopez and Hynes (2003) Index		
New York-Newark-Bridgeport, NY-NJ-CT-PA	Northeast	6.72
Los Angeles-Long Beach-Riverside, CA	West	10.61
San Diego-Carlsbad-San Marcos, CA	West	14.89
Miami-Fort Lauderdale-Miami Beach, FL	South	15.73
Stockton, CA	West	21.52
Las Vegas-Paradise-Pahrump, NV	West	25.54
San Antonio, TX	South	26.85
Chicago-Naperville-Michigan City, IL-IN-WI	Midwest	30.71
Philadelphia-Camden-Vineland, PA-NJ-DE-MD	Northeast	31.46
Denver-Aurora-Boulder, CO	West	32.19
Nasser and Overberg (2001) -- USA Today Index		
Colorado Springs, CO	West	55
Sacramento--Arden-Arcade--Truckee, CA-NV	West	60
San Diego-Carlsbad-San Marcos, CA	West	62
San Antonio, TX	South	66
Miami-Fort Lauderdale-Miami Beach, FL	South	69
Omaha-Council Bluffs-Fremont, NE-IA	Midwest	77
Los Angeles-Long Beach-Riverside, CA	West	78
New York-Newark-Bridgeport, NY-NJ-CT-PA	Northeast	82
Norfolk-Virginia Beach-Newport News, VA-NC	South	94
El Paso, TX	South	97
Sutton (2003) High Threshold Index		
New York-Newark-Bridgeport, NY-NJ-CT-PA	Northeast	53
Los Angeles-Long Beach-Riverside, CA	West	52

San Antonio, TX	South	51
Phoenix-Mesa-Scottsdale, AZ	West	46
Stockton, CA	West	46
Fresno-Madera, CA	West	42
New Orleans-Metairie-Bogalusa, LA	South	41
Springfield, MA	Northeast	35
El Paso, TX	South	30
Bakersfield, CA	West	30
Sutton (2003) Low Threshold Index		
Fresno-Madera, CA	West	48
Los Angeles-Long Beach-Riverside, CA	West	45
Bakersfield, CA	West	41
San Diego-Carlsbad-San Marcos, CA	West	41
New Orleans-Metairie-Bogalusa, LA	South	32
Stockton, CA	West	29
El Paso, TX	South	29
Sacramento--Arden-Arcade--Truckee, CA-NV	West	28
Buffalo-Niagara-Cattaraugus, NY	Northeast	27
San Antonio, TX	South	25
Burchfield et al. (2006) Index		
Miami-Fort Lauderdale-Miami Beach, FL	South	21.7
Memphis, TN-MS-AR	South	27.4
Philadelphia-Camden-Vineland, PA-NJ-DE-MD	Northeast	27.5
Dallas-Fort Worth, TX	South	28.1
Denver-Aurora-Boulder, CO	West	28.6
New York-Newark-Bridgeport, NY-NJ-CT-PA	Northeast	28.8
San Diego-Carlsbad-San Marcos, CA	West	30.5
Chicago-Naperville-Michigan City, IL-IN-WI	Midwest	31.7
Sacramento--Arden-Arcade--Truckee, CA-NV	West	31.9
Minneapolis-St. Paul-St. Cloud, MN-WI	Midwest	32.1

*Among MSAs and CSAs with populations > 500,000.

Table 17. Descriptive statistics for sprawl indices and Ewing et al. (2003) sprawl index components.

Spatial Metric	Number	Mean	Maximum	Minimum	Range	Standard Deviation
Ewing et al. (2003	64	102	178	46.8	131	22.9
Street Connectivity	64	97.4	155	37.2	118	25.0
Centrality	64	104	149	51.9	96.7	20.6
Mixed Use	64	97.5	141	39.5	101	23.0
Residential Density	64	98.3	243	71.22	171	24.9
Sutton (2003) Low Threshold	76	-9.05	48.0	-118	166	32.1
Sutton (2003) High Threshold	84	2.11	53.0	-95.0	148	26.2
Lopez and Hynes (2003)	85	58.2	98.8	6.72	92.0	21.0
Nasser and Overberg (2001)	86	258	478	55.0	423	113
Burchfield et al. (2006)	40	38.9	57.7	20.73	37.0	8.63

Table 18. Descriptive statistics for spatial metrics calculated at the high and low urban threshold at the metropolitan scale.

Spatial Metric	Threshold	Mean	Maximum	Minimum	Range	Standard Deviation
ED	High	49.3	91.7	26.9	64.7	14.4
	Low	45.1	67.0	23.9	43.1	9.3
LPI	High	47.6	71.9	20.0	51.9	10.2
	Low	25.3	56.8	9.3	47.4	9.04
AWMSI	High	49.7	167	14.7	153	28.0
	Low	89.9	268	26.6	242	47.1
AWMPFD	High	1.364	1.463	1.288	0.175	0.038
	Low	1.418	1.500	1.320	0.170	0.033
CONTAG	High	32.8	45.1	21.1	24.0	5.24
	Low	39.5	54.5	28.7	25.8	5.37
CLUMPY	High	0.846	0.960	0.724	0.236	0.043
	Low	0.832	0.910	0.738	0.172	0.037
LSI	High	73.1	233	27.0	206	44.1
	Low	140	341	61.9	279	59.1
AWMCONTIG	High	0.922	0.963	0.853	0.110	0.029
	Low	0.868	0.953	0.789	0.163	0.036
PLADJ	High	92.8	96.7	74.1	22.6	3.17
	Low	88.1	94.9	80.4	14.5	3.37

Table 19. Descriptive statistics for spatial metrics calculated at the high and low urban threshold at the megapolitan scale.

Spatial Metric	Threshold	Mean	Maximum	Minimum	Range	Standard Deviation
ED	High	47.2	76.0	29.9	46.0	12.8
	Low	44.5	60.3	33.9	26.4	7.96
LPI	High	34.8	59.2	15.4	43.7	13.5
	Low	27.5	50.7	19.3	31.4	8.98
AWMSI	High	63.4	133	27.6	105	29.5
	Low	121	232	56.8	175	55.5
AWMPFD	High	1.372	1.437	1.310	0.126	0.033
	Low	1.416	1.472	1.356	0.117	0.034
CONTAG	High	33.9	43.3	24.5	18.7	5.85
	Low	36.7	41.8	30.1	11.7	3.28
CLUMPY	High	0.843	0.889	0.770	0.119	0.038
	Low	0.844	0.888	0.780	0.108	0.034
LSI	High	138	269	74.3	194	59.7
	Low	259	451	105	346	93.2
AWMCONTIG	High	0.927	0.960	0.869	0.091	0.028
	Low	0.884	0.942	0.829	0.113	0.033
PLADJ	High	93.6	96.7	88.2	8.45	2.53
	Low	90.0	94.9	84.9	10.0	2.82

Table 20. Paired t-test of spatial metrics for 86 metropolitan-scale areas calculated and the high and low urban threshold.

Spatial Metric	Mean	Std. Dev.	t	Sig.
AWMPFDh* – AWMPFDl	-0.0532	0.0311	-15.87	0.000
AWMSIh – AWMSIl	-40.24	28.12	-13.27	0.000
CLUMPYh – CLUMPYl	0.0141	0.0265	4.947	0.000
CONTAGh – CONTAGl	-6.690	7.464	-8.312	0.000
CONTIGh – CONTIGl	0.0544	0.0239	21.08	0.000
EDh – Edl	4.184	8.142	4.765	0.000
LPIh – LPIl	22.29	6.220	33.23	0.000
LSIh – LSIl	-67.03	26.02	-23.88	0.000
PLADJh – PLADJl	4.644	2.433	17.69	0.000

*h refers to high urban threshold; l refers to low urban threshold

Table 21. Paired t-test of spatial metrics for 19 megapolitan-scale areas calculated and the high and low urban threshold.

Spatial Metric	Mean	Std. Dev.	t	Sig.
AWMPFDh* – AWMPFDl	-0.0447	0.0229	-8.516	0.000
AWMSIh – AWMSIl	-195.5	83.53	-10.20	0.000
CLUMPYh – CLUMPYl	-0.0013	0.0147	-0.3847	0.705
CONTAGh – CONTAGl	-2.785	7.261	-1.671	0.112
CONTIGh – CONTIGl	0.0433	0.0131	14.416	0.000
EDh – Edl	2.688	7.8195	1.498	0.151
LPIh – LPIl	7.287	13.05	2.434	0.026
LSIh – LSIl	-120.15	46.04	-11.37	0.000
PLADJh – PLADJl	3.591	1.4679	10.66	0.000

*h refers to high urban threshold; l refers to low urban threshold

Figure 22. Independent samples t-test indicating difference in spatial metrics calculated at the metropolitan vs. megapolitan scale. High and low threshold values were averaged for each scale.

Spatial Metric	Scale	Mean	t	Mean Diff. (metro-mega)	Sig.
AWMPFD	Metro	1.391			
	Mega	1.395	-0.396	-0.003	0.695
AWMSI	Metro	69.820			
	Mega	92.422	-2.3	-22.6	0.030
CLUMPY	Metro	0.839			
	Mega	0.844	-0.496	-0.004	0.624
CONTAG	Metro	36.190			
	Mega	35.320	1.073	0.870	0.292
CONTIG	Metro	0.896			
	Mega	0.906	-1.368	-0.010	0.183
ED	Metro	47.186			
	Mega	45.908	0.493	1.28	0.625
LPI	Metro	36.405			
	Mega	31.184	2.202	5.22	0.037
LSI	Metro	106.571			
	Mega	198.871	-5.123	-92.3	0.000
PLADJ	Metro	90.435			
	Mega	91.810	-2.035	-1.37	0.051

Table 23. ANOVA of spatial metrics calculated at the metropolitan scale between four U.S. regions: Northeast, Midwest, South, and West.

Spatial Metric		Sum of Squares	df	Mean Square	F	Sig.
AWMPFD	Between	0.012	3	0.004	4.417	0.006
	Within	0.077	82	0.001		
	Total	0.089	85			
AWMSI	Between	10539	3	3,513	2.870	0.041
	Within	100,378	82	1,224		
	Total	110,917	85			
CLUMPY	Between	0.013	3	0.004	3.108	0.031
	Within	0.110	82	0.001		
	Total	0.122	85			
CONTAG	Between	120	3	40.3	3.037	0.034
	Within	1,087	82	13.3		
	Total	1,208	85			
CONTIG	Between	0.011	3	0.004	4.661	0.005
	Within	0.064	82	0.001		
	Total	0.075	85			
ED	Between	1,114	3	371	3.062	0.033
	Within	9,948	82	121		
	Total	11,063	85			
LPI	Between	625	3	208	2.669	0.053
	Within	6,408	82	78.1		
	Total	7,034	85			
LSI	Between	20,642	3	6,880	2.877	0.041
	Within	196,096	82	2,391		
	Total	216,739	85			
PLADJ	Between	100	3	33.5	4.023	0.010
	Within	682	82	8.33		
	Total	783	85			

Table 24. Top 10 MSAs and CSAs by the urban form factors urban "continuity" and urban "shape complexity" at the high urban threshold.

MSA or CSA	Region	Score*
Highest Continuity		
Sacramento--Arden-Arcade--Truckee, CA-NV	West	1.56
San Francisco-San-Jose-Oakland, CA	West	1.47
Salt Lake City-Ogden-Clearfield, UT	West	1.43
Tulsa-Bartlesville, OK	South	1.26
Omaha-Council Bluffs-Fremont, NE-IA	Midwest	1.25
Detroit-Warren-Flint, MI	Midwest	1.24
Dayton-Springfield-Greenville, OH	Midwest	1.18
Stockton, CA	West	1.15
Toledo-Fremont, OH	Midwest	1.13
Wichita-Winfield, KS	Midwest	1.10
Lowest Continuity		
Philadelphia-Camden-Vineland, PA-NJ-DE-MD	Northeast	-2.64
Atlanta-Sandy Springs-Gainesville, GA-AL	South	-2.62
Greenville-Spartanburg-Anderson, SC	South	-2.41
Washington-Baltimore, DC-MD-VA-WV	South	-2.31
Norfolk-Virginia Beach-Newport News, VA-NC	South	-2.27
Richmond, VA	South	-2.12
Tucson, AZ	West	-1.76
Boston-Worcester-Manchester, MA-NH	Northeast	-1.75
Cincinnati-Middletown-Wilmington, OH-KY-IN	Midwest	-1.17
New York-Newark-Bridgeport, NY-NJ-CT-PA	Northeast	-1.16
Highest Shape Complexity		
New York-Newark-Bridgeport, NY-NJ-CT-PA	Northeast	2.49
Atlanta-Sandy Springs-Gainesville, GA-AL	South	2.20
Los Angeles-Long Beach-Riverside, CA	West	2.20
Boston-Worcester-Manchester, MA-NH	Northeast	2.09
Miami-Fort Lauderdale-Miami Beach, FL	South	2.08
Chicago-Naperville-Michigan City, IL-IN-WI	Midwest	1.68
Seattle-Tacoma-Olympia, WA	West	1.54
San Diego-Carlsbad-San Marcos, CA	West	1.39
Cleveland-Akron-Elyria, OH	South	1.35
Dallas-Fort Worth, TX	South	1.32
Lowest Shape Complexity		
Portland-Lewiston-South Portland, ME	West	-2.01

Lexington-Fayette--Frankfort--Richmond, KY	Midwest	-1.72
Norfolk-Virginia Beach-Newport News, VA-NC	South	-1.56
Madison-Baraboo, WI	Midwest	-1.52
Charleston-North Charleston, SC	South	-1.44
New Orleans-Metairie-Bogalusa, LA	South	-1.43
Little Rock-North Little Rock-Pine Bluff, AR	South	-1.29
Stockton, CA	West	-1.22
Bakersfield, CA	West	-1.21
Mobile-Daphne-Fairhope, AL	South	-1.16

*Scores represent standard deviations from the mean.

Table 25. Top 10 MSAs and CSAs by the urban form factors urban "continuity" and urban "shape complexity" at the low urban threshold.

MSA or CSA	Region	Score*
Highest Continuity		
Salt Lake City-Ogden-Clearfield, UT	West	1.92
Las Vegas-Paradise-Pahrump, NV	West	1.89
New Orleans-Metairie-Bogalusa, LA	South	1.83
Denver-Aurora-Boulder, CO	West	1.58
Miami-Fort Lauderdale-Miami Beach, FL	South	1.56
Sacramento--Arden-Arcade--Truckee, CA-NV	West	1.31
Wichita-Winfield, KS	Midwest	1.29
San Francisco-San-Jose-Oakland, CA	West	1.15
Memphis, TN-MS-AR	South	1.14
Omaha-Council Bluffs-Fremont, NE-IA	Midwest	1.13
Lowest Continuity		
Greenville-Spartanburg-Anderson, SC	South	-2.77
Atlanta-Sandy Springs-Gainesville, GA-AL	South	-2.74
Boston-Worcester-Manchester, MA-NH	Northeast	-1.88
Knoxville-Sevierville-La Follette, TN	South	-1.80
Philadelphia-Camden-Vineland, PA-NJ-DE-MD	Northeast	-1.51
Pittsburgh-New Castle, PA	Northeast	-1.50
Bakersfield, CA	West	-1.42
Washington-Baltimore-Northern Virginia, DC-MD-VA-WV	South	-1.25
Columbia-Newberry, SC	South	-1.18
Tucson, AZ	West	-1.15
Highest Shape Complexity		
Atlanta-Sandy Springs-Gainesville, GA-AL	South	1.96
New York-Newark-Bridgeport, NY-NJ-CT-PA	Northeast	1.91
Los Angeles-Long Beach-Riverside, CA	West	1.77
Boston-Worcester-Manchester, MA-NH	Northeast	1.76
Chicago-Naperville-Michigan City, IL-IN-WI	Midwest	1.74
Detroit-Warren-Flint, MI	Midwest	1.63
San Diego-Carlsbad-San Marcos, CA	West	1.50
Miami-Fort Lauderdale-Miami Beach, FL	South	1.40
Tampa-St. Petersburg-Clearwater, FL	South	1.35
Cleveland-Akron-Elyria, OH	South	1.28
Lowest Shape Complexity		
Lafayette-Acadiana, LA	South	-2.22

Madison-Baraboo, WI	Midwest	-1.89
Syracuse-Auburn, NY	Northeast	-1.80
Lexington-Fayette--Frankfort--Richmond, KY	Midwest	-1.45
Charleston-North Charleston, SC	South	-1.34
Bakersfield, CA	West	-1.17
Mobile-Daphne-Fairhope, AL	South	-1.16
Louisville-Elizabethtown-Scottsburg, KY-IN	Midwest	-1.05
Baton Rouge-Pierre Part, LA	South	-1.05
Scranton--Wilkes-Barre, PA	Northeast	-1.03

*Scores represent standard deviations from the mean.

Table 26. Nineteen megapolitan areas ranked (from high to low) in terms of the urban form factors urban "continuity" calculated at a high and low urban threshold.

Megapolitan Area	Score*		Score
Continuity – High Threshold		**Continuity – Low Threshold**	
Steel Corridor	1.39	Treasure Coast	2.02
Metroplex	1.13	Southern California	1.52
Michigan Corridor	1.04	Texas Gulf	0.76
Front Range	0.75	Northern California	0.75
Treasure Coast	0.71	Florida	0.64
Cascadia	0.66	Metroplex	0.63
Ohio Valley	0.65	Cascadia	0.45
Florida	0.54	Lake Front	0.29
Texas Corridor	0.41	Michigan Corridor	0.17
Lake Front	0.41	Front Range	0.13
Northern California	0.20	Sun Corridor	-0.01
Carolina Piedmont	0.03	Steel Corridor	-0.11
Texas Gulf	-0.32	Ohio Valley	-0.26
Chesapeake Megalopolis	-0.70	Texas Corridor	-0.42
Southern California	-0.77	New England	-0.86
Sun Corridor	-1.05	Core Megalopolis	-1.09
New England	-1.26	Georgia Piedmont	-1.27
Georgia Piedmont	-1.80	Carolina Piedmont	-1.67
Core Megalopolis	-2.01	Chesapeake Megalopolis	-1.67

*Scores represent standard deviations from the mean.

Table 27. Nineteen megapolitan areas ranked (from high to low) in terms of the urban form factor urban "shape complexity" calculated at a high and low urban threshold.

Megapolitan Area	Score*		Score
Shape Complexity – High Threshold		**Shape Complexity – Low Threshold**	
New England	1.39	Georgia Piedmont	1.73
Southern California	1.30	Southern California	1.71
Georgia Piedmont	1.14	Carolina Piedmont	0.93
Metroplex	1.12	Florida	0.86
Lake Front	1.11	Sun Corridor	0.81
Treasure Coast	1.02	New England	0.65
Sun Corridor	0.85	Cascadia	0.02
Texas Gulf	0.37	Texas Corridor	-0.02
Cascadia	-0.02	Metroplex	-0.06
Front Range	-0.17	Northern California	-0.14
Steel Corridor	-0.42	Treasure Coast	-0.14
Northern California	-0.62	Steel Corridor	-0.33
Chesapeake Megalopolis	-0.67	Texas Gulf	-0.43
Texas Corridor	-0.67	Core Megalopolis	-0.67
Florida	-0.75	Lake Front	-0.67
Michigan Corridor	-0.76	Chesapeake Megalopolis	-0.71
Carolina Piedmont	-1.09	Front Range	-1.16
Ohio Valley	-1.56	Michigan Corridor	-1.65
Core Megalopolis	-1.56	Ohio Valley	-1.66

*Scores represent standard deviations from the mean.

Table 28. ANOVA of the urban form factors urban "continuity" and urban "shape complexity" calculated at the metropolitan scale between four U.S. regions: Northeast, Midwest, South, and West. "High" refers to the high urban threshold; "Low" refers to the low urban threshold.

Urban Form Factor		Sum of Squares	df	Mean Square	F	Sig.
Continuity	Between	13.5	3	4.5	5.172	0.003
High	Within	71.5	82	0.872		
	Total	85	85			
Continuity	Between	14.1	3	4.71	5.456	0.002
Low	Within	70.9	82	0.864		
	Total	85	85			
Shape	Between	1.64	3	0.546	0.537	0.658
Complexity	Within	83.4	82	1.017		
High	Total	85	85			
Shape	Between	2.25	3	0.751	0.744	0.529
Complexity	Within	82.7	82	1.01		
Low	Total	85	85			

Table 29a. Pearson correlations between air pollutant concentrations and urban sprawl indices.

		Urban Sprawl Indices & Components									
Pollutant		Ewing	Street Con.[1]	Centered.	Mixed Use	Res. Den.	Sutton high	Sutton low	Lopez	Nasser	Burchfield
O3 (ppm)	r^2	-.364**	-.328**	-.228	-.099	-.141	-.354**	-.098	.224*	.330**	.192
	Sig.	.003	.009	.072	.439	.271	.002	.383	.042	.002	.236
	N	63	63	63	63	63	74	82	83	84	40
O3	r^2	-.416**	-.284*	-.269*	-.205	-.131	-.210	-.406**	.254*	.266*	.265
exceedances	Sig.	.001	.024	.033	.107	.307	.058	.000	.020	.015	.099
	N	63	63	63	63	63	82	74	83	84	40
PM2.5	r^2	-.353**	-.222	-.278*	-.164	-.045	-.230*	-.117	.193	.320**	.154
(mg/m^3)	Sig.	.004	.078	.026	.196	.725	.045	.292	.078	.003	.342
	N	64	64	64	64	64	76	83	84	85	40
PM10	r^2	-.100	-.028	-.200	.026	-.023	.215	.166	-.240*	-.076	.070
(mg/m3)	Sig.	.472	.840	.148	.850	.870	.096	.173	.045	.530	.683
	N	54	54	54	54	54	61	69	70	71	36

[1]Street connectivity, centeredness, mixed use, and residential density are components of the Ewing et al. (2003) sprawl index.
**Correlation is significant at the 0.01 level. *Correlation is significant at the 0.05 level.

Table 29b. Pearson correlations between air pollutant non-point source emissions and urban sprawl indices.

		Urban Sprawl Indices & Components									
Pollutant		Ewing	Street Con.[1]	Centered.	Mixed Use	Res. Den.	Sutton high	Sutton low	Lopez	Nasser	Burchfield
O3 non-pt.	r^2	.267*	.394**	-.157	.220	.786**	.267*	.000	-.475**	-.341**	-.153
emissions	Sig.	.033	.001	.216	.081	.000	.014	.997	.000	.001	.347
	N	64	64	64	64	64	84	76	85	86	40
O3 non-pt.	r^2	-.370**	-.438**	.140	-.402**	-.354**	-.518**	-.184	.547**	.558**	.136
emissions	Sig.	.003	.000	.270	.001	.001	.000	.111	.000	.000	.403
per capita	N	64	64	64	64	84	64	76	85	86	40
PM2.5 non-pt.	r^2	.171	.302*	-.195	.176	.656**	.142	-.120	-.420**	-.305**	-.112
emissions	Sig.	.177	.015	.123	.164	.000	.199	.302	.000	.004	.490
	N	64	64	64	64	64	84	76	85	86	40
PM2.5 non-	r^2	-.130	-.269*	.210	-.140	-.257*	-.278*	-.072	.262*	.312**	.056
pt. emissions	Sig.	.305	.032	.096	.270	.018	.026	.534	.015	.003	.732
per capita	N	64	64	64	64	84	64	76	85	86	40
PM10 non-pt.	r^2	.074	.193	-.213	.146	.454**	.034	-.190	-.327**	-.269*	-.083
emissions	Sig.	.563	.126	.091	.249	.000	.758	.101	.002	.012	.611
	N	64	64	64	64	64	84	76	85	86	40
PM10 non-pt.	r^2	-.080	-.206	.174	-.042	-.249*	-.214	-.061	.216*	.197	.016
emissions	Sig.	.531	.103	.169	.745	.022	.090	.599	.047	.070	.921
per capita	N	64	64	64	64	84	64	76	85	86	40
CO2 on-road	r^2	-.309*	-.315*	.026	-.225	-.397**	-.328**	-.395**	.376**	.410**	.113
emissions	Sig.	.013	.011	.837	.073	.000	.008	.000	.000	.000	.488
per capita	N	64	64	64	64	84	64	76	85	86	40

[1]Street connectivity, centeredness, mixed use, and residential density are components of the Ewing et al. (2003) sprawl index.
**Correlation is significant at the 0.01 level. *Correlation is significant at the 0.05 level.

Table 30a. Pearson correlations between air pollutant concentrations and spatial metrics calculated at the metropolitan scale, high urban threshold.

		Spatial Metrics (high threshold)								
Pollutant		ED	LPI	AWMSI	AWMPFD	CONTAG	CLUMPY	LSI	CONTIG	PLADJ
O3 (ppm)	r^2	.235*	-.270*	.218*	.164	-.280*	-.256*	.299**	-.228*	-.202
	Sig.	.031	.013	.047	.137	.010	.019	.006	.037	.065
	N	84	84	84	84	84	84	84	84	84
O3 exceedances	r^2	.297**	-.161	.236*	.210	-.276*	-.324**	.333**	-.243*	-.258*
	Sig.	.006	.144	.030	.056	.011	.003	.002	.026	.018
	N	84	84	84	84	84	84	84	84	84
PM2.5 (mg/m^3)	r^2	.059	-.139	.071	-.057	-.015	-.103	.173	-.063	-.066
	Sig.	.589	.206	.519	.604	.890	.346	.113	.568	.548
	N	85	85	85	85	85	85	85	85	85
PM10 (mg/m3)	r^2	-.149	.230	-.071	-.113	.117	.114	-.107	.156	.120
	Sig.	.216	.053	.554	.350	.330	.343	.373	.195	.320
	N	71	71	71	71	71	71	71	71	71

**Correlation is significant at the 0.01 level. *Correlation is significant at the 0.05 level.

Table 30b. Pearson correlations between air pollutant non-point source emissions and spatial metrics calculated at the metropolitan scale using a high urban threshold.

		Spatial Metrics (high threshold)								
Pollutant		ED	LPI	AWMSI	AWMPFD	CONTAG	CLUMPY	LSI	CONTIG	PLADJ
O3 non-pt.	r^2	.072	.208	.646**	.417**	.104	-.118	.685**	.061	.051
emissions	Sig.	.507	.055	.000	.000	.339	.279	.000	.575	.641
	N	86	86	86	86	86	86	86	86	86
O3 non-pt.	r^2	-.001	-.335**	-.371**	-.318**	-.134	.043	-.335**	-.075	-.097
emissions	Sig.	.993	.002	.000	.003	.218	.695	.002	.493	.373
per capita	N	86	86	86	86	86	86	86	86	86
PM2.5 non-pt.	r^2	-.009	.259*	.625**	.376**	.151	-.009	.612**	.117	.093
emissions	Sig.	.931	.016	.000	.000	.165	.937	.000	.282	.394
	N	86	86	86	86	86	86	86	86	86
PM2.5 non-	r^2	-.151	-.095	-.337**	-.319**	.039	.190	-.355**	.019	.016
pt. emissions	Sig.	.165	.385	.001	.003	.721	.079	.001	.862	.884
per capita	N	86	86	86	86	86	86	86	86	86
PM10 non-pt.	r^2	-.070	.308**	.536**	.315**	.181	.067	.477(**)	.177	.134
emissions	Sig.	.522	.004	.000	.003	.096	.537	.000	.103	.218
	N	86	86	86	86	86	86	86	86	86
PM10 non-pt.	r^2	-.156	.066	-.276*	-.270*	.069	.187	-.328**	.105	.076
emissions	Sig.	.152	.547	.010	.012	.526	.084	.002	.337	.487
per capita	N	86	86	86	86	86	86	86	86	86
CO2 on-road	r^2	.064	-.133	-.155	-.117	-.141	-.013	-.142	-.074	-.079
emissions	Sig.	.557	.223	.155	.283	.195	.907	.192	.496	.468
per capita	N	86	86	86	86	86	86	86	86	86

**Correlation is significant at the 0.01 level. *Correlation is significant at the 0.05 level.

Table 31. Pearson correlations between air pollutants and control variables at the metropolitan scale.

		Control Variables								
Pollutant		Temp. Factor	Moisture Factor	Avg. Wind Speed	Metro. Population	Population within 500k	Area (km^2)	Industrial Emission voc + nox	Industrial Emissions $PM_{2.5}$	Industrial Emissions PM_{10}
O3 non-pt. emissions	r^2	.045	.013	.088	.969**	.163	.591**	.434**	.262*	.280**
	Sig.	.679	.905	.423	.000	.134	.000	.000	.015	.009
	N	86	86	86	86	86	86	86	86	86
O3 non-pt. emissions per capita	r^2	.151	.324**	-.184	-.494**	-.167	-.214*	-.076	-.029	-.043
	Sig.	.165	.002	.090	.000	.125	.048	.486	.794	.693
	N	86	86	86	86	86	86	86	86	86
PM2.5 non-pt. emissions	r^2	.073	.000	.146	.844**	.036	.610**	.549**	.369**	.398**
	Sig.	.502	.999	.181	.000	.740	.000	.000	.000	.000
	N	86	86	86	86	86	86	86	86	86
PM2.5 non-pt. emissions per capita	r^2	.059	-.024	.069	-.355**	-.334**	-.043	-.133	-.042	-.051
	Sig.	.586	.828	.531	.001	.002	.697	.221	.704	.641
	N	86	86	86	86	86	86	86	86	86
PM10 non-pt. emissions	r^2	.101	.000	.202	.649**	-.069	.541**	.558**	.335**	.370**
	Sig.	.356	.998	.062	.000	.531	.000	.000	.002	.000
	N	86	86	86	86	86	86	86	86	86
PM10 non-pt. emissions per capita	r^2	.116	-.078	.201	-.303**	-.385**	.020	-.103	-.073	-.067
	Sig.	.287	.477	.063	.005	.000	.854	.343	.505	.537
	N	86	86	86	86	86	86	86	86	86
CO2 on-road emissions per capita	r^2	-.091	.153	-.133	-.260*	-.062	-.087	.058	.035	.054
	Sig.	.402	.159	.221	.016	.572	.426	.598	.749	.618
	N	86	86	86	86	86	86	86	86	86

**Correlation is significant at the 0.01 level. *Correlation is significant at the 0.05 level.

Table 32a. Pearson correlations between the urban form factors urban "continuity" and urban "shape complexity" calculated at the metropolitan scale, and control variables.

		Control Variables								
Urban Form Factor		Temp. Factor	Moisture Factor	Avg. Wind Speed	Metro. Population	Population within 500k	Area (km^2)	Industrial Emissions voc + nox	Industrial Emissions $PM_{2.5}$	Industrial Emissions PM_{10}
Continuity	r^2	-.130	-.040	.158	-.157	-.254*	.022	-.038	-.029	-.061
High	Sig.	.233	.713	.146	.150	.018	.838	.727	.791	.579
	N	86	86	86	86	86	86	86	86	86
Continuity	r^2	.087	-.097	.201	-.046	-.405**	.155	.064	.065	.028
Low	Sig.	.425	.372	.064	.672	.000	.155	.561	.552	.797
	N	86	86	86	86	86	86	86	86	86
Complexity	r^2	.087	-.038	.188	.655**	-.070	.456**	.364**	.347**	.370**
High	Sig.	.424	.728	.082	.000	.524	.000	.001	.001	.000
	N	86	86	86	86	86	86	86	86	86
Complexity	r^2	.098	-.102	.130	.579**	-.054	.349**	.306**	.229*	.258*
Low	Sig.	.371	.351	.231	.000	.623	.001	.004	.034	.016
	N	86	86	86	86	86	86	86	86	86

**Correlation is significant at the 0.01 level. *Correlation is significant at the 0.05 level.

Table 32b. Pearson correlations between the urban form factors urban "continuity" and urban "shape complexity" calculated at the megapolitan scale, and control variables.

		Control Variables								
Urban Form Factor		Temp. Factor	Moisture Factor	Avg. Wind Speed	Mega. Population	Population within 500k	Area (km^2)	Industrial Emissions voc + nox	Industrial Emissions $PM_{2.5}$	Industrial Emissions PM_{10}
Continuity	r^2	-.045	.038	-.005	-.212	-.410	-.134	.050	-.083	-.148
High	Sig.	.855	.877	.985	.384	.081	.585	.840	.737	.545
	N	19	19	19	19	19	19	19	19	19
Continuity	r^2	.366	-.042	-.181	-.065	-.633**	.055	-.051	-.081	-.138
Low	Sig.	.123	.866	.457	.792	.004	.823	.836	.742	.573
	N	19	19	19	19	19	19	19	19	19
Complexity	r^2	.202	-.139	.124	-.154	-.437	.026	.007	.263	.257
High	Sig.	.407	.570	.612	.529	.061	.916	.976	.277	.287
	N	19	19	19	19	19	19	19	19	19
Complexity	r^2	.443	-.125	-.324	.014	-.269	.394	-.154	.010	.053
Low	Sig.	.058	.611	.176	.956	.266	.095	.529	.969	.829
	N	19	19	19	19	19	19	19	19	19

**Correlation is significant at the 0.01 level. *Correlation is significant at the 0.05 level.

Table 33a. Pearson correlations between air pollutant concentrations and spatial metrics at the metropolitan scale using a low urban threshold.

		Spatial Metrics (low threshold)								
Pollutant		ED	LPI	AWMSI	AWMPFD	CONTAG	CLUMPY	LSI	CONTIG	PLADJ
O3 conc.	r^2	.224*	-.230*	.322**	.296**	.030	-.278*	.436**	-.287**	-.308**
	Sig.	.041	.035	.003	.006	.786	.011	.000	.008	.004
	N	84	84	84	84	84	84	84	84	84
O3 exceedances	r^2	.324**	-.133	.320**	.285**	-.127	-.308**	.460**	-.254*	-.279*
	Sig.	.003	.227	.003	.009	.251	.004	.000	.020	.010
	N	84	84	84	84	84	84	84	84	84
PM2.5 conc.	r^2	.173	-.144	.172	.112	-.027	-.175	.315**	-.171	-.160
	Sig.	.113	.189	.117	.308	.808	.109	.003	.119	.143
	N	85	85	85	85	85	85	85	85	85
PM10 conc.	r^2	-.046	.059	-.115	-.169	-.071	.131	-.096	.138	.144
	Sig.	.706	.624	.338	.158	.554	.278	.424	.252	.231
	N	71	71	71	71	71	71	71	71	71

**Correlation is significant at the 0.01 level. *Correlation is significant at the 0.05 level.

Table 33b. Pearson correlations between air pollutants and spatial metrics at the metropolitan scale and using a low urban threshold.

		Spatial Metrics (low threshold)								
Pollutant		ED	LPI	AWMSI	AWMPFD	CONTAG	CLUMPY	LSI	CONTIG	PLADJ
O3 non-pt. emissions	r^2	.139	.413**	.567**	.264*	-.423**	.110	.658**	.291**	.267*
	Sig.	.201	.000	.000	.014	.000	.315	.000	.007	.013
	N	86	86	86	86	86	86	86	86	86
O3 non-pt. emissions per capita	r^2	-.082	-.542**	-.315**	-.251*	.427**	-.184	-.212	-.366**	-.326**
	Sig.	.453	.000	.003	.020	.000	.089	.050	.001	.002
	N	86	86	86	86	86	86	86	86	86
PM2.5 non-pt. emissions	r^2	.064	.391**	.561**	.247*	-.383**	.169	.617**	.306**	.296**
	Sig.	.558	.000	.000	.022	.000	.120	.000	.004	.006
	N	86	86	86	86	86	86	86	86	86
PM2.5 non-pt. emissions per capita	r^2	-.158	-.340**	-.296**	-.245*	.367**	-.058	-.275*	-.237*	-.182
	Sig.	.146	.001	.006	.023	.001	.595	.011	.028	.094
	N	86	86	86	86	86	86	86	86	86
PM10 non-pt. emissions	r^2	.021	.387**	.504**	.230*	-.386**	.227*	.498**	.338**	.335**
	Sig.	.845	.000	.000	.033	.000	.036	.000	.001	.002
	N	86	86	86	86	86	86	86	86	86
PM10 non-pt. emissions per capita	r^2	-.116	-.162	-.226*	-.181	.127	.071	-.281**	-.055	-.003
	Sig.	.287	.137	.037	.095	.244	.518	.009	.616	.981
	N	86	86	86	86	86	86	86	86	86
CO2 on-road emissions per capita	r^2	.003	-.306**	-.116	-.039	.202	-.135	-.048	-.221*	-.218*
	Sig.	.975	.004	.289	.722	.062	.216	.661	.041	.043
	N	86	86	86	86	86	86	86	86	86

**Correlation is significant at the 0.01 level. *Correlation is significant at the 0.05 level.

Table 34a. Pearson correlations between air pollutant concentrations and the urban form factors urban "continuity" and urban "shape complexity" calculated at the metropolitan scale.

		Urban Form Factors			
Pollutant		Continuity High	Continuity Low	Complexity High	Complexity Low
O3 conc.	r^2	-.285**	-.388**	-.029	.028
	Sig.	.009	.000	.795	.804
	N	84	84	84	84
O3 exceedances	r^2	-.317**	-.399**	.031	.116
	Sig.	.003	.000	.781	.294
	N	84	84	84	84
PM2.5 conc.	r^2	-.080	-.236*	-.026	.022
	Sig.	.467	.030	.813	.840
	N	85	85	85	85
PM10 conc.	r^2	.154	.147	.078	.014
	Sig.	.200	.222	.519	.910
	N	71	71	71	71

**Correlation is significant at the 0.01 level. *Correlation is significant at the 0.05 level.

Table 34b. Pearson correlations between air pollutant non-point source emissions and the urban form factors urban "continuity" and urban "shape complexity" calculated at the metropolitan scale.

		Urban Form Factors			
Pollutant		Continuity High	Continuity Low	Complexity High	Complexity Low
O3 non-pt. emissions	r^2	-.192	-.080	.684**	.606**
	Sig.	.077	.466	.000	.000
	N	86	86	86	86
O3 non-pt. emissions per capita	r^2	.058	-.090	-.521**	-.545**
	Sig.	.594	.412	.000	.000
	N	86	86	86	86
PM2.5 non-pt. emissions	r^2	-.120	-.035	.693**	.583**
	Sig.	.271	.748	.000	.000
	N	86	86	86	86
PM2.5 non-pt. emissions per capita	r^2	.179	.029	-.343**	-.431**
	Sig.	.099	.793	.001	.000
	N	86	86	86	86
PM10 non-pt. emissions	r^2	-.041	.028	.649**	.561**
	Sig.	.710	.799	.000	.000
	N	86	86	86	86
PM10 non-pt. emissions per capita	r^2	.202	.113	-.202	-.219*
	Sig.	.062	.299	.063	.043
	N	86	86	86	86
CO2 on-road emissions per capita	r^2	-.016	-.111	-.242*	-.258*
	Sig.	.881	.311	.025	.016
	N	86	86	86	86

**Correlation is significant at the 0.01 level. *Correlation is significant at the 0.05 level.

Table 35a. Pearson correlations between air pollutant concentrations and the urban form factors urban "continuity" and urban "shape complexity" calculated at the megapolitan scale.

		Urban Form Factors			
Pollutant		Continuity High	Continuity Low	Complexity High	Complexity Low
O3 conc.	r^2	-.453	-.571*	-.145	-.064
	Sig.	.051	.011	.553	.796
	N	19	19	19	19
O3 exceedances	r^2	-.411	-.416	-.015	.201
	Sig.	.081	.076	.950	.408
	N	19	19	19	19
PM2.5 conc.	r^2	-.228	-.278	-.070	.077
	Sig.	.347	.249	.777	.753
	N	19	19	19	19
PM10 conc.	r^2	.021	.163	.249	.257
	Sig.	.934	.517	.318	.303
	N	18	18	18	18

**Correlation is significant at the 0.01 level. *Correlation is significant at the 0.05 level.

Table 35b. Pearson correlations between air pollutant non-point source emissions and the urban form factors urban "continuity" and urban "shape complexity" calculated at the megapolitan scale.

		Urban Form Factors			
Pollutant		Continuity High	Continuity Low	Complexity High	Complexity Low
O3 non-pt. emissions	r^2	-.292	-.169	-.145	.035
	Sig.	.225	.490	.553	.887
	N	19	19	19	19
O3 non-pt. emissions per capita	r^2	-.213	-.330	-.016	.117
	Sig.	.382	.168	.950	.632
	N	19	19	19	19
PM2.5 non-pt. emissions	r^2	-.262	-.214	-.190	.047
	Sig.	.278	.380	.436	.848
	N	19	19	19	19
PM2.5 non-pt. emissions per capita	r^2	-.042	-.221	-.017	.065
	Sig.	.866	.363	.944	.793
	N	19	19	19	19
PM10 non-pt. emissions	r^2	-.119	-.175	-.080	-.015
	Sig.	.628	.474	.744	.953
	N	19	19	19	19
PM10 non-pt. emissions per capita	r^2	.063	-.116	.051	-.011
	Sig.	.799	.635	.837	.966
	N	19	19	19	19
CO2 on-road emissions per capita	r^2	-.251	-.273	.053	-.052
	Sig.	.300	.258	.829	.833
	N	19	19	19	19

**Correlation is significant at the 0.01 level. *Correlation is significant at the 0.05 level

Table 36. Pearson correlations between air pollutants and control variables at the metropolitan scale.

		Control Variables								
Pollutant		Temp. Factor	Moisture Factor	Avg. Wind Speed	Metro. Population	Population within 500k	Area (km^2)	Industrial Emissions voc + nox	Industrial Emissions $PM_{2.5}$	Industrial Emissions PM_{10}
O3 conc.	r^2	-.056	.298**	-.186	.141	.607**	-.017	.261*	.144	.170
	Sig.	.615	.006	.090	.201	.000	.880	.016	.190	.123
	N	84	84	84	84	84	84	84	84	84
O3 exceedances	r^2	-.007	.169	-.308**	.192	.445**	.109	.229*	.124	.160
	Sig.	.952	.124	.004	.081	.000	.322	.036	.261	.147
	N	84	84	84	84	84	84	84	84	84
PM2.5 conc.	r^2	-.053	.291**	-.307**	.184	.448**	.016	.277*	.260*	.287**
	Sig.	.628	.007	.004	.092	.000	.885	.010	.016	.008
	N	85	85	85	85	85	85	85	85	85
PM10 conc.	r^2	.287*	-.512**	-.399**	.023	-.248*	.411**	.027	-.010	.004
	Sig.	.015	.000	.001	.852	.037	.000	.825	.934	.971
	N	71	71	71	71	71	71	71	71	71

**Correlation is significant at the 0.01 level. *Correlation is significant at the 0.05 level.

Table 37. Pearson correlations among urban sprawl indices and the four Ewing sprawl components.

		Ewing	Street Con.	Centered.	Mixed Use	Res. Den.	Sutton L	Sutton H	Lopez	Nasser	Burchfield
Street Connectivity	r^2	.695**	1								
	Sig.	.000									
	N	64	64								
Centeredness	r^2	.571**	.011	1							
	Sig.	.000	.930								
	N	64	64	64							
Mixed Use	r^2	.726**	.297*	.244	1						
	Sig.	.000	.017	.052							
	N	64	64	64	64						
Residential Density	r^2	.670**	.614**	.140	.435**	1					
	Sig.	.000	.000	.271	.000						
	N	64	64	64	64	64					
Sutton low	r^2	.457**	.239	.177	.407**	.303*	1				
	Sig.	.000	.076	.191	.002	.023					
	N	56	56	56	56	56	76				
Sutton high	r^2	.468**	.301*	.201	.405**	.488**	.743**	1			
	Sig.	.000	.017	.118	.001	.000	.000				
	N	62	62	62	62	62	75	84			
Lopez & Hynes	r^2	-.550**	-.516**	.040	-.497**	-.688**	-.596**	-.673**	1		
	Sig.	.000	.000	.757	.000	.000	.000	.000			
	N	63	63	63	63	63	75	83	85		
Nasser & Overberg	r^2	-.503**	-.509**	.052	-.467**	-.498**	-.461**	-.479**	.721**	1	
	Sig.	.000	.000	.681	.000	.000	.000	.000	.000		
	N	64	64	64	64	64	76	84	85	86	
Burchfield et al.	r^2	-.297	-.236	-.026	-.319	-.286	-.295	-.078	.604**	.542**	1
	Sig.	.074	.159	.880	.054	.086	.081	.638	.000	.000	
	N	37	37	37	37	37	36	39	39	40	40

**Correlation is significant at the 0.01 level. *Correlation is significant at the 0.05 level

Table 38. Multiple linear regression of the urban form factors urban "continuity" and urban "shape complexity" versus the concentration of ozone (O_3), fine particulate matter ($PM_{2.5}$) and coarse particulate matter (PM_{10}) (Regression model set 1, metropolitan scale). Urban form factors were calculated at the metropolitan scale using the high urban threshold.

		O_3 Conc.	O_3 Exceed.	$PM_{2.5}$ Conc.	PM_{10} Conc.
Model Adj. R^2		0.458	0.309	0.391	0.346
Model Significance		< 0.001	< 0.001	< 0.001	< 0.001
Constant	B	79.32	22.19	17.63	34.77
	Sig.	< 0.001	< 0.001	< 0.001	< 0.001
Temperature Factor	B	1.539	0.402	-0.137	1.107
	Sig.	0.106	0.702	0.698	0.162
Moisture Factor	B	0.765	0.463	0.584	-2.773
	Sig.	0.361	0.618	0.046	< 0.001
Wind Speed	B	-0.885	-1.812	-0.851	-1.136
	Sig.	0.121	0.005	< 0.001	0.022
Population	B	-0.173	0.114	0.174	-0.052
	Sig.	0.597	0.754	0.132	0.839
Population 500 km	B	0.295	0.189	0.064	0.019
	Sig.	< 0.001	0.001	< 0.001	0.664
Industrial Emissions	B	< 0.001	< 0.001	< 0.001	< 0.001
	Sig.	0.052	0.268	0.081	0.352
Continuity High	B	-0.552	-1.120	0.396	1.101
	Sig.	0.479	0.198	0.154	0.083
Shape Complexity High	B	0.052	0.339	-0.250	0.539
	Sig.	0.959	0.761	0.491	0.514

Table 39. Multiple linear regression of the urban form factors urban "continuity" and urban "shape complexity" versus the concentration of ozone (O_3), fine particulate matter ($PM_{2.5}$) and coarse particulate matter (PM_{10}) (Regression model set 1, metropolitan scale). Urban form factors were calculated at the metropolitan scale using the low urban threshold.

		O_3 Conc.	O_3 Exceed.	$PM_{2.5}$ Conc.	PM_{10} Conc.
Model Adj. R^2		0.470	0.334	0.373	0.325
Model Significance		< 0.001	< 0.001	< 0.001	< 0.001
Constant	B	78.97	21.60	18.23	35.35
	Sig.	< 0.001	< 0.001	< 0.001	< 0.001
Temperature Factor	B	1.632	0.621	-0.265	0.822
	Sig.	0.075	0.535	0.448	0.288
Moisture Factor	B	0.705	0.373	0.624	-2.696
	Sig.	0.401	0.687	0.037	< 0.001
Wind Speed	B	-0.793	-1.695	-0.882	-1.186
	Sig.	0.167	0.009	< 0.001	0.021
Population	B	-0.249	0.019	0.100	0.066
	Sig.	0.404	0.954	0.355	0.784
Population 500 km	B	0.287	0.182	0.061	0.005
	Sig.	0.000	< 0.001	0.001	0.903
Industrial Emissions	B	< 0.001	< 0.001	< 0.001	< 0.001
	Sig.	0.043	0.226	0.114	0.268
Continuity Low	B	-1.040	-1.545	0.111	0.843
	Sig.	0.201	0.087	0.706	0.205
Shape Complexity Low	B	0.503	1.004	0.078	-0.185
	Sig.	0.579	0.317	0.811	0.818

Table 40. Multiple linear regression of the urban form factors urban "continuity" and urban "shape complexity" versus the non-point source emission of the ozone (O_3) precursors volatile organic compounds (VOCs) and nitrogen oxides (NOx), fine particulate matter ($PM_{2.5}$), coarse particulate matter (PM_{10}) and carbon dioxide (CO_2) from on-road sources (Regression model set 2, metropolitan scale). Urban form factors were calculated at the metropolitan scale using the high urban threshold.

		O_3 Emissions	$PM_{2.5}$ Emissions	PM_{10} Emissions	CO_2 Emissions
Model Adj. R^2		0.952	0.764	0.521	0.902
Model Significance		< 0.001	< 0.001	< 0.001	< 0.001
Constant	B	41,445	10,158	45,519	-985,407
	Sig.	< 0.001	< 0.001	< 0.001	0.003
Temperature Factor	B	-192	-29	1,171	-162,193
	Sig.	0.969	0.980	0.847	0.378
Moisture Factor	B	18,070	2,627	10,922	172,964
	Sig.	0.001	0.036	0.103	0.391
Population	B	52,835	3,616	6,374	1,375,375
	Sig.	< 0.001	< 0.001	0.026	< 0.001
Area (km^2)	B	1.849	0.394	1.727	86.062
	Sig.	< 0.001	0.001	0.009	< 0.001
Continuity High	B	-11,685	-668	108	-122,375
	Sig.	0.019	0.552	0.986	0.504
Shape Complexity High	B	15,837	4,402	26,707	-202,365
	Sig.	0.014	0.003	< 0.001	0.394

Table 41. Multiple linear regression of the urban form factors urban "continuity" and urban "shape complexity" versus the non-point source emission of the ozone (O_3) precursors volatile organic compounds (VOCs) and nitrogen oxides (NOx), fine particulate matter ($PM_{2.5}$), coarse particulate matter (PM_{10}) and carbon dioxide (CO_2) from on-road sources (Regression model set 2, metropolitan scale). Urban form factors were calculated at the metropolitan scale using the low urban threshold.

		O_3 Emissions	$PM_{2.5}$ Emissions	PM_{10} Emissions	CO_2 Emissions
Model Adj. R^2		0.953	0.753	0.507	0.902
Model Significance		< 0.001	< 0.001	< 0.001	< 0.001
Constant	B	36,871	8,648	38,205	-889,668
	Sig.	< 0.001	< 0.001	< 0.001	0.005
Temperature Factor	B	1,628	60	436	-145,305
	Sig.	0.737	0.958	0.943	0.424
Moisture Factor	B	19,675	3,077	14,198	162,218
	Sig.	< 0.001	0.017	0.038	0.422
Population	B	53,319	3,854	7,065	1,331,802
	Sig.	< 0.001	< 0.001	0.012	< 0.001
Area (km^2)	B	2.068	0.456	2.089	86.171
	Sig.	< 0.001	< 0.001	0.002	< 0.001
Continuity Low	B	-10,331	-770	322	-221,617
	Sig.	0.034	0.495	0.957	0.219
Shape Complexity Low	B	14,913	3,055	22,096	20,873
	Sig.	0.012	0.027	0.003	0.923

Table 42. Multiple linear regression of the Ewing et al. (2003) urban sprawl index versus the concentration of ozone (O_3), fine particulate matter ($PM_{2.5}$) and coarse particulate matter (PM_{10}) (Regression model set 3, metropolitan scale).

		O_3 Conc.	O_3 Exceed.	$PM_{2.5}$ Conc.	PM_{10} Conc.
Model Adj. R^2		0.502	0.351	0.456	0.258
Model Significance		< 0.001	< 0.001	< 0.001	0.003
Constant	B	81.16	30.21	19.80	36.35
	Sig.	< 0.001	< 0.001	< 0.001	< 0.001
Temperature Factor	B	1.993	0.531	-0.351	0.514
	Sig.	0.054	0.636	0.348	0.591
Moisture Factor	B	0.386	0.031	0.541	-3.014
	Sig.	0.675	0.976	0.111	< 0.001
Wind Speed	B	0.099	-0.857	-0.606	-0.744
	Sig.	0.880	0.239	0.012	0.267
Population	B	0.063	0.625	0.245	0.146
	Sig.	0.833	0.061	0.019	0.575
Population 500 km	B	0.292	0.157	0.048	-0.008
	Sig.	< 0.001	0.008	0.012	0.864
Industrial Emissions	B	< 0.001	< 0.001	< 0.001	0.000
	Sig.	0.143	0.780	0.143	0.414
Ewing et al.	B	-0.105	-0.156	-0.041	-0.045
	Sig.	0.018	0.002	0.011	0.289

Table 43. Multiple linear regression of the Sutton (2003) urban sprawl index (high threshold) versus the concentration of ozone (O_3), fine particulate matter ($PM_{2.5}$) and coarse particulate matter (PM_{10}) (Regression model set 3, metropolitan scale).

		O_3 Conc.	O_3 Exceed.	$PM_{2.5}$ Conc.	PM_{10} Conc.
Model Adj. R^2		0.494	0.423	0.399	0.320
Model Significance		< 0.001	< 0.001	< 0.001	< 0.001
Constant	B	79.258	20.22	17.470	34.012
	Sig.	< 0.001	< 0.001	< 0.001	< 0.001
Temperature Factor	B	1.885	1.120	-0.181	0.805
	Sig.	0.037	0.233	0.603	0.307
Moisture Factor	B	0.139	-0.723	0.463	-2.875
	Sig.	0.869	0.415	0.132	< 0.001
Wind Speed	B	-0.996	-1.861	-0.820	-0.981
	Sig.	0.073	0.002	< 0.001	0.055
Population	B	0.044	0.561	0.154	0.062
	Sig.	0.870	0.048	0.107	0.782
Population 500 km	B	0.321	0.241	0.063	-0.010
	Sig.	< 0.001	< 0.001	< 0.001	0.808
Industrial Emissions	B	< 0.001	< 0.001	< 0.001	< 0.001
	Sig.	0.089	0.439	0.130	0.275
Sutton (high)	B	-0.063	-0.123	-0.018	-0.008
	Sig.	0.040	< 0.001	0.116	0.774

Table 44. Multiple linear regression of the Sutton (2003) urban sprawl index (low threshold) versus the concentration of ozone (O_3), fine particulate matter ($PM_{2.5}$) and coarse particulate matter (PM_{10}) (Regression model set 3, metropolitan scale).

		O_3 Conc.	O_3 Exceed.	$PM_{2.5}$ Conc.	PM_{10} Conc.
Model Adj. R^2		0.535	0.411	0.403	0.320
Model Significance		< 0.001	< 0.001	< 0.001	< 0.001
Constant	B	75.27	17.25	18.14	35.68
	Sig.	< 0.001	0.007	< 0.001	< 0.001
Temperature Factor	B	2.364	1.182	-0.244	0.490
	Sig.	0.009	0.242	0.498	0.555
Moisture Factor	B	-0.208	-0.809	0.477	-2.886
	Sig.	0.793	0.372	0.138	< 0.001
Wind Speed	B	-0.566	-1.479	-0.884	-1.139
	Sig.	0.301	0.020	< 0.001	0.038
Population	B	0.002	0.377	0.122	0.053
	Sig.	0.995	0.178	0.203	0.805
Population 500 km	B	0.296	0.204	0.061	-0.001
	Sig.	< 0.001	< 0.001	< 0.001	0.980
Industrial Emissions	B	< 0.001	< 0.001	< 0.001	< 0.001
	Sig.	0.053	0.459	0.163	0.475
Sutton (low)	B	-0.070	-0.105	-0.011	-0.008
	Sig.	0.004	< 0.001	0.260	0.712

Table 45. Multiple linear regression of the Lopez and Hynes (2003) urban sprawl index versus the concentration of ozone (O_3), fine particulate matter ($PM_{2.5}$) and coarse particulate matter (PM_{10}) (Regression model set 3, metropolitan scale).

		O_3 Conc.	O_3 Exceed.	$PM_{2.5}$ Conc.	PM_{10} Conc.
Model Adj. R^2		0.487	0.308	0.387	0.325
Model Significance		< 0.001	< 0.001	< 0.001	< 0.001
Constant	B	69.26	5.97	16.14	36.50
	Sig.	< 0.001	0.425	< 0.001	< 0.001
Temperature Factor	B	1.849	0.955	-0.192	0.822
	Sig.	0.040	0.322	0.583	0.287
Moisture Factor	B	-0.280	-1.221	0.423	-2.605
	Sig.	0.759	0.218	0.206	0.002
Wind Speed	B	-0.591	-1.335	-0.788	-1.119
	Sig.	0.290	0.029	< 0.001	0.028
Population	B	0.163	0.694	0.177	-0.013
	Sig.	0.572	0.028	0.095	0.958
Population 500 km	B	0.310	0.212	0.061	< 0.001
	Sig.	< 0.001	< 0.001	< 0.001	0.988
Industrial Emissions	B	< 0.001	< 0.001	< 0.001	< 0.001
	Sig.	0.025	0.116	0.092	0.263
Lopez and Hynes	B	0.104	0.164	0.019	-0.023
	Sig.	0.023	0.001	0.276	0.583

Table 46. Multiple linear regression of the Nasser and Overberg (USA Today) (2001) urban sprawl index versus the concentration of ozone (O_3), fine particulate matter ($PM_{2.5}$) and coarse particulate matter (PM_{10}) (Regression model set 3, metropolitan scale).

		O_3 Conc.	O_3 Exceed.	$PM_{2.5}$ Conc.	PM_{10} Conc.
Model Adj. R^2		0.493	0.328	0.402	0.318
Model Significance		< 0.001	< 0.001	< 0.001	< 0.001
Constant	B	71.68	15.13	15.82	34.15
	Sig.	< 0.001	0.040	< 0.001	< 0.001
Temperature Factor	B	1.815	0.853	-0.225	0.785
	Sig.	0.043	0.396	0.510	0.310
Moisture Factor	B	0.108	-0.178	0.453	-2.818
	Sig.	0.899	0.853	0.134	< 0.001
Wind Speed	B	-0.541	-1.534	-0.736	-1.005
	Sig.	0.339	0.018	< 0.001	0.056
Population	B	0.059	0.395	0.175	0.058
	Sig.	0.827	0.201	0.072	0.795
Population 500 km	B	0.293	0.198	0.054	-0.015
	Sig.	< 0.001	< 0.001	0.001	0.730
Industrial Emissions	B	< 0.001	< 0.001	< 0.001	< 0.001
	Sig.	0.044	0.264	0.103	0.256
Nasser and Overberg	B	0.016	0.014	0.005	0.001
(USA Today)	Sig.	0.032	0.096	0.091	0.862

Table 47. Multiple linear regression of the Burchfield et al. (2006) urban sprawl index versus the concentration of ozone (O_3), fine particulate matter ($PM_{2.5}$) and coarse particulate matter (PM_{10}) (Regression model set 3, metropolitan scale).

		O_3 Conc.	O_3 Exceed.	$PM_{2.5}$ Conc.	PM_{10} Conc.
Model Adj. R^2		0.395	0.279	0.413	0.175
Model Significance		0.001	0.012	0.001	0.082
Constant	B	76.25	15.22	16.94	28.70
	Sig.	< 0.001	0.229	< 0.001	0.013
Temperature Factor	B	2.388	1.779	-0.712	0.851
	Sig.	0.130	0.271	0.128	0.529
Moisture Factor	B	-0.984	-0.665	0.870	-4.115
	Sig.	0.596	0.729	0.104	0.011
Wind Speed	B	-0.371	-1.414	-0.814	-0.309
	Sig.	0.724	0.198	0.010	0.751
Population	B	-0.509	-0.011	0.154	-0.095
	Sig.	0.167	0.978	0.142	0.744
Population 500 km	B	0.361	0.251	0.048	0.018
	Sig.	< 0.001	0.004	0.049	0.791
Industrial Emissions	B	< 0.001	< 0.001	< 0.001	< 0.001
	Sig.	0.100	0.438	0.158	0.495
Burchfield et al.	B	-0.046	0.071	0.027	-0.017
	Sig.	0.758	0.646	0.548	0.893

Table 48. Multiple linear regression of the Ewing (2003) urban sprawl index components street connectivity, centeredness, mixed use, and residential density versus the concentration of ozone (O_3), fine particulate matter ($PM_{2.5}$) and coarse particulate matter (PM_{10}) (Regression model set 4, metropolitan scale).

		O_3 Conc.	O_3 Exceed.	$PM_{2.5}$ Conc.	PM_{10} Conc.
Model Adj. R^2		0.556	0.410	0.469	0.237
Model Significance		< 0.001	< 0.001	< 0.001	< 0.001
Constant	B	92.39	43.54	23.16	40.48
	Sig.	< 0.001	< 0.001	< 0.001	< 0.001
Temperature Factor	B	2.592	1.024	-0.222	0.726
	Sig.	0.012	0.357	0.559	0.474
Moisture Factor	B	0.391	-0.529	0.546	-2.876
	Sig.	0.686	0.623	0.144	0.004
Wind Speed	B	-0.128	-0.798	-0.640	-0.825
	Sig.	0.847	0.281	0.011	0.243
Population	B	1.372	2.426	0.569	0.477
	Sig.	0.022	< 0.001	0.010	0.398
Population 500 km	B	0.272	0.146	0.043	-0.017
	Sig.	< 0.001	0.011	0.027	0.739
Industrial Emissions	B	< 0.001	< 0.001	< 0.001	< 0.001
	Sig.	0.331	0.902	0.159	0.483
Street Connectivity	B	-0.057	-0.038	-0.019	-0.021
	Sig.	0.206	0.452	0.252	0.672
Centeredness	B	-0.004	0.010	-0.011	-0.029
	Sig.	0.937	0.849	0.521	0.504
Mixed Use	B	0.063	0.006	0.012	0.034
	Sig.	0.171	0.902	0.481	0.450
Residential Density	B	-0.229	-0.325	-0.061	-0.069
	Sig.	0.015	0.002	0.082	0.450

Table 49. Multiple linear regression of the Ewing (2003) urban sprawl index versus the non-point source emission of the ozone (O_3) precursors volatile organic compounds (VOCs) and nitrogen oxides (NOx), fine particulate matter ($PM_{2.5}$), coarse particulate matter (PM_{10}) and carbon dioxide (CO_2) from on-road sources (Regression model set 5, metropolitan scale).

		O_3 Emissions	$PM_{2.5}$ Emissions	PM_{10} Emissions	CO_2 Emissions
Model Adj. R^2		0.946	0.726	0.402	0.903
Model Significance		< 0.001	< 0.001	< 0.001	< 0.001
Constant	B	87,896	16,339	66,251	973,217
	Sig.	0.016	0.048	0.147	0.446
Temperature Factor	B	2,956	596.9	2,511	-179,693
	Sig.	0.645	0.684	0.759	0.436
Moisture Factor	B	17,635	2,804	13,108	-44,629
	Sig.	0.024	0.111	0.180	0.870
Population	B	57,788	4,570	11,106	1,435,056
	Sig.	< 0.001	< 0.001	0.001	< 0.001
Area (km^2)	B	1.443	0.368	1.824	73.53
	Sig.	0.032	0.017	0.034	0.003
Ewing et al.	B	-456.0	-65.05	-248.8	-20,123
	Sig.	0.169	0.388	0.554	0.092

Table 50. Multiple linear regression of the Sutton (2003) urban sprawl index (high threshold) versus the non-point source emission of the ozone (O_3) precursors volatile organic compounds (VOCs) and nitrogen oxides (NOx), fine particulate matter ($PM_{2.5}$), coarse particulate matter (PM_{10}) and carbon dioxide (CO_2) from on-road sources (Regression model set 5, metropolitan scale).

		O_3 Emissions	$PM_{2.5}$ Emissions	PM_{10} Emissions	CO_2 Emissions
Model Adj. R^2		0.947	0.749	0.475	0.901
Model Significance		< 0.001	< 0.001	< 0.001	< 0.001
Constant	B	33,938	7,957	31,400	-862,032
	Sig.	< 0.001	< 0.001	0.004	0.006
Temperature Factor	B	3,060	534	3,661	-154,576
	Sig.	0.557	0.646	0.564	0.403
Moisture Factor	B	16,449	1,825	6,871	148,381
	Sig.	0.011	0.200	0.375	0.510
Population	B	57,343	4,802	13,001	1,353,317
	Sig.	< 0.001	< 0.001	< 0.001	< 0.001
Area (km^2)	B	1.719	0.382	1.760	81.297
	Sig.	0.003	0.003	013	< 0.001
Sutton (high)	B	-140.5	-86.7	-475.3	-996.2
	Sig.	0.528	0.084	0.083	0.900

Table 51. Multiple linear regression of the Sutton (2003) urban sprawl index (low threshold) versus the non-point source emission of the ozone (O_3) precursors volatile organic compounds (VOCs) and nitrogen oxides (NOx), fine particulate matter ($PM_{2.5}$), coarse particulate matter (PM_{10}) and carbon dioxide (CO_2) from on-road sources (Regression model set 5, metropolitan scale).

Set 5: Sutton (low)

		O_3 Emissions	$PM_{2.5}$ Emissions	PM_{10} Emissions	CO_2 Emissions
Model Adj. R^2		0.949	0.751	0.476	0.898
Model Significance		< 0.001	< 0.001	< 0.001	< 0.001
Constant	B	34,066	7,720	29,350	-879,778
	Sig.	0.001	< 0.001	0.011	0.012
Temperature Factor	B	4,030	574	3,536	-181,464
	Sig.	0.473	0.639	0.598	0.372
Moisture Factor	B	15,007	1,410	5,023	232,693
	Sig.	0.025	0.328	0.523	0.330
Population	B	56,689	4,532	11,432	1,343,520
	Sig.	< 0.001	< 0.001	< 0.001	< 0.001
Area (km^2)	B	1.676	0.375	1.769	85.432
	Sig.	0.005	0.005	0.014	< 0.001
Sutton (low)	B	-244	-106	-558	5,111
	Sig.	0.202	0.012	0.016	0.457

Table 52. Multiple linear regression of the Lopez and Hynes(2003) urban sprawl index (high threshold) versus the non-point source emission of the ozone (O_3) precursors volatile organic compounds (VOCs) and nitrogen oxides (NOx), fine particulate matter ($PM_{2.5}$), coarse particulate matter (PM_{10}) and carbon dioxide (CO_2) from on-road sources (Regression model set 5, metropolitan scale).

		O_3 Emissions	$PM_{2.5}$ Emissions	PM_{10} Emissions	CO_2 Emissions
Model Adj. R^2		0.945	0.732	0.447	0.900
Model Significance		< 0.001	< 0.001	< 0.001	< 0.001
Constant	B	34,836	9,199	40,003	-1,648,234
	Sig.	0.115	0.068	0.147	0.0359477
Temperature Factor	B	2,728	347	2,686	-154,000
	Sig.	0.593	0.765	0.673	0.394
Moisture Factor	B	18,391	2,993	13,396	43,730
	Sig.	0.005	0.043	0.097	0.847
Population	B	56,358	4,325	10,613	1,392,852
	Sig.	< 0.001	< 0.001	< 0.001	< 0.001
Area (km^2)	B	1.825	0.435	2.037	79.934
	Sig.	0.001	< 0.001	0.003	< 0.001
Lopez and Hynes	B	-25.30	-24.06	-156.0	12,369
	Sig.	0.936	0.739	0.694	0.271

Table 53. Multiple linear regression of the Nasser and Overberg (2001) (USA Today) urban sprawl index versus the non-point source emission of the ozone (O_3) precursors volatile organic compounds (VOCs) and nitrogen oxides (NOx), fine particulate matter ($PM_{2.5}$), coarse particulate matter (PM_{10}) and carbon dioxide (CO_2) from on-road sources (Regression model set 5, metropolitan scale).

		O_3 Emissions	$PM_{2.5}$ Emissions	PM_{10} Emissions	CO_2 Emissions
Model Adj. R^2		0.947	0.740	0.460	0.904
Model Significance		< 0.001	< 0.001	< 0.001	< 0.001
Constant	B	32,706	8,689	43,870	-1,468,570
	Sig.	0.046	0.020	0.031	0.011
Temperature Factor	B	2,662	321	2,522	-147,326
	Sig.	0.602	0.782	0.690	0.411
Moisture Factor	B	18,053	2,912	13,955	70,185
	Sig.	0.004	0.036	0.064	0.740
Population	B	56,826	4,427	10,478	1,384,480
	Sig.	< 0.001	< 0.001	< 0.001	< 0.001
Area (km^2)	B	1.807	0.434	2.073	78.999
	Sig.	0.001	< 0.001	0.003	< 0.001
Nasser and Overberg	B	1.885	-3.747	-50.51	2,229
(USA Today)	Sig.	0.970	0.744	0.420	0.210

Table 54. Multiple linear regression of the Burchfield (2006) urban sprawl index versus the non-point source emission of the ozone (O_3) precursors volatile organic compounds (VOCs) and nitrogen oxides (NOx), fine particulate matter ($PM_{2.5}$), coarse particulate matter (PM_{10}) and carbon dioxide (CO_2) from on-road sources (Regression model set 5, metropolitan scale).

		O_3 Emissions	$PM_{2.5}$ Emissions	PM_{10} Emissions	CO_2 Emissions
Model Adj. R^2		0.937	0.687	0.312	0.908
Model Significance		< 0.001	< 0.001	0.003	< 0.001
Constant	B	4,194	5,427	37,664	-2,145,012
	Sig.	0.935	0.630	0.551	0.218
Temperature Factor	B	5,130	563.4	3,858	-151,435
	Sig.	0.590	0.787	0.742	0.636
Moisture Factor	B	24,796	4,671	22,175	32,189
	Sig.	0.080	0.131	0.199	0.945
Population	B	53,929	3,990	8,162	1,239,467
	Sig.	< 0.001	< 0.001	0.041	< 0.001
Area (km^2)	B	2.257	0.492	2.420	145.2
	Sig.	0.030	0.031	0.057	< 0.001
Burchfield et al.	B	1,122	136.5	248.3	8,770
	Sig.	0.343	0.597	0.864	0.824

Table 55. Multiple linear regression of the Ewing (2003) urban sprawl index components street connectivity, centeredness, mixed use, and residential density versus the non-point source emission of the ozone (O_3) precursors volatile organic compounds (VOCs) and nitrogen oxides (NOx), fine particulate matter ($PM_{2.5}$), coarse particulate matter (PM_{10}) and carbon dioxide (CO_2) from on-road sources (Regression model set 6, metropolitan scale).

		O_3 Emissions	$PM_{2.5}$ Emissions	PM_{10} Emissions	CO_2 Emissions
Model Adj. R^2		0.946	0.720	0.397	0.920
Model Significance		< 0.001	< 0.001	< 0.001	< 0.001
Constant	B	124,962	16,914	61,225	4,467,587
	Sig.	0.033	0.203	0.404	0.019
Temperature Factor	B	6,116	1,367	6,884	-142,963
	Sig.	0.394	0.406	0.451	0.537
Moisture Factor	B	17,402	3,562	18,367	-370,481
	Sig.	0.046	0.074	0.097	0.185
Population	B	61,841	4,441	9,654	1,974,833
	Sig.	< 0.001	< 0.001	0.152	< 0.001
Area (km^2)	B	1.396	0.396	1.995	56.22
	Sig.	0.045	0.014	0.025	0.014
Street Connectivity	B	-264.7	-90.12	-431.1	16,536
	Sig.	0.455	0.270	0.341	0.152
Centrality	B	-178.5	-60.69	-406.2	6,226
	Sig.	0.633	0.479	0.394	0.606
Mixed Use	B	275.9	73.47	565.2	8,800
	Sig.	0.435	0.366	0.212	0.442
Residential Density	B	-777.2	6.524	104.2	-100,331
	Sig.	0.311	0.970	0.915	< 0.001

Table 56. Multiple linear regression of the urban form factors urban "continuity" and urban "shape complexity" versus the concentration of ozone (O_3), fine particulate matter ($PM_{2.5}$) and coarse particulate matter (PM_{10}) (Regression model set 1, megapolitan scale). Urban form factors were calculated at the megapolitan scale using the high urban threshold.

		O3 Conc.	O3 Exceed.	PM2.5 Conc.	PM10 Conc.
Model Adj. R2		0.472	0.239	0.615	0.683
Model Significance		0.053	0.211	0.014	0.009
Constant	B	57.49	22.35	18.81	28.147
	Sig.	0.007	0.285	0.002	0.003
Temperature Factor	B	3.942	1.211	-0.697	1.761
	Sig.	0.146	0.687	0.365	0.147
Moisture Factor	B	-1.636	-0.170	0.594	-4.002
	Sig.	0.450	0.946	0.355	0.001
Wind Speed	B	1.184	-2.379	-1.317	-0.900
	Sig.	0.524	0.283	0.022	0.243
Population	B	-0.344	0.003	0.058	-0.116
	Sig.	0.275	0.992	0.494	0.369
Population 500 km	B	0.312	0.300	0.110	0.108
	Sig.	0.013	0.033	0.004	0.033
Industrial Emissions	B	< 0.001	< 0.001	< 0.001	< 0.001
	Sig.	0.113	0.861	0.654	0.415
Continuity High	B	-1.399	-0.588	0.475	1.417
	Sig.	0.493	0.803	0.405	0.115
Shape Complexity High	B	0.519	3.353	1.441	1.377
	Sig.	0.808	0.199	0.052	0.196

Table 57. Multiple linear regression of the urban form factors urban "continuity" and urban "shape complexity" versus the concentration of ozone (O_3), fine particulate matter ($PM_{2.5}$) and coarse particulate matter (PM_{10}) (Regression model set 1, megapolitan scale). Urban form factors were calculated at the megapolitan scale using the low urban threshold.

		O3 Conc.	O3 Exceed.	PM2.5 Conc.	PM10 Conc.
Model Adj. R2		0.500	0.193	0.611	0.663
Model Significance		0.042	0.257	0.015	0.012
Constant	B	56.56	8.93	14.00	24.57
	Sig.	0.005	0.659	0.009	0.005
Temperature Factor	B	4.745	1.708	-0.862	1.204
	Sig.	0.073	0.573	0.253	0.302
Moisture Factor	B	-1.673	-1.294	0.129	-4.368
	Sig.	0.410	0.603	0.823	0.001
Wind Speed	B	1.425	-0.776	-0.797	-0.496
	Sig.	0.391	0.701	0.102	0.479
Population	B	-0.233	-0.120	-0.044	-0.241
	Sig.	0.489	0.771	0.642	0.116
Population 500 km	B	0.264	0.270	0.121	0.121
	Sig.	0.038	0.077	0.004	0.039
Industrial Emissions	B	< 0.001	< 0.001	< 0.001	< 0.001
	Sig.	0.081	0.458	0.206	0.203
Continuity Low	B	-2.453	-0.272	1.252	2.103
	Sig.	0.323	0.928	0.103	0.088
Shape Complexity Low	B	0.129	2.718	1.113	0.767
	Sig.	0.949	0.287	0.085	0.417

Table 58. Multiple linear regression of the urban form factors urban "continuity" and urban "shape complexity" versus the non-point source emission of the ozone (O_3) precursors volatile organic compounds (VOCs) and nitrogen oxides (NOx), fine particulate matter ($PM_{2.5}$), coarse particulate matter (PM_{10}) and carbon dioxide (CO_2) from on-road sources (Regression model set 2, megapolitan scale). Urban form factors were calculated at the megapolitan scale using the high urban threshold.

		O3 Emiss.	PM2.5 Emiss.	PM10 Emiss.	CO2 Emiss.
Model Adj. R2		0.940	0.685	0.055	0.941
Model Significance		< 0.001	0.002	0.382	< 0.001
Constant	B	42,470	40,702	217,723	2,658,792
	Sig.	0.610	0.034	0.047	0.117
Temperature Factor	B	-35,284	1,498	9,689	-55,540
	Sig.	0.203	0.790	0.766	0.915
Moisture Factor	B	103,695	4,386	11,263	524,871
	Sig.	0.006	0.519	0.773	0.408
Population	B	54,790	5,022	12,915	1,222,610
	Sig.	< 0.001	< 0.001	0.053	< 0.001
Area (km^2)	B	3.172	0.058	-0.353	-10.238
	Sig.	0.076	0.869	0.862	0.753
Continuity High	B	-43,333	-3,087	1,596	-694,987
	Sig.	0.112	0.570	0.959	0.182
Shape Complexity High	B	13,694	-1,998	2,579	-83,964
	Sig.	0.602	0.716	0.935	0.868

Table 59. Multiple linear regression of the urban form factors urban "continuity" and urban "shape complexity" versus the non-point source emission of the ozone (O3) precursors volatile organic compounds (VOCs) and nitrogen oxides (NOx), fine particulate matter ($PM_{2.5}$), coarse particulate matter (PM_{10}) and carbon dioxide (CO_2) from on-road sources (Regression model set 2, megapolitan scale). Urban form factors were calculated at the megapolitan scale using the low urban threshold.

		O3 Emiss.	PM2.5 Emiss.	PM10 Emiss.	CO2 Emiss.
Model Adj. R2		0.937	0.722	0.103	0.950
Model Significance		< 0.001	0.001	0.311	< 0.001
Constant	B	22,760	37,297	199,265	1,392,377
	Sig.	0.812	0.061	0.090	0.409
Temperature Factor	B	-11,702	4,693	24,252	641,350
	Sig.	0.722	0.462	0.525	0.272
Moisture Factor	B	101,012	4,720	13,145	660,201
	Sig.	0.010	0.469	0.734	0.268
Population	B	55,906	5,133	12,368	1,224,883
	Sig.	< 0.001	< 0.001	0.056	< 0.001
Area (km^2)	B	3.342	0.100	0.047	11.173
	Sig.	0.106	0.791	0.984	0.742
Continuity Low	B	-43,598	-7,757	-25,820	-996,629
	Sig.	0.145	0.175	0.439	0.062
Shape Complexity Low	B	-2,670	-1,019	-12,547	-714,964
	Sig.	0.937	0.876	0.749	0.239

Table 60. Exurban area and population among selected large metropolitan areas. Source: Sutton (2006).

Metro	Urban Area (km^2)	Exurban Area (km^2)	% Exurban Area (km^2)	Urban Pop.	Exurban Pop.	% Exurban Pop.
New York	6,366	17,555	73.4	10,443,497	2,055,822	16.4
Los Angeles	5,060	13,733	73.1	9,056,845	1,883,055	17.2
Chicago	5,313	22,321	80.8	4,970,777	1,131,023	18.5
Miami	2,987	4,619	60.7	3,708,042	452,270	10.9
Washington-Baltimore	5,313	26,552	83.3	3,444,641	1,985,356	36.6
Detroit	3,143	25,042	88.8	2,579,779	1,235,907	32.4
Boston	1,845	14,599	88.8	1,718,846	1,496,005	46.5
Las Vegas	744	2,669	78.2	855,447	111,235	11.5
St. Louis	1,930	14,128	88.0	1,173,411	723,077	38.1
Denver	1,397	7,225	83.8	1,238,270	449,862	26.6
San Diego	907	2,359	72.2	1,646,181	541,241	24.7
Portland	874	5,850	87.0	718,111	624,159	46.5
El Paso	572	2,269	79.9	1,074,367	171,841	13.8
Dallas-Ft. Worth	3,320	11,433	77.5	2,800,483	1,003,921	26.4
Phoenix	1,750	5,523	75.9	1,838,568	464,487	20.2
Atlanta[1]	2,119	16,741	88.8	1,482,878	1,873,347	55.8
Memphis	869	8,166	90.4	549,916	444,341	44.7
Charlotte	620	15,533	96.2	357,651	1,457,915	80.3
Birmingham	675	10,055	93.7	352,683	668,578	65.5
Nashville	1,005	14,195	93.4	433,648	647,703	59.9

Table 61. Nineteen megapolitan areas ranked (from high to low) in terms of O_3 concentration and number of O_3 exceedances (1998 – 2002).

Megapolitan Area	O_3 Conc.(µg/m^3)	O_3 Exceed. (days)	
Georgia Piedmont	107.4	Georgia Piedmont	30.6
Texas Gulf	99.4	Southern California	28.6
Chesapeake Megalopolis	97.2	Metroplex	28.0
Metroplex	96.9	Carolina Piedmont	26.6
Carolina Piedmont	96.4	Chesapeake Megalopolis	24.7
Southern California	96.3	Ohio Valley	20.5
Steel Corridor	93.7	Core Megalopolis	20.4
Ohio Valley	93.4	Steel Corridor	19.8
Core Megalopolis	91.5	Texas Gulf	17.3
Michigan Corridor	86.7	Michigan Corridor	13.5
Florida	86.5	Northern California	12.3
New England	84.1	Texas Corridor	11.4
Texas Corridor	83.8	Sun Corridor	11.2
Front Range	82.1	New England	10.0
Lake Front	80.8	Lake Front	9.8
Northern California	79.5	Florida	6.8
Sun Corridor	79.5	Front Range	5.3
Treasure Coast	79.2	Treasure Coast	2.5
Cascadia	66.8	Cascadia	0.8

Table 62. Nineteen megapolitan areas ranked (from high to low) in terms of $PM_{2.5}$ and PM_{10} concentration (1998 – 2002).

Megapolitan Area	$PM_{2.5}$ Conc.($\mu g/m^3$)	PM_{10} Conc. ($\mu g/m^3$)	
Southern California	17.8	Sun Corridor	35.0
Georgia Piedmont	17.3	Southern California	28.2
Ohio Valley	16.7	Texas Gulf	27.7
Chesapeake Megalopolis	15.2	Georgia Piedmont	27.1
Carolina Piedmont	14.9	Metroplex	26.7
Lake Front	14.6	Texas Corridor	26.0
Michigan Corridor	14.4	Ohio Valley	25.9
Core Megalopolis	14.0	Lake Front	25.8
Steel Corridor	13.6	Michigan Corridor	25.0
Metroplex	12.8	Carolina Piedmont	24.9
Texas Gulf	12.1	Steel Corridor	23.9
Northern California	11.9	Florida	23.5
New England	11.1	Northern California	22.8
Florida	10.7	Core Megalopolis	22.7
Texas Corridor	10.2	Front Range	21.8
Sun Corridor	9.5	Chesapeake Megalopolis	21.6
Cascadia	9.4	Treasure Coast	20.3
Treasure Coast	8.7	New England	18.7
Front Range	8.5	Cascadia	17.3

Figure 1. The metropolitan-scale analysis included 23 metropolitan statistical areas (MSAs) and 63 combined statistical areas (CSAs)

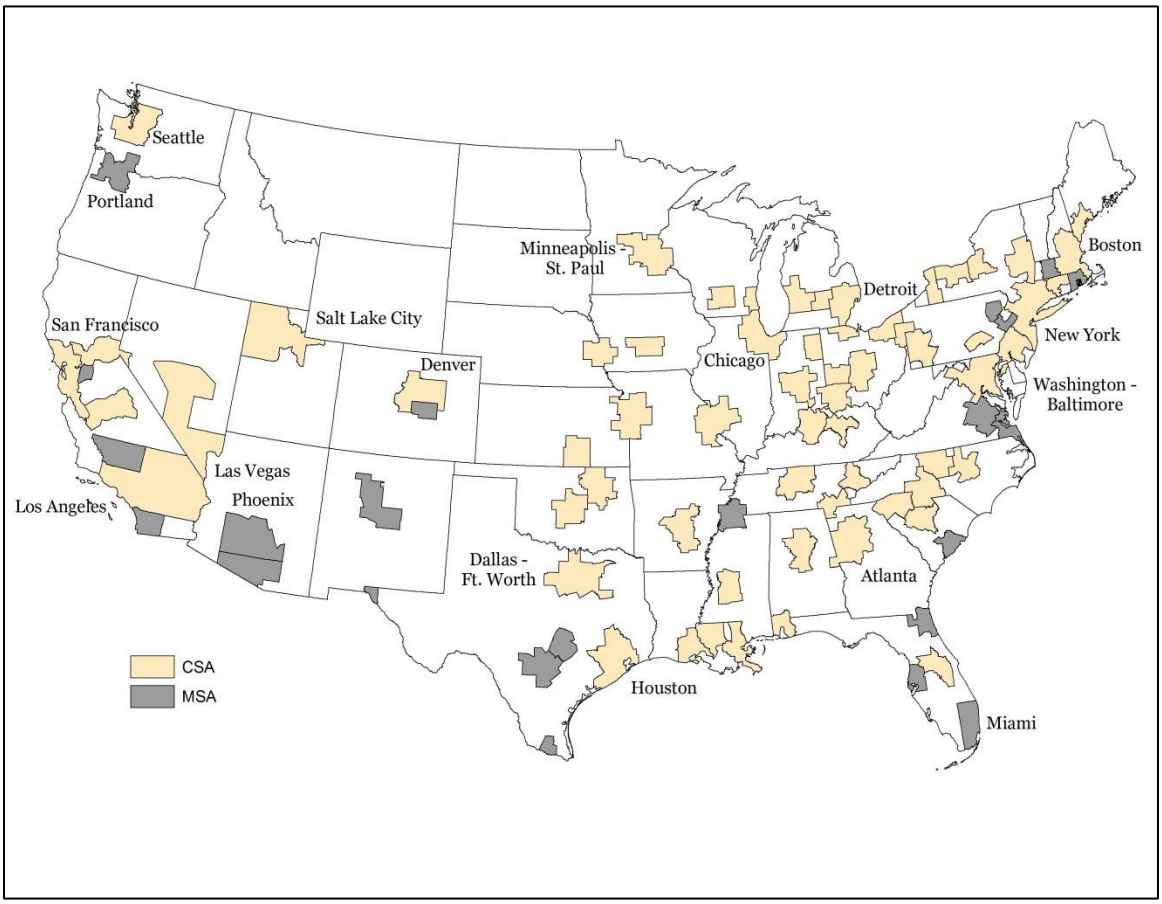

Figure 2. Nineteen megapolitan areas as described by Lang (2006).

Figure 3. Intensity of city lights at night in the United States. Data was acquired from the Defense Meteorological Satellite Program's Operational Linescan System (DMSP-OLS).

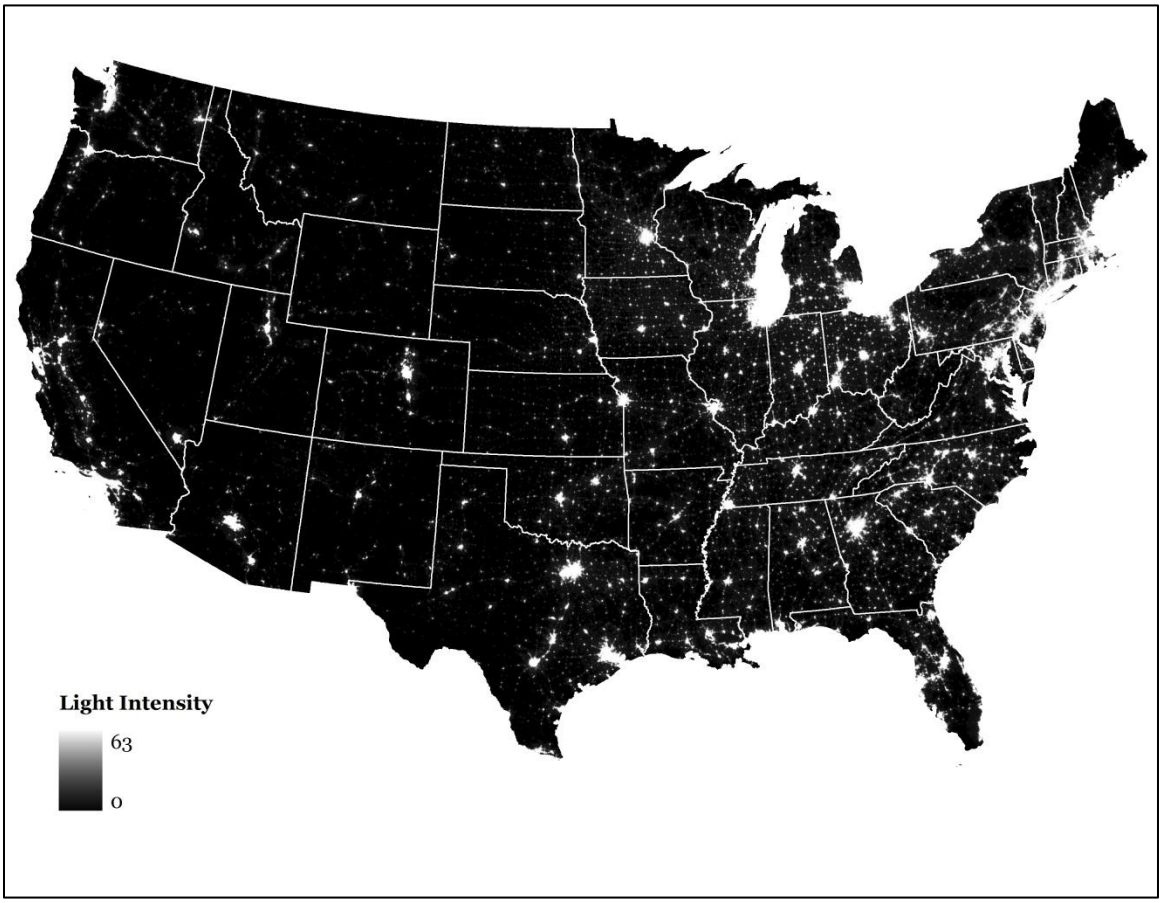

Figure 4. High and low urban thresholds in the Greensboro-Winston-Salem-High Point CSA based on intensity of city lights at night.

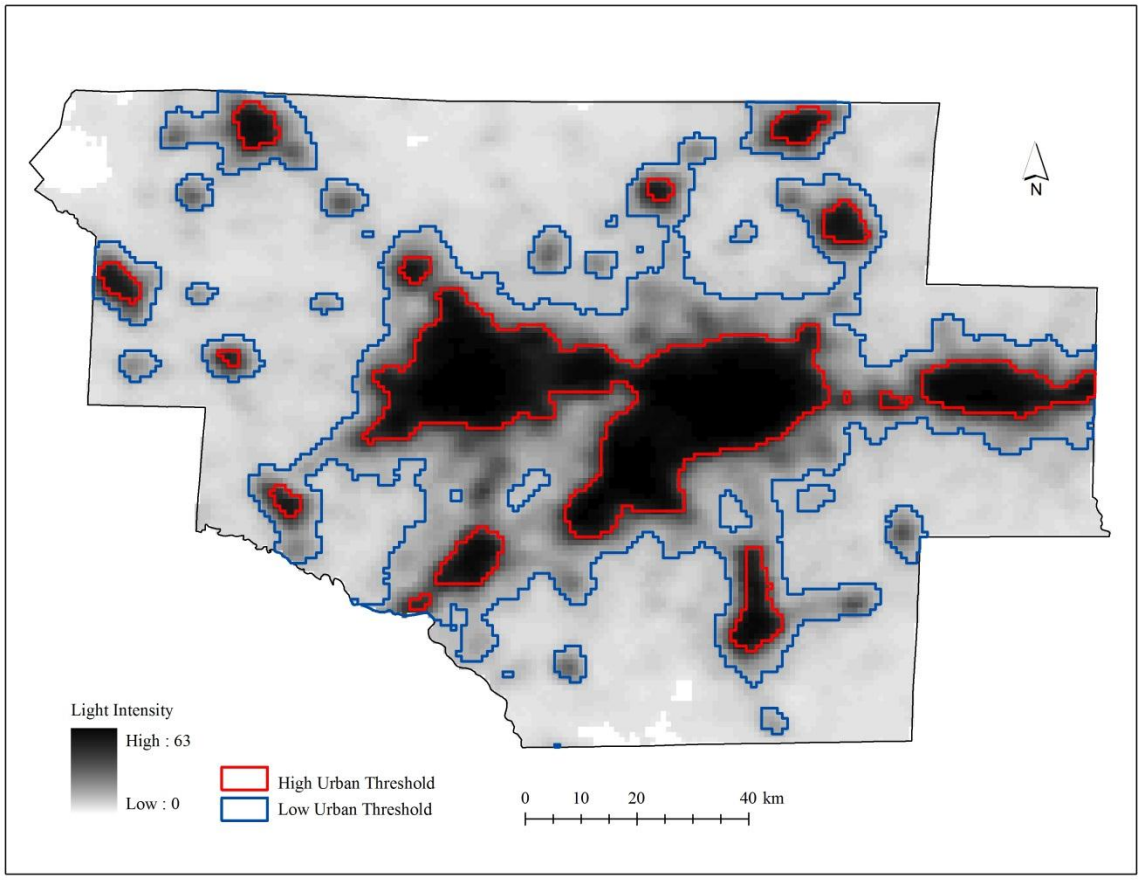

Figure 5. Urban landcover within the high and low urban thresholds in Greensboro—Winston-Salem—High Point CSA.

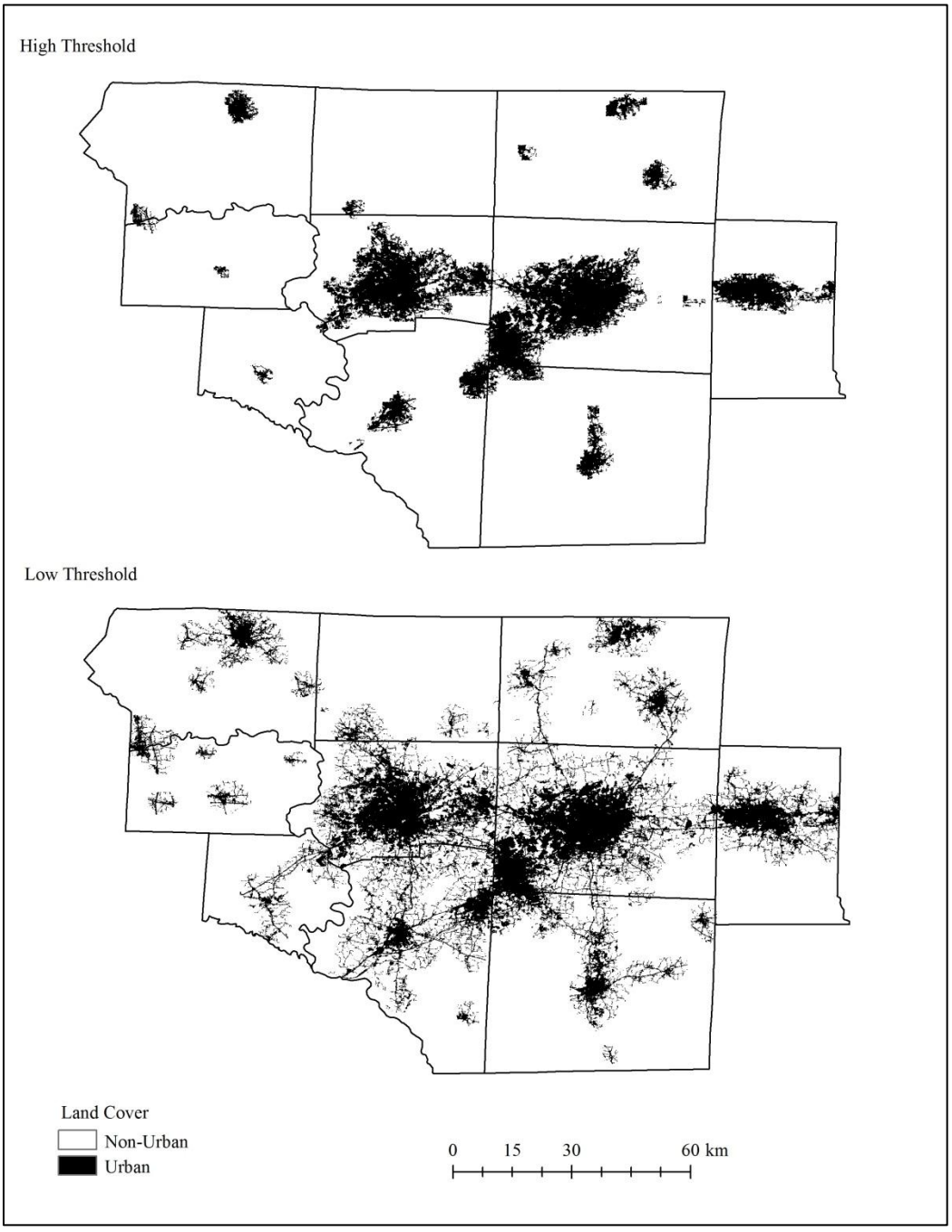

Figure 6. Non-point emission of volatile organic compounds (VOCs) and nitrogen oxides (NOx) by county in 2000.

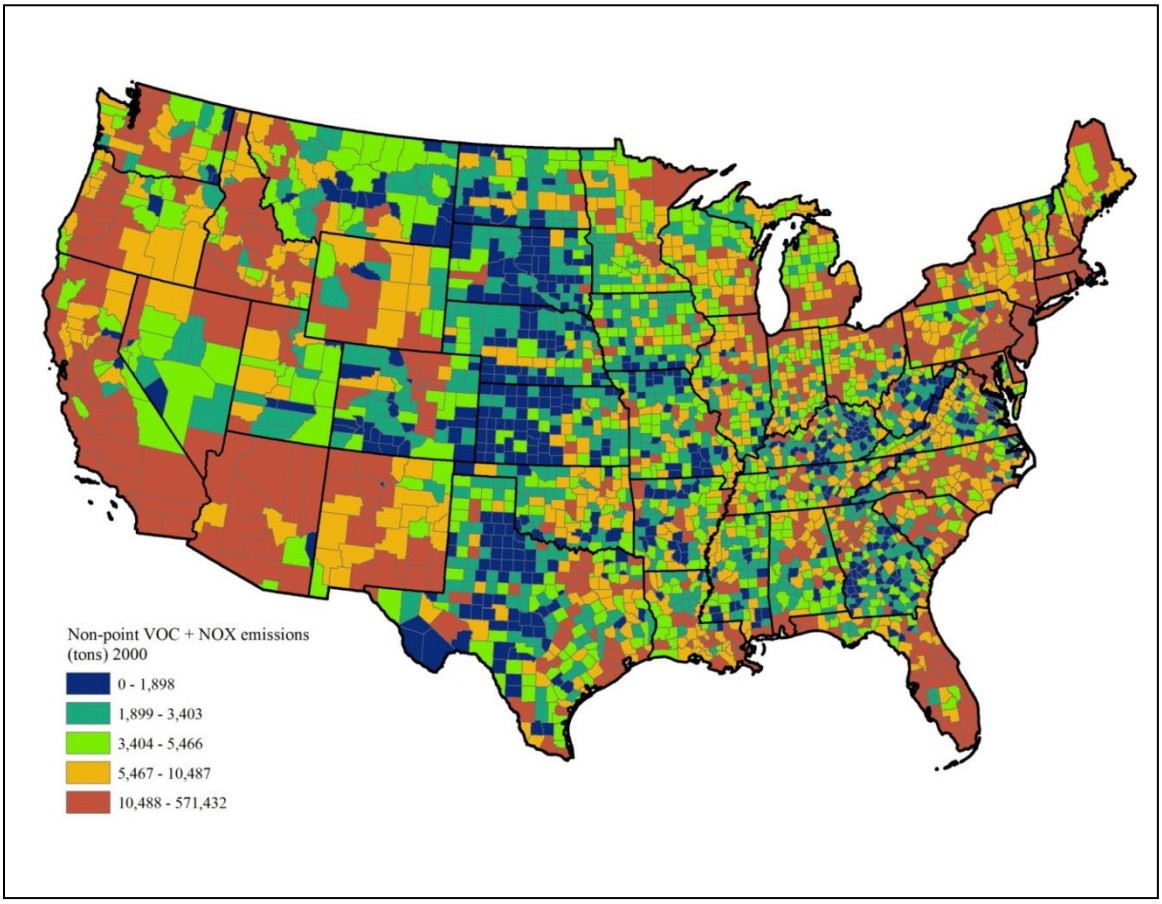

Figure 7. Non-point emission of $PM_{2.5}$ by county in 2000.

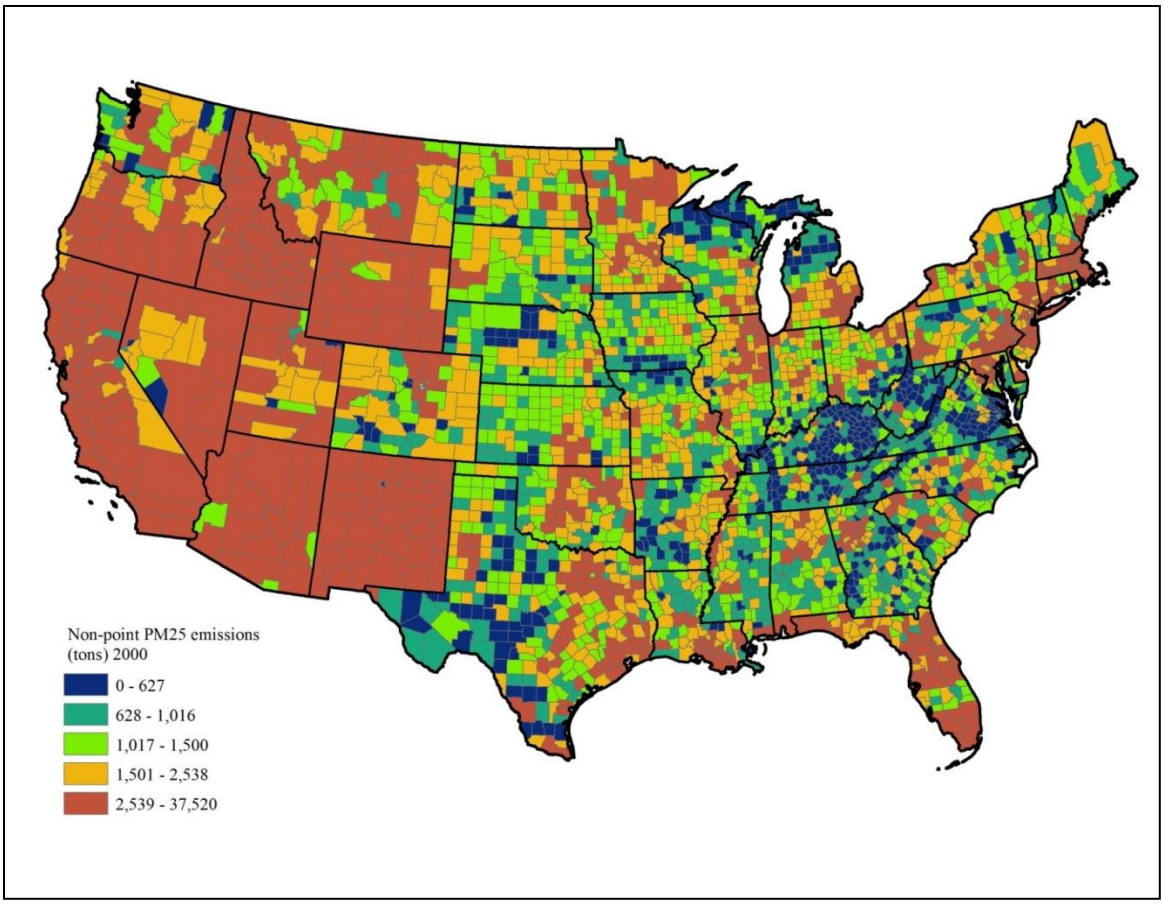

Figure 8. Non-point emission of PM_{10} by county in 2000.

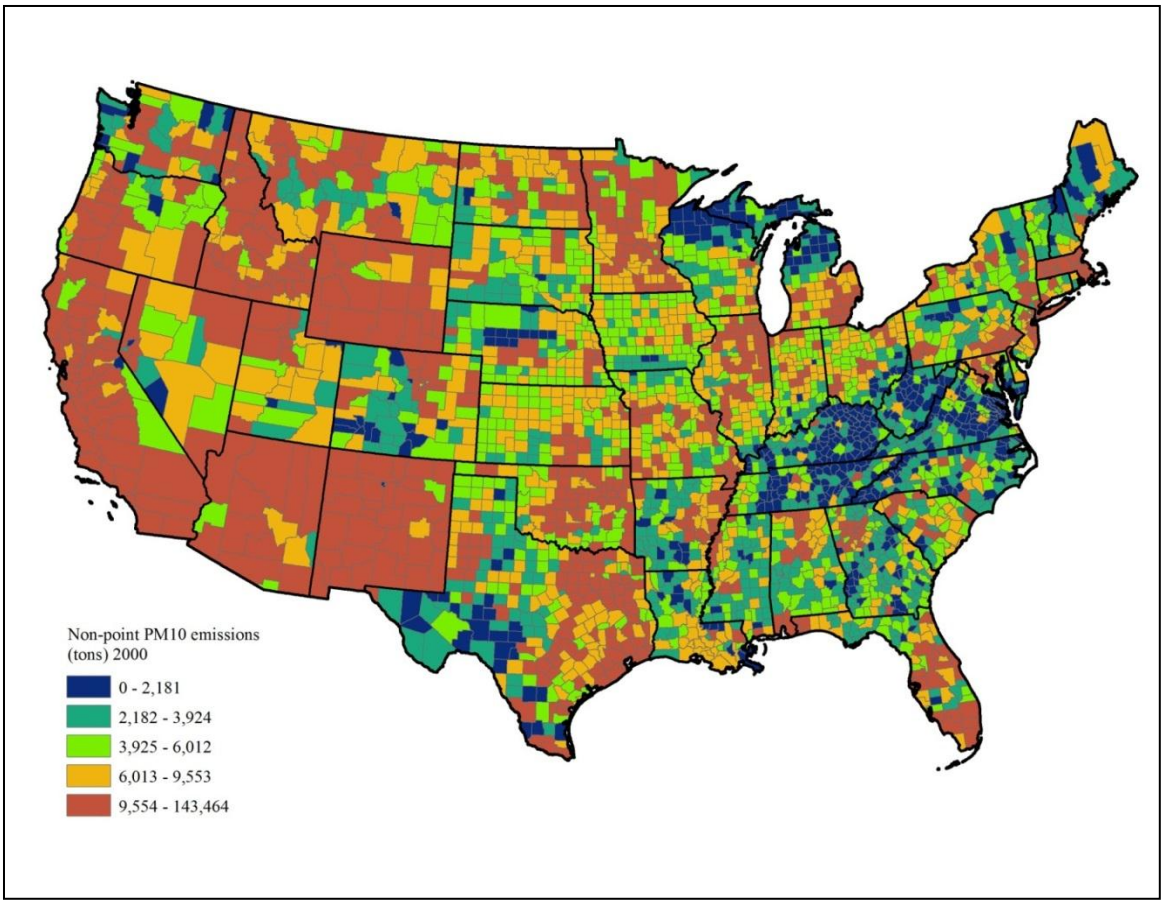

Figure 9. On-road emission of CO_2 by county in 2002.

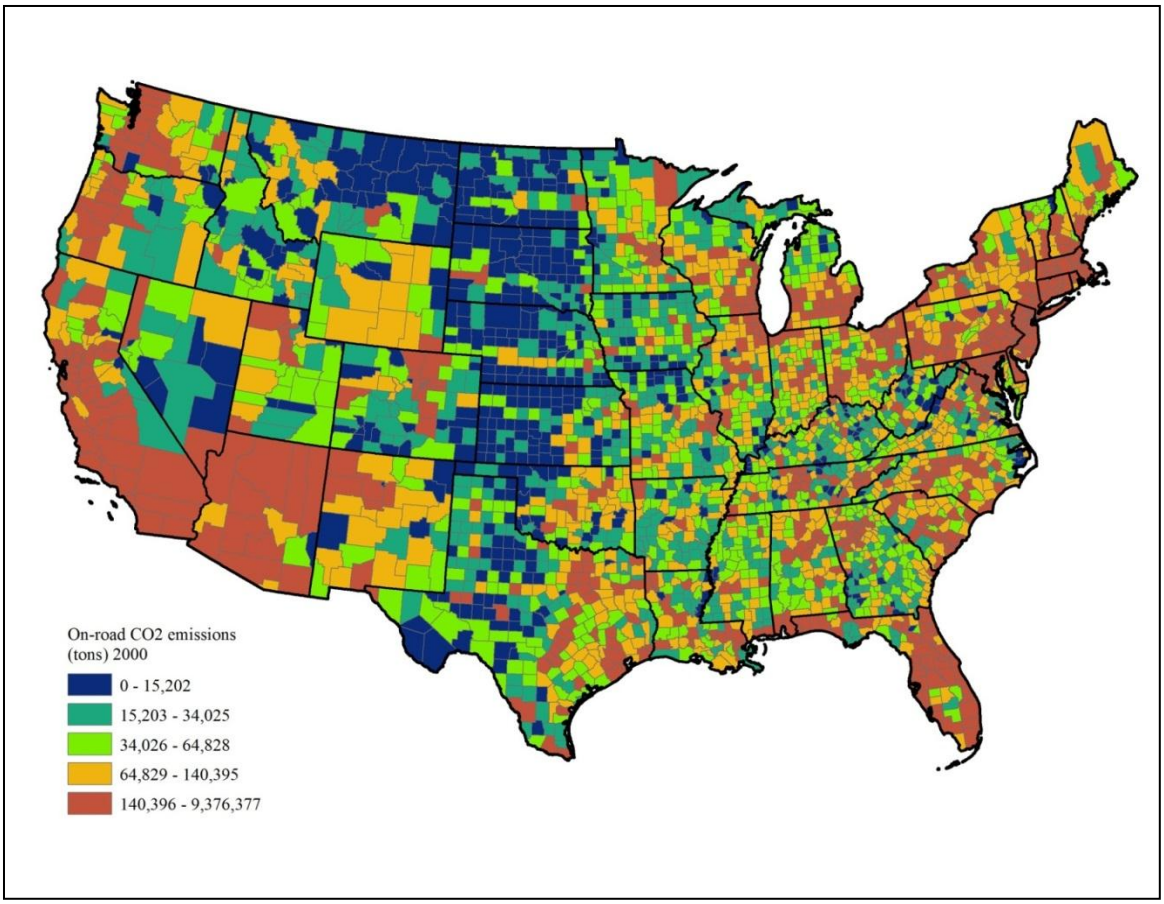

Figure 10. Non-point emission density of volatile organic compounds (VOCs) and nitrogen oxides (NOx) by county in 2000.

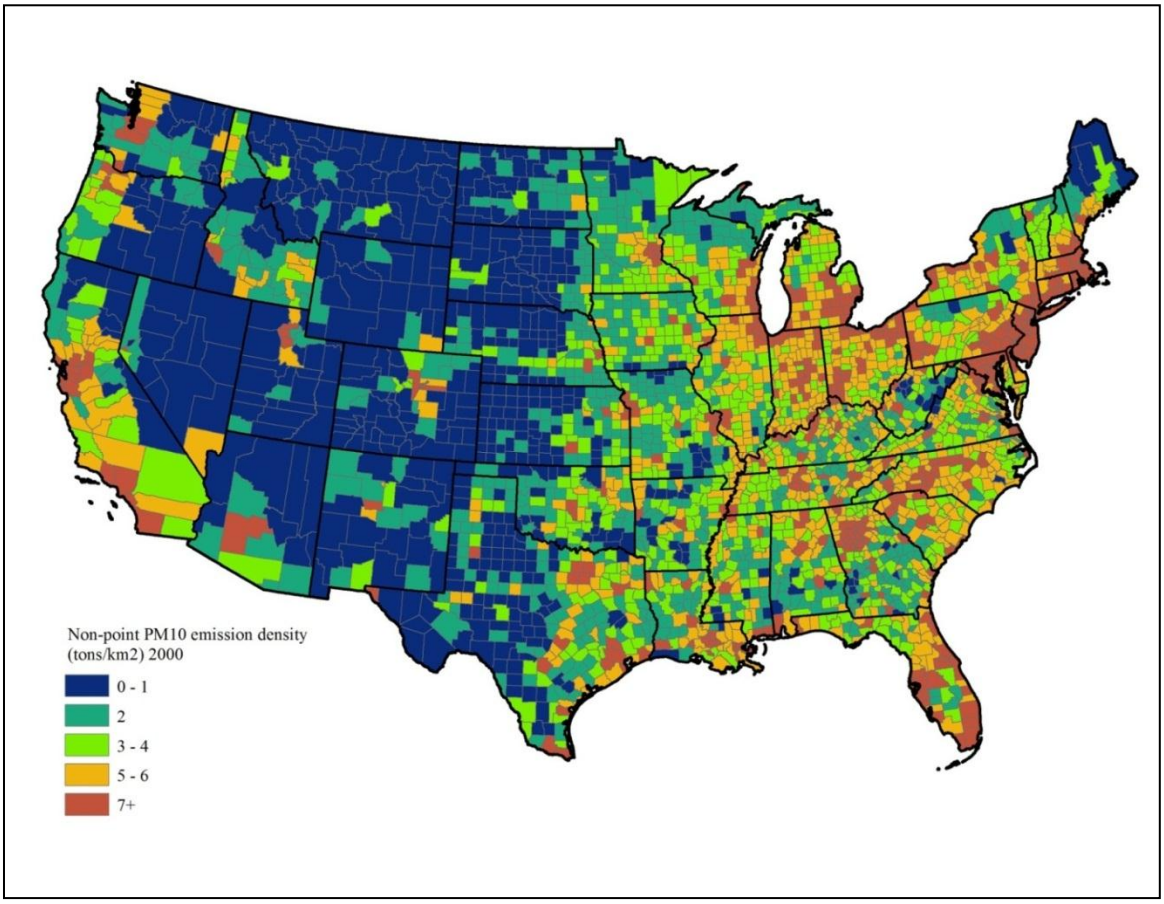

Figure 11. Non-point emission density of $PM_{2.5}$ by county in 2000.

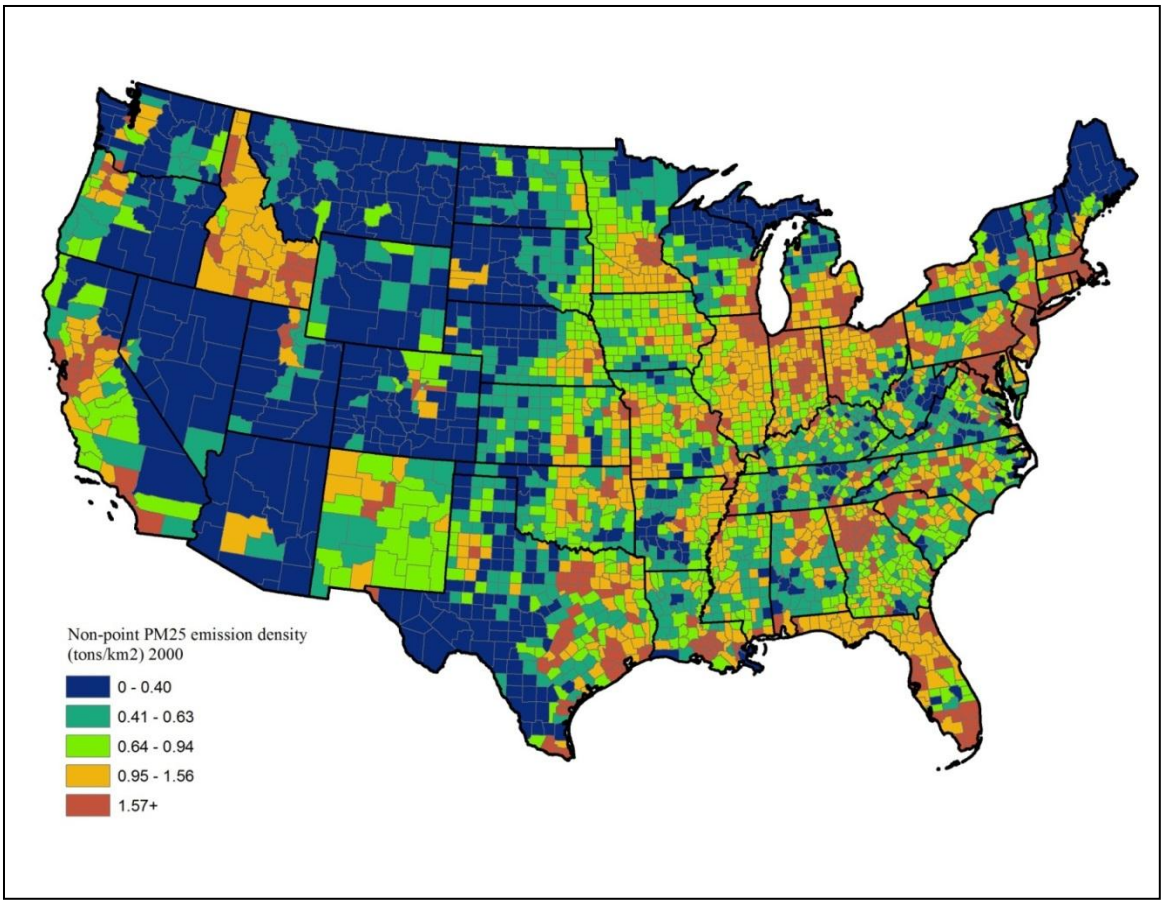

Figure 12. Non-point emission density of PM_{10} by county in 2000.

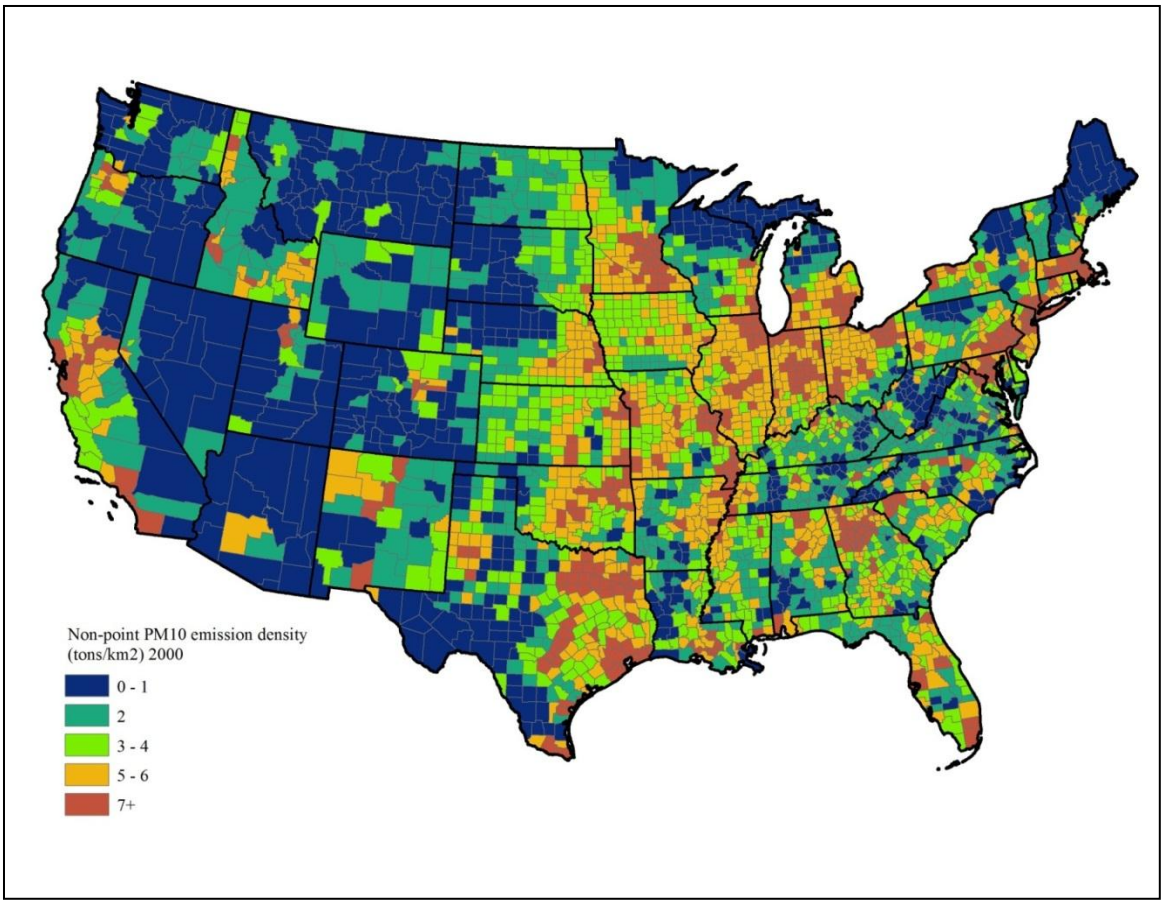

Figure 13. Non-point emission density of on-road CO_2 by county in 2000.

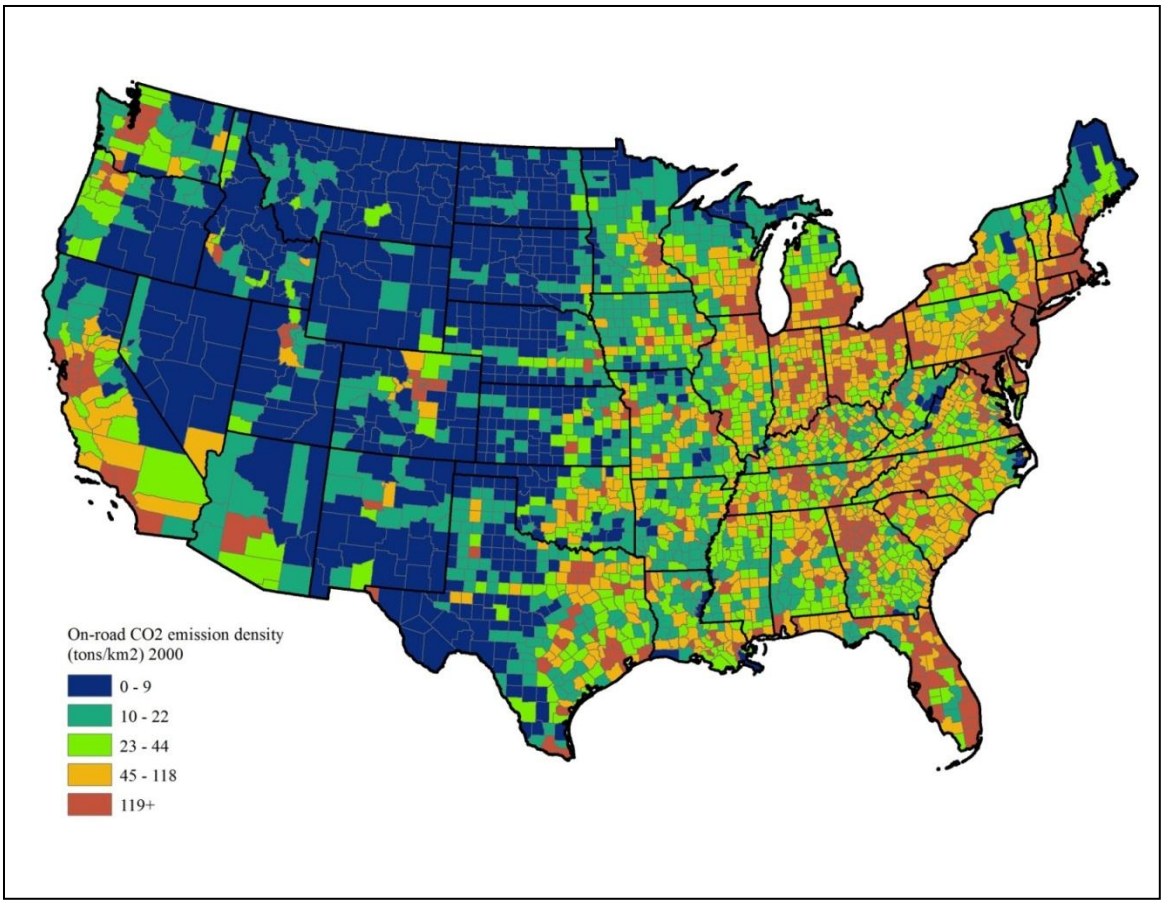

Figure 14. Per capita non-point emission of volatile organic compounds (VOCs) and nitrogen oxides (NOx) by county in 2000.

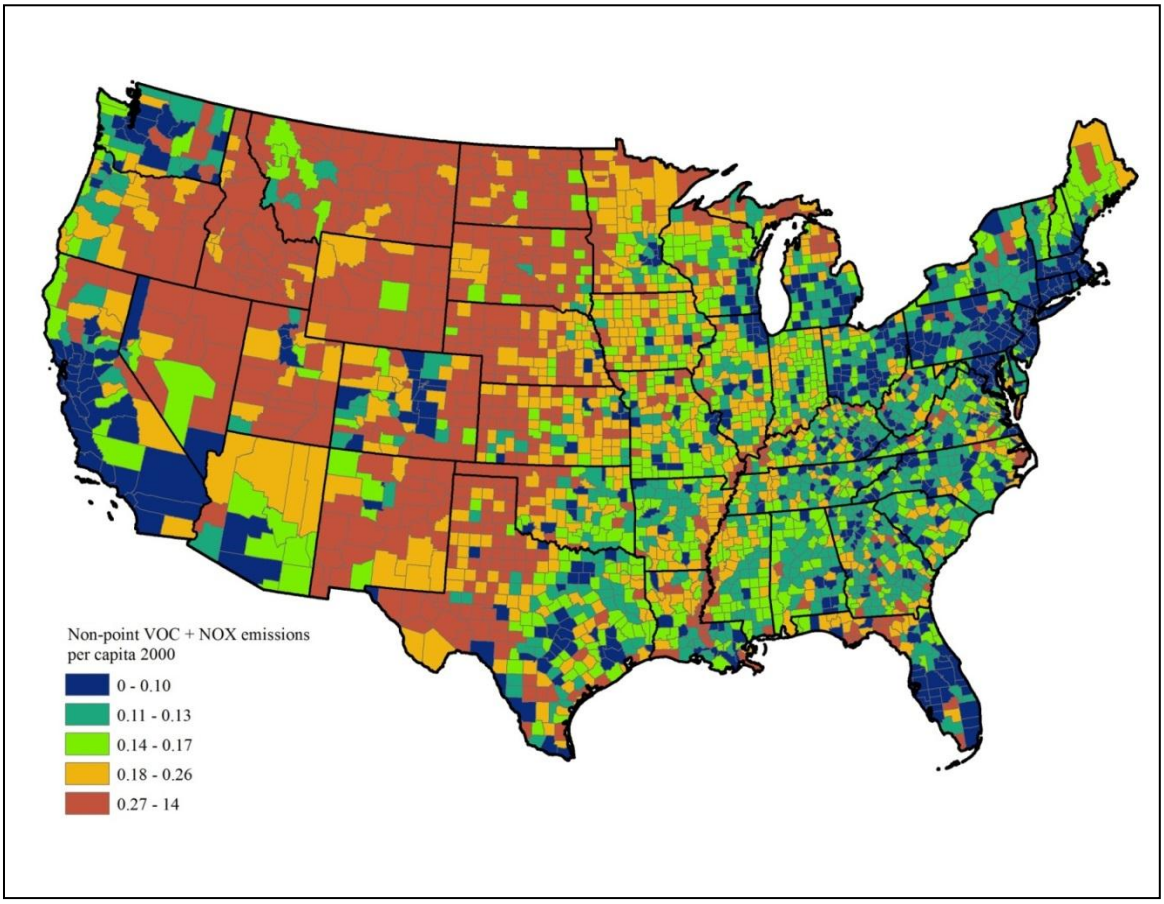

Figure 15. Per capita non-point emission of $PM_{2.5}$ by county in 2000.

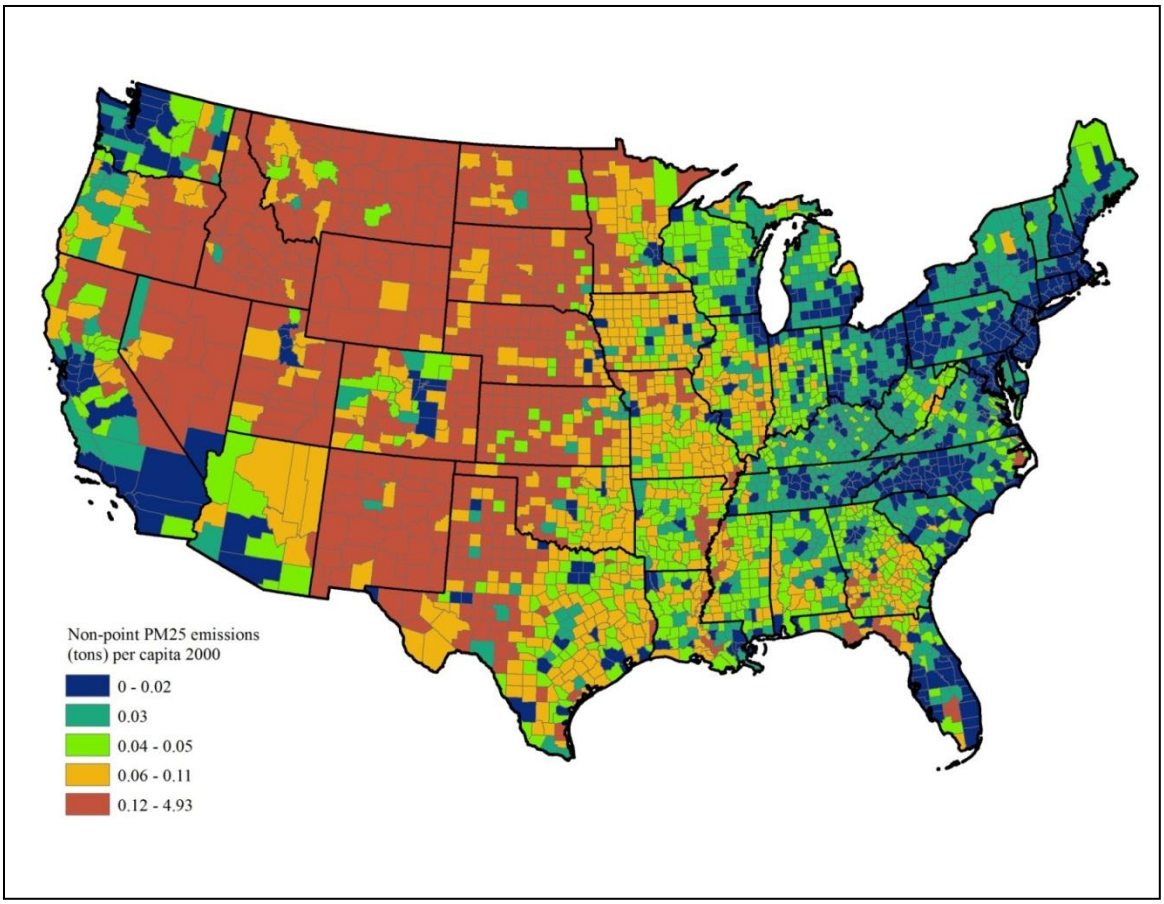

Figure 16. Per capita non-point emission of PM_{10} by county in 2000.

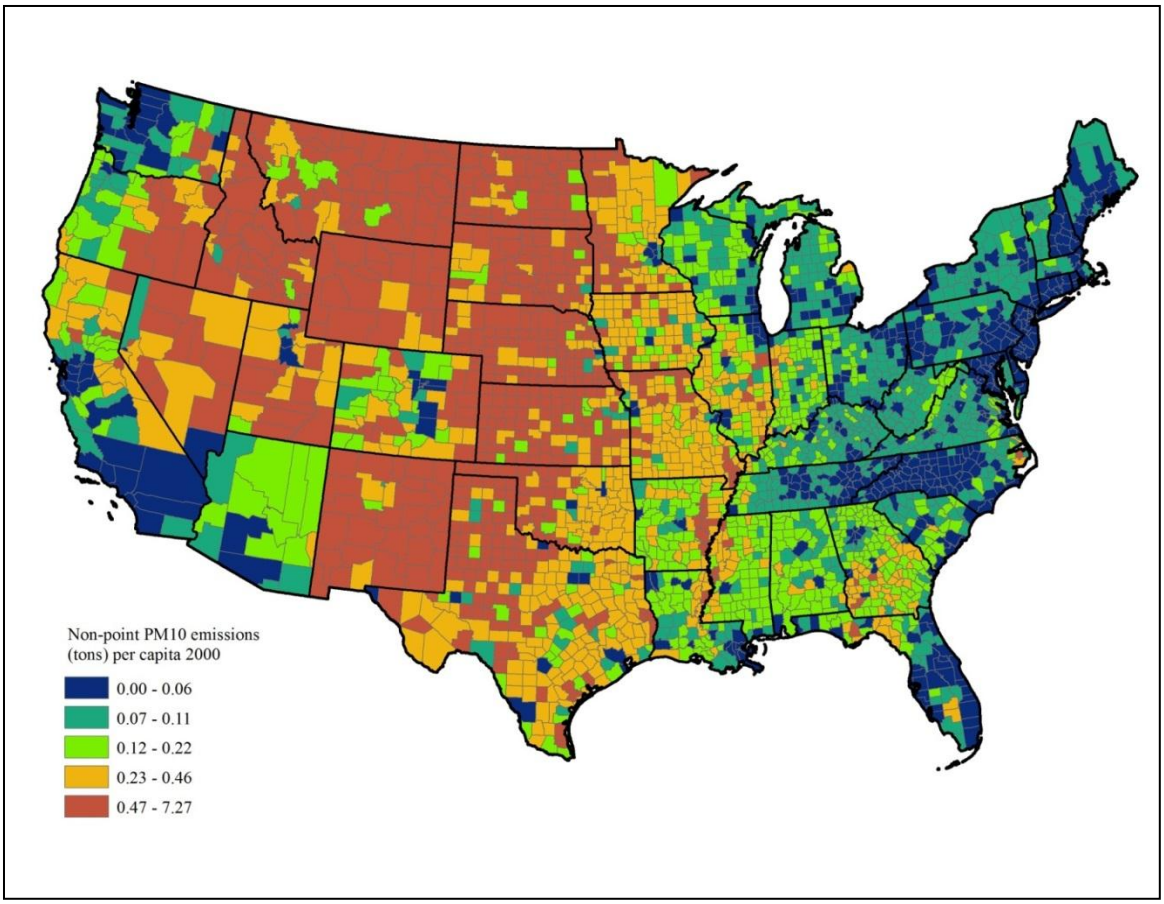

Figure 17. Per capita non-point emission of on-road CO_2 by county in 2000.

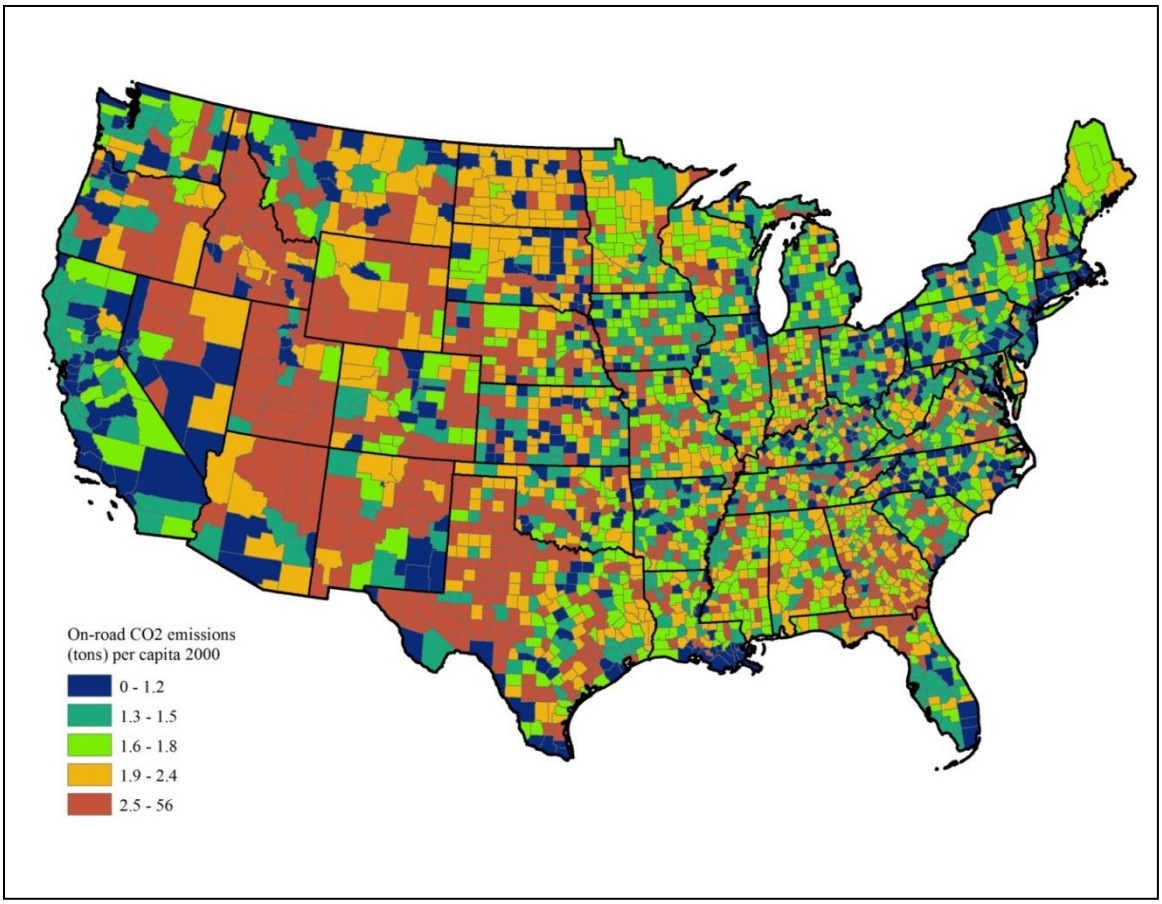

Figure 18. Major U.S. regions.

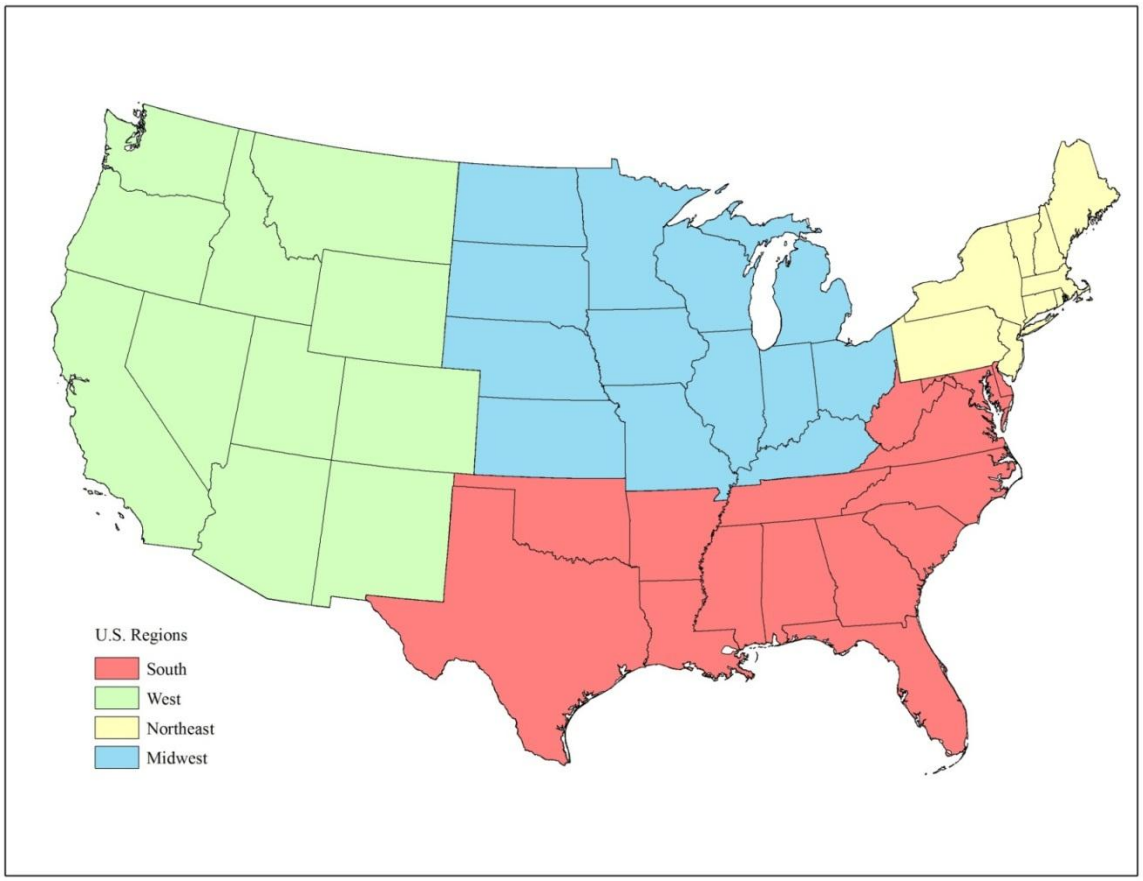

Figure 19. Annual average fourth maximum 8-hour ozone concentration (ppm) 1998 to 2002.

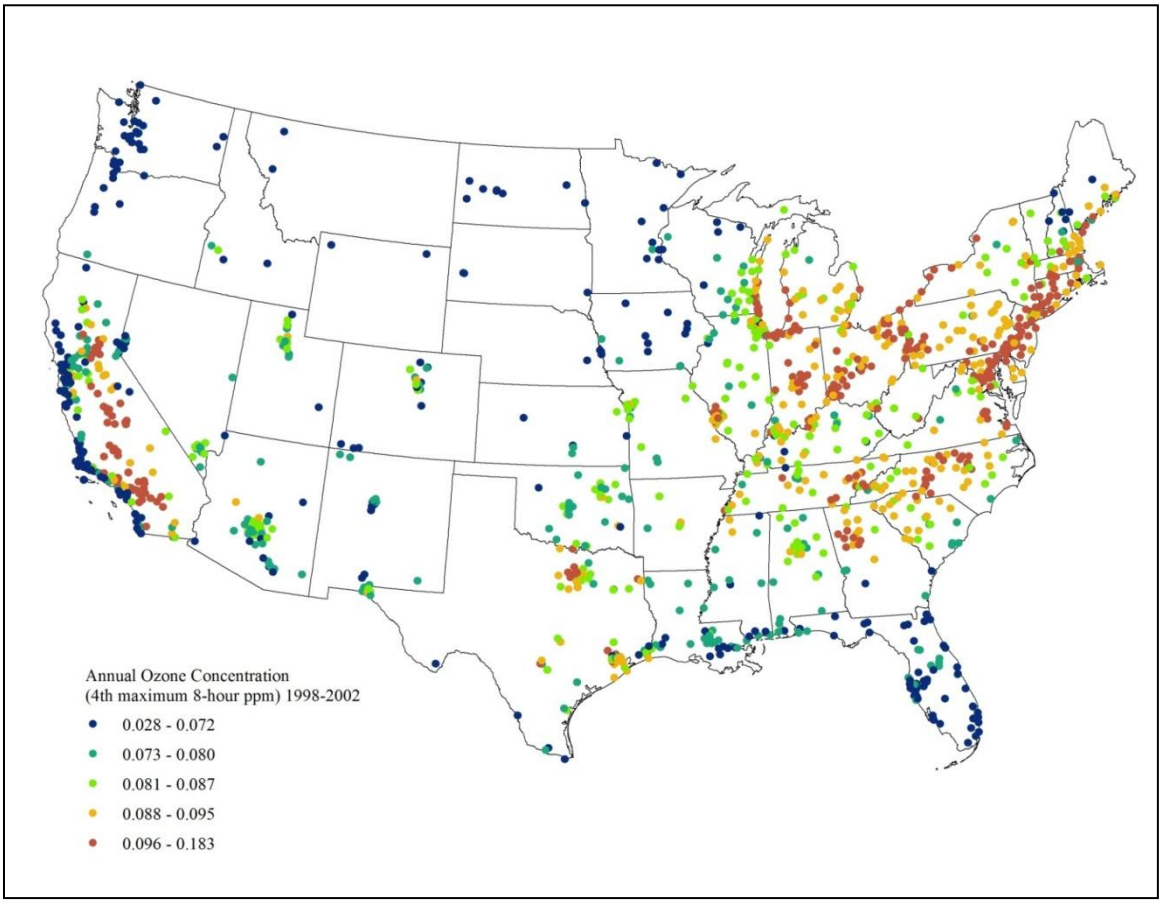

Figure 20. Kriging-based model of annual average fourth maximum 8-hour ozone concentration (ppm) between 1998 and 2002.

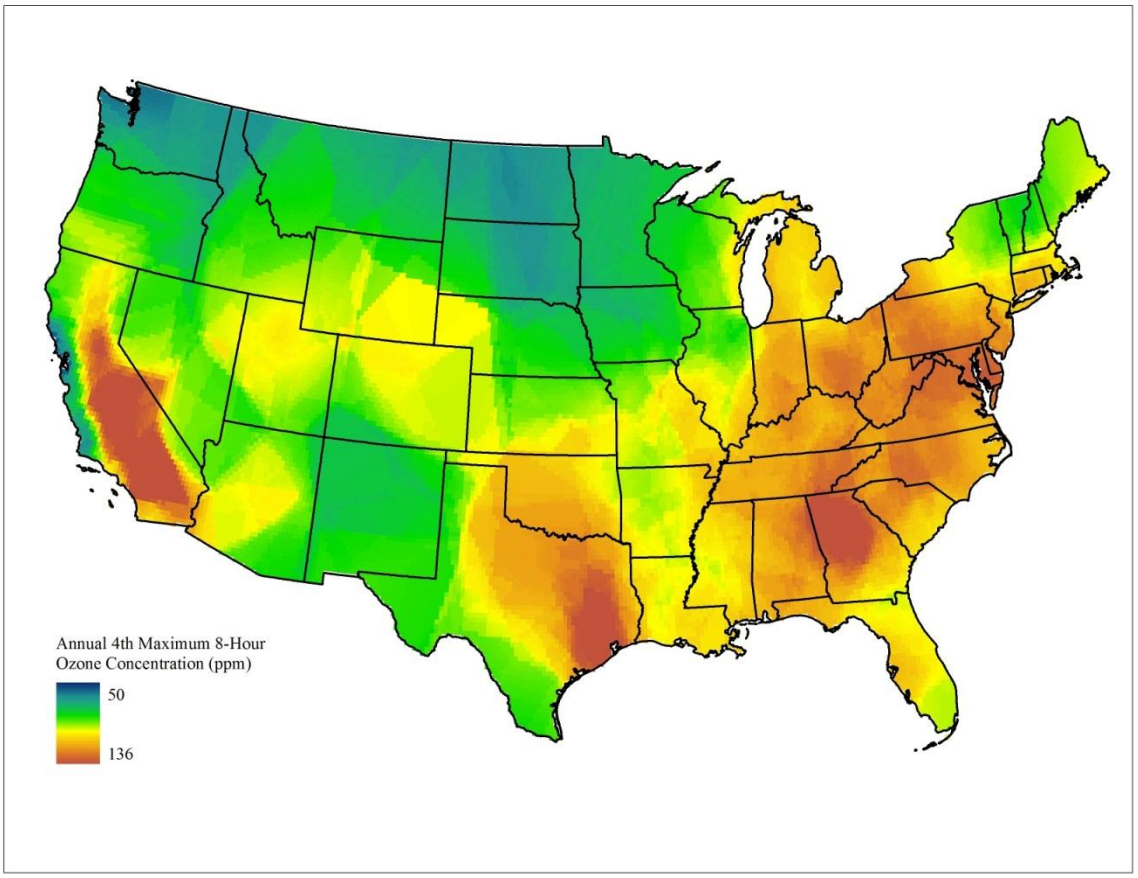

Figure 21. Annual average PM_{25} concentration ($\mu g/m^3$) 1998 to 2002.

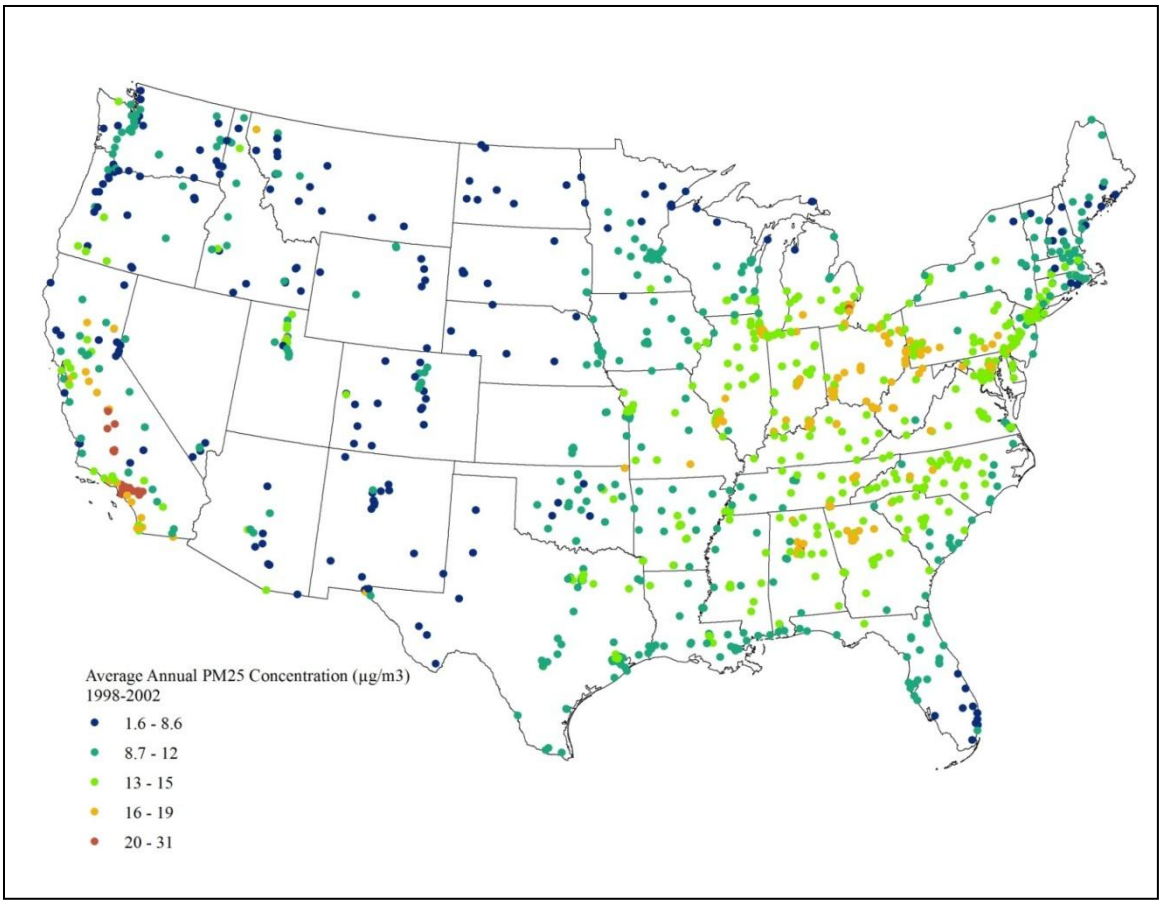

Figure 22. Kriging-based model of annual average PM_{25} concentration ($\mu g/m^3$) between 1998 and 2002.

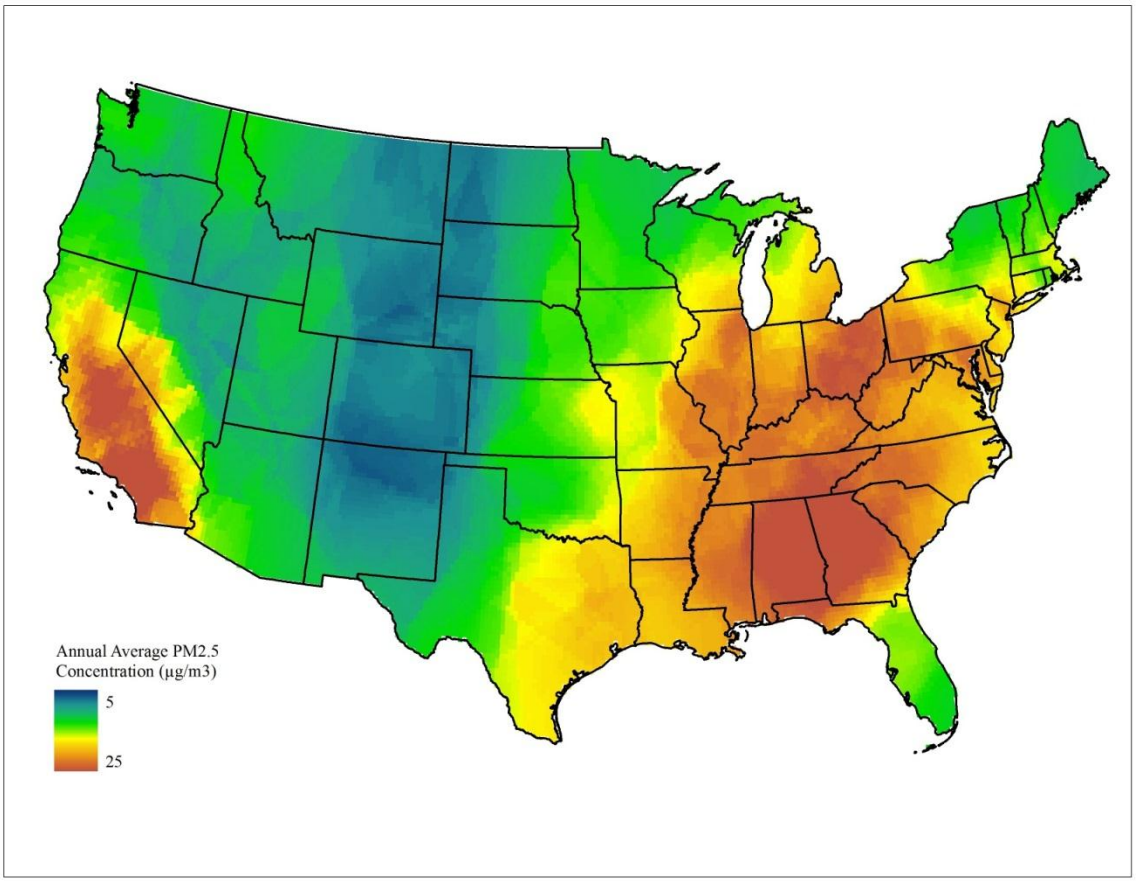

Figure 23. Annual average PM_{10} concentration ($\mu g/m^3$) 1998 to 2002.

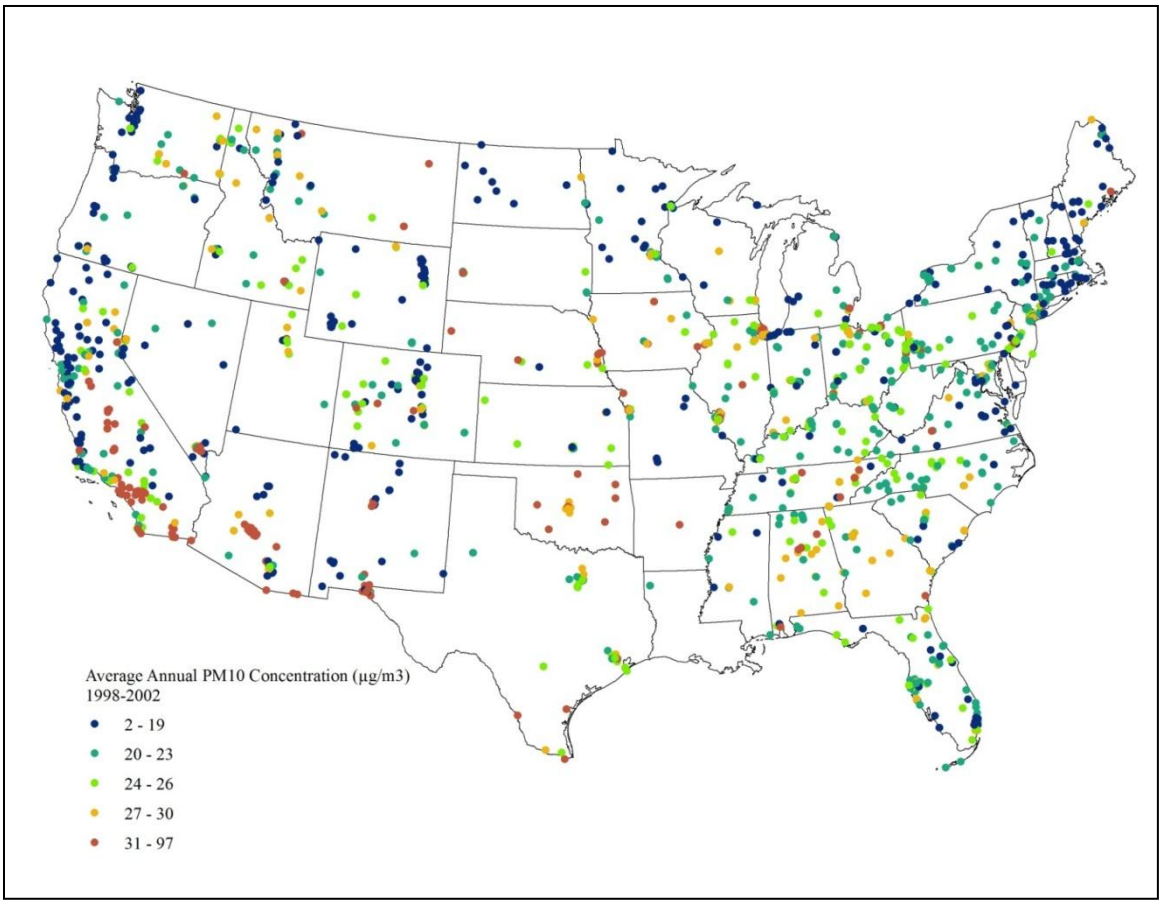

Figure 24. Kriging-based model of annual average PM_{10} concentration ($\mu g/m^3$) between 1998 and 2002.

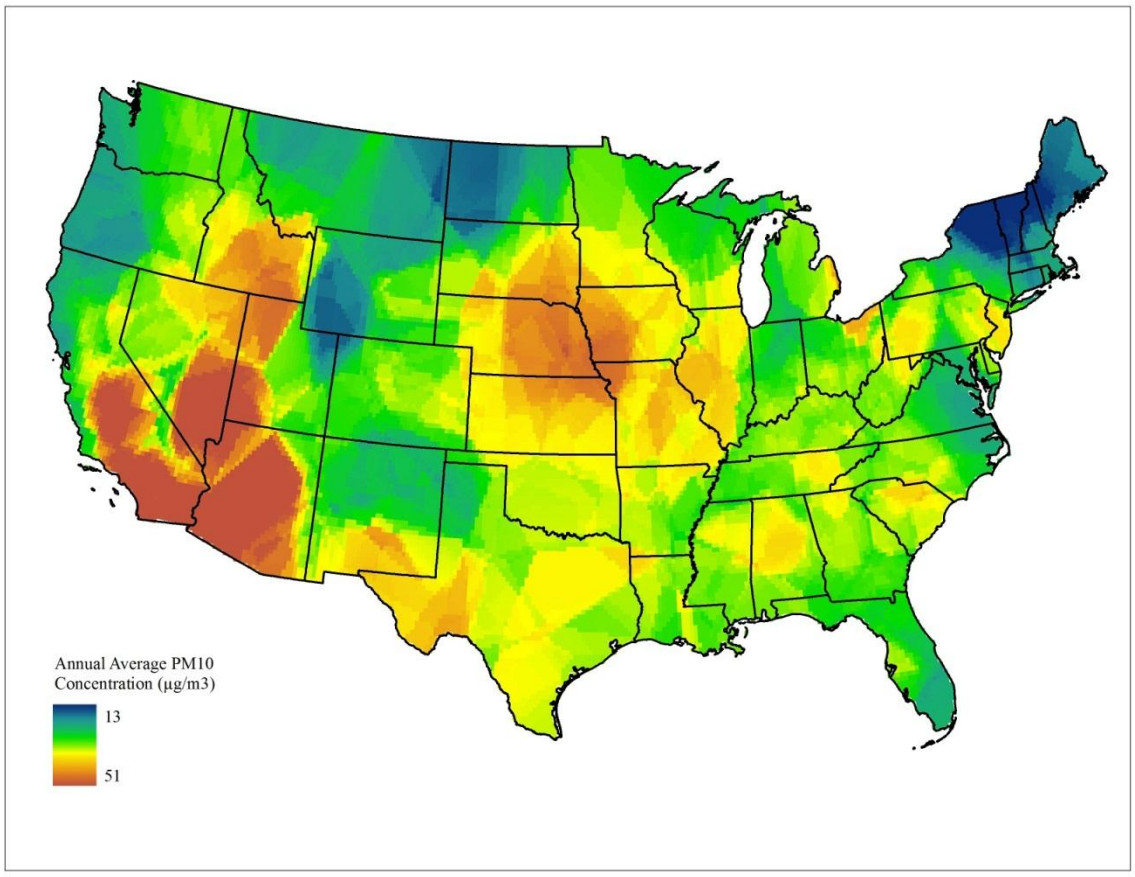

Figure 25. The number of sprawl indices (max: 6) that rank each MSA/CSA within the top 10 most sprawling in the United States.

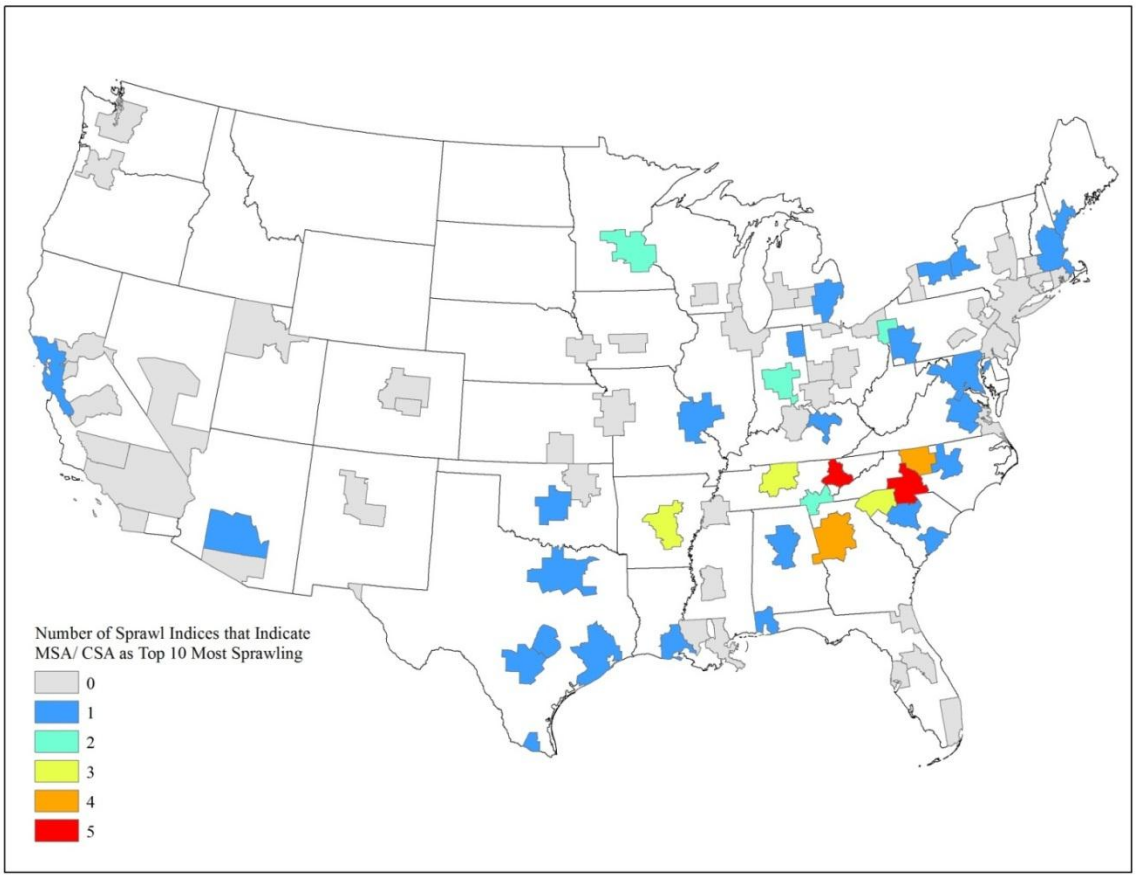

Figure 26. The number of sprawl indices (max: 6) that rank each MSA/CSA within the top 10 least sprawling in the United States.

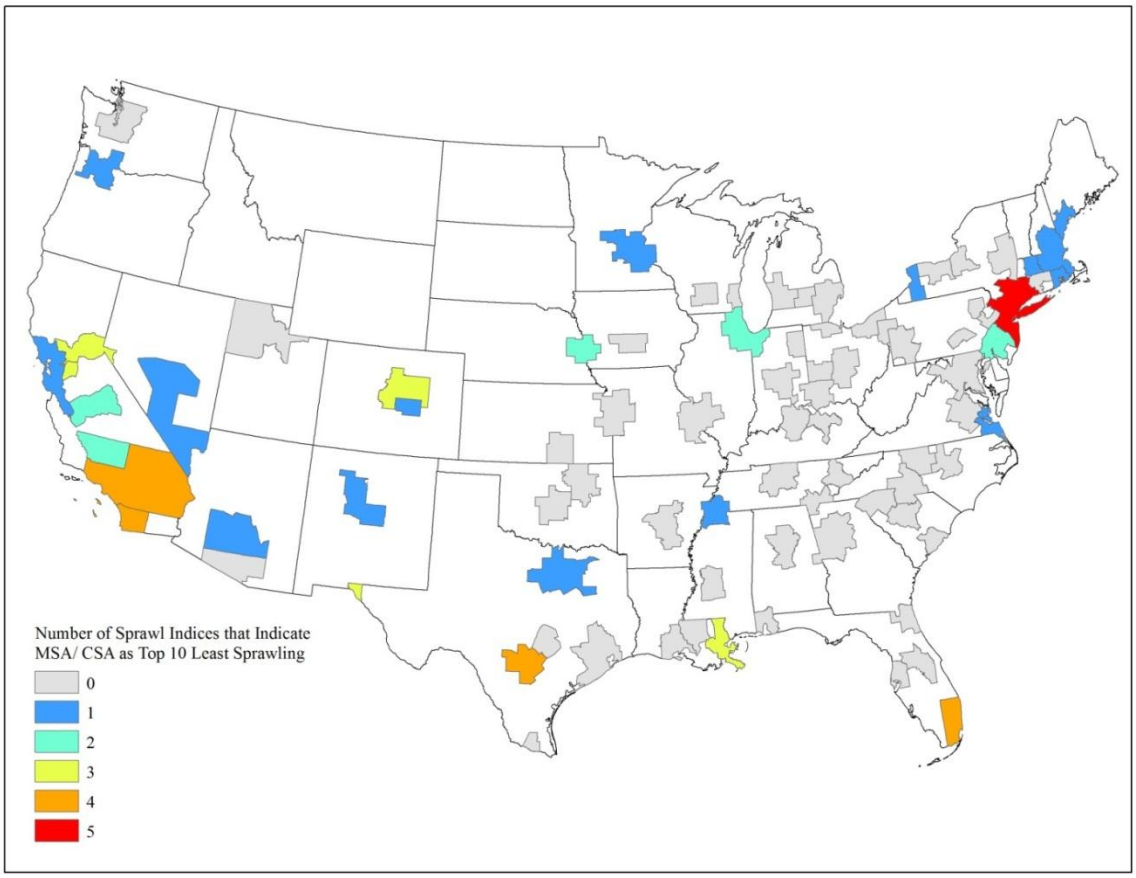

Figure 27. Urban landcover, Carolina Piedmont megapolitan area. Megapolitan areas often form complex shapes and exhibit both inter-urban and intra-urban polycentrism. At this scale, the Carolina Piedmont mega forms a linear corridor along I-85.

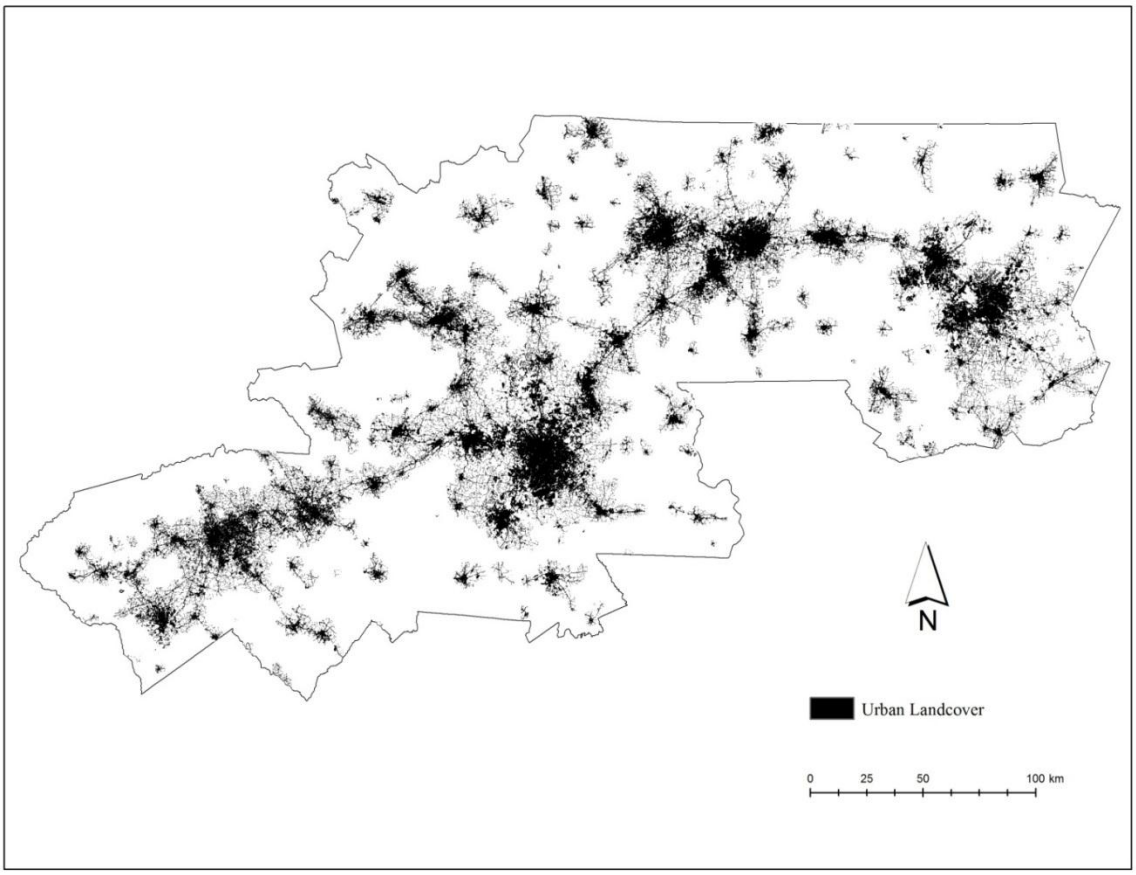

Figure 28. Urban landcover, Georgia Piedmont megapolitan area. Megapolitan areas often form complex shapes and exhibit both inter-urban and intra-urban polycentrism. At this scale, the Carolina Piedmont mega forms a “galactic” pattern with several major and minor urban centers arranged in a cluster.

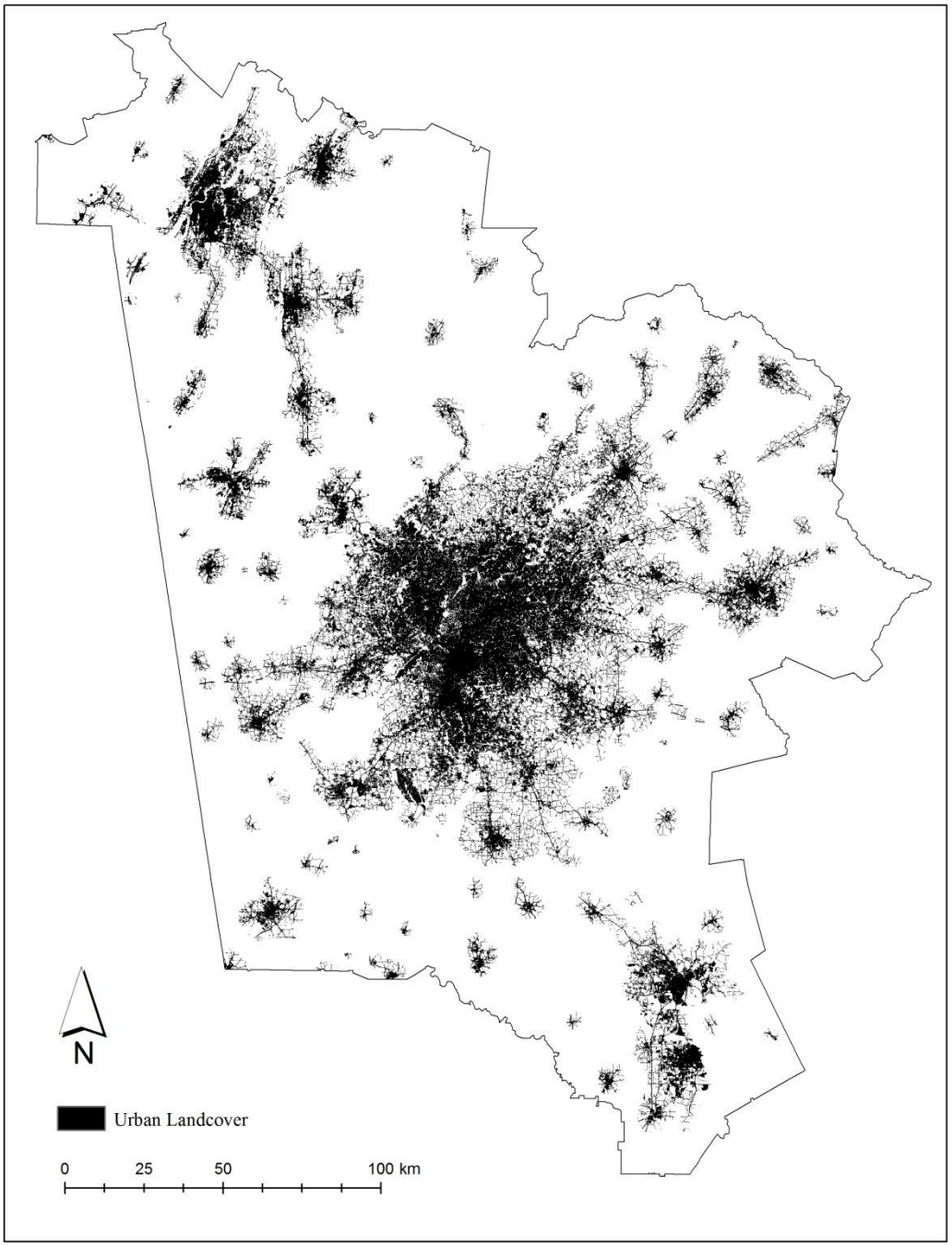

Figure 29. Two common urban spatial patterns at the megapolitan scale include the linear corridor and the galactic cluster. Black dots indicate urban cores, circles demarcate the boundary of contiguous suburban area surrounding urban cores, and lines indicate major highways.

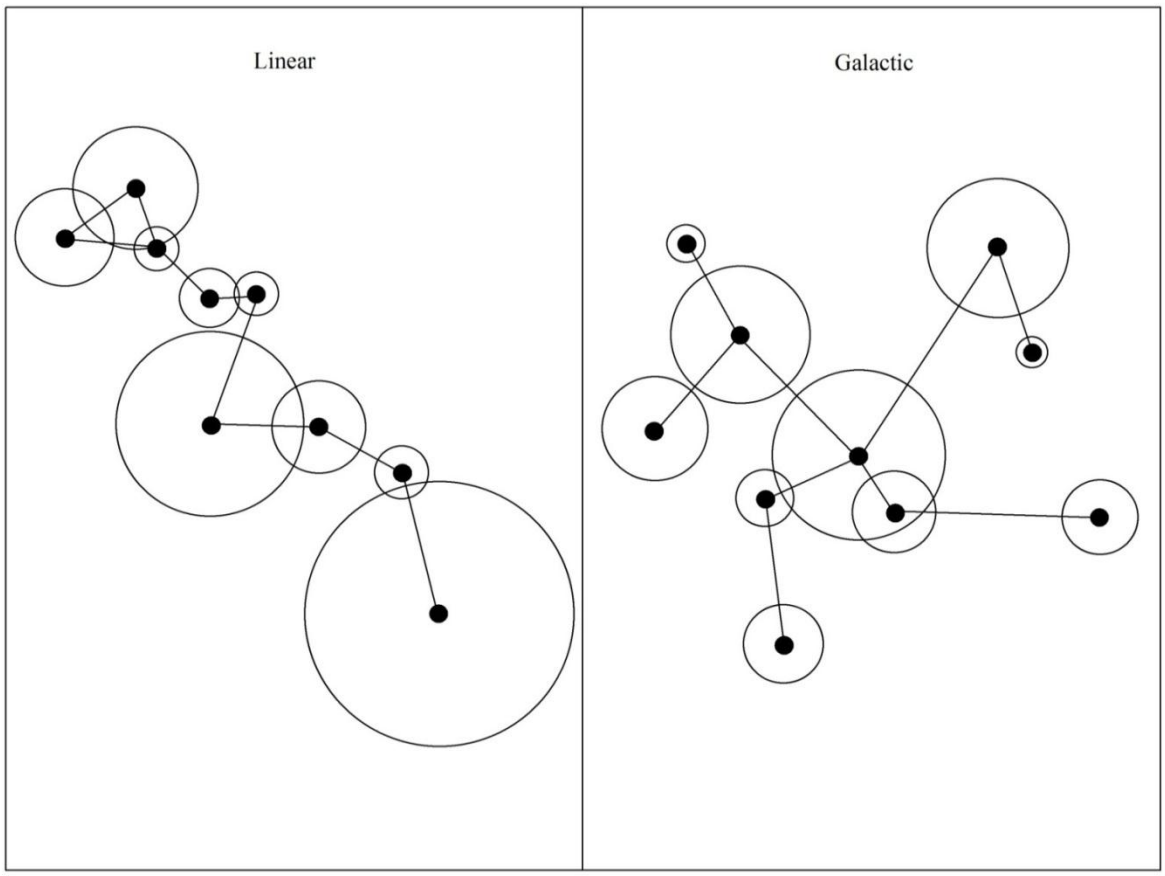

Figure 30. Edge density (ED) of urban landcover by MSA/CSA. Values calculated at the high and low urban threshold have been averaged. Higher values of ED may indicate more “sprawl-like” conditions.

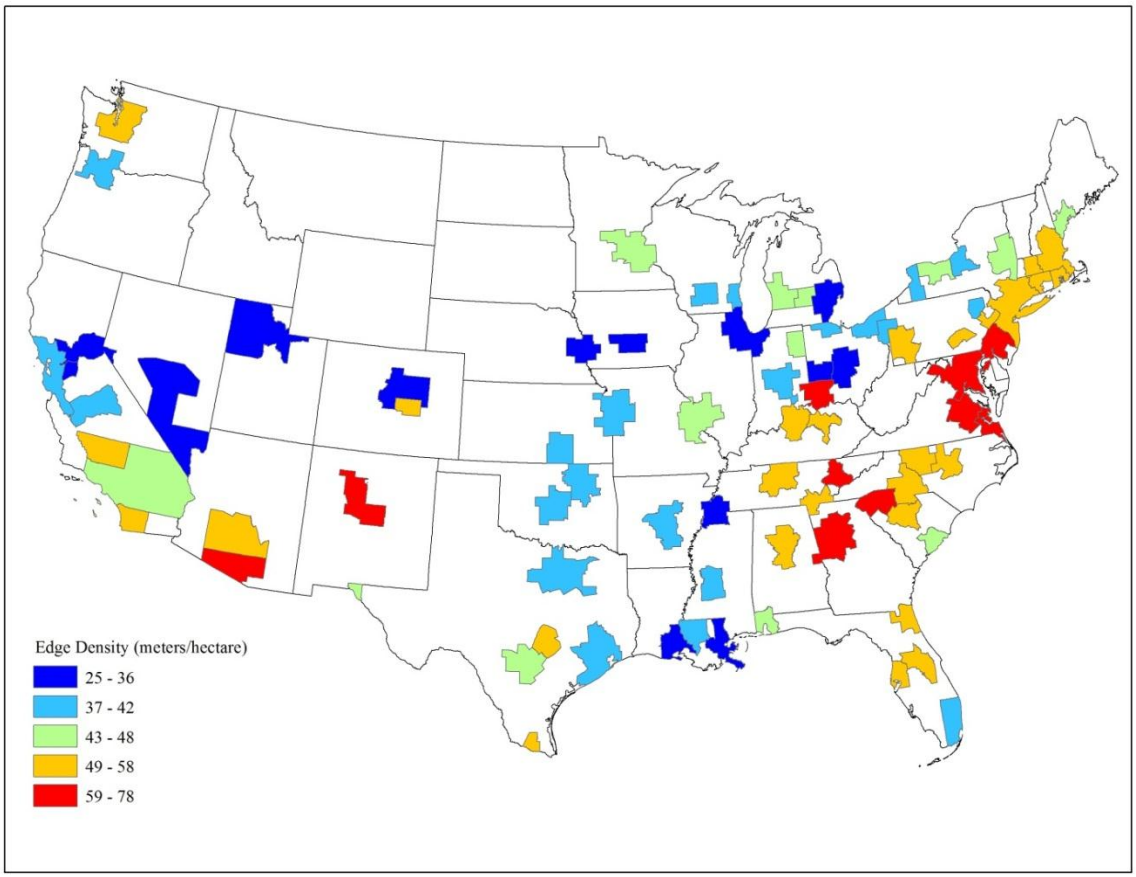

Figure 31. Landscape shape index (LSI) of urban landcover by MSA/CSA. Values calculated at the high and low urban threshold have been averaged. Higher values of LSI may indicate more “sprawl-like” conditions.

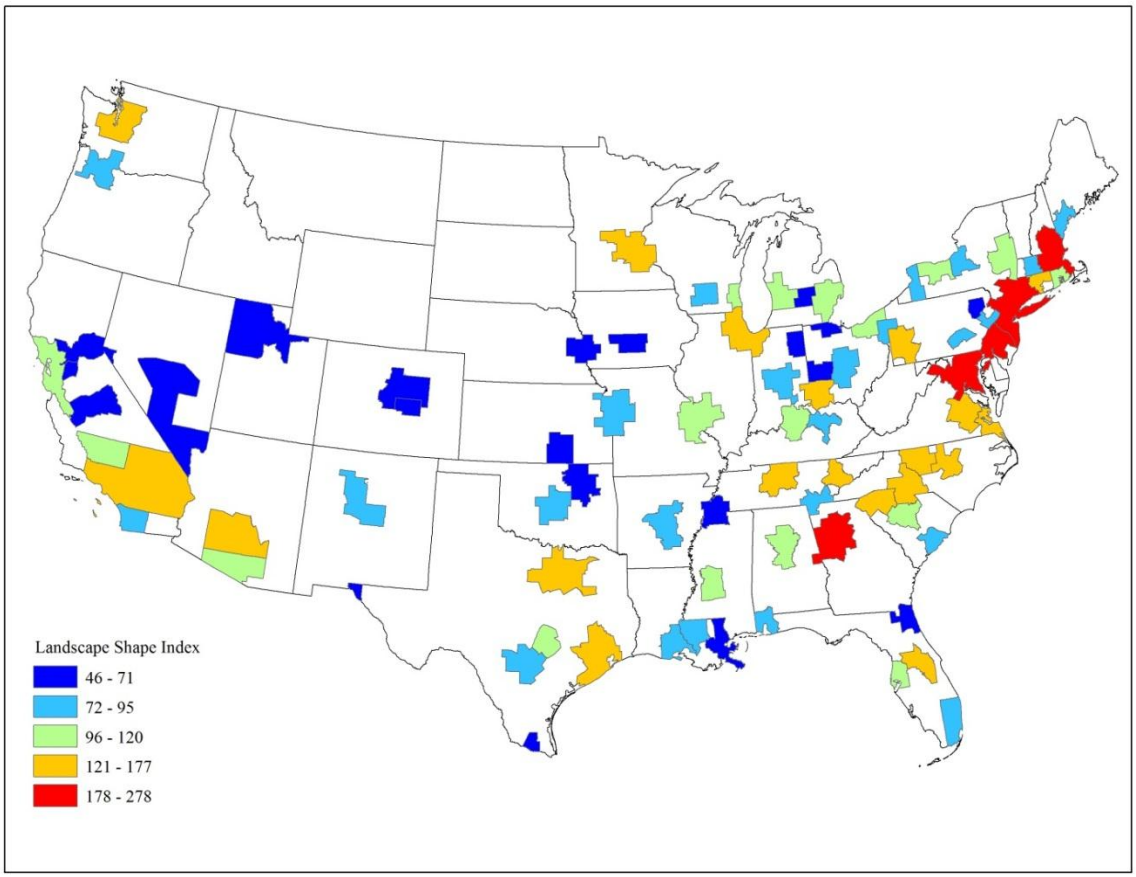

Figure 32. Largest patch index (LPI) of urban landcover by MSA/CSA. Values calculated at the high and low urban threshold have been averaged. Lower values of LPI may indicate more “sprawl-like” conditions.

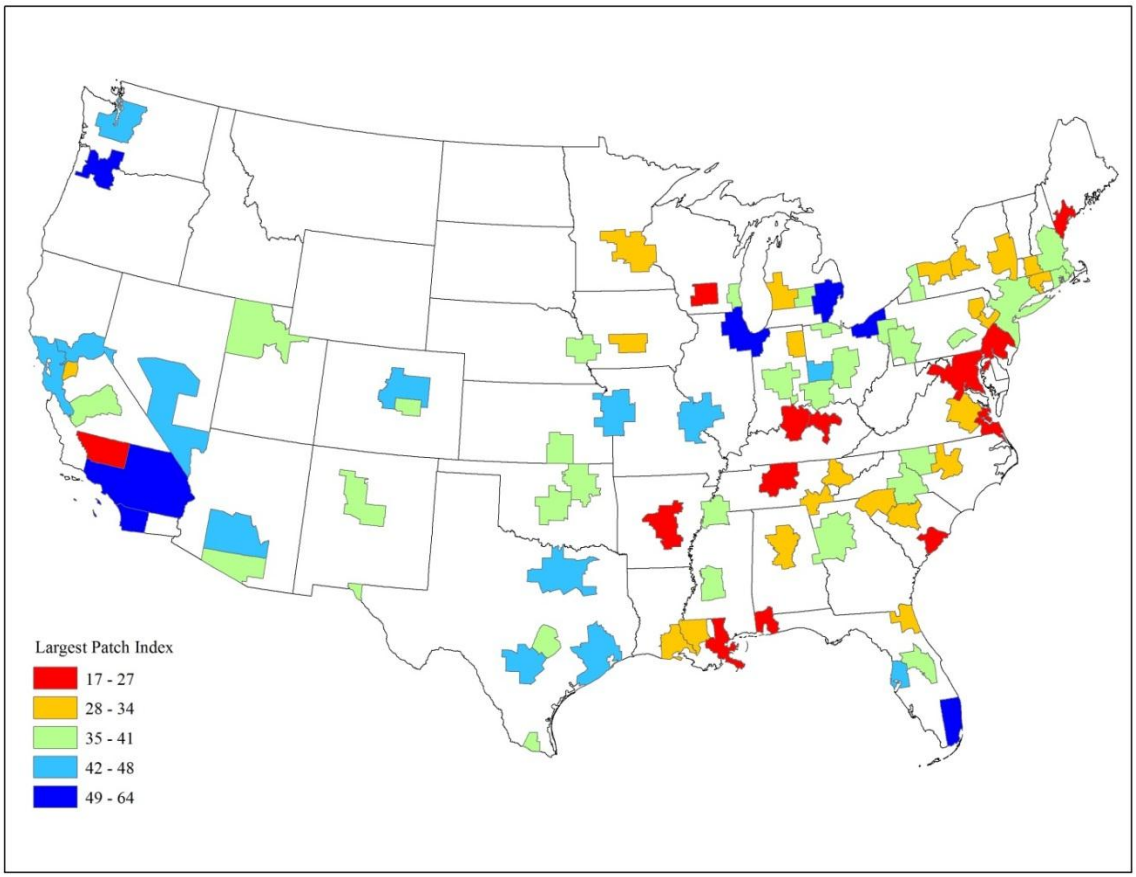

Figure 33. Area-weighted mean shape index (AWMSI) of urban landcover by MSA/CSA. Values calculated at the high and low urban threshold have been averaged. Higher values of AWMSI may indicate more “sprawl-like” conditions.

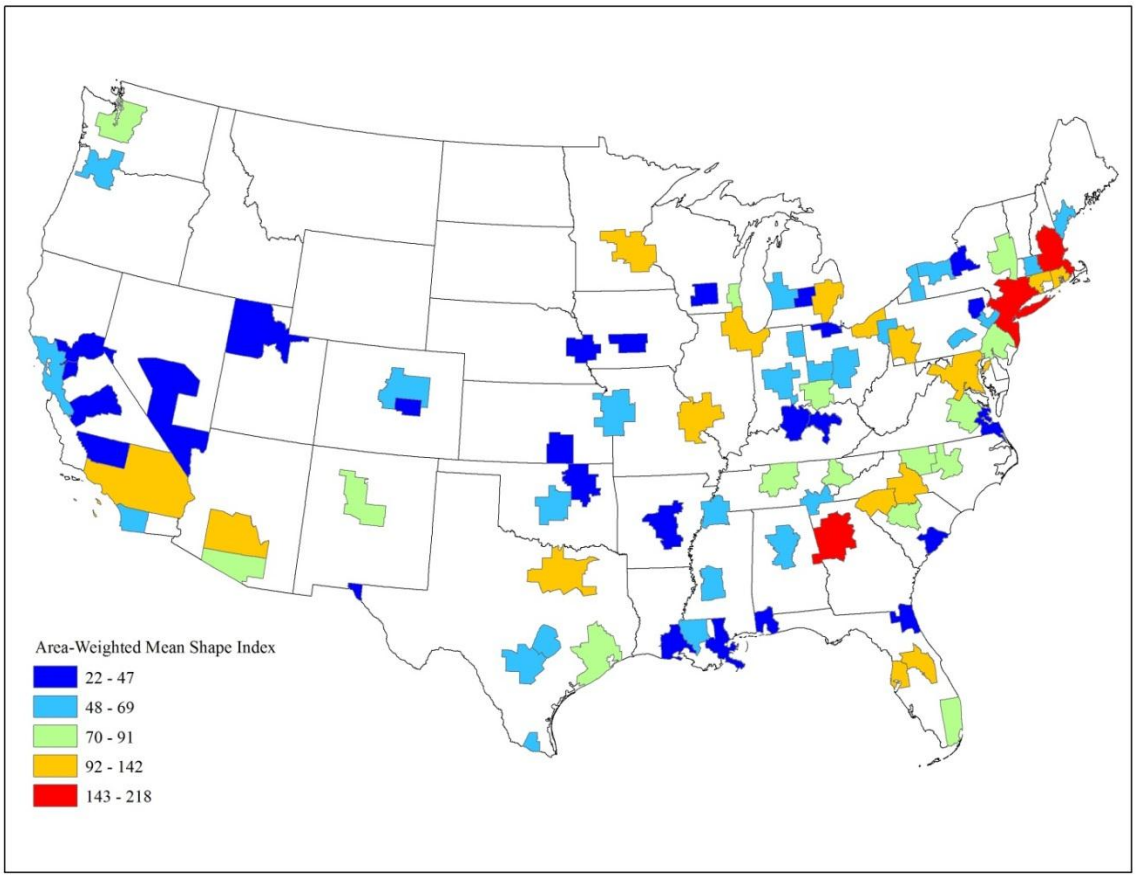

Figure 34. Area-weighted mean patch fractal dimension (AWMPFD) of urban landcover by MSA/CSA. Values calculated at the high and low urban threshold have been averaged. Higher values of AWMPFD may indicate more “sprawl-like” conditions.

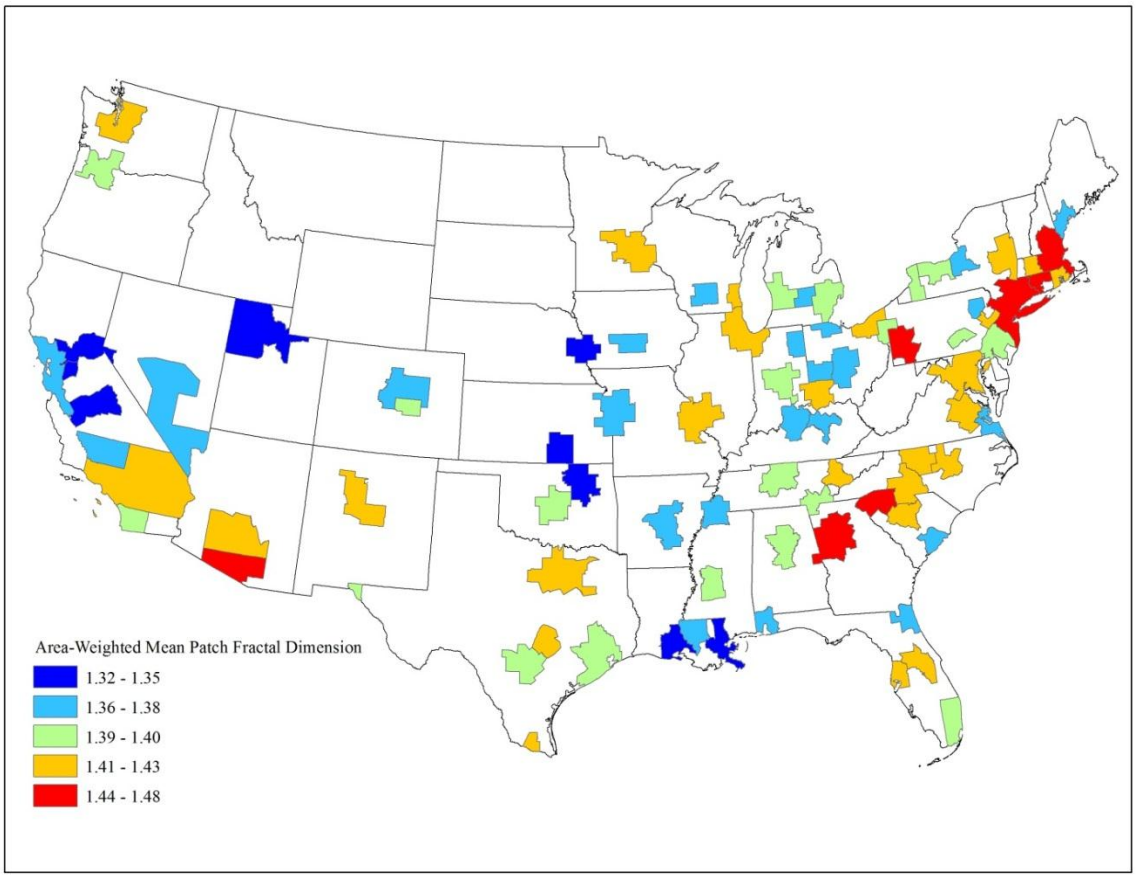

Figure 35. Contiguity (CONTIG) of urban landcover by MSA/CSA. Values calculated at the high and low urban threshold have been averaged. Lower values of CONTIG may indicate more “sprawl-like” conditions.

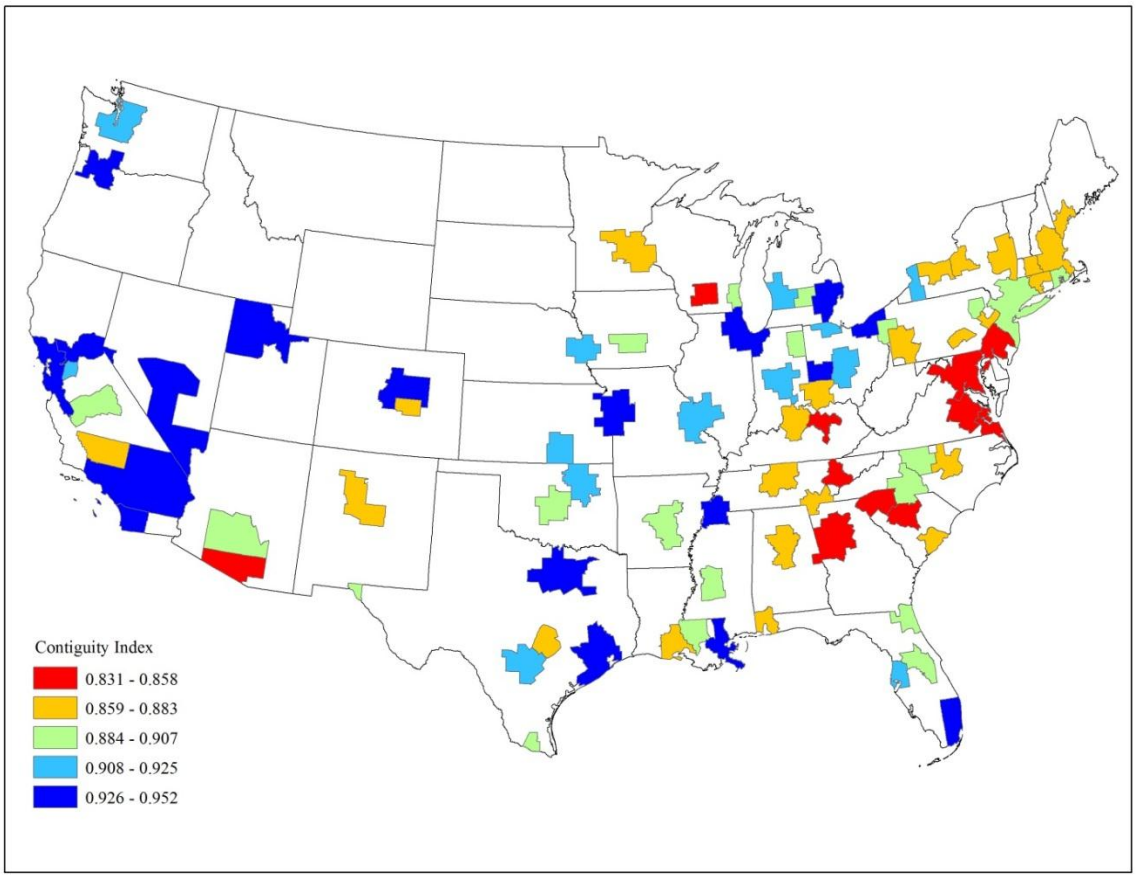

Figure 36. Contagion (CONTAG) of urban landcover by MSA/CSA. Values calculated at the high and low urban threshold have been averaged. Lower values of CONTAG may indicate more “sprawl-like” conditions.

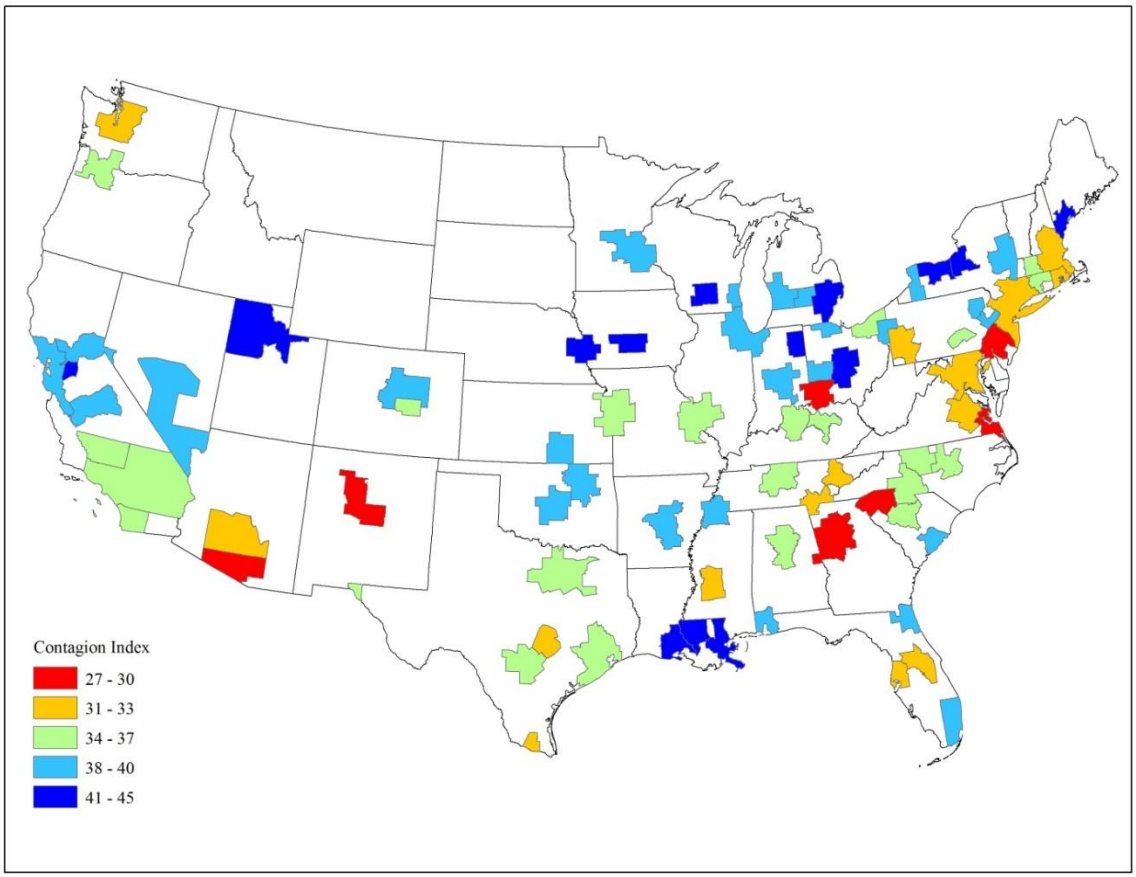

Figure 37. Percentage of like adjacencies (PLADJ) index of urban landcover by MSA/ CSA. Values calculated at the high and low urban threshold have been averaged. Lower values of PLADJ may indicate more “sprawl-like” conditions.

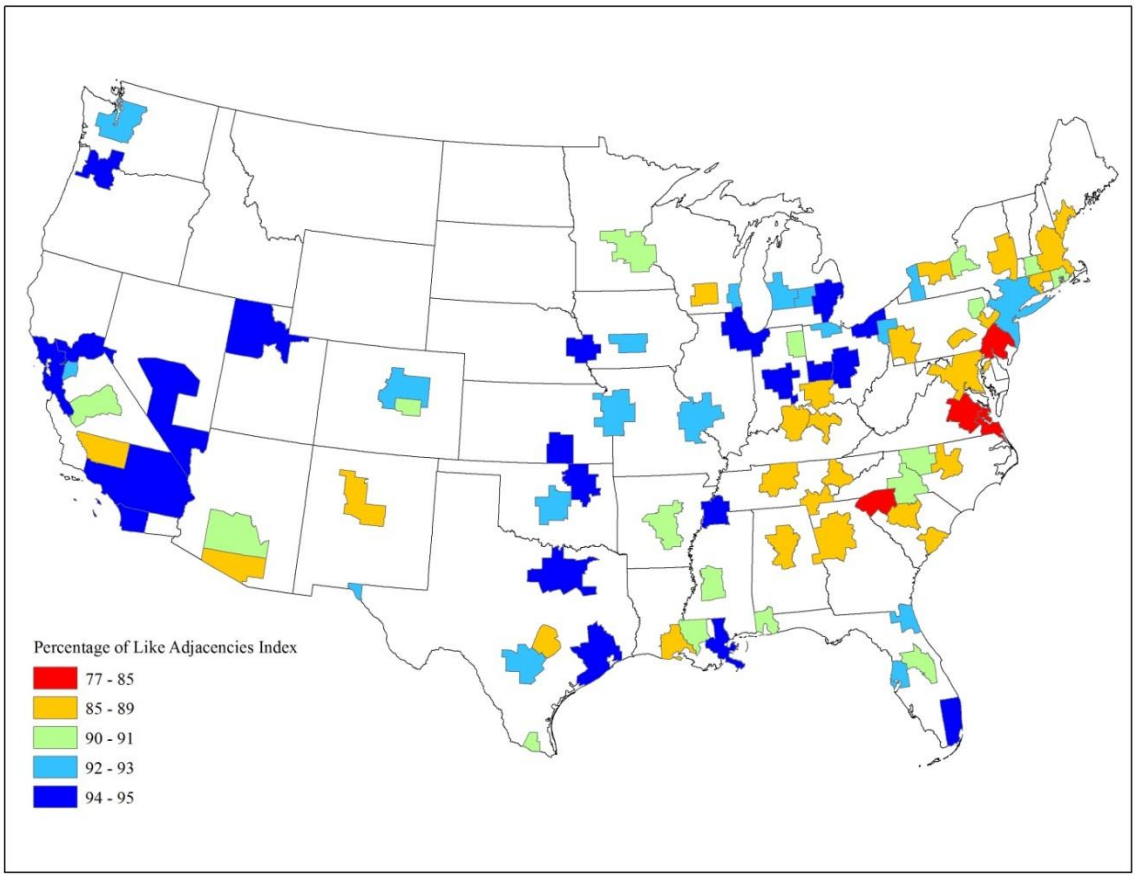

Figure 38. Clumpiness (CLUMPY) of urban landcover by MSA/CSA. Values calculated at the high and low urban threshold have been averaged. Lower values of CLUMPY may indicate more “sprawl-like” conditions.

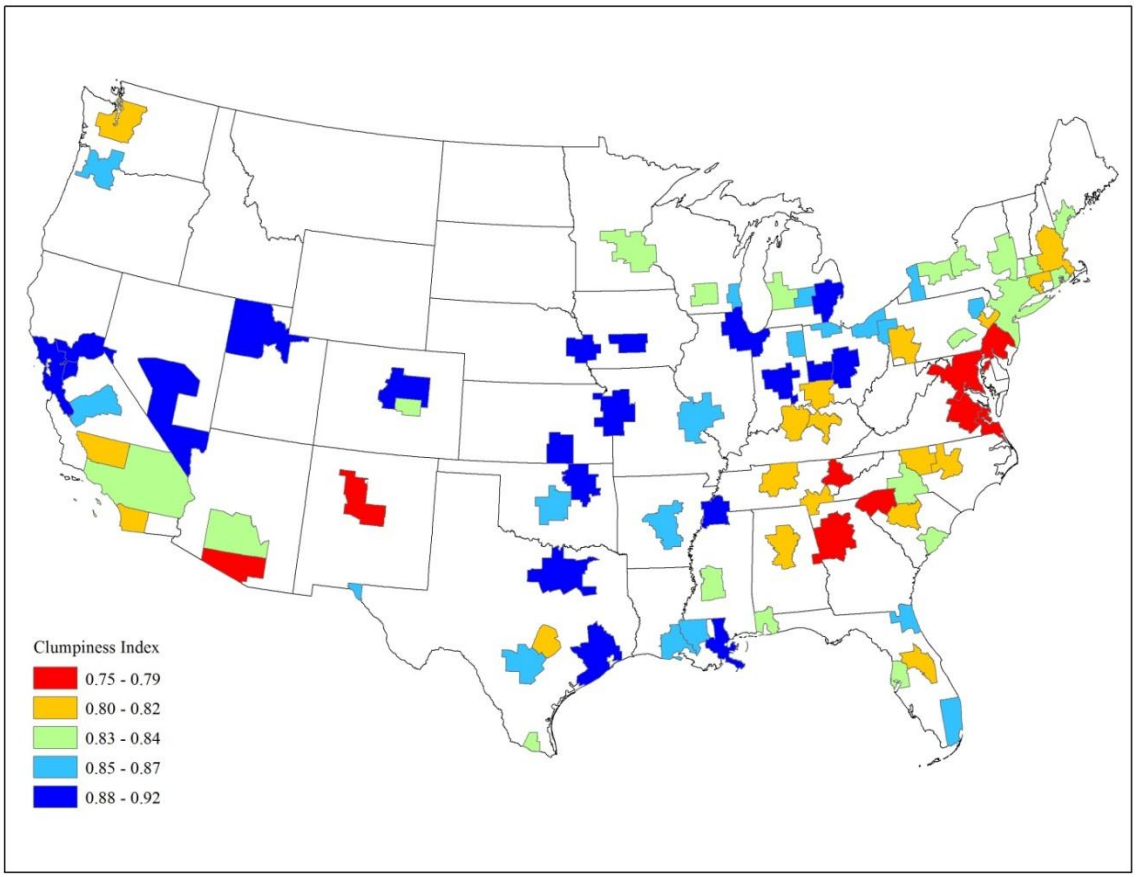

Figure 39. Getis-Ord Gi* hot-spot analysis for edge density (ED). Higher Z scores (red) indicate more intense clustering of high values; lower negative Z scores (blue) indicate more intense clustering of low values.

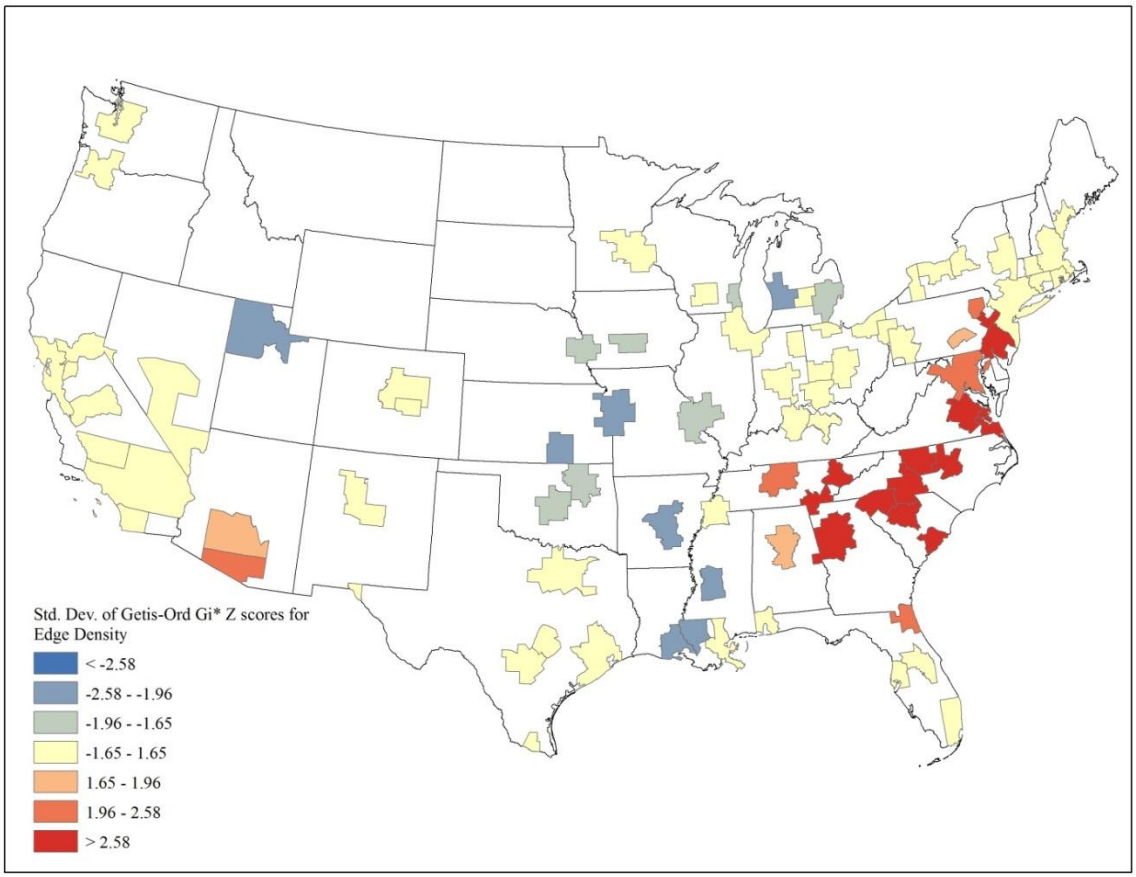

Figure 40. Getis-Ord Gi* hot-spot analysis for landscape shape index (LSI). Higher Z scores (red) indicate more intense clustering of high values; lower negative Z scores (blue) indicate more intense clustering of low values.

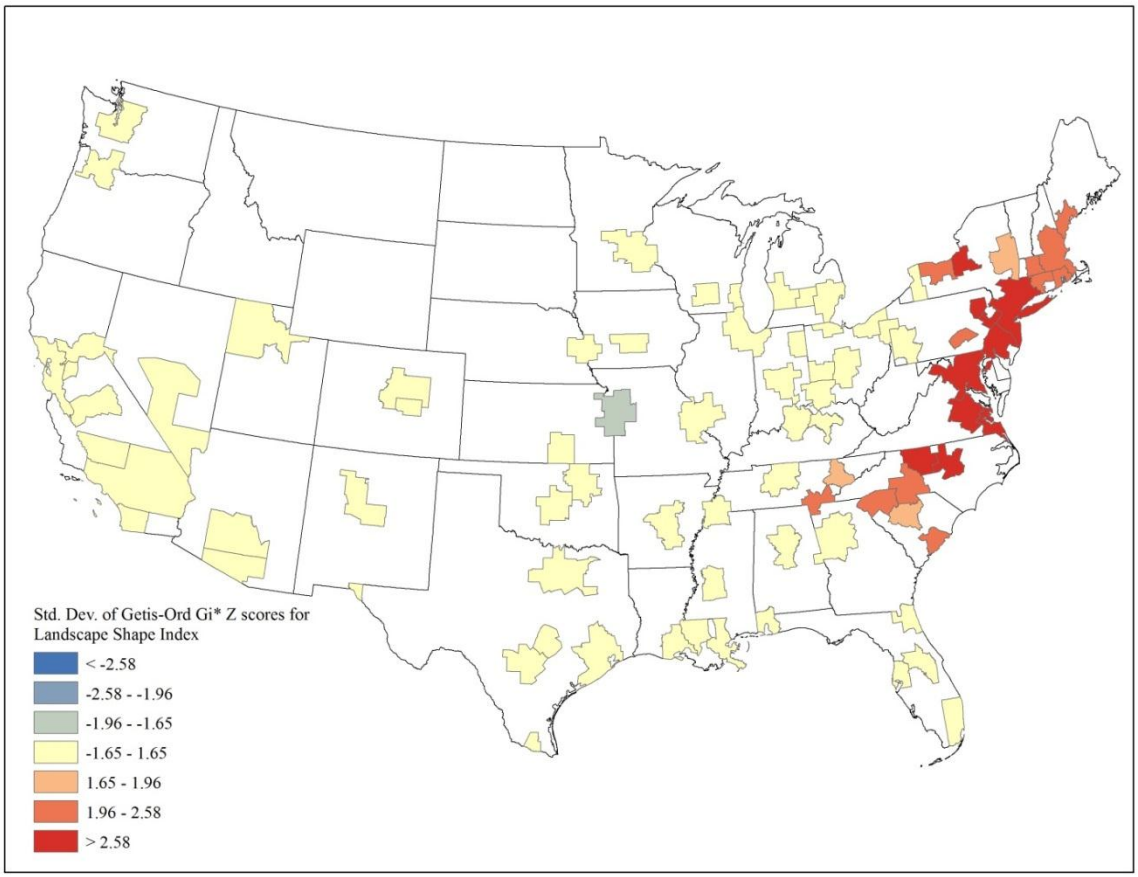

Figure 41. Getis-Ord Gi* hot-spot analysis for largest patch index (LPI). Higher Z scores (red) indicate more intense clustering of high values; lower negative Z scores (blue) indicate more intense clustering of low values.

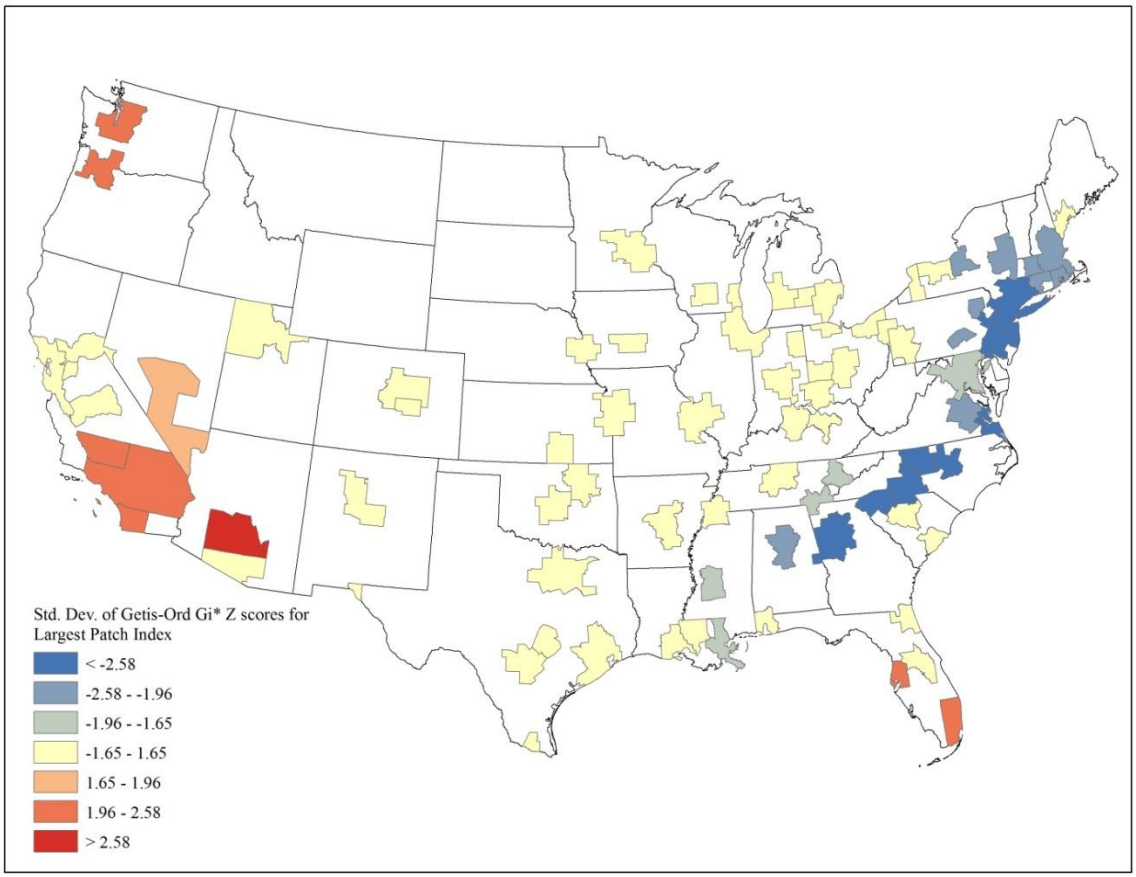

Figure 42. Getis-Ord Gi* hot-spot analysis for area-weighted mean shape index (AWMSI). Higher Z scores (red) indicate more intense clustering of high values; lower negative Z scores (blue) indicate more intense clustering of low values.

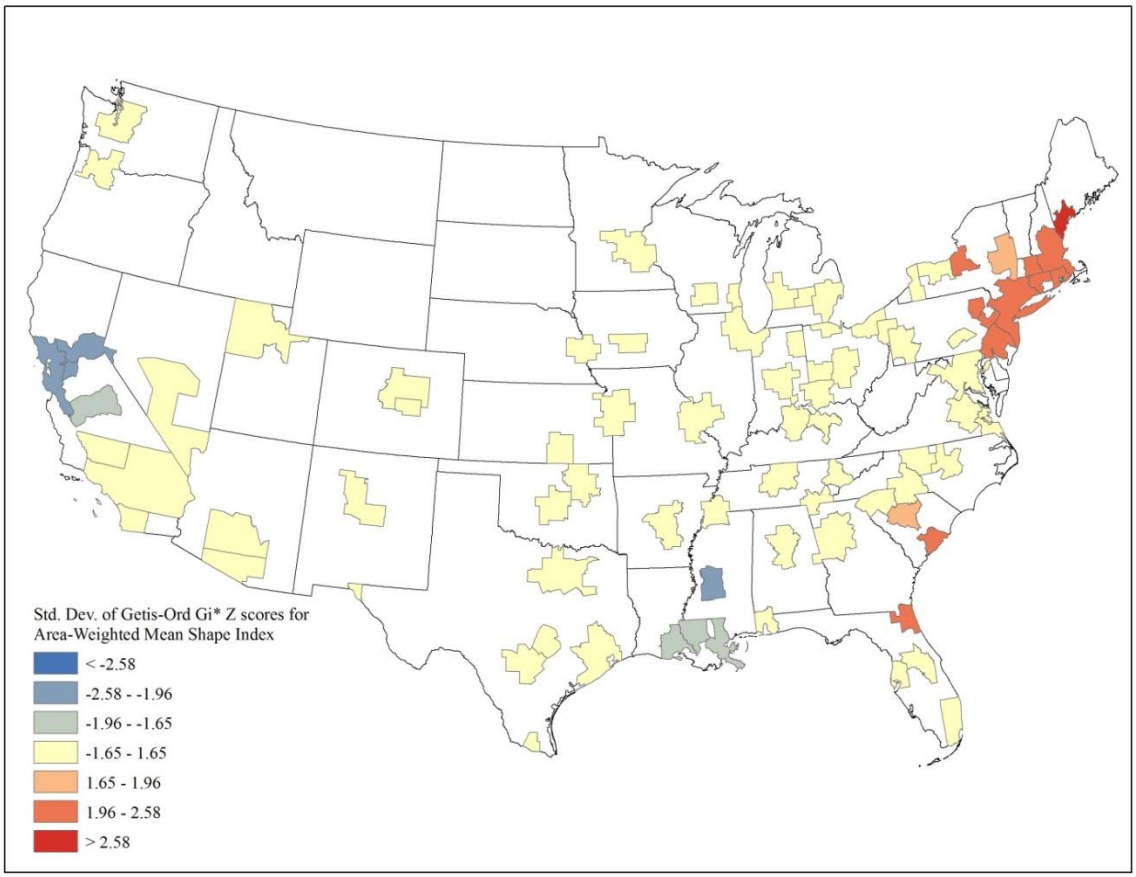

Figure 43. Getis-Ord Gi* hot-spot analysis for area-weighted mean patch fractal dimension (AWMPFD). Higher Z scores (red) indicate more intense clustering of high values; lower negative Z scores (blue) indicate more intense clustering of low values.

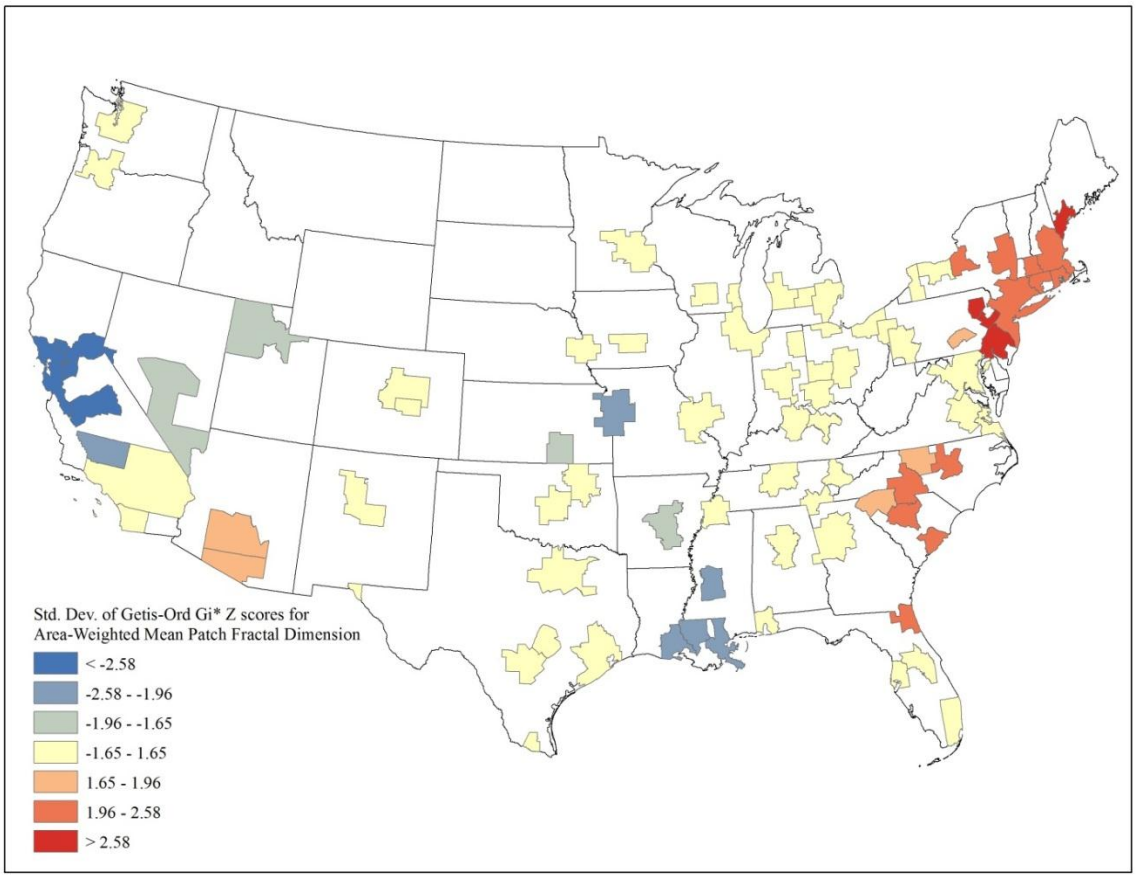

Figure 44. Getis-Ord Gi* hot-spot analysis for contiguity (CONTIG). Higher Z scores (red) indicate more intense clustering of high values; lower negative Z scores (blue) indicate more intense clustering of low values.

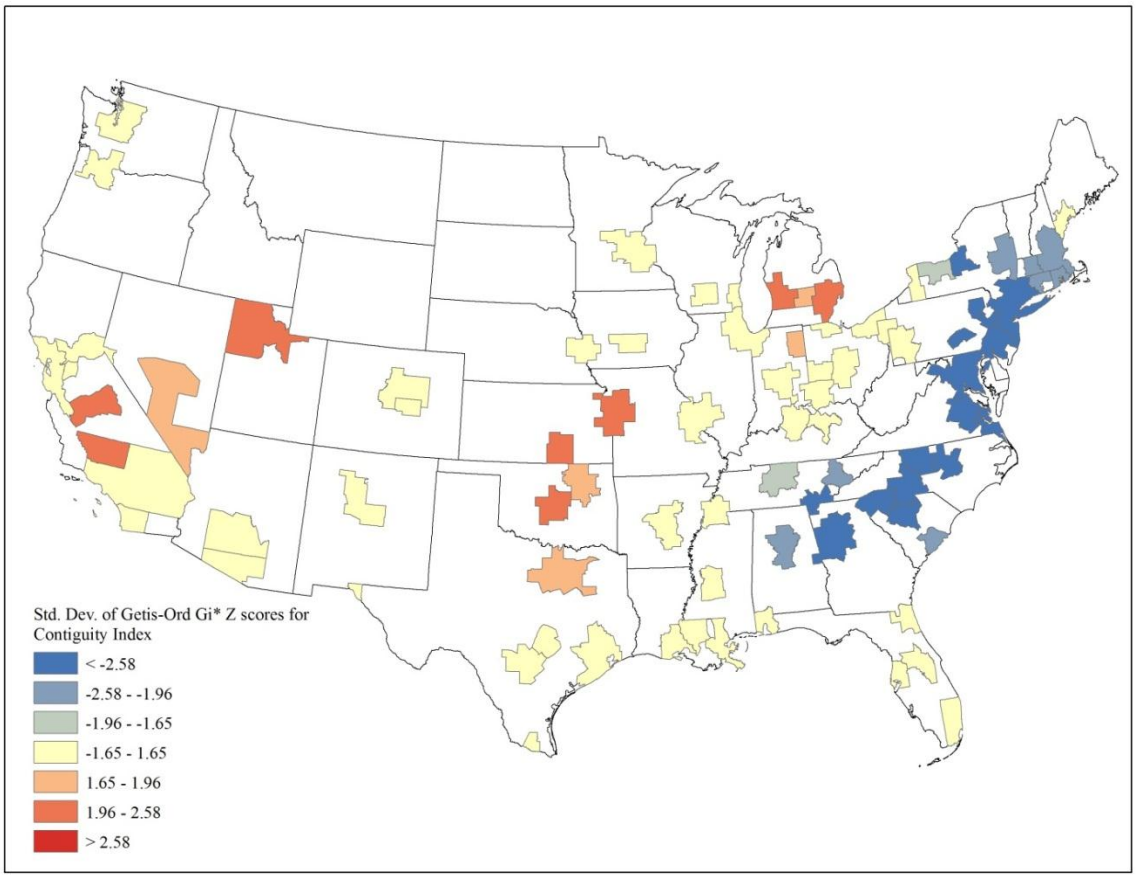

Figure 45. Getis-Ord Gi* hot-spot analysis for percentage of like adjacencies (PLADJ) index. Higher Z scores (red) indicate more intense clustering of high values; lower negative Z scores (blue) indicate more intense clustering of low values.

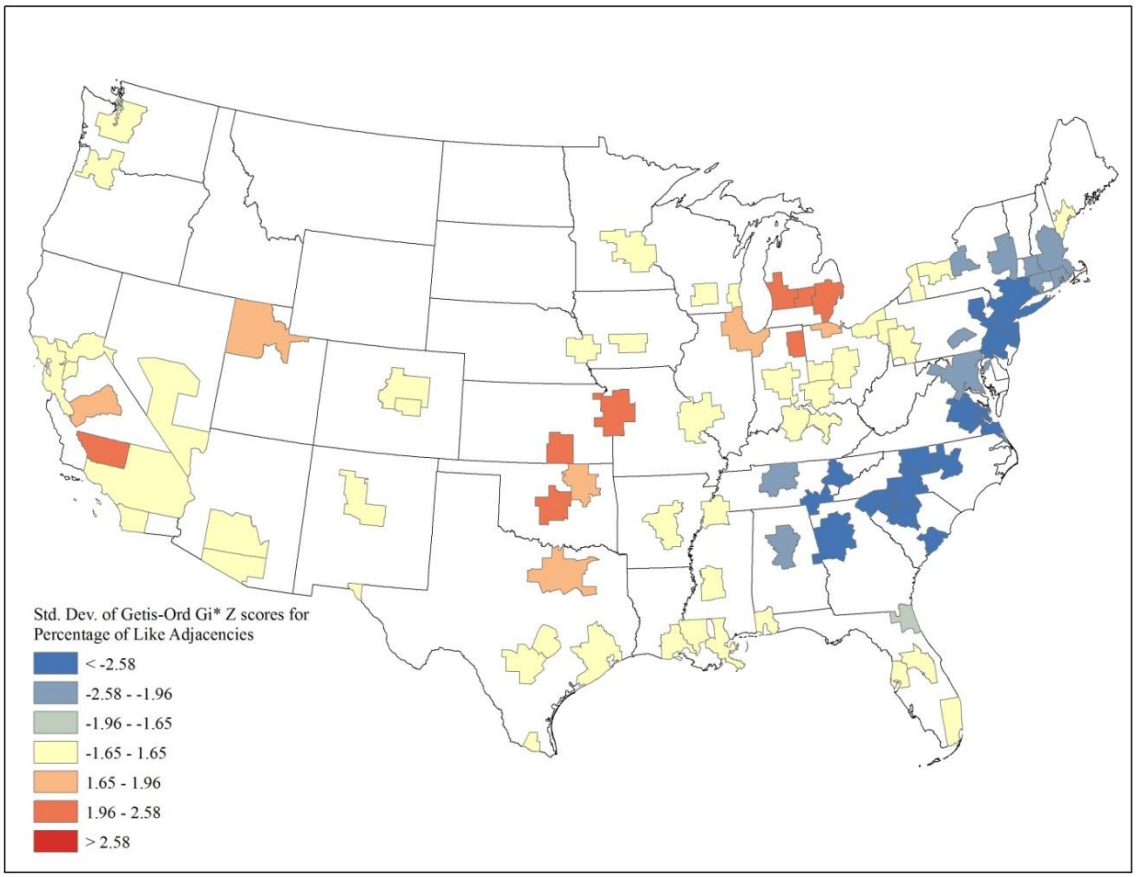

Figure 46. Getis-Ord Gi* hot-spot analysis for clumpiness (CLUMPY). Higher Z scores (red) indicate more intense clustering of high values; lower negative Z scores (blue) indicate more intense clustering of low values.

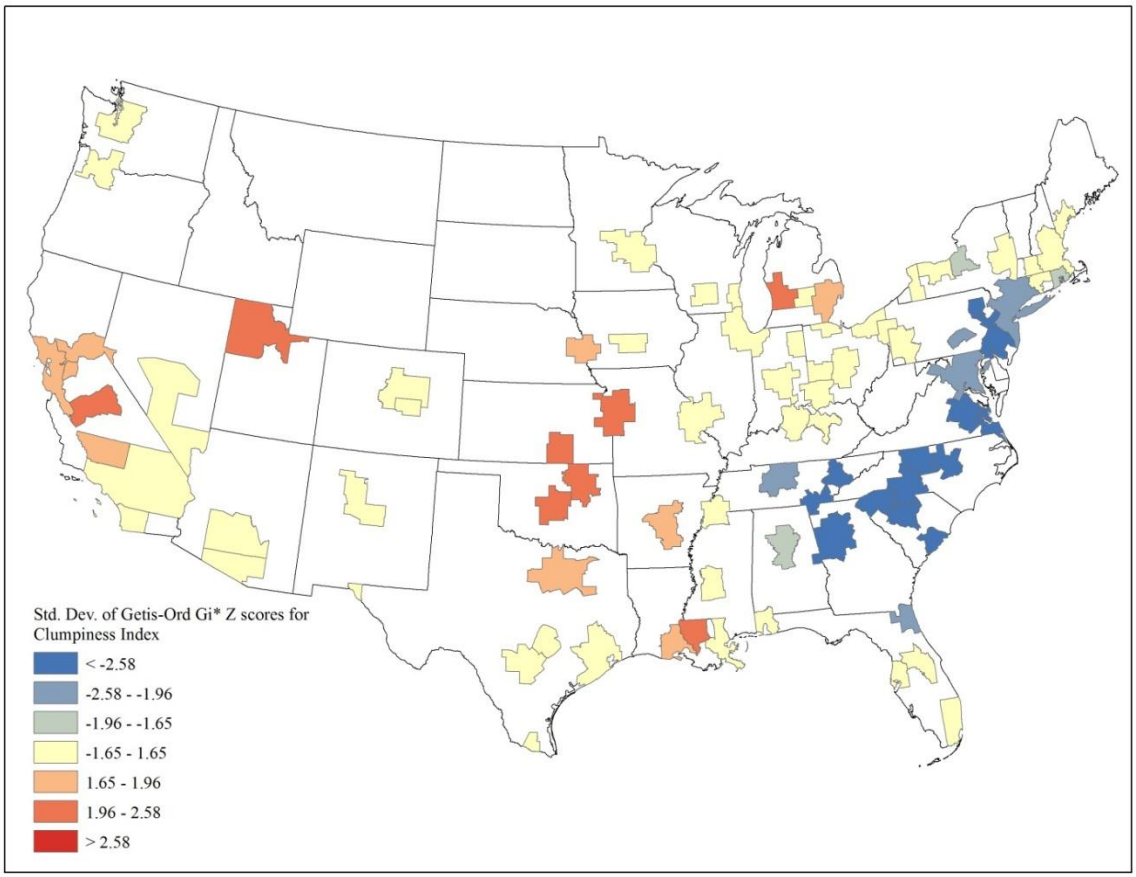

Figure 47. Getis-Ord Gi* hot-spot analysis for contagion (CONTAG). Higher Z scores (red) indicate more intense high values; lower negative Z scores (blue) indicate more intense clustering of low values

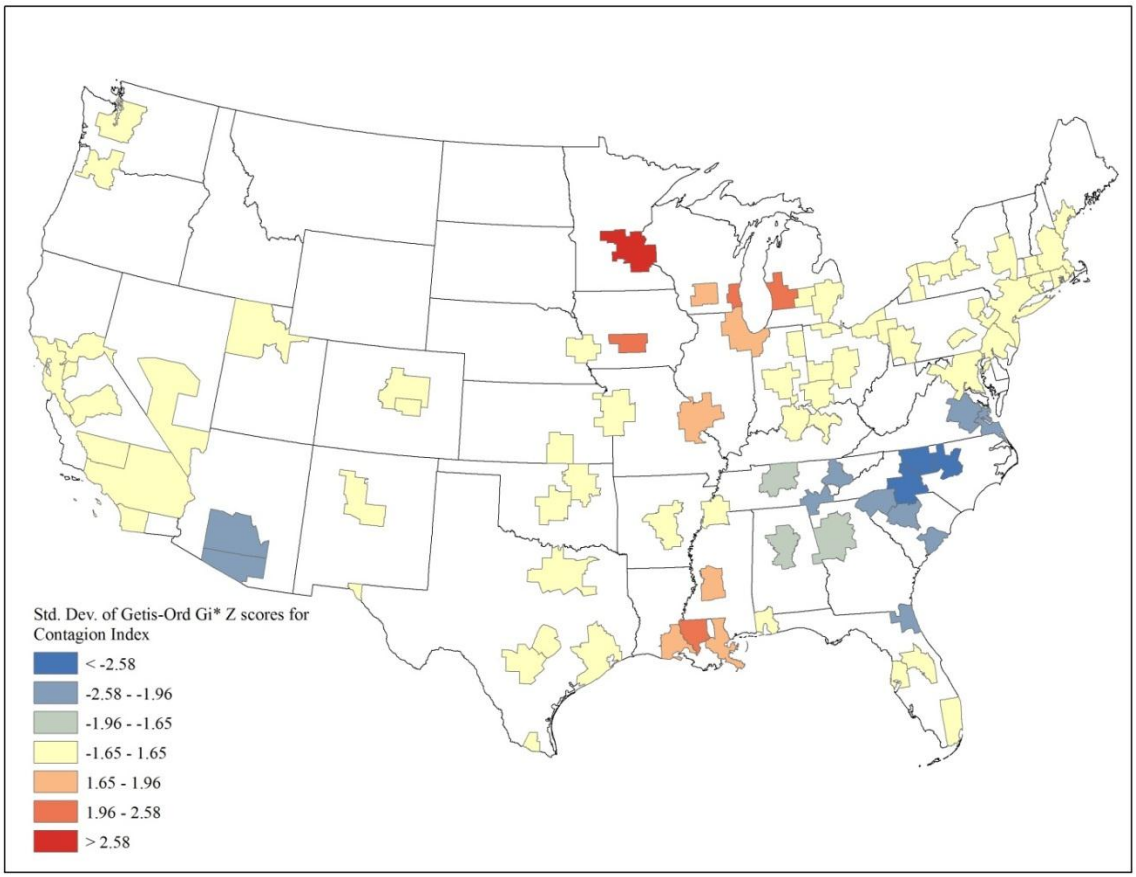

Figure 48. Largest patch index (LPI) among 86 metropolitan-scale areas within four U.S. regions. Values calculated at the high and low urban threshold have been averaged.

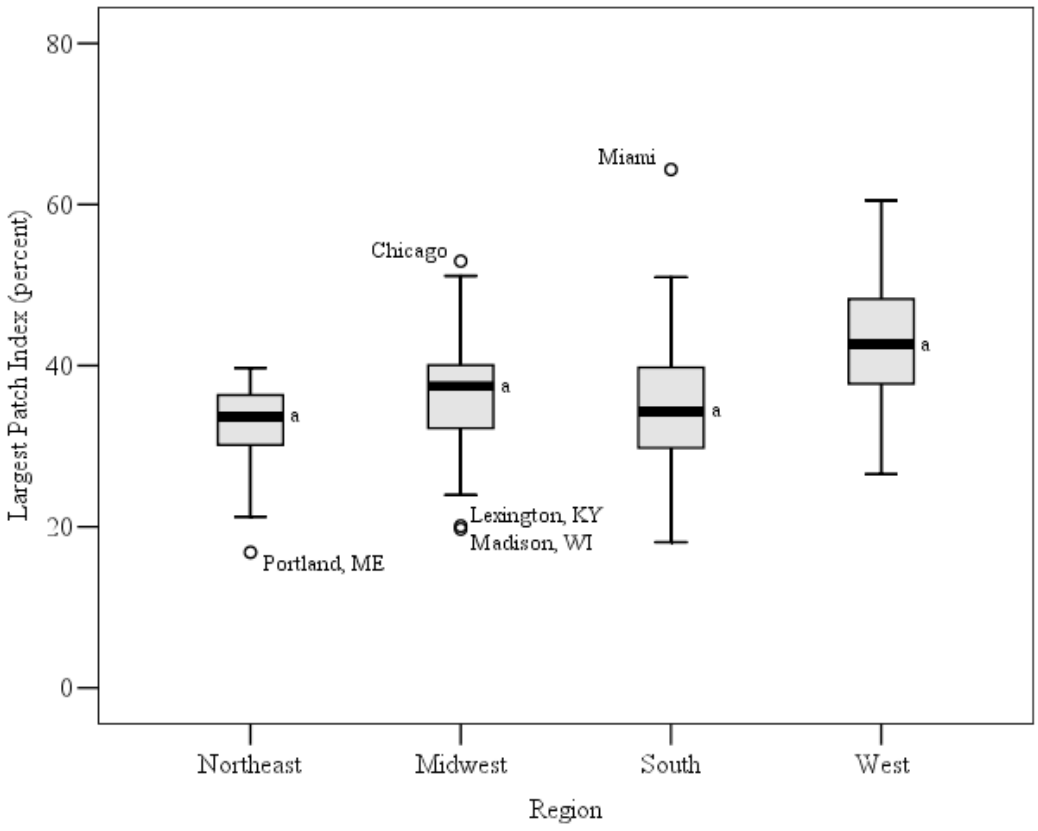

Figure 49. Landscape shape index (LSI) among 86 metropolitan-scale areas within four U.S. regions. Values calculated at the high and low urban threshold have been averaged.

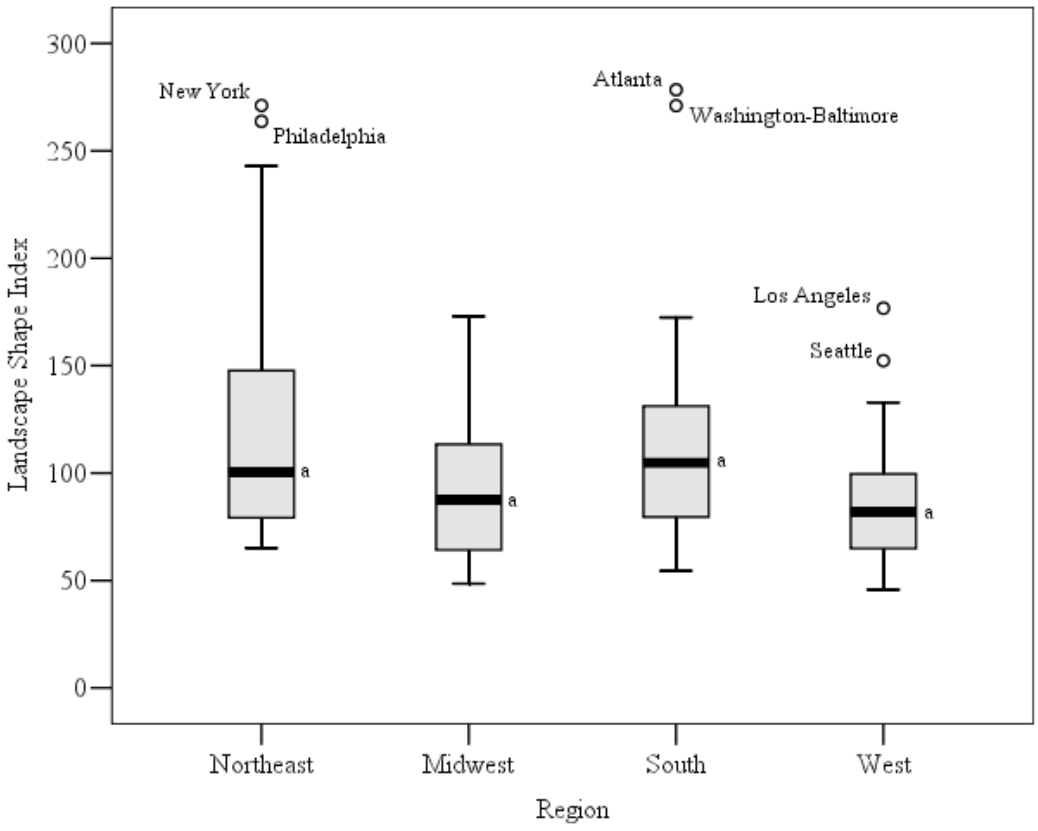

Figure 50. Edge density (ED) among 86 metropolitan-scale areas within four U.S. regions. Values calculated at the high and low urban threshold have been averaged.

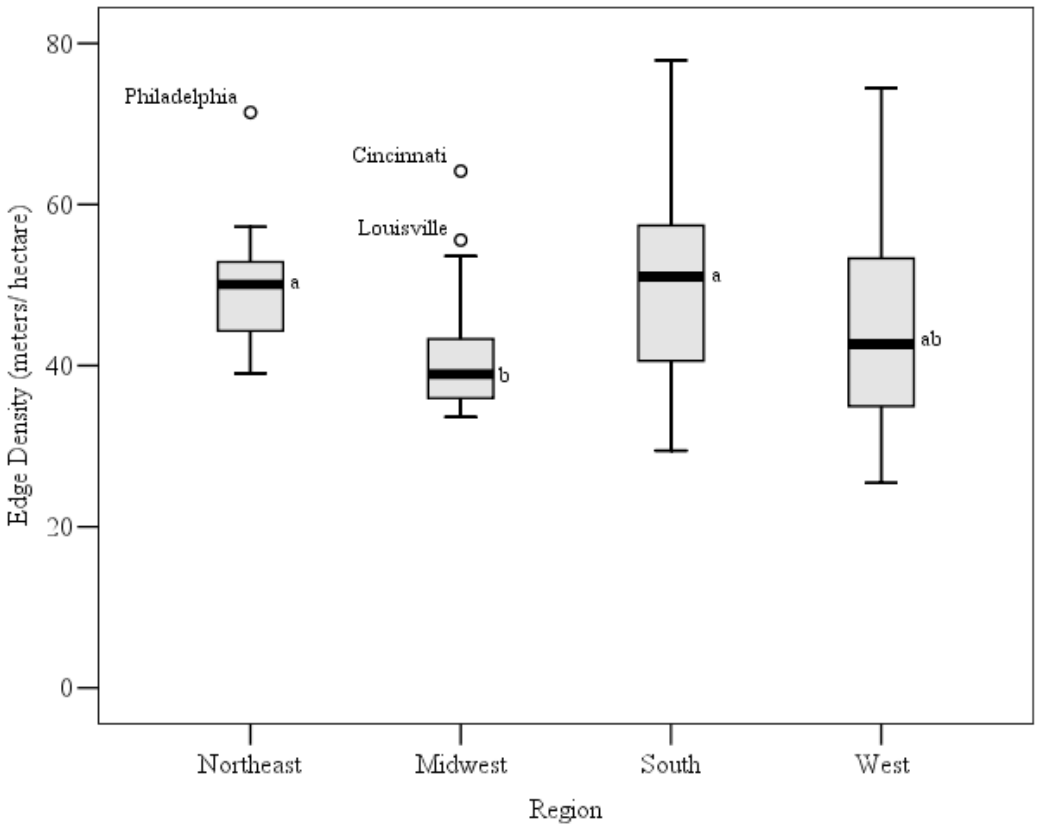

Figure 51. Area-weighted mean shape index (AWMSI) among 86 metropolitan-scale areas within four U.S. regions. Values calculated at the high and low urban threshold have been averaged.

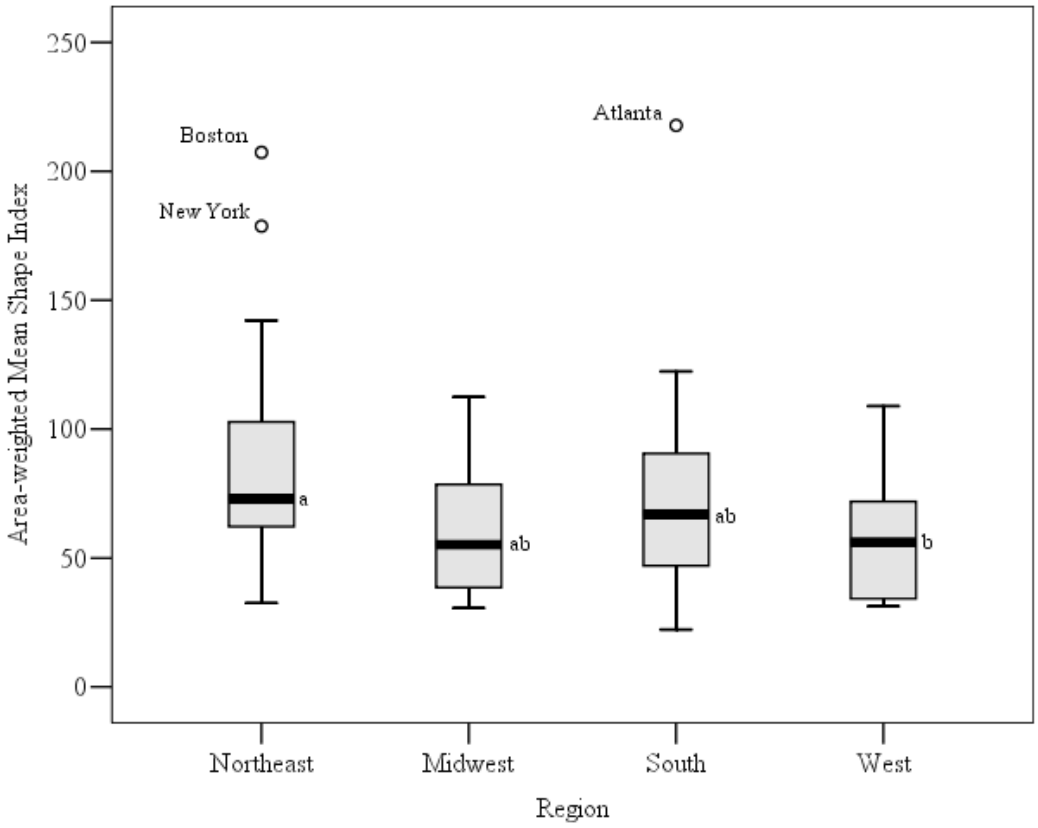

Figure 52. Area-weighted mean patch fractal dimension (AWMPFD) among 86 metropolitan-scale areas within four U.S. regions. Values calculated at the high and low urban threshold have been averaged.

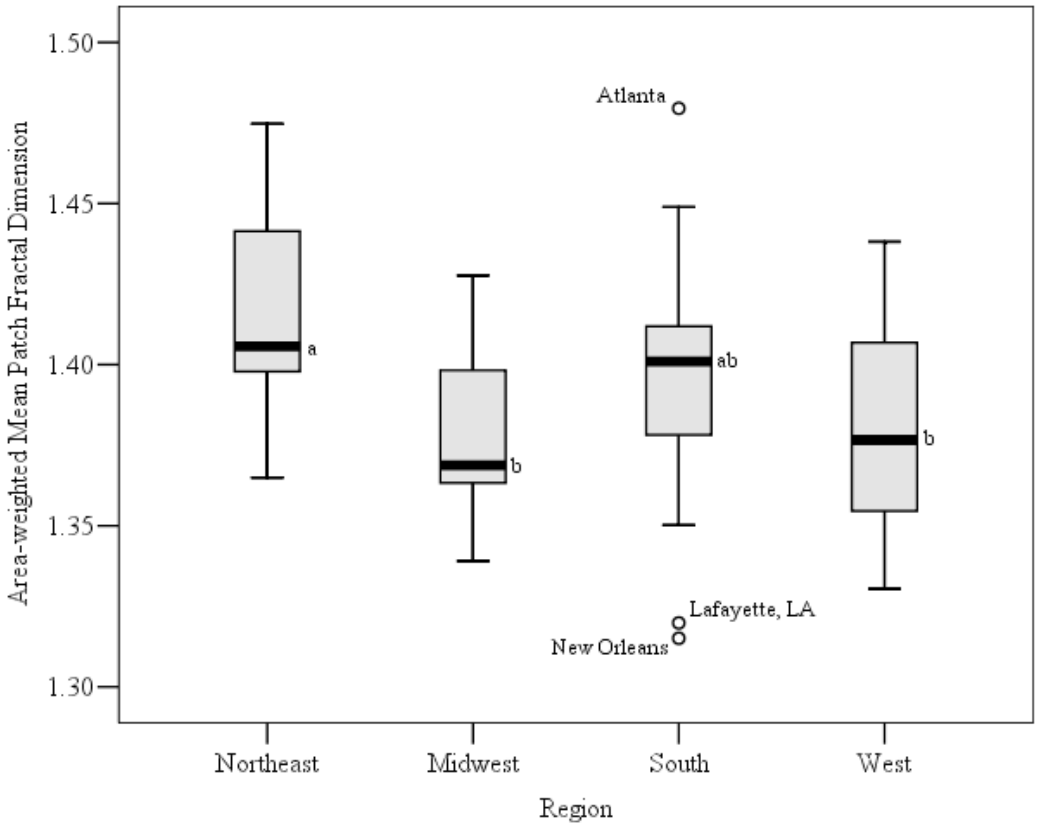

Figure 53. Contiguity (CONTIG) among 86 metropolitan-scale areas b within four U.S. regions. Values calculated at the high and low urban threshold have been averaged.

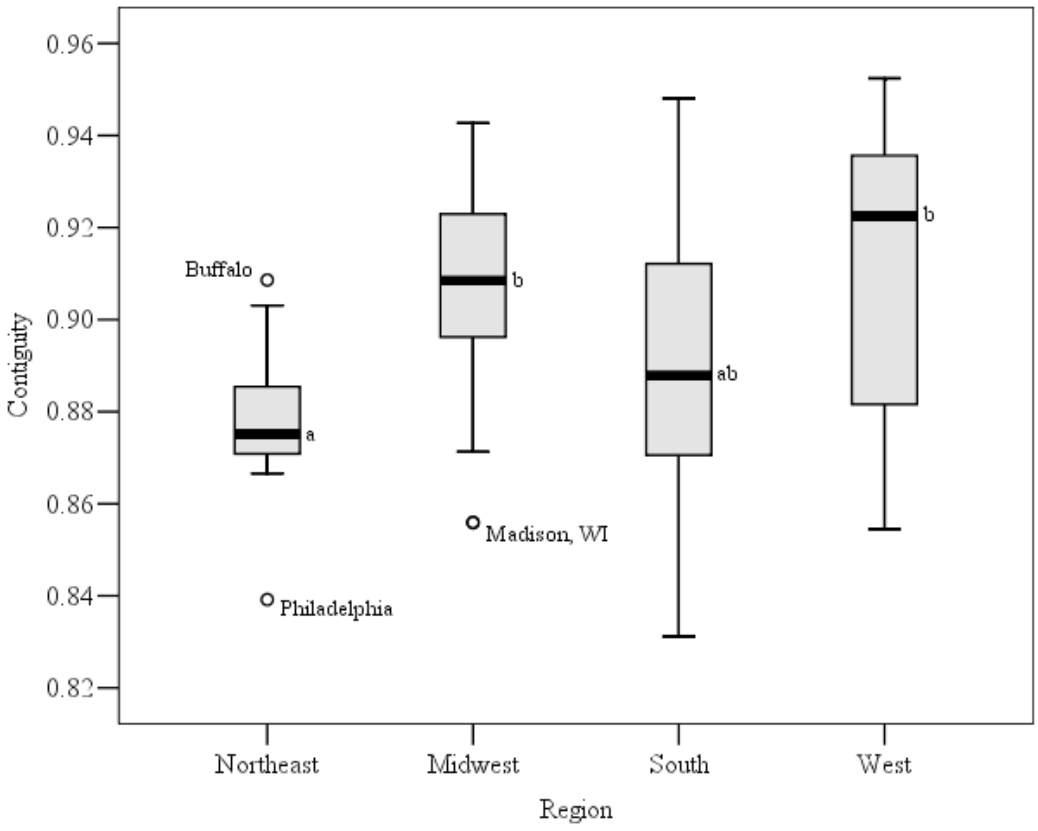

Figure 54. Contagion (CONTAG) among 86 metropolitan-scale areas within four U.S. regions. Values calculated at the high and low urban threshold have been averaged.

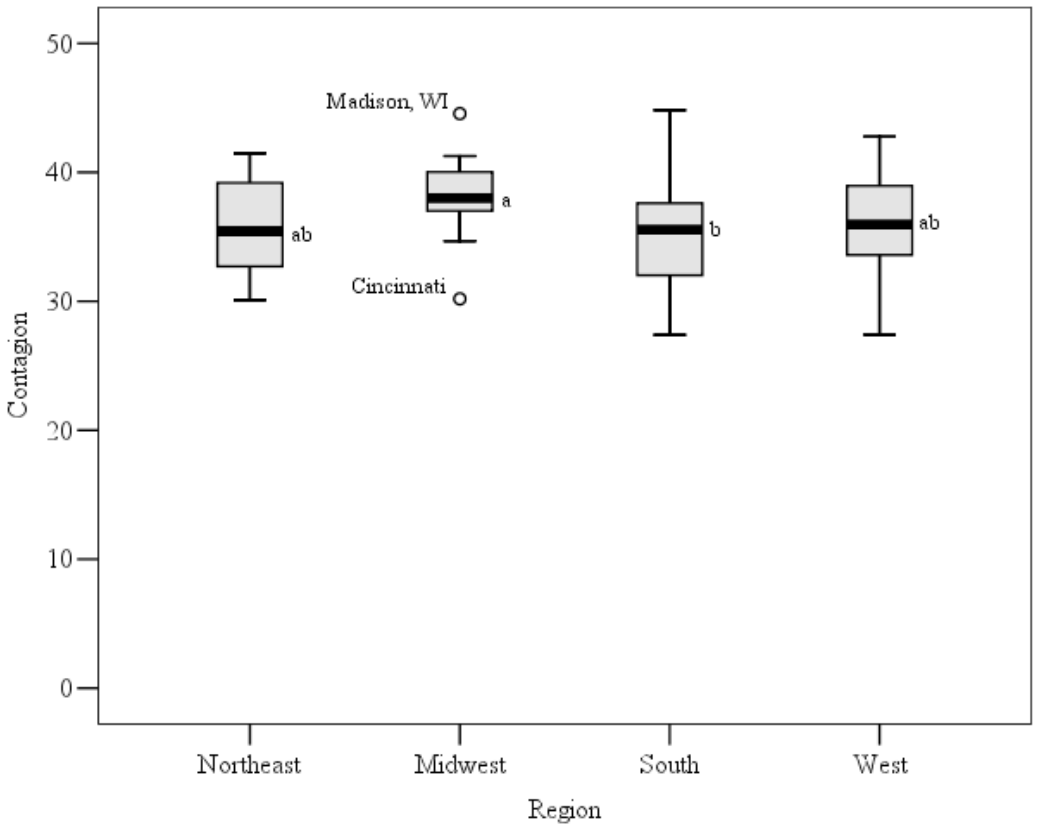

Figure 55. Percentage of like adjacencies (PLADJ) index among 86 metropolitan-scale areas within four U.S. regions. Values calculated at the high and low urban threshold have been averaged.

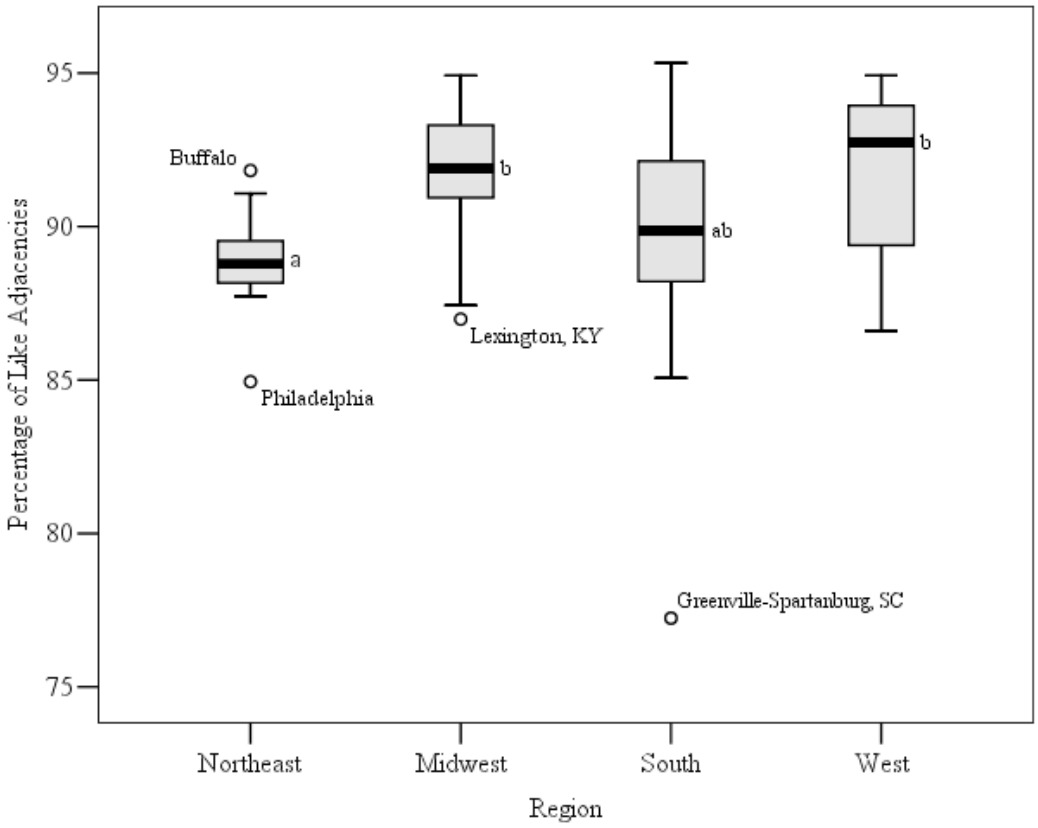

Figure 56. Clumpiness (CLUMPY) among 86 metropolitan-scale areas within four U.S. regions. Values calculated at the high and low urban threshold have been averaged.

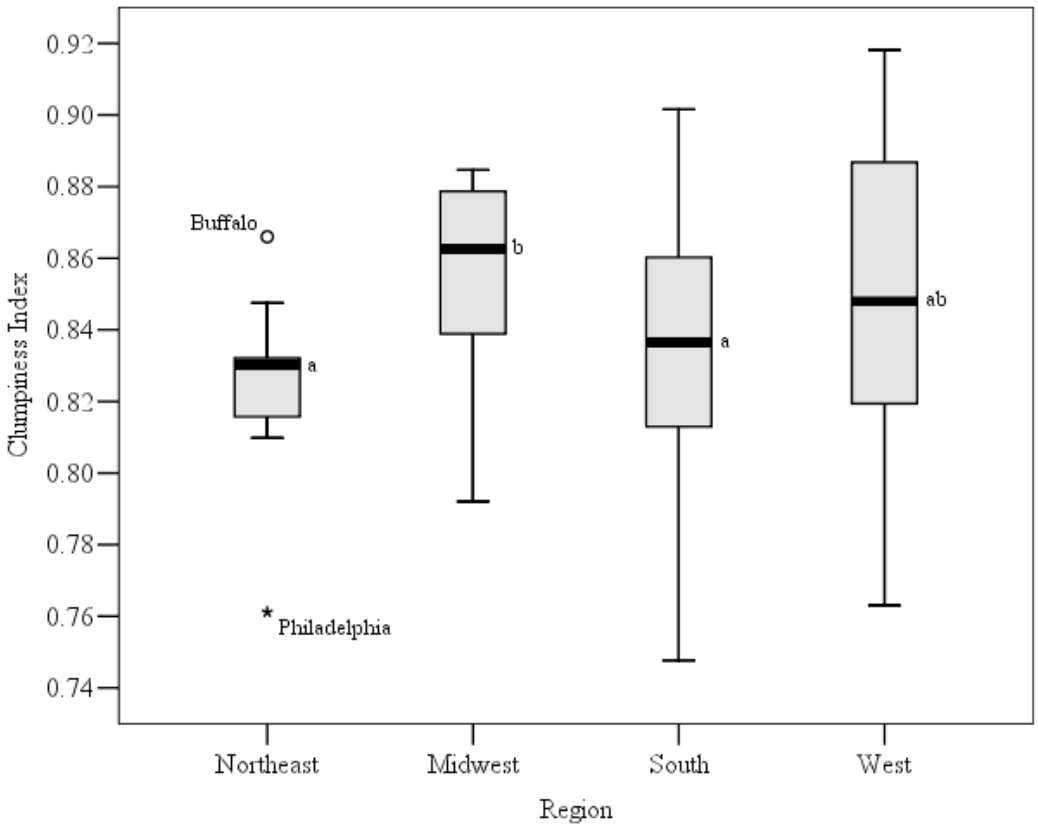

Figure 57. Urban “continuity,” derived from spatial metrics calculated at the high urban threshold, by MSA/ CSA. Lower values of urban “continuity” may indicate more “sprawl-like” conditions.

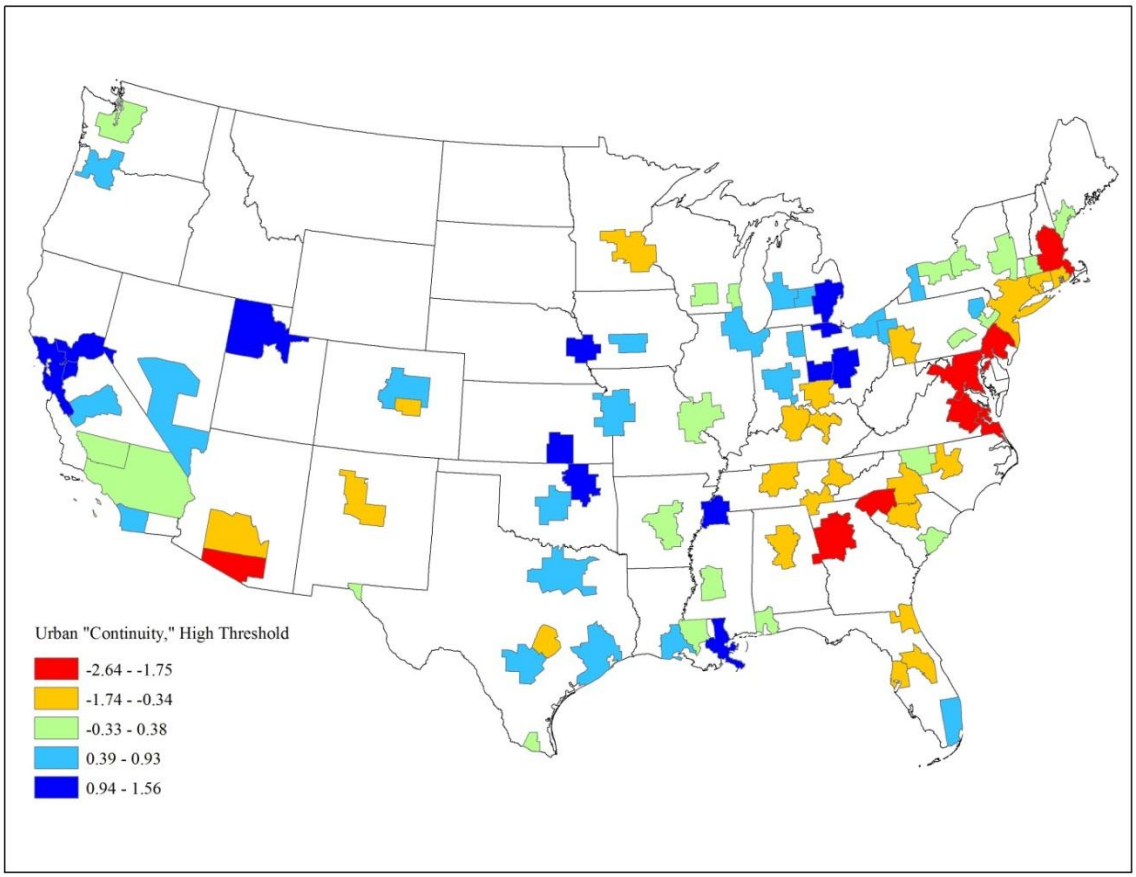

Figure 58. Urban “continuity,” derived from spatial metrics calculated at the low urban threshold, by MSA/ CSA. Lower values of urban “continuity” may indicate more “sprawl-like” conditions.

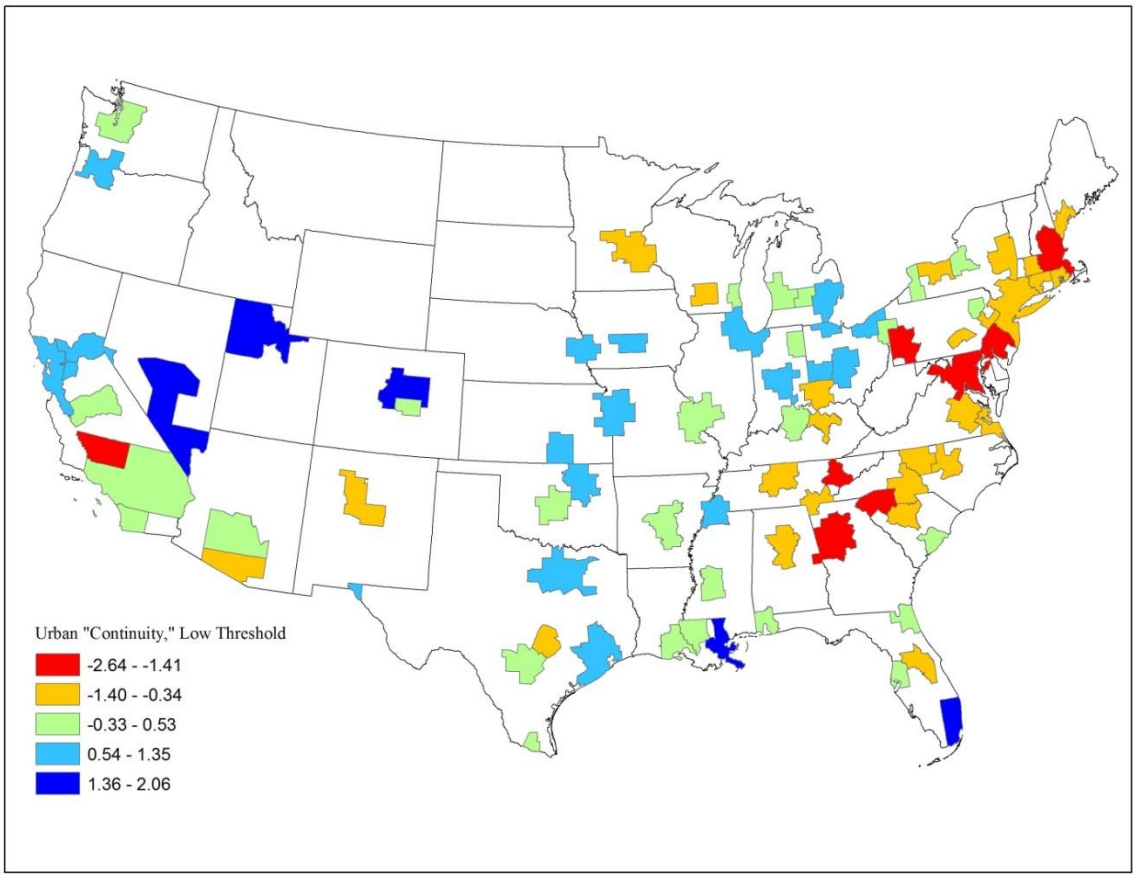

Figure 59. Urban “shape complexity,” derived from spatial metrics calculated at the high urban threshold, by MSA/ CSA. Higher values of urban “shape complexity” may indicate more “sprawl-like” conditions.

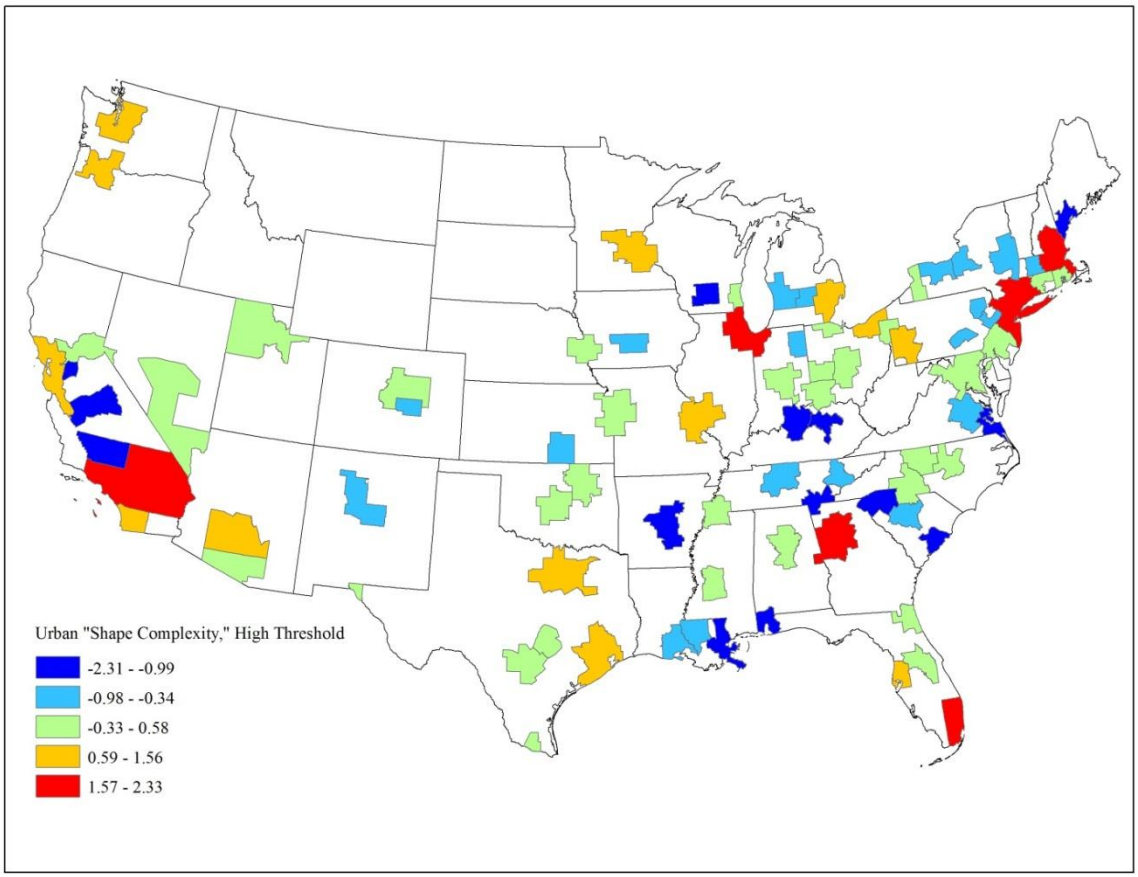

Figure 60. Urban “shape complexity,” derived from spatial metrics calculated at the low urban threshold, by MSA/ CSA. Higher values of urban “shape complexity” may indicate more “sprawl-like” conditions.

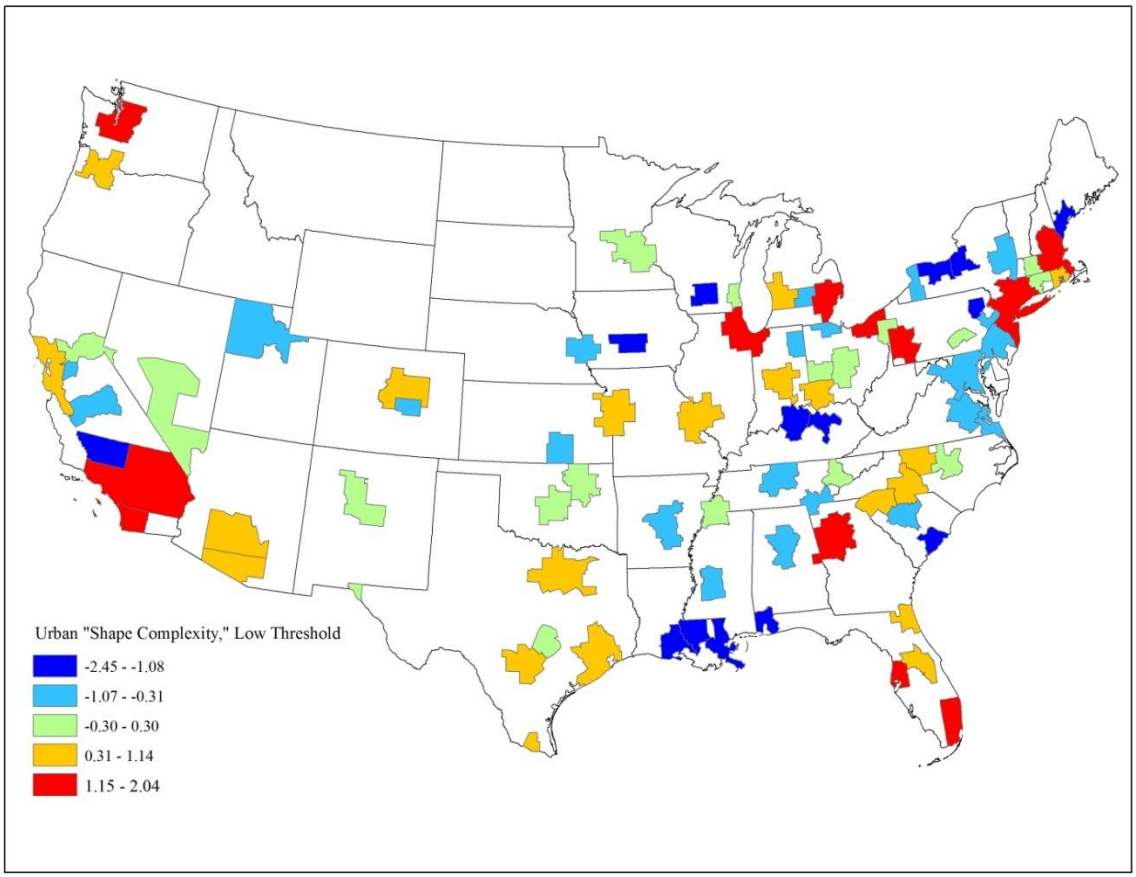

Figure 61. Hot spot analysis using Getis-Ord Gi* for the urban form factor urban "continuity," derived from spatial metrics calculated at the high urban threshold. Higher Z scores (red) indicate more intense clustering of high values; lower negative Z scores (blue) indicate more intense clustering of low values.

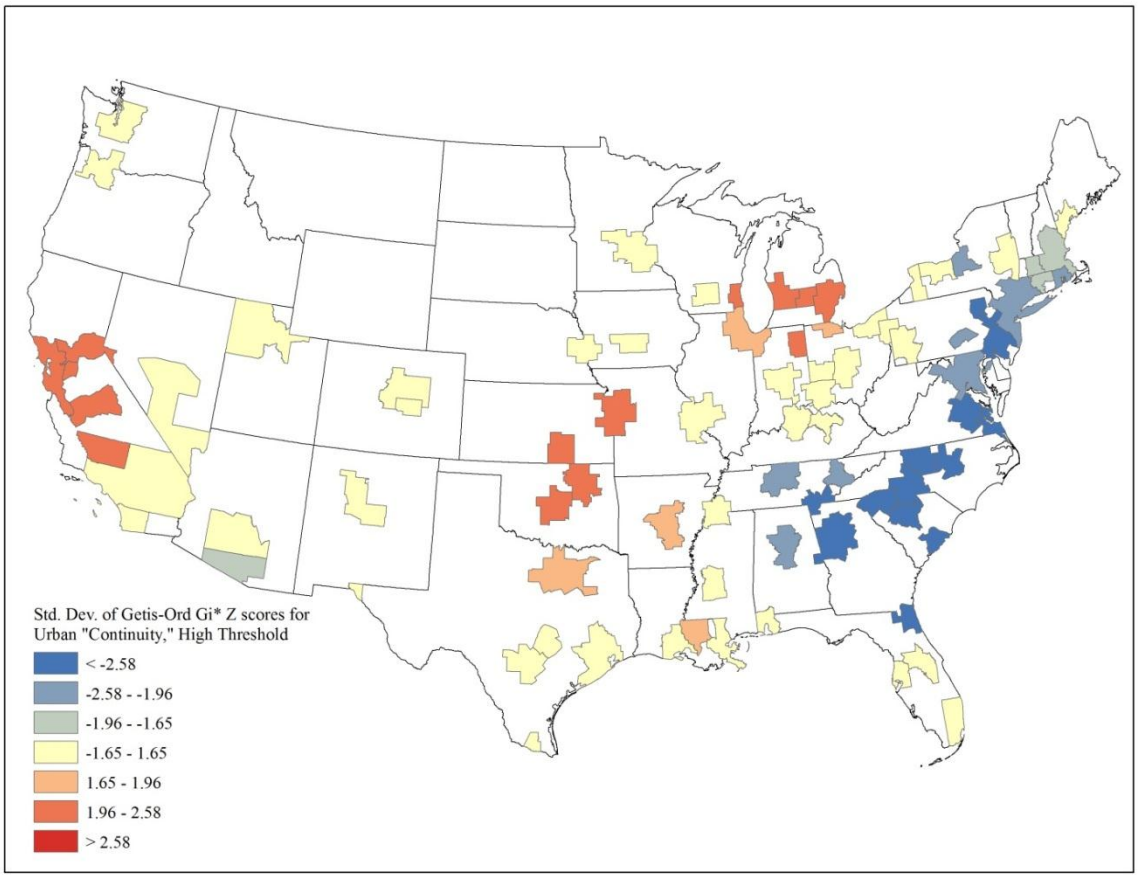

Figure 62. Hot spot analysis using Getis-Ord Gi* for the urban form factor urban "continuity," derived from spatial metrics calculated at the low urban threshold. Higher Z scores (red) indicate more intense clustering of high values; lower negative Z scores (blue) indicate more intense clustering of low values.

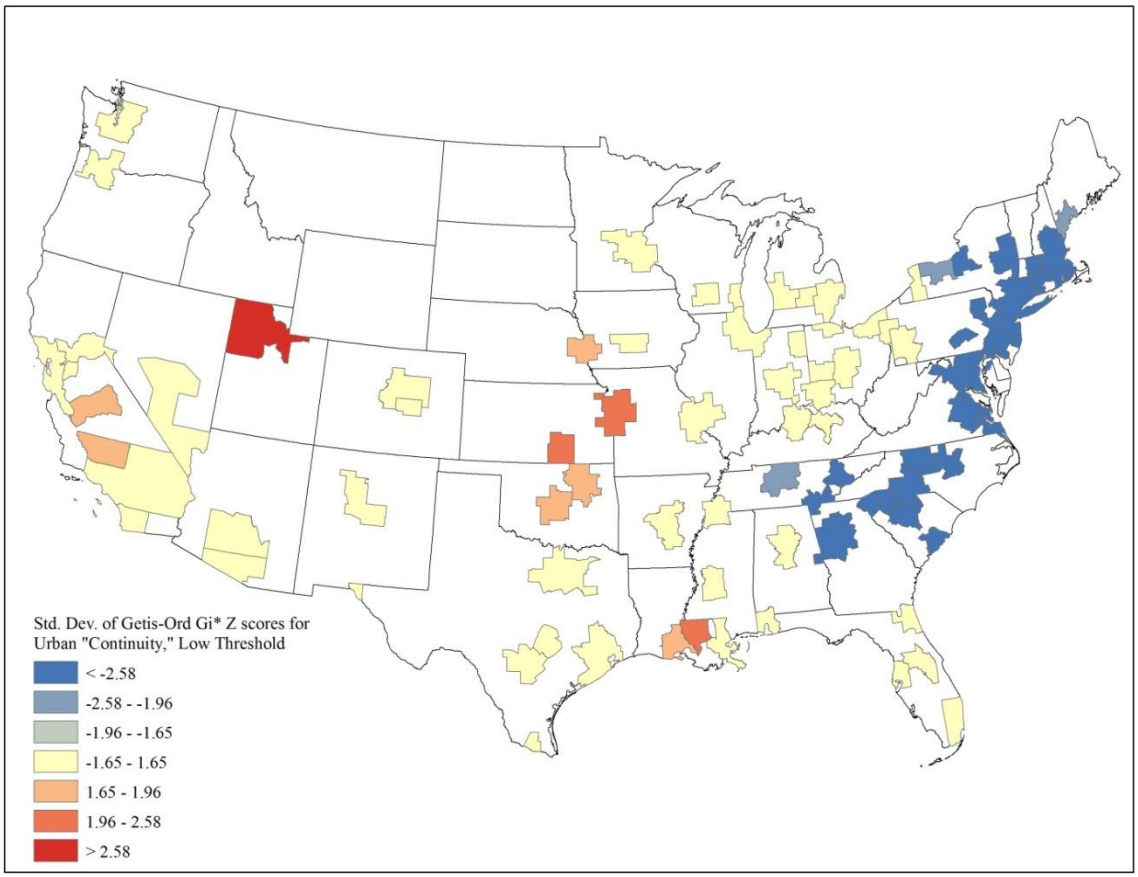

Figure 63. Hot spot analysis using Getis-Ord Gi* for the urban form factor urban "shape complexity," derived from spatial metrics calculated at the high urban threshold. Higher Z scores (red) indicate more intense clustering of high values; lower negative Z scores (blue) indicate more intense clustering of low values.

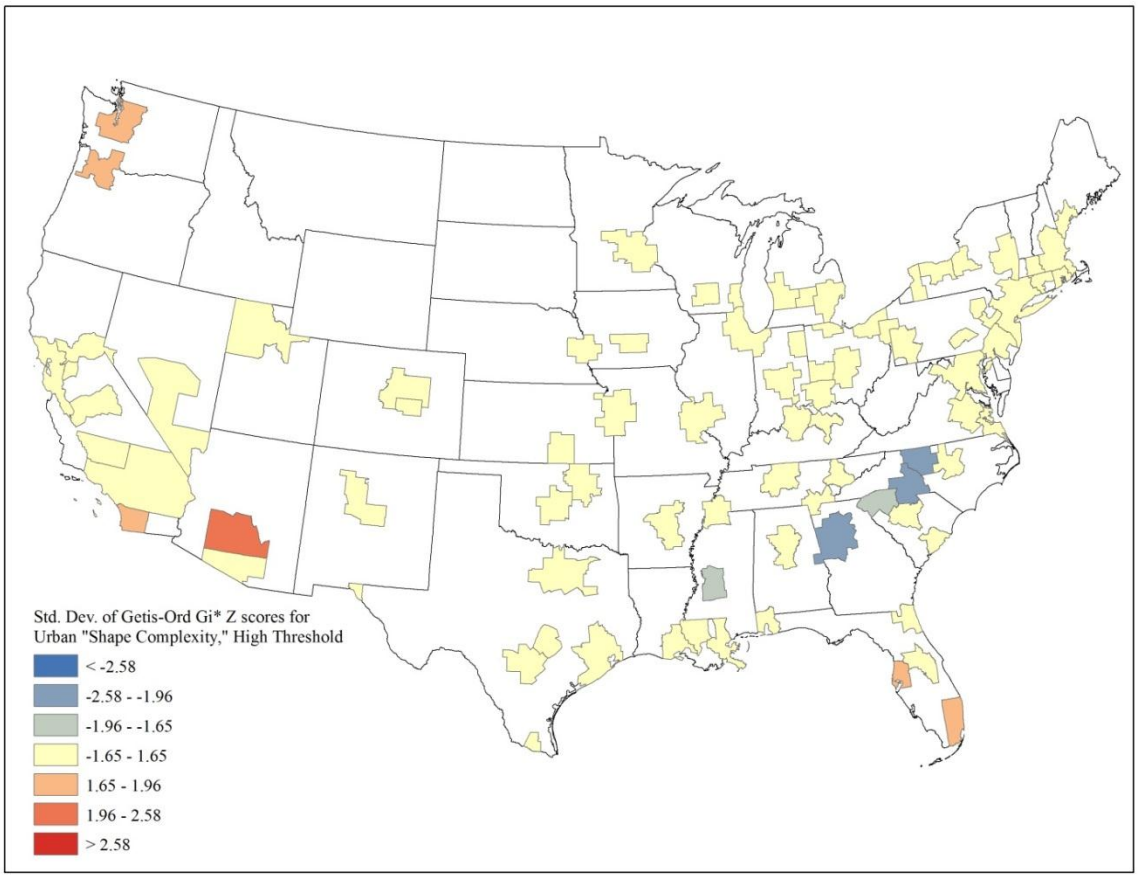

Figure 64. Hot spot analysis using Getis-Ord Gi* for the urban form factor urban “shape complexity,” derived from spatial metrics calculated at the low urban threshold. Higher Z scores (red) indicate more intense clustering of high values; lower negative Z scores (blue) indicate more intense clustering of low values.

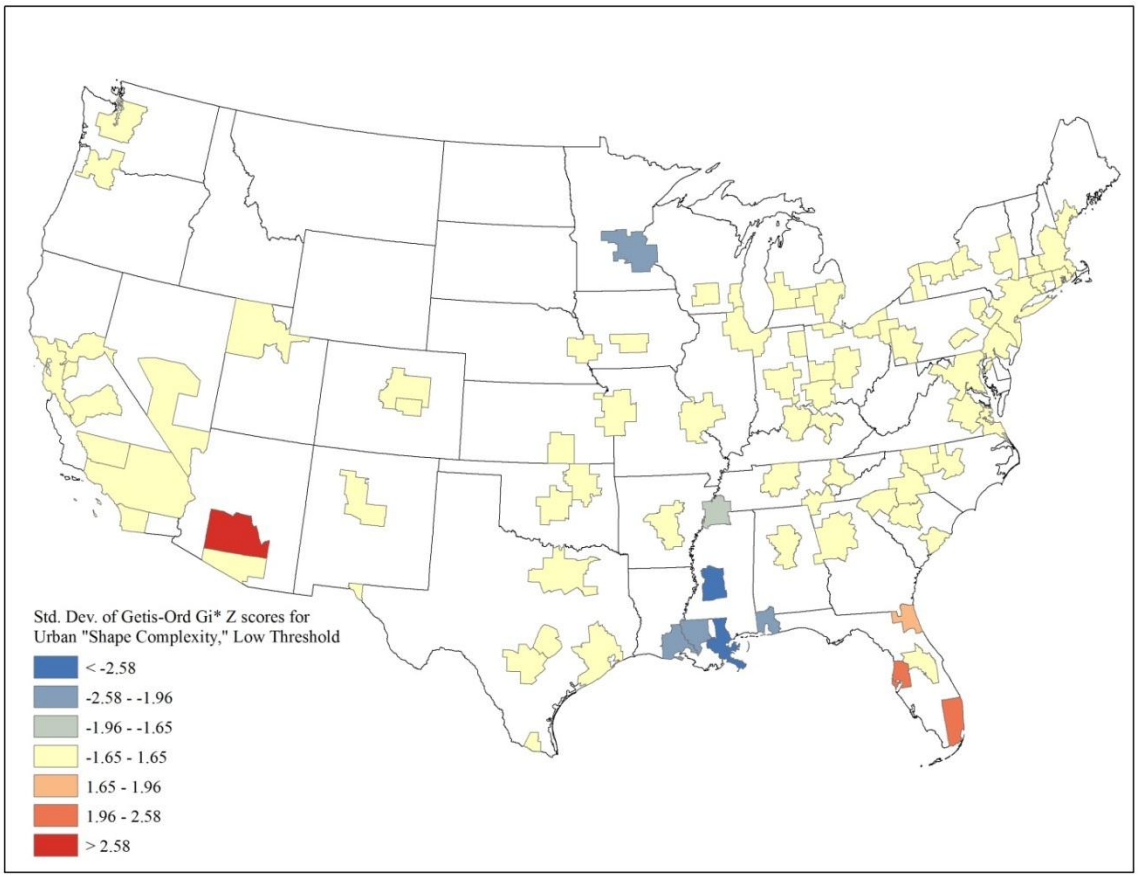

Figure 65. Urban “continuity,” calculated at the high urban threshold, among 86 metropolitan-scale areas by U.S. region.

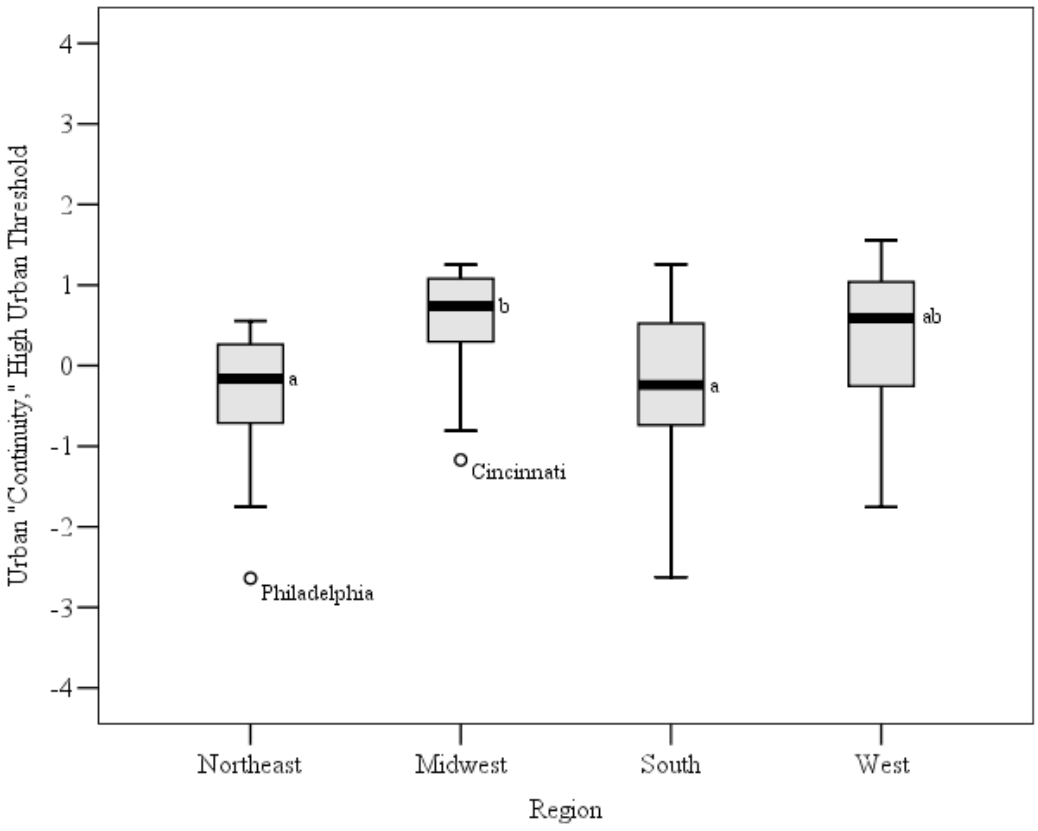

Figure 66. Urban “continuity,” calculated at the low urban threshold, among 86 metropolitan-scale areas by U.S. region.

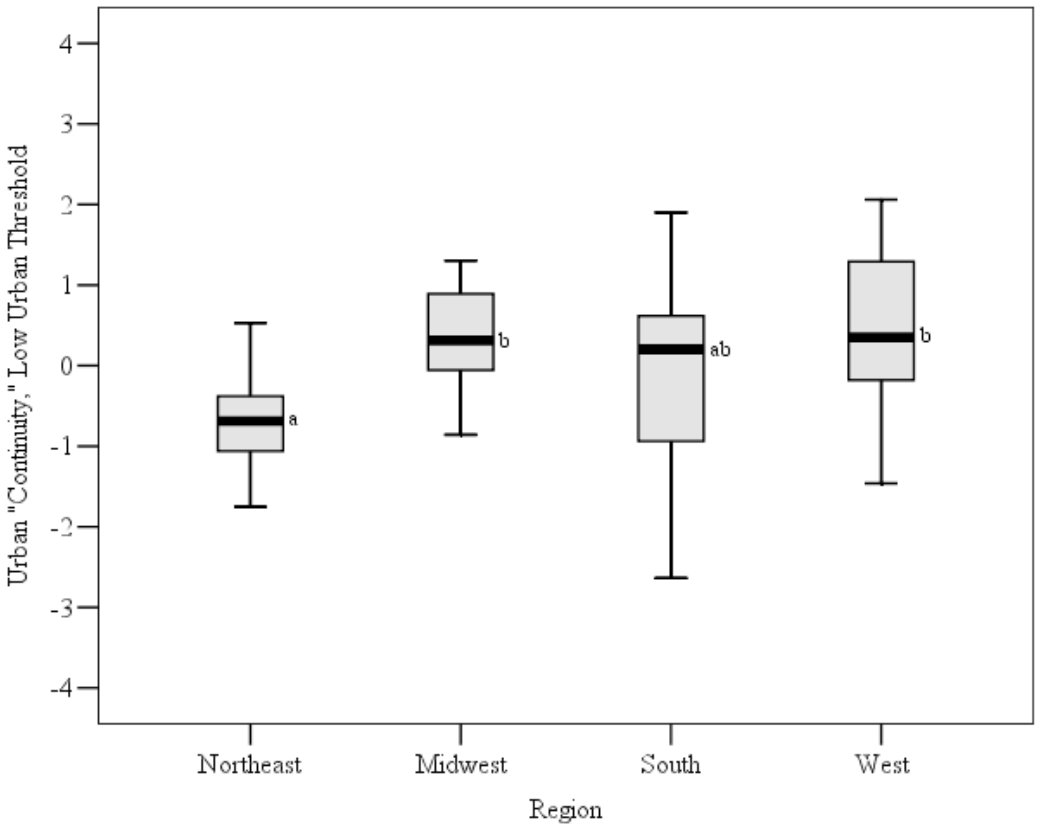

Figure 67. Urban “shape complexity,” calculated at the high urban threshold, among 86 metropolitan-scale areas by U.S. region.

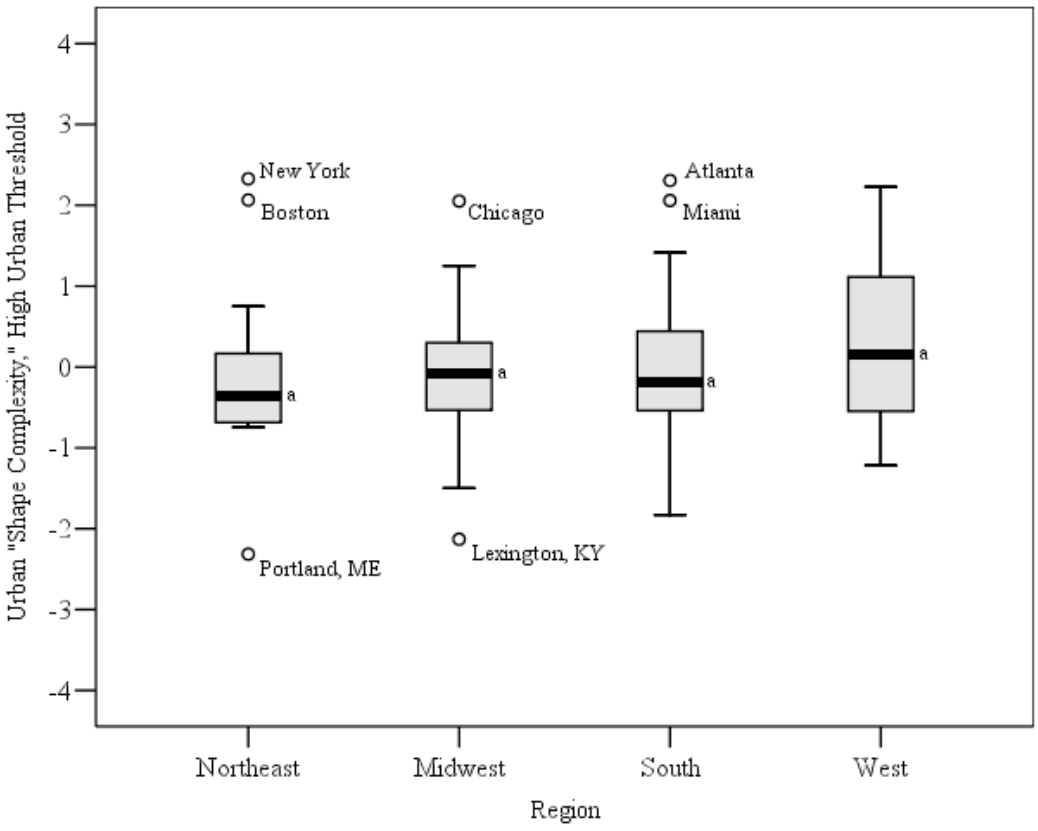

Figure 68. Urban “shape complexity,” calculated at the low urban threshold, among 86 metropolitan-scale areas by U.S. region.

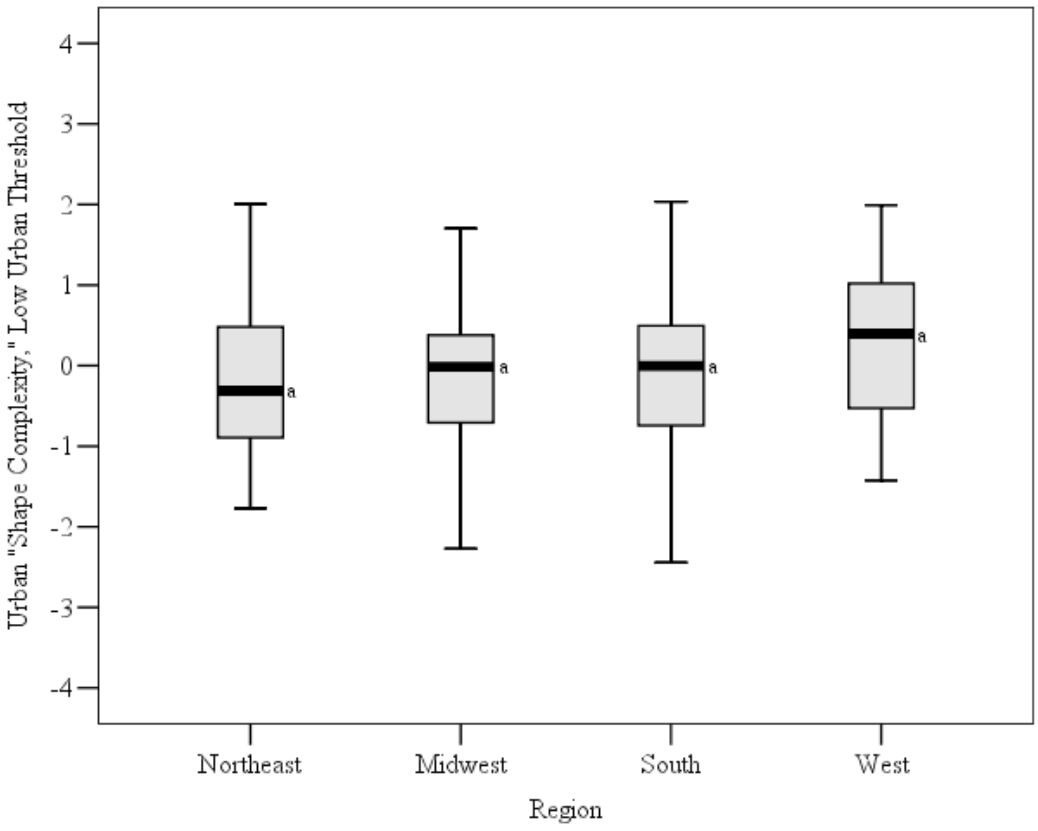

Figure 69. The urban "continuity" and urban "shape complexity" of 86 MSAs and CSAs, calculated at the high urban threshold. "Triangle" represents the Raleigh-Durham-Cary, NC CSA; "Triad" represents the Greensboro—Winston-Salem—High-Point, NC CSA.

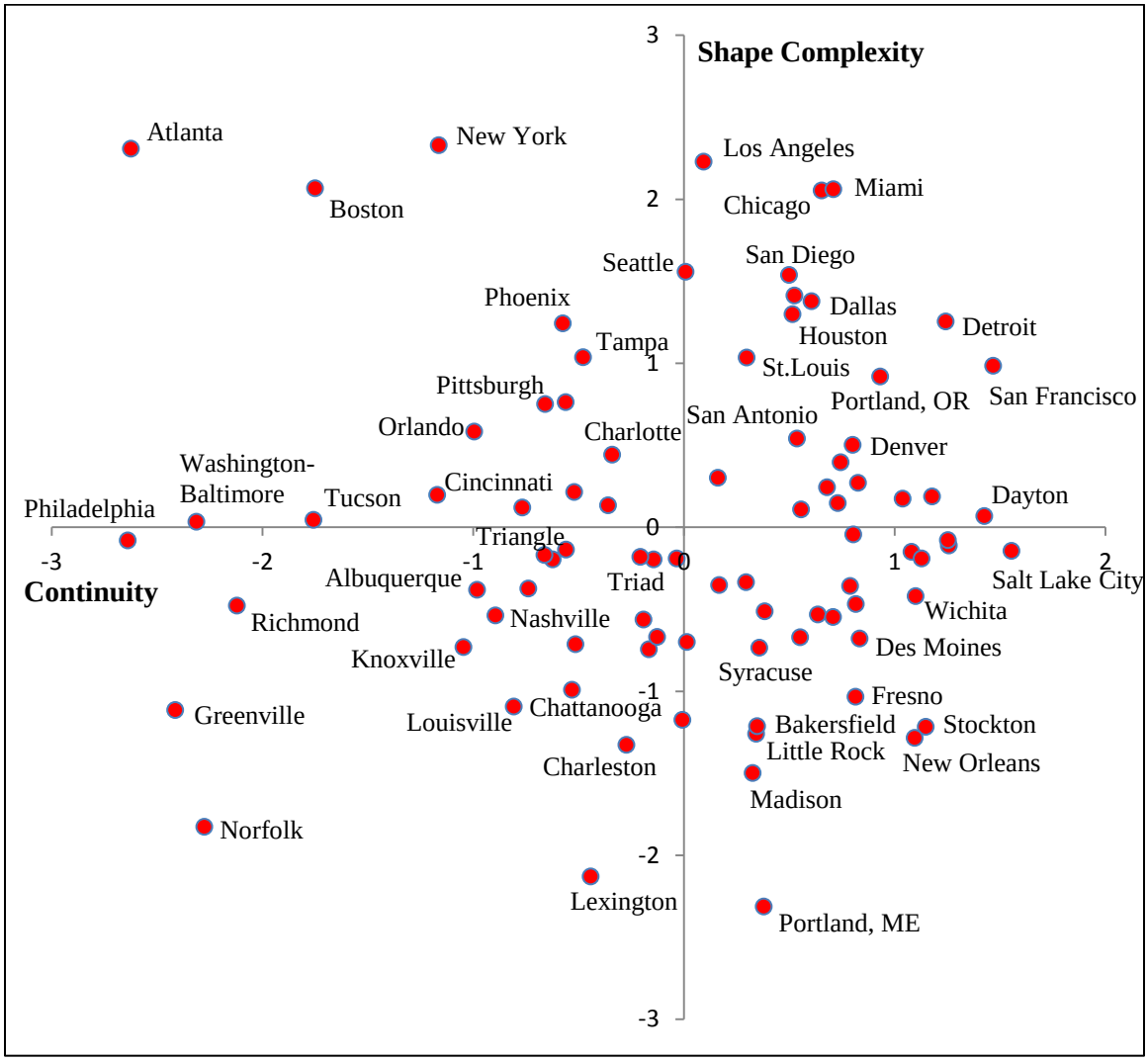

Figure 70. Urban “continuity” and urban “shape complexity” of 86 MSAs and CSAs, calculated at the low urban threshold. “Triangle” represents the Raleigh-Durham-Cary, NC CSA; “Triad” represents the Greensboro—Winston-Salem—High-Point, NC CSA.

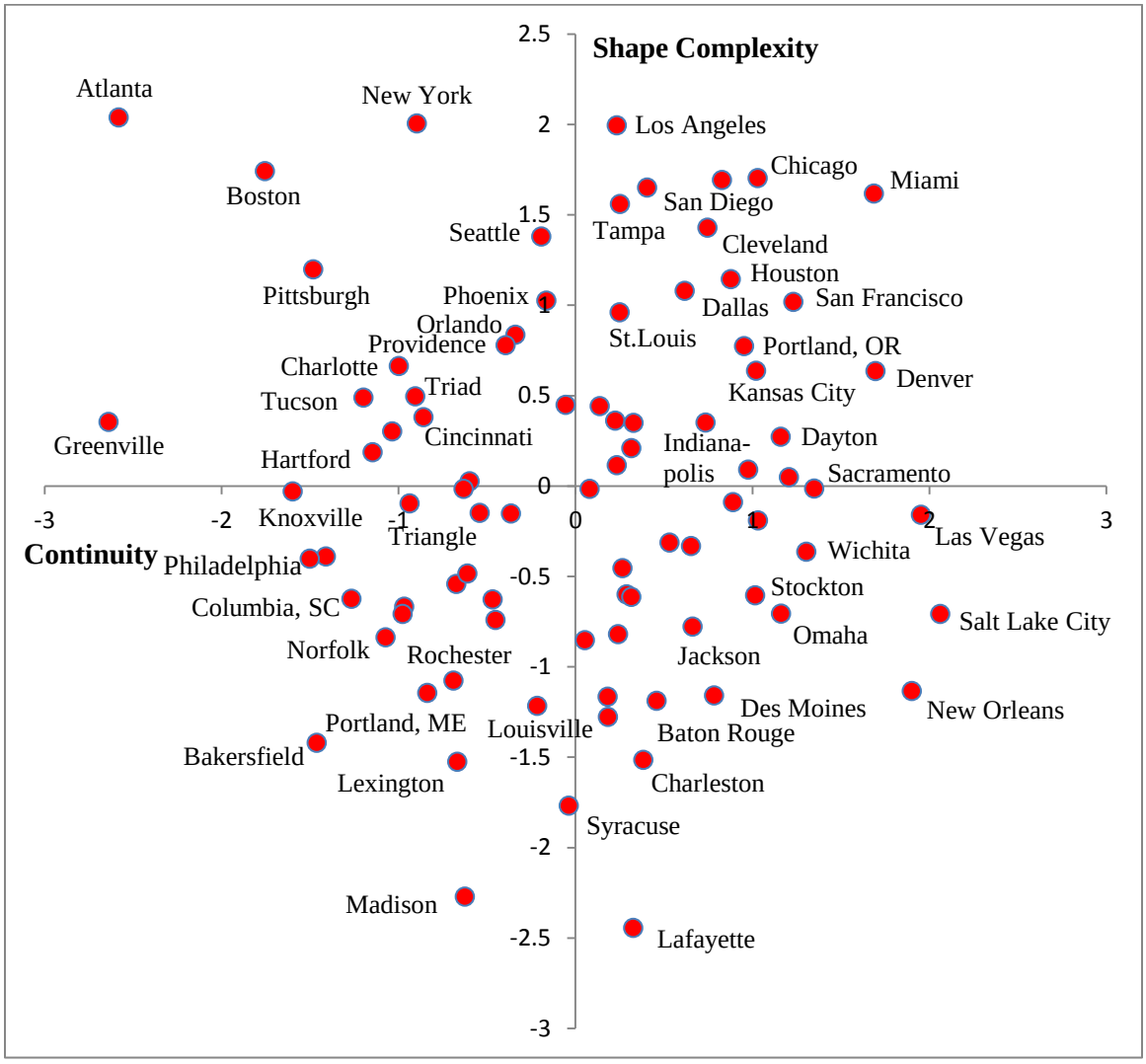

Figure 71. Urban “continuity” and urban “shape complexity” of 19 megapolitan areas, calculated at the high urban threshold.

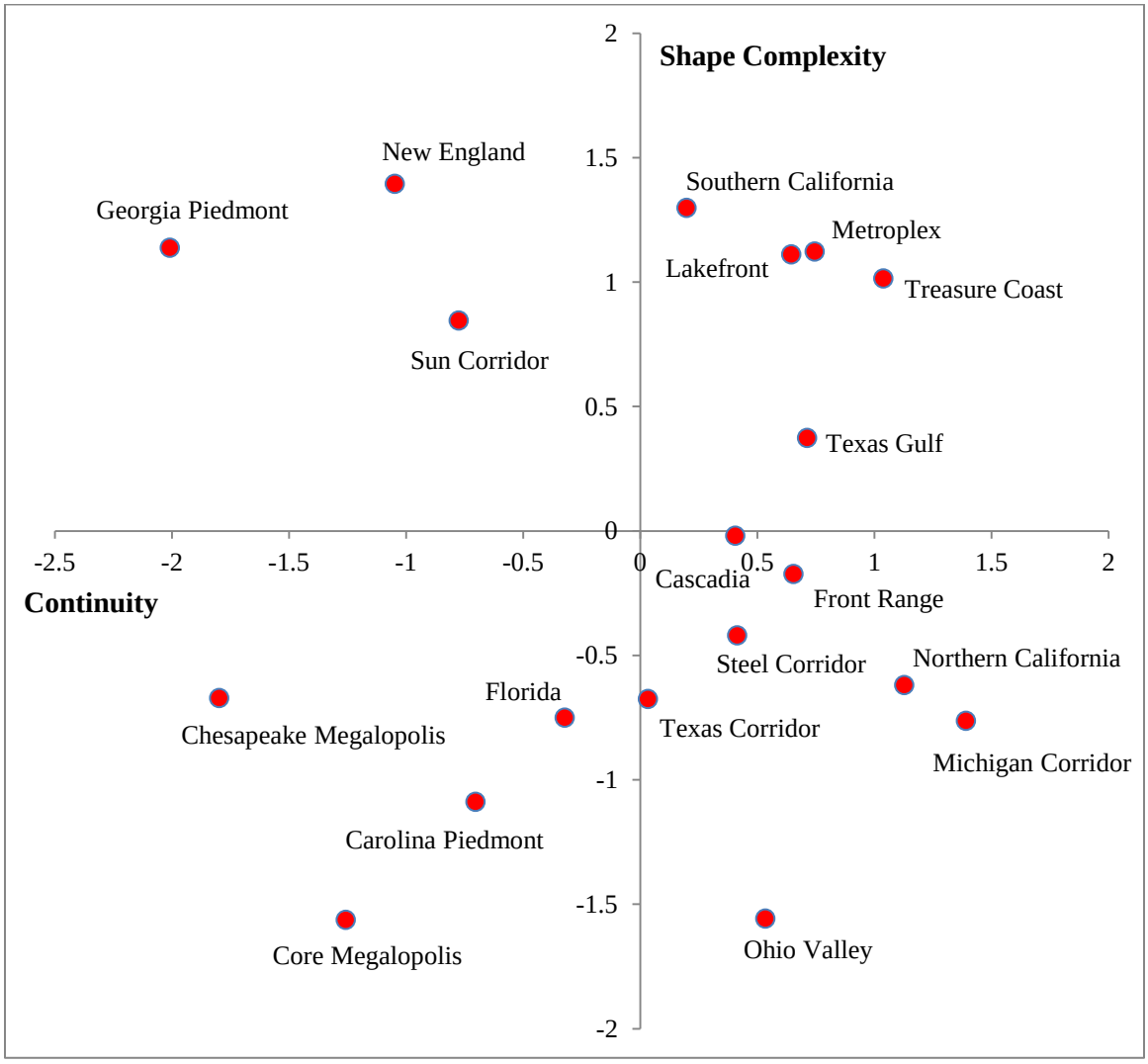

Figure 72. Urban “continuity” and urban “shape complexity” of 19 megapolitan areas, calculated at the low urban threshold.

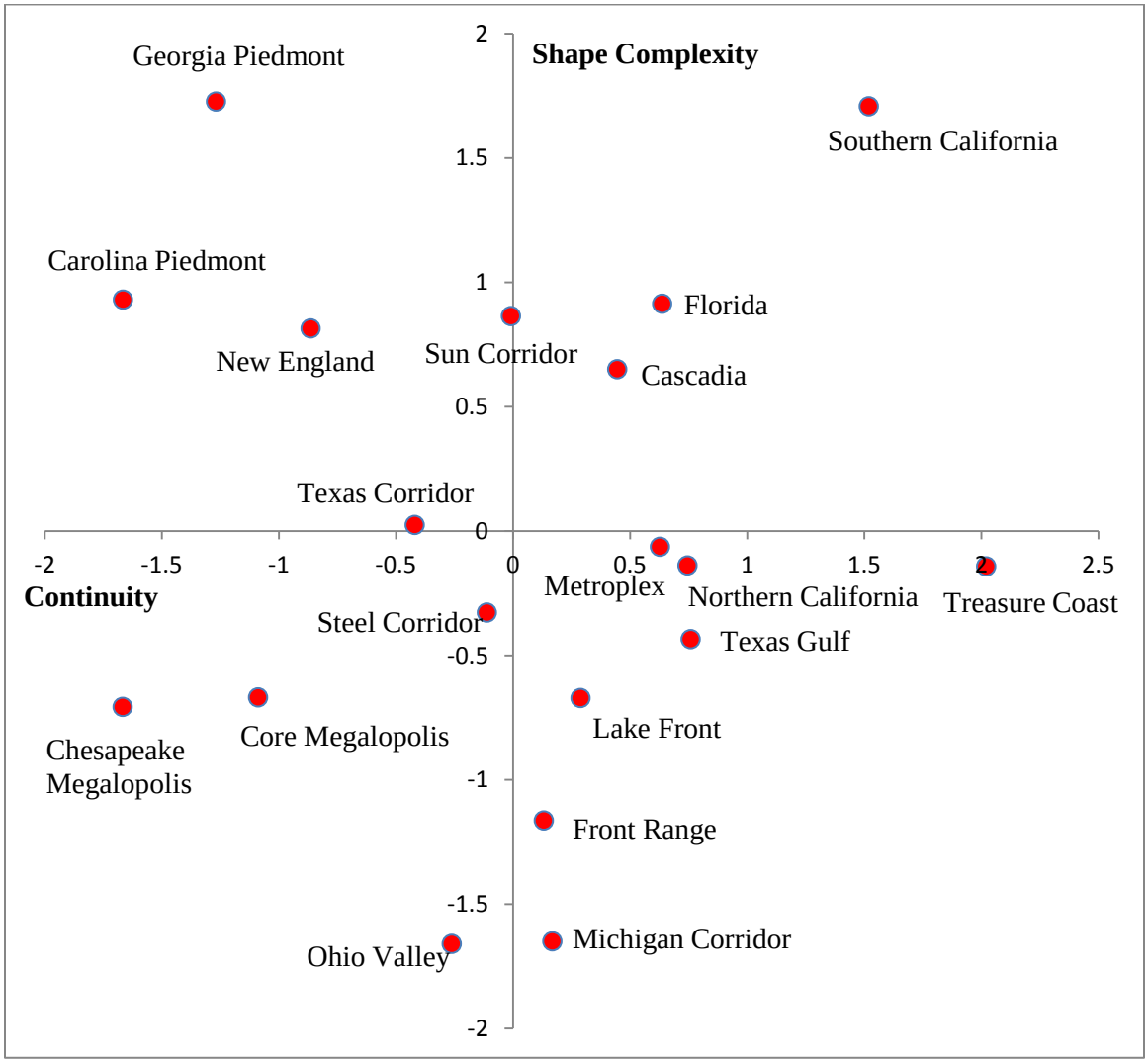

Figure 73. Annual average 4th maximum 8-hr concentration of ozone (O_3) from 1998 to 2002 throughout Los Angeles, CA.

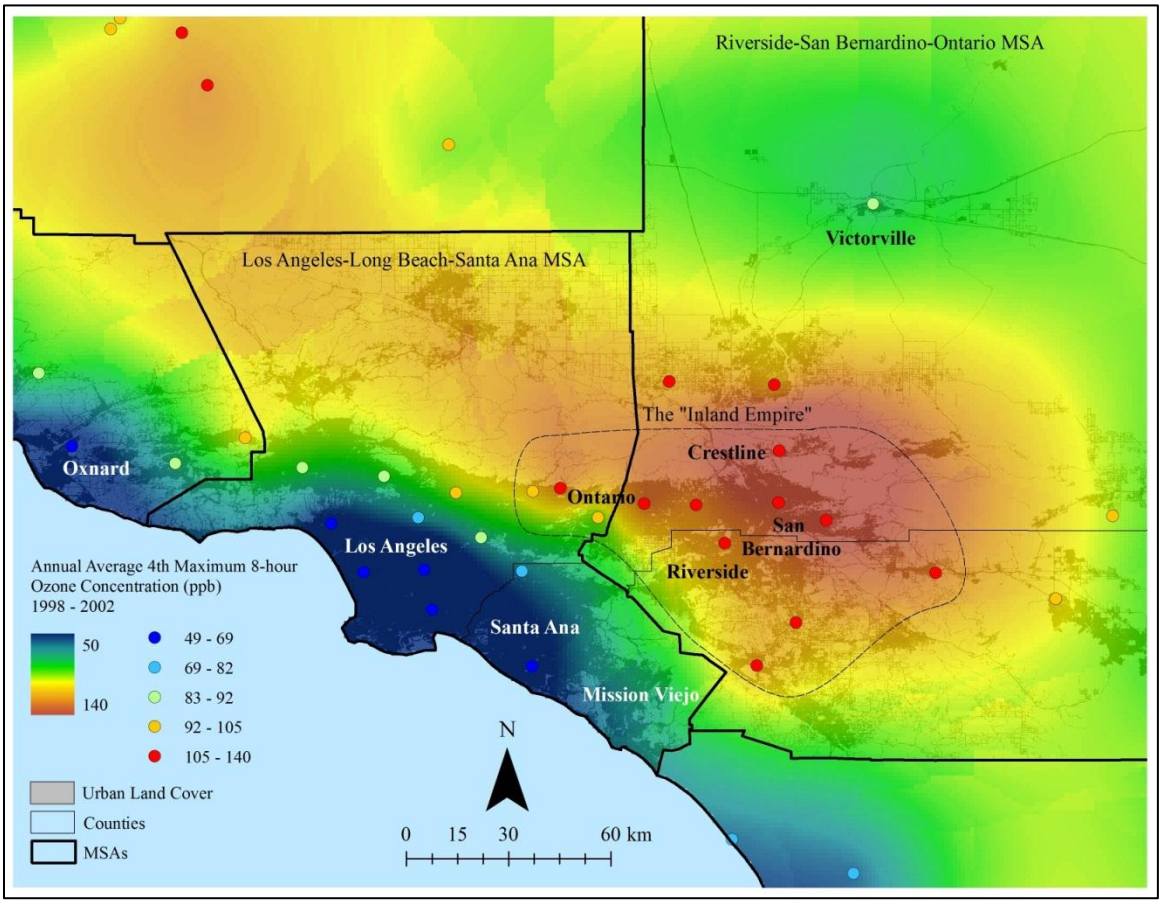

Figure 74. Annual average 24-hr concentration of fine particulate matter ($PM_{2.5}$) from 1998 to 2002 throughout Los Angeles, CA.

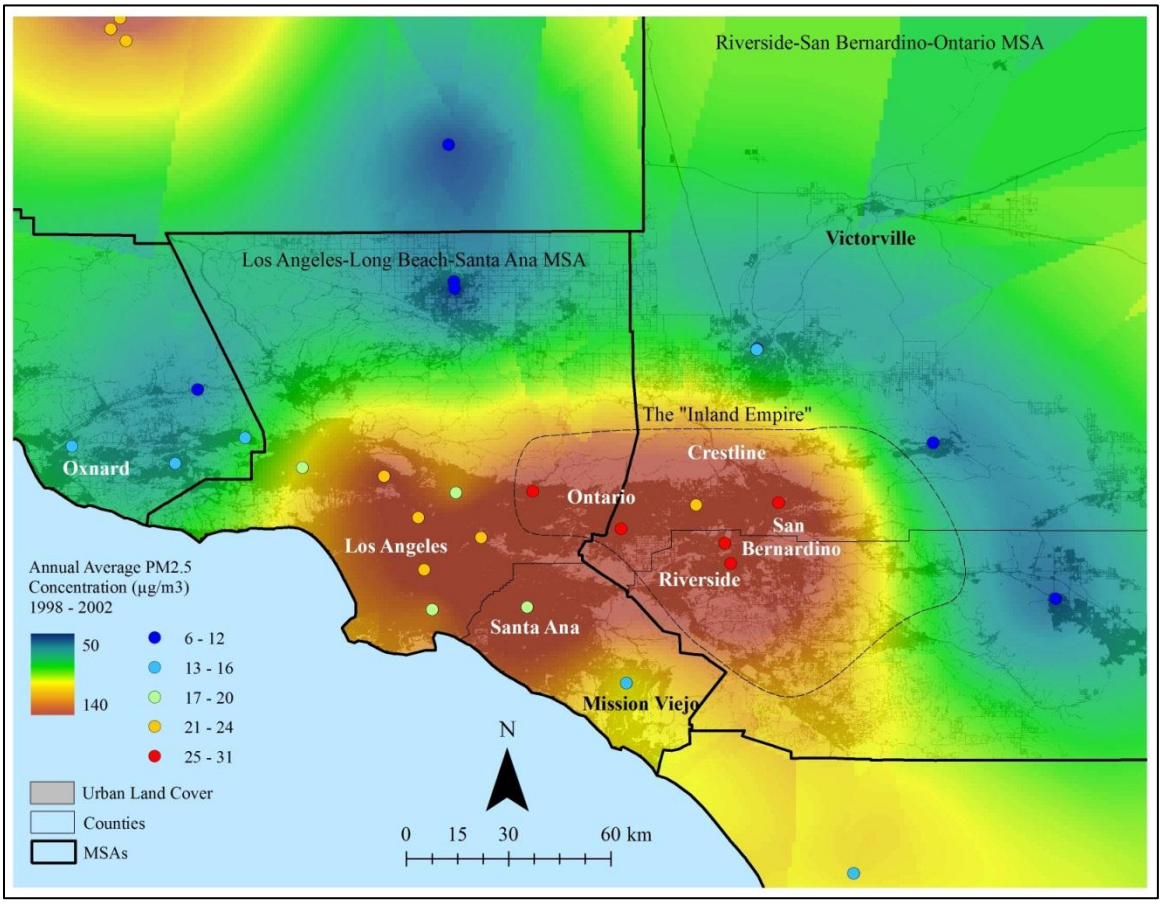

Figure 75. Urban landcover, Los Angeles, CA. Data provided by the National Landcover Dataset (NLCD 2001).

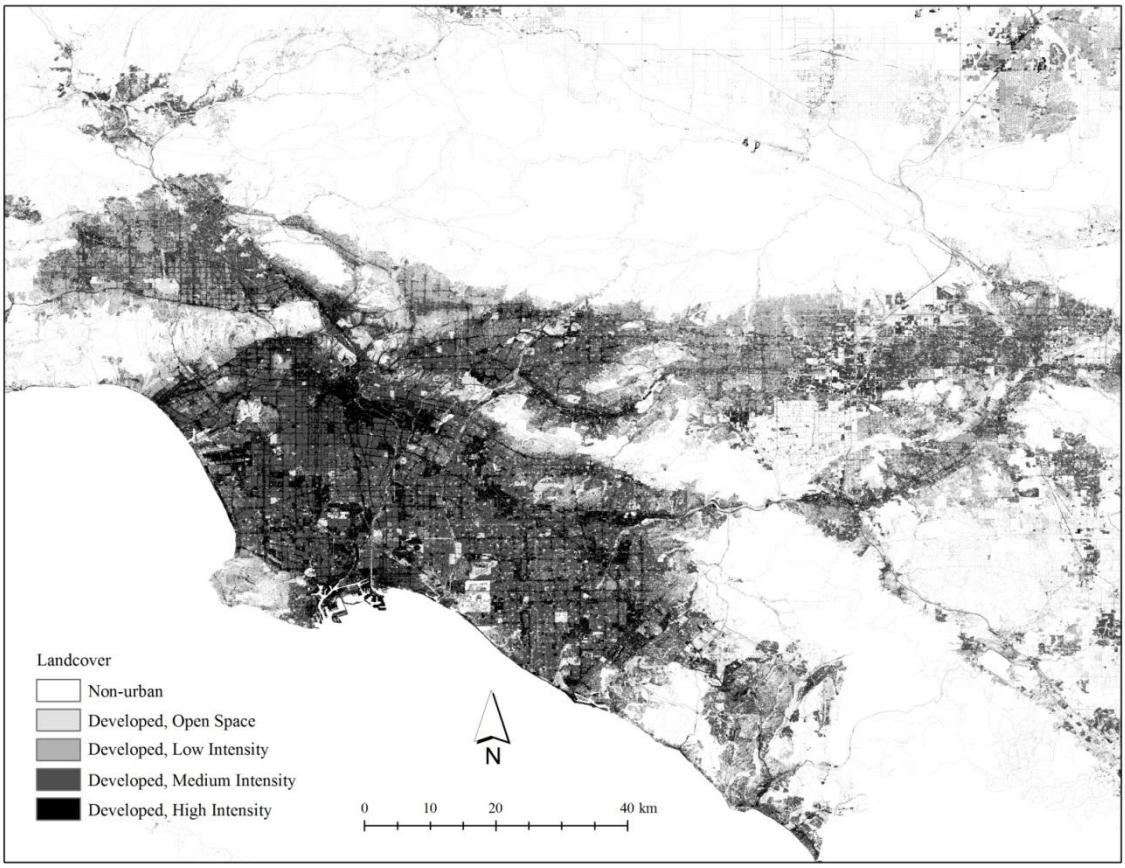

Figure 76. Annual average 4th maximum 8-hour concentration of ozone (O_3) from 1998 to 2002 in central California.

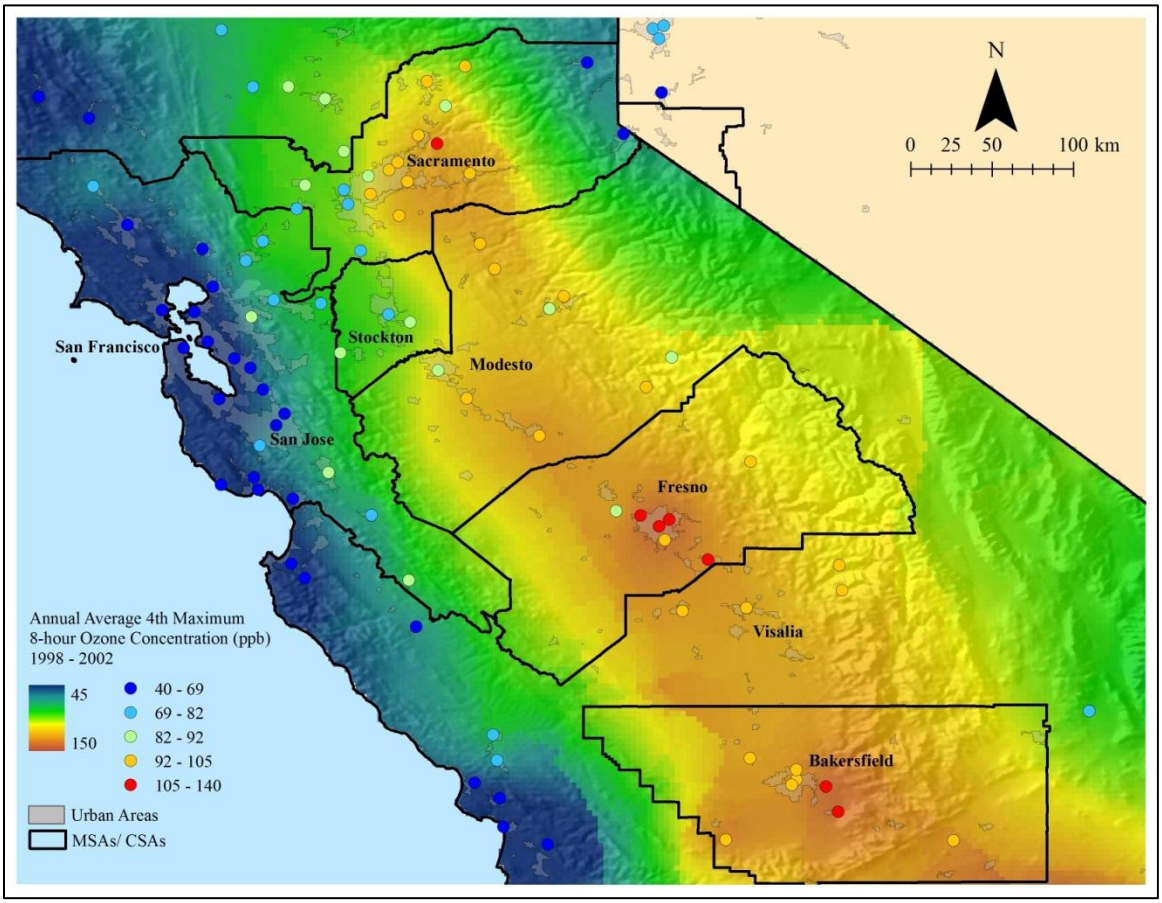

Figure 77. Annual average 24-hour concentration of fine particulate matter ($PM_{2.5}$) from 1998 to 2002 in central California.

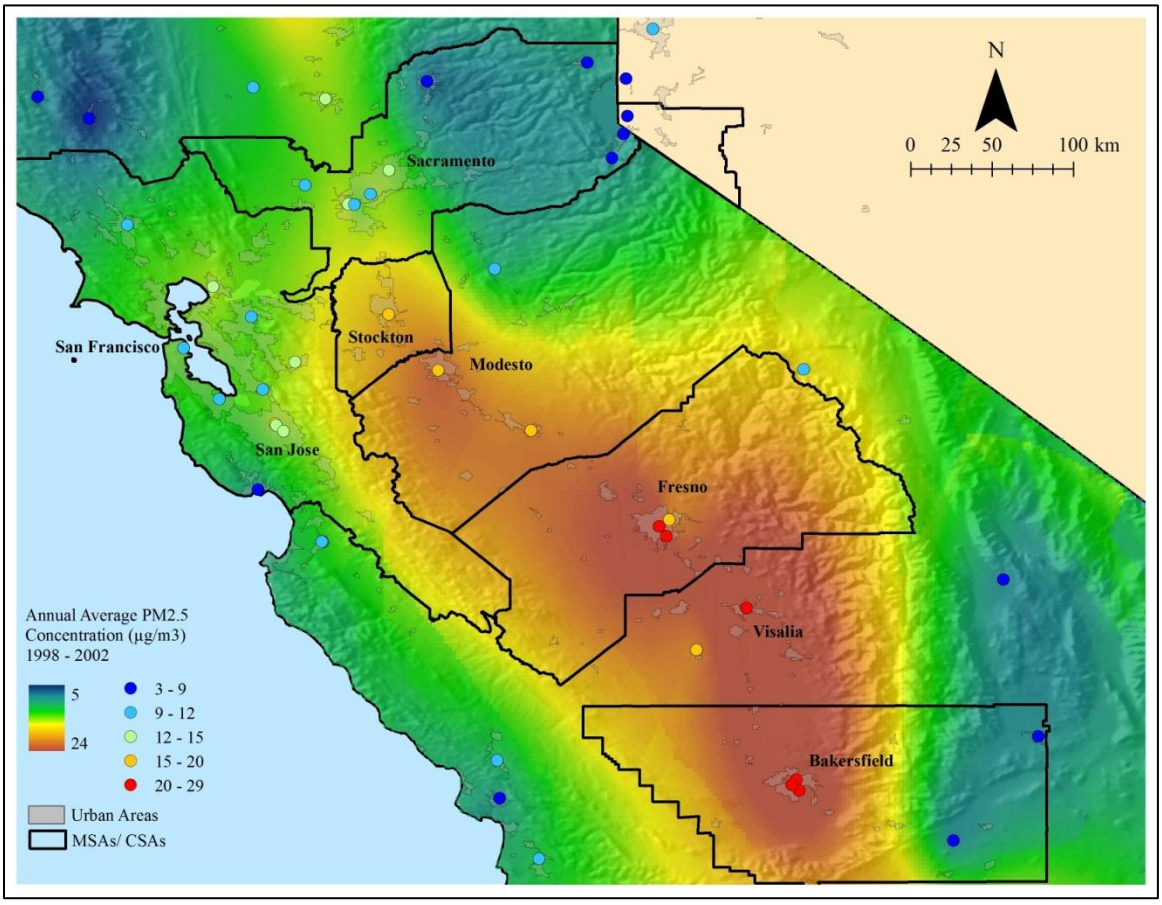

Figure 78. Annual average 4th maximum 8-hour concentration of ozone (O_3) from 1998 to 2002 in the Atlanta, GA area.

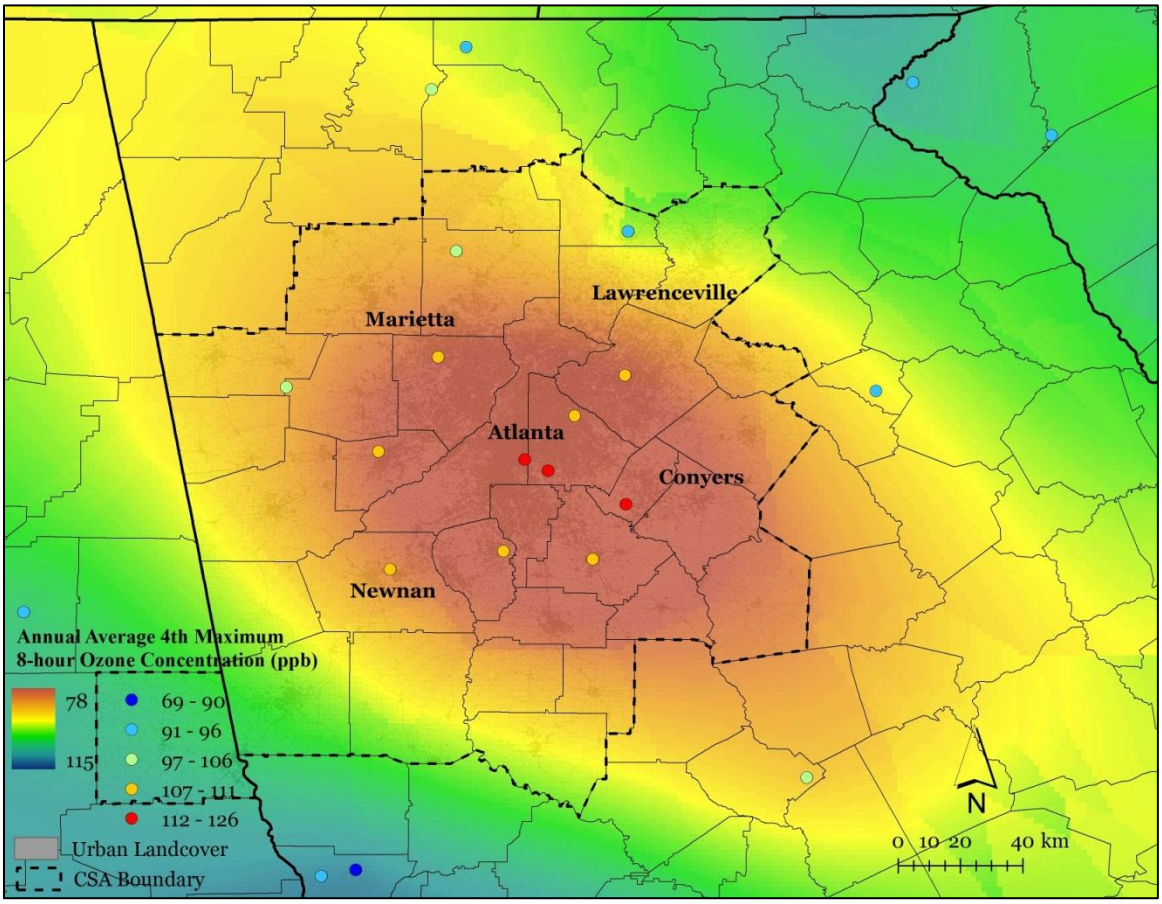

Figure 79. Annual average 4th maximum 8-hour concentration of ozone (O_3) from 1998 to 2002 along the Northeast Megalopolis from Washington, D.C. to Boston, MA ("BosWash").

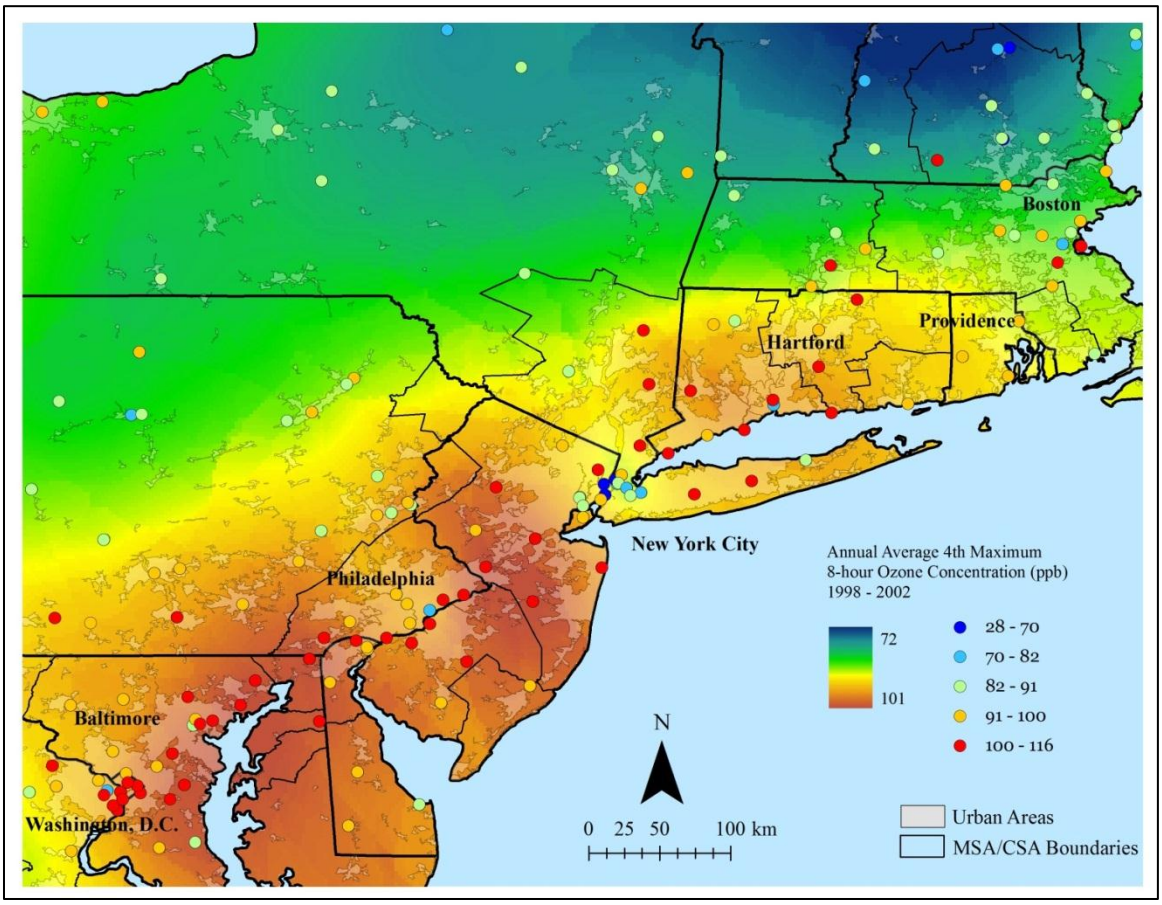

Figure 80. Annual average 24-hour concentration of fine particulate matter ($PM_{2.5}$) from 1998 to 2002 along the Northeast Megalopolis from Washington, D.C. to Boston, MA ("BosWash").

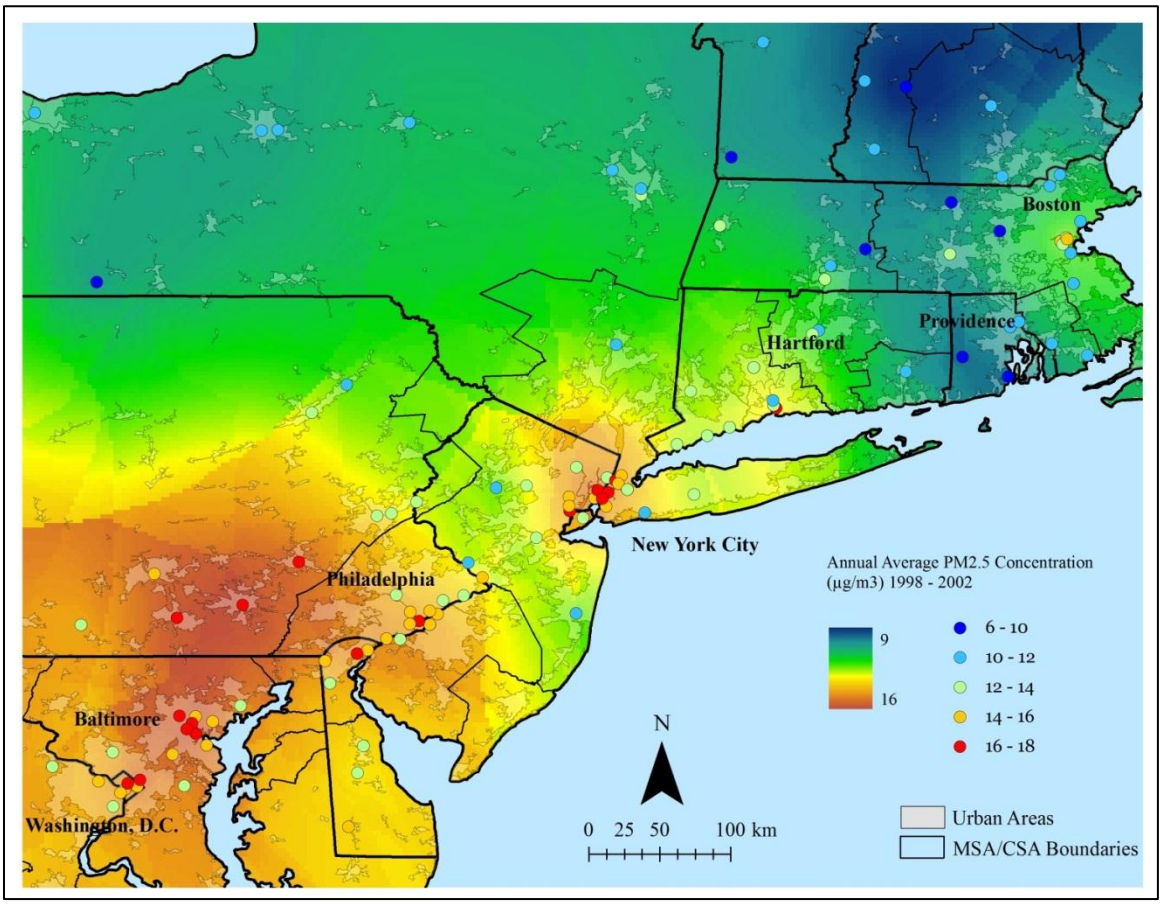

Figure 81. Location of the Southeast “Sprawl Belt” in relation to the “Rust Belt” and Northeast Megalopolis.

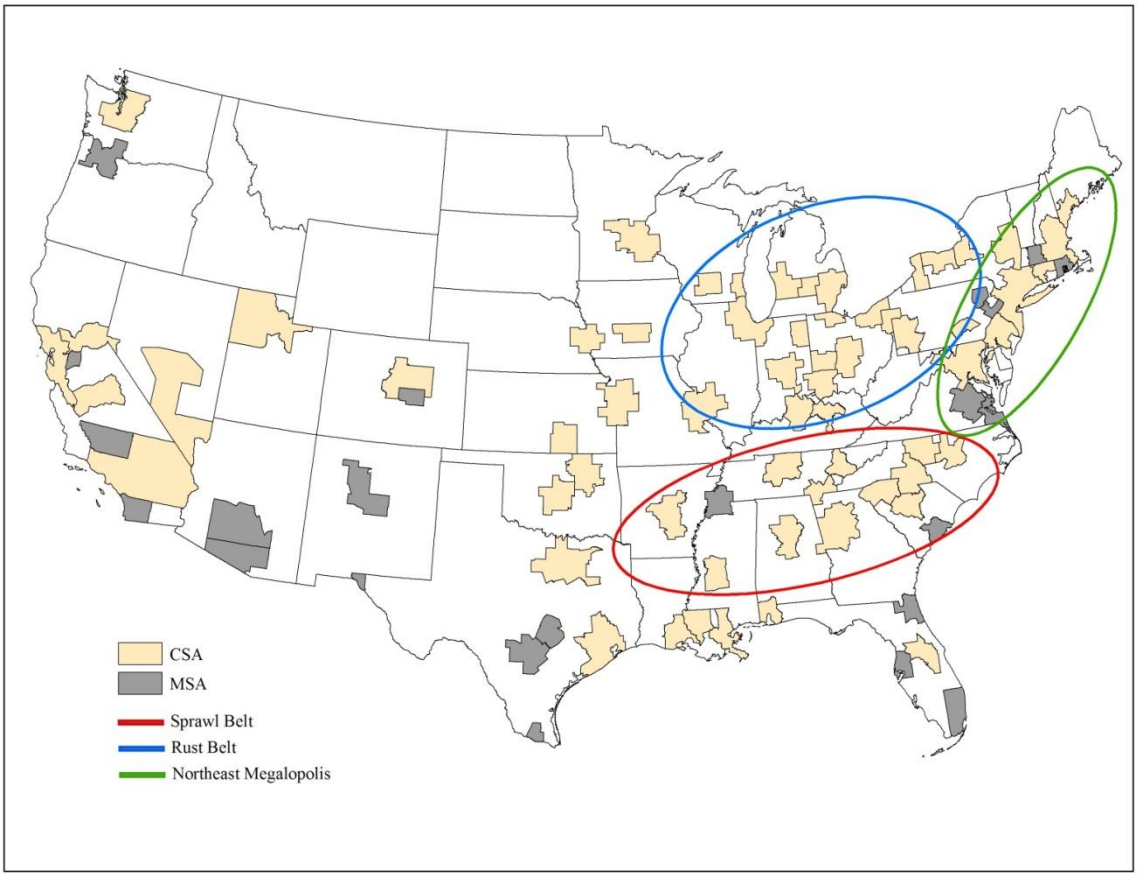

Figure 82. Urban landcover, Portland, OR.